UNIVERSITÀ DEGLI STUDI DI TRIESTE

XXVII CICLO DEL DOTTORATO DI RICERCA IN BIOMEDICINA MOLECOLARE

Tumor Suppressor DAB2IP as a target for post-transcriptional inactivation in cancer

Settore scientifico disciplinare BIO/13

DOTTORANDA Arianna Bellazzo

COORDINATORE Prof. Guidalberto Manfioletti

SUPERVISORE DI TESI Prof. Licio Collavin

ANNO ACCADEMICO 2014 / 2015

UNIVERSITÀ DEGLI STUDI DI TRIESTE

XXVII CICLO DEL DOTTORATO DI RICERCA IN BIOMEDICINA MOLECOLARE

Tumor Suppressor DAB2IP as a target for post-transcriptional inactivation in cancer

Settore scientifico disciplinare BIO/13

DOTTORANDA Arianna Bellazzo

COORDINATORE Prof. Guidalberto Manfioletti

SUPERVISORE DI TESI Prof. Licio Collavin

ANNO ACCADEMICO 2014 / 2015

To my Mom and my sister Fabiana,
always on my mind.

TABLE OF CONTENTS

ABSTRACT

The tumor suppressor DAB2IP is a cytoplasmic signaling protein that modulates the intricate network of information established among cancer cells and their microenvironment. Behaving as a guardian of signal transduction, DAB2IP modulates pathways activated by several growth factors and inflammatory cytokines, including TNFα, thus affecting the cancer cells' responses to extrinsic inputs. The gene is seldom mutated in cancer, but DAB2IP inactivation mediated by epigenetic or post-transcriptional means is frequently observed in human malignancies. Since DAB2IP inactivation can potentially favor progression of tumors driven by a variety of diverse genetic mutations, post-transcriptional inactivation of this protein may be even more diffuse.
This Thesis describes two different projects aimed to identify additional molecular mechanisms to counteract DAB2IP tumor suppressive functions in cancer.

The first project describes a mechanism of DAB2IP inactivation mediated by physical interaction with mutant forms of the p53 tumor suppressor. I demonstrated that mutant p53 binds DAB2IP in the cytoplasm, blocking its inhibitory role on NF-κB and counteracting the activation of JNK/ASK1 pathway, thus reprogramming the way cancer cells respond to TNF. Importantly, through this mechanism, mutant p53 sustains a pro-invasive response to inflammation, also restraining apoptosis. Intriguingly, this action is coupled to increased expression of a set of chemokines that can expose tumor cells to host immunity, potentially affecting response to therapy and patient outcome.
Finally, I obtained proof-of-concept evidence that overexpression of a decoy protein able to displace mutp53-DAB2IP interaction reduces tumor growth and invasion *in vivo*, suggesting that this molecular axis may be a promising therapeutic target.

The second project is focused on DAB2IP inactivation by microRNAs. Performing a high-throughput screen of a large collection of human miRNA mimics, I identified a consistent number of miRNAs targeting the DAB2IP mRNA. Among the hits, I demonstrated that two different miRNAs can efficiently down-regulate DAB2IP protein in multiple transformed cell lines, strongly enhancing cancer cells motility and invasivity. Focusing on the most active miRNA isolated, I confirmed that it promotes cancer cell invasivity by reducing DAB2IP levels, and this phenotype is likely mediated by sustained activation of NF-κB and increased expression of pro-inflammatory cytokines. Importantly, I demonstrated that the use of specific miRNA

inhibitors, or target protectors, restores DAB2IP activity and strongly reduces invasiveness of PC-3 prostate cancer cells.

Collectively, my results provide additional knowledge on the post-transcriptional mechanisms of DAB2IP inactivation in cancer, and offer solid conceptual grounds to hypothesize that therapeutic tools able to restore DAB2IP functions in tumor cells, by counteracting the mechanisms of its inactivation, would efficiently contrast cancer progression.

FOREWORD

This Thesis is composed of two different projects. Although they concern the analysis of mechanisms involved in the inactivation of the tumor suppressor DAB2IP in cancer, they are markedly distinct; for this reason I discussed them separately.

In Part 1, I wrote an extensive introduction on the tumor suppressor DAB2IP.

In Part 2, I described studies on the interaction between mutant p53 and DAB2IP in cancer progression. Since this work has been recently published, I enclosed the paper reprint, correlated with a specific introduction.

Part 3 is relative to unpublished work focused on the identification of microRNAs targeting DAB2IP. It includes a specific introduction, results, discussion and description of experimental procedures used.

PART 1: DAB2IP AS A KEY GUARDIAN OF CYTOPLASMIC SIGNAL TRANSDUCTION

1.1 CANCER: AN OVERVIEW

Cancer formation, as we currently understand it, involves multiple changes in the regulatory circuits that finely modulate proliferation and homeostasis of normal cells. Cancer has traditionally been viewed as a set of diseases driven by the activation of proto-oncogenes and by the inactivation of tumor suppressor genes (Hanahan and Weinberg, 2000).

In addition to mutations, the disruption of epigenetic regulatory mechanisms is also prevalent in cancer cells, so that genetic and epigenetic alterations interplay and synergize during tumorigenesis (You and Jones, 2012). In addition, long non-coding RNAs (ncRNAs) and micro-RNAs (miRNAs) are emerging as important regulatory molecules in tumor suppressor and oncogenic pathways (Huarte and Rinn, 2010), and defects in miRNA activity and processing are a common hallmark of the disease (Esteller, 2011).

As normal cell evolves progressively to a neoplastic state, it acquires a set of common features that include self-sufficiency in growth signals, insensitivity to growth inhibition, evasion of programmed cell death (apoptosis), limitless replicative potential, sustained angiogenesis, and tissue invasion and metastasis (Hanahan and Weinberg, 2000). In addition to these hallmarks of cancer, tumors benefit from changes in cell metabolism to sustain increased proliferation (Hanahan and Weinberg, 2011) and from the inflammatory microenvironment and the ability to avoid immune control (Colotta et al., 2009).

Notably, tumors are much more than insular masses of proliferating cells; they are complex tissues composed by multiple cell types that establish dynamic interactions with one another. The complexity of the tumor tissue also resides in the intricate network established between tumor cells and the surrounding environment, and the traffic of information shared among distinct cells.

Evidences collected in the last decade have introduced DAB2IP (Disable-2 Interactin Protein) as a new tumor suppressor able to modulate different cytoplasmic signaling pathways; this protein is frequently down-regulated in tumors, and loss of its oncosuppressive role seems to strongly impact tumor progression.

1.2 THE TUMOR SUPPRESSOR DAB2IP

DAB2IP was initially identified as a novel member of the RAS GTP-ase (RAS GAP) protein family, cloned specifically as a protein interacting with the tumor suppressor DOC-2/DAB2 (differentially expressed in ovarian carcinoma-2/Disable-2) both in normal tissues and in prostate cancer (Chen et al., 2002; Wang et al., 2002). The heterogeneous role of DAB2IP emerged immediately: indeed this protein was concomitantly cloned and identified as an ASK1-interacting protein; hence the alternative name ASK-interacting protein 1 (AIP1) (Zhang et al., 2003). In the subsequent years a lot of works have explored the important role of DAB2IP as modulator of other signaling pathways, pointing out its relevance as guardian of cytoplasmic signaling transduction. This protein turned out to be a regulator of cell response to different extracellular stimuli, such as TNF (tumor necrosis factor) or EGF (epidermal growth factor), affecting cell survival, migration and apoptosis with obvious implications for cancer development and progression.

1.2.1 Human DAB2IP gene

The human DAB2IP gene is located on chromosome 9q33.1-q33.3. It is rather complex, and can express multiple transcripts and proteins. Two human transcripts and proteins are annotated in RefSeq: hDAB2IP transcript variant 1 (NM_032552.3), and hDAB2IP transcript variant 2 (NM_138709.1). They are transcribed by different promoters, and encode predicted proteins that differ in their N-terminus (variant 1 being 96 amino acids longer) and have an alternative C-terminal exon (Chen et al., 2006; Chen et al., 2002).

The hDAB2IP gene is ubiquitously expressed in different tissues and organs. Low levels of its transcript are found only in seminal vesicle, ventral prostate, epididymis, and bladder (Wang et al., 2002). hDAB2IP transcript variant 1 seems to be the dominant isoform expressed in normal tissues (Qiu et al., 2007). During development, hDAB2IP is expressed in most human fetal tissues, in a gestational age- and tissue-type specific manner. These data suggest that DAB2IP plays a unique physiological role in organogenesis and in regulation of tissues or cells differentiation (Liu et al., 2012).

1.2.2 DAB2IP protein structure

DAB2IP can modulate the response of cells to a variety of extracellular signals. Its function strongly depends on its complex structure, well conserved in mammalians, which contains several domains (Chen et al., 2002).

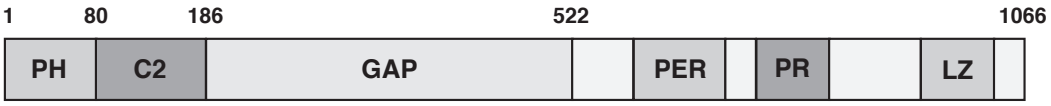

Figure 1.1. DAB2IP functional domains.
Schematic representation of DAB2IP (isoform 2) domains (see the text for additional details).

- *Pleckstring homology domain* (*PH domain*): it is an approximately 100-residue protein module, localized on the N-terminal of DAB2IP. It characterizes a wide range of proteins involved in intracellular signaling. This domain can bind phosphatidylinositol lipids within biological membranes, such as phosphatidylinositol (3,4,5)-triphosphate and phosphatidylinositol (4,5)-bisphosphate (Musacchio et al., 1993).
- *Protein kinase C conserved region 2* (*C2 domain*): it is a $Ca2^{+}$ binding motif, approximately 130 residues in length; single and multiple copies of C2 domains have been identified in several signaling proteins that mediate a broad array of critical intracellular processes. This domain displays the remarkable property of binding a variety of different ligand and substrates such as $Ca2^{+}$, phospholipids, inositol polyphosphates, and intracellular proteins (Nalefski and Falke, 1996).
- *Ras GTPase-activator protein* (*RasGAP domain*): it is found in proteins involved in protein synthesis and signal transduction. Many of these proteins are much larger and more complex than their targets, containing multiple domains capable of interacting with an intricate network of cellular enzymes and structures (Boguski and McCormick, 1993).
- *Proline rich domain* (*PR domain*): it is a domain implicated in protein-protein interactions, in particular it is a docking site for proteins with SH3 domains (Feller et al., 1994).
- *Period-like domain* (*PER domain*): a non-described structure, involved in protein-protein interaction.
- *Leucine zipper domain*: it is a hydrophobic motif, usually found within the DNA-binding domain of transcription factors. It is involved in the formation of protein dimers.

In humans, there are at least two DAB2IP isoforms, derived from the alternative transcripts described above. Human DAB2IP isoform 1 (NP_115941) is composed of 1132 amino acids, with a molecular weight of approximately 130kDa. Human DAB2IP isoform 2 (NP_619723) is composed of 1066 amino acids, with a molecular weight of 110 kDa. Both isoforms share the same structure (Figure 1.1), but differ at their N- and C-terminal ends. hDAB2IP variant 1 has a longer PH domain compared to hDAB2IP variant 2. Variant 2 has an alternative C-terminal sequence, encoding a class-I PDZ interacting motif that may allow additional protein-protein interactions. However, very little information is currently available on the expression and function of the different proteins potentially encoded by this complex gene, with most published functional studies performed with isoform 2.

The abundance of DAB2IP's domains underlies the multiple functions of this protein. First, DAB2IP has an enzymatic activity, whose core lies in its RasGAP domain. In addition, through its domains specialized in protein-protein binding, DAB2IP can act on one side as an adaptor, or scaffold, to promote formation of protein complexes involved in signal transduction, and on the other side it can act as a competitor, or scavenger, binding signaling proteins and preventing their interaction with upstream activators, or downstream effectors. Table 1.1 summarizes currently known interactors of DAB2IP, and the domains involved in the binding.

Table 1.1: DAB2IP can interact with several proteins involved in signal transduction, affecting the outcome of multiple cellular inputs			
DAB2IP domain	Interacting protein	Biological effect of the binding:	Ref.
PH	**IRE1α**	It enhances IRE1α, and ASK1-JNK activation upon ER stress	(Luo et al., 2008)
C2	**ASK1** (K154-161 residues-KA2)	It prevents ASK1 binding to 14-3-3 and enhances TNF-induced ASK1-JNK activation	(Zhang et al., 2003)
	GSK3β	It facilitates GSK3β de-phosphorylation and decreases transcriptional activity of β-catenin	(Xie et al., 2010)
	VEGFR-2 (K104-106 residues-KA1)	It inhibits auto-phosphorylation of VEGFR-2 and counteracts VEGFR-2 mediated angiogenic signals	(Zhang et al., 2008)
	mutant p53	It counteracts the binding of DAB2IP with ASK1, prevents JNK phosphorylation and enhances NF-κB activation in response to TNF	(Di Minin et al., 2014)
PH-C2	**JAK2**	It inhibits JAK2, STAT1 and STAT3 phosphorylation and activation upon IFN-γ treatment	(Yu et al., 2011)
N-terminal	**VEGFR-3**	It facilitates VEGFR-3 stabilization and activity (mechanism not completely understood)	(Zhou et al., 2014b)
GAP	**RAS**	Inactivates RAS	(Wang et al., 2002)
	PP2A	DAB2IP facilitates PP2A-ASK1 interaction, and the subsequent dephosphorylation and activation of ASK1 in response to TNF	(Min et al., 2008)
	HIPK1	It induces dissociation of ASK1 from its inhibitors 14-3-3 and thioredoxin, and induces ASK1 activation.	(Li et al., 2005)
	RIP-1	It promotes DAB2IP phosphorylation is ser-604 and stimulates DAB2IP activation upon TNF treatment	(Zhang et al., 2007)
PER	**TRAF2**	It enhances TNF- induced JNK activation, while counteracts NF-κB cascade	(Zhang et al., 2004)
	14-3-3	It prevents the binding between 14-3-3- and ASK1	(Zhang et al., 2007)
	AKT1	It counteracts activation of AKT1	(Xie et al., 2009)
PR	**p85(PI3K)**	It sequesters p85-p110 complex and inhibits PI3K activity and AKT activation	(Xie et al., 2009)
	c-Src	It disrupts the interaction between c-Src and AR, and blocks AR activation	(Wu et al., 2014)
LZ	**GATA-1**	It regulates CD117 expression	(Yun et al., 2015)
Undefined	**DOC/DAB-2**	It negatively modulates RAS pathway	(Wang et al., 2002)
	DAB-1	It negatively modulates RAS pathway	(Wang et al., 2002)
	FBW7	It promotes the degradation of DAB2IP	(Dai et al., 2014)
	TNFR-2	TNFR-2 binds to DAB2IP and ASK1 to activate JNK	(Ji et al., 2012)
	Skp2 (N-term and C-term)	It mediates DAB2IP ubiquitination and proteasome degradation	(Tsai et al., 2014)

1.2.3 DAB2IP functional activities

DAB2IP as a GTPase Activating Protein

The RasGAP domain of DAB2IP shows a high degree of amino acids homology (40%-90%) with other RasGAPs, such as GAP120 and *homo sapiens* neurofibrin (NF1) (Chen et al., 2002). DAB2IP is able to stimulate *in-vitro* and *in-vivo* activity of several RAS protein (i.e. H-Ras, K-Ras and N-Ras) in prostate and hepatocellular cancer cell lines, and in acute myeloid leukemia cells (Calvisi et al., 2011; Homayouni et al., 2003; Min et al., 2010; von Bergh et al., 2004). In the absence of Ras mutations, down-regulation of DAB2IP was found in highly proliferative human liver and in prostate cancers (Calvisi et al., 2011; Min et al., 2010). The reactivation of DAB2IP activity, through protein overexpression inhibits tumor cells proliferation and induced apoptosis (Calvisi et al., 2011). The GAP domain of DAB2IP is necessary for this function: mutation of a key amino acid in this domain (R289L) abolishes selectively the Ras-GAP activity (Min et al., 2010).

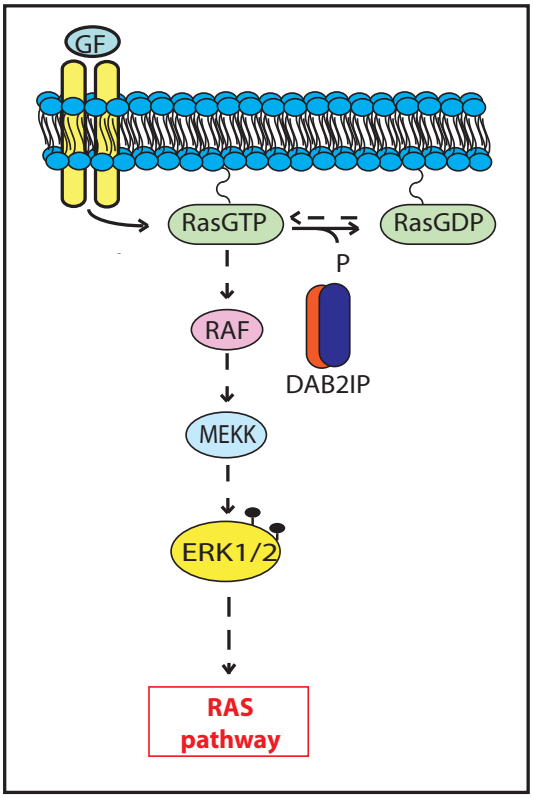

In Acute Myeloid Leukemia, DAB2IP was identified as a novel MLL fusion partner, because of the translocation t(9,11)(q34;q23). The PH domain of DAB2IP is disrupted, and the normal function of DAB2IP is aborted; that implies a deregulation of RAS activity, which could be involved in leukemia transformations (von Bergh et al., 2004).

In endothelial cells, the GAP activity of DAB2IP may also play an inhibitory role in LPS-induced NF-κB and MAPK signaling pathways, by acting on the trafficking regulator Arf6, the best characterized activator of PIP5K (phosphatidylinositol 4-phosphate 5-kinase) (Wan et al., 2010). Although the authors could not clearly demonstrate that DAB2IP functions as a GTPase-activating protein for Arf6, they demonstrated that DAB2IP down-regulates cellular PIP2 (phosphatidylinositol 4,5-bisphosphate) levels, and inhibits TLR4-dependent activation of NF-κB and MAPK signaling pathways in a way that requires its Ras GAP domain (Wan et al., 2010).

DAB2IP as a cytoplasmic scaffold or competitor

DAB2IP was initially identified as an interactor of the adaptor protein DAB2/DOC-2 (Disable-2/ differentially express in ovarian carcinoma-2) in human prostate cancer cell (Wang et al., 2002). DAB2/DOC2 and DAB2IP appear to form a unique regulatory complex that acts as negative feedback machinery for several exogenous stimuli. The protein kinase PKC can phosphorylate the N-terminal domain of DAB2/DOC2, which recruits DAB2IP to inactivate Ras protein through its Ras GAP activity (Wang et al., 2002). On the other hand, shortly after the stimulation with growth factors, DAB2/DOC2 competes with SOS for the binding with Grb2, which leads to the inactivation of MAP kinase signaling (Wang et al., 2002). Therefore, the DAB2/DOC2 binding with DAB2IP has an important role in the control of cell proliferation and differentiation. Altered expression of these two proteins is often detected in prostate, ovarian, and breast cancer cells, and induces uncontrolled tumor growth and increased tumor aggressiveness (Wang et al., 2002).

Similarly, DAB2IP modulates many cellular pathways, by forming specific and dynamic protein complexes with a remarkable number of different signal transducers.

Activation of the ASK1-JNK signaling cascade

ASK1 (apoptosis signal-regulating kinase 1) is a member of the MAP kinases family (MAP3K) and is an upstream activator of JNK (c-Jun N-terminal kinase) and p38 MAPK (Davis, 2000). ASK1 can be activated in response to various extracellular signals, including pro-apoptotic stimuli such as pro-inflammatory cytokines, and reactive oxygen species; one of the most important activator of ASK1 is TNF alpha (tumor necrosis factor alpha) (Davis, 2000). DAB2IP carries out a key role in ASK1 activation upon TNFα stimulation. In endothelial and cancer cells, TNFα stimulates the activation of two distinct and opposite cytoplasmic pathways: ASK1/JNK or NF-κB signaling. The regulation of this cytoplasmic signal transduction is rather complex. When TNFα binds its receptor, TNFR1, it induces detachment between TNRF1 and its inhibitor SODD (silencer of death-domains). Once activated, TNFR1 can be bound by TRADD (TNFR-associated death domain protein), and recruits TRAF2 and RIP1 (receptor-interacting protein-1) (Hsu et al., 1995; Jiang et al., 1999). This minimal complex catalyzes the formation of a multi-proteins complex, recruiting either the IκB kinase complex (IKK) or ASK1, leading to activation of the NF-κB and JNK pathways, respectively (Kalliolias and Ivashkiv, 2016). DAB2IP functions by specifying TRAF2 towards ASK1-JNK pathway activation, enforcing at different levels this signaling cascade. In particular, DAB2IP, through PH/C2 domain, binds the cytoplasmic membrane, in a closed and inactive conformation.

Upon TNFα stimulation, this protein detaches from plasma membrane and shuttles in the cytoplasm, where it binds TRAF2 (Zhang et al., 2004; Zhang et al., 2003). This interaction sequesters TRAF2 from the NF-κB activating complex, allowing formation of a complex composed of TRADD, TRAF2, RIP1 and DAB2IP (the so called AIP1 complex) in the cytoplasm (Zhang et al., 2004). In the formation of this complex, RIP1 seems to be important to modulate DAB2IP activity (Zhang et al., 2007): this kinase binds DAB2IP on its GAP domain (Table 1.1), and mediates its phosphorylation on Serine 604, inducing a conformational change and allowing the binding of DAB2IP with the other protein complex members, especially with ASK1. Protein 14-3-3, a phosphoserine-binding protein, binds to ASK1, when phosphorylated on Ser-967 and inhibits its function. When phosphorylated on Ser-604, DAB2IP binds ASK1 causing the release of inhibitory 14-3-3 protein, thus activating ASK1 (Zhang et al., 2007). Mutation of Ser-604 in DAB2IP blocks formation of the AIP1 complex, as well as TNF-induced ASK1-JNK activation, suggesting that it plays a critical role in this mechanism (Zhang et al., 2007). Indeed, in cells that express this particular mutant, TNF stimulation mainly sustains NF-κB pathway activation, promoting EMT and cell invasion (Min et al., 2010).

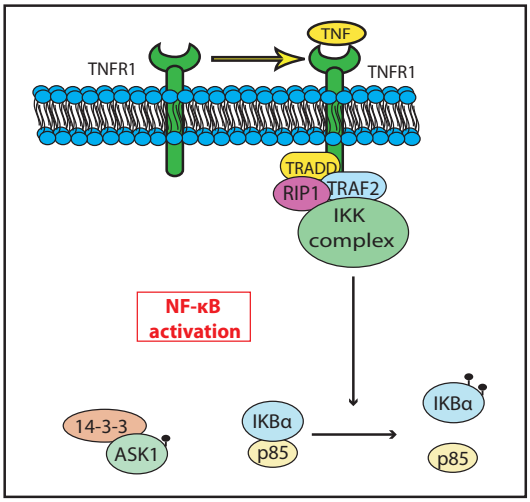

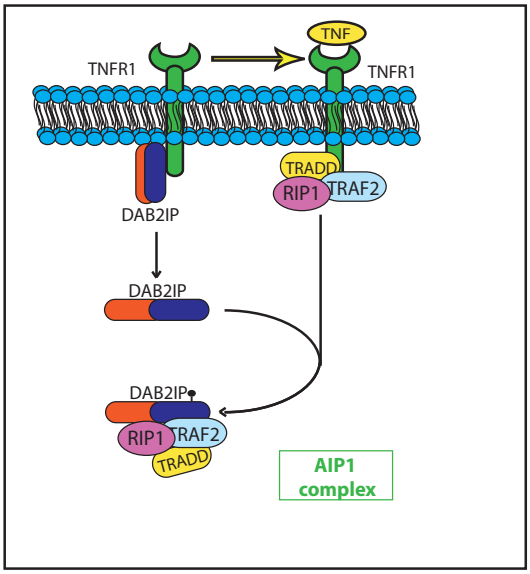

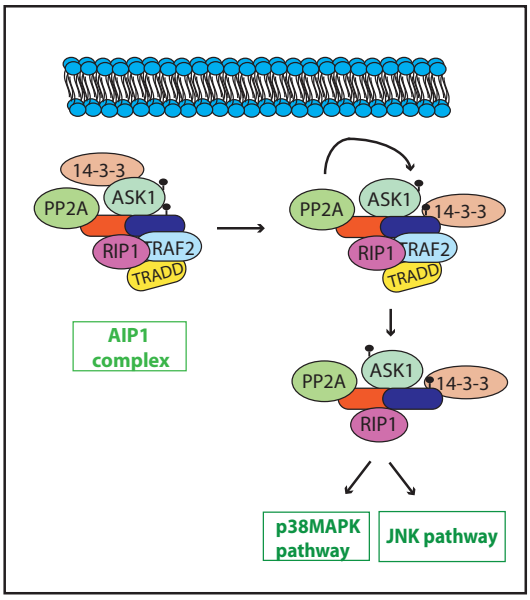

The activation of ASK1 is protracted also by PP2A-dependent dephosphorylation of Ser-967. DAB2IP binds the Ser/Thr phosphatase PP2A through the GAP domain (Table 1.1) in resting and TNF-stimulated cells (Min et al., 2008), and functions as a scaffold in TNF-induced recruitment of

PP2A to ASK1, leading to de-phosphorylation of Ser-967 and further activation of ASK1 (Min et al., 2008). Notably, PP2A is one of the major Ser/Thr phosphates implicated in the regulation of many cellular processes and signal transduction pathways (Sangodkar et al., 2015). Despite the high number of signaling kinases, a relatively limited number of Ser/Thr-specific phosphatases are known to antagonize them. Therefore, substrate specificity is determined by adaptor proteins, such as DAB2IP, which thus play a crucial regulatory role.
This model is well characterized in endothelial cells (Zhang et al., 2004), but is likely conserved in most cell types, including cancer cells, and defines DAB2IP as a determinant in driving the response to TNFα toward TRAF2- dependent ASK1/JNK activation, while indirectly inhibiting IKK/NF-κB branch (Zhang et al., 2004).
TNFR2 expression is limited to specific cell types, including endothelial cells, cardiac myocytes and hematopoietic cells (Carpentier et al., 2004) and is involved in the activation of canonical, and non-canonical NF-κB pathway as well as JNK pathway (Carpentier et al., 2004). Again, DAB2IP association with TNFR2 is required for TNFR2-dependent JNK and apoptotic signaling in vascular endothelial cells, where it can affect vascular disease progression (Ji et al., 2012).

Notably, DAB2IP can sustain ASK1/JNK pathway activation also acting as a scaffold in another protein complex. HIPK1 (Homeodomain-interacting protein kinase 1), a kinase that leads to activation of apoptotic pathways upon various stress signals (Isono et al., 2006), was shown to form a ternary complex with DAB2IP and ASK1 upon TNF stimulation in endothelial cells (Table 1.1) (Li et al., 2005). Under these conditions DAB2IP and HIPK1 synergize to promote stress-induced activation of the ASK1-JNK/p38 pathway (Li et al., 2005).

Another condition in which DAB2IP promotes ASK1-JNK/p38 signaling is during the Unfolded Protein Response (UPR). In the lumen of the endoplasmic reticulum (ER) maturation of proteins requires the coordinated activity of many chaperones and folding enzymes. When unfolded proteins accumulate, the cell is said to undergo “ER stress” and elicits a homeostatic UPR (Clarke et al., 2014). Three different receptors, localized on the ER membrane, act as sensors of ER stress, and induce the activation of various effectors and cellular process. These sensors are activating transcription factor (ATF) 6, the trans-membrane kinase PERK (PKR-like ER kinase) and the kinase with ribonuclease activity IRE1α (inositol-requiring enzyme-1) (Jager et al., 2012).

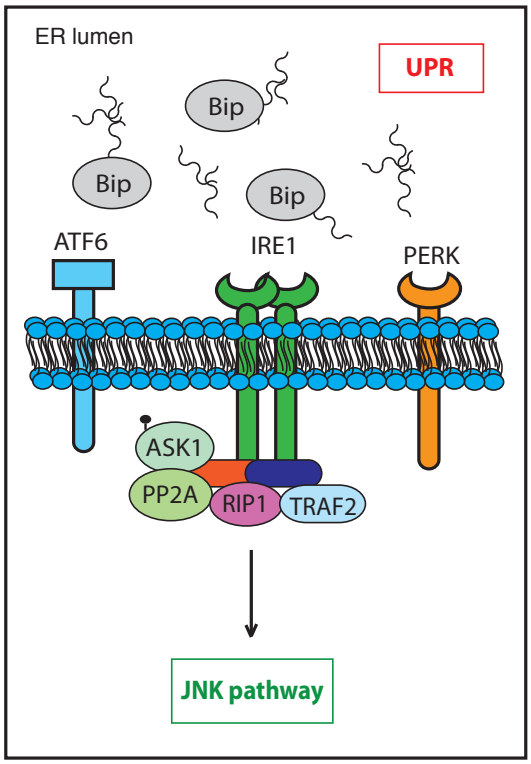

Activated IRE1α catalyzes cytoplasmic splicing of the mRNA encoding the Xbp1 transcription factor, which translates an alternative protein, Xbp1s that activates expression of a broad set of UPR response genes. In addition, IRE1α also triggers the activation of pro-apoptotic JNK signaling through recruitment of the TRAF2-ASK1 complex (Jager et al., 2012).

Endothelial cells from DAB2IP knockout (KO) mice show dramatic reduction in the response to ER-stress mediated by IRE1α/JNK axis (Luo et al., 2008). Apparently, the other UPR signaling axes are not blunted in DAB2IP KO mice. This because DAB2IP binds directly to IRE1α (Table 1.1), facilitates its dimerization, and behaves as a scaffold protein to mediate JNK phosphorylation by the kinase IRE1α (Luo et al., 2008).

Cancer cells are constantly exposed to ER stress by expression of aberrant proteins, limited availability of sugars for protein glycosylation, chronic hypoxia and inflammation in the tumor niche, and also the effects of chemotherapeutic drugs (Clarke et al., 2014). The impact of the UPR in cancer remains controversial, as it can lead to cell elimination by apoptosis, but also to cell survival and adaptation. In this scenario, the role of DAB2IP in promoting ER-stress induced activation of the ASK1-JNK axis might have a tumor-suppressive function.

Negative modulation of Androgen receptor signaling

The androgen receptor (AR) regulates normal prostate development as well as critical growth and survival programs in prostate carcinoma. Multiple mechanisms lead to hyperactive AR signaling, including AR mutation or amplification, altered expression of AR co-activators and co-repressor or presence of androgen regulated promoters fused with ERG and other ETS-family transcription factors (Robinson et al., 2015). DAB2IP can inhibit AR-mediated prostate cancer cell growth via distinct mechanism (Wu et al., 2014). First, AR activity is inhibited by DAB2IP/PP2A complex (Wu et al., 2014). DAB2IP acts as a scaffold protein for PP2A, driving this phosphatase to multiple substrates. Phosphorylation in Ser-81 is essential for AR function, and appears to mediate chromatin binding and transcriptional activation in response to androgen stimulation (Chen et al., 2012). DAB2IP, through the binding with PP2A, is able to suppress

DHT-elicited Ser-81 phosphorylation of AR, preventing its nuclear translocation and binding to androgen response elements. Notably, DAB2IP can exert this inhibition on different AR splice variants (Wu et al., 2014). Moreover, DAB2IP inhibits the non-genomic pathways activated by AR, disrupting its binding with c-Src and counteracting AR-induced ERK phosphorylation and proliferation of prostate cells (Wu et al., 2014). Taken together, these data demonstrate that DAB2IP is a unique intrinsic negative modulator of AR activity in normal and cancer cells, and likely can be further developed into a therapeutic agent for PCa.

Activation of GSK3β – βcatenin signaling pathway

GSK3β is a serine/threonine kinase that phosphorylates numerous substrates, in many cases promoting their routing to proteasome degradation. GSK3β is constitutively active under resting conditions; different signaling cascades (such as Wnt/βcatenin and PI3K-AKT) promote its inactivation through N-terminal Ser-9 phosphorylation. In canonical WNT signaling, in the absence of ligand, the serine/threonine kinases CK1 and GSK3β phosphorylate βcatenin, rapidly stimulating its destruction by the proteasome. Upon Wnt stimulation, GSK3β-mediated βcatenin degradation is inhibited, leading to the stabilization of βcatenin, that shuttles in the nucleus to promote gene transcription (Clevers, 2006). DAB2IP interacts via its C2 domain with GSK3β, directing PP2A activities on Ser-9 dephosphorylation, and leading to GSK3β activation (Xie et al., 2010). Loss of DAB2IP expression increases inhibitory phosphorylation of GSK3β, sustains repression of E-cadherin and up-regulation of vimentin in both human normal epithelial and prostate carcinoma cells, initiating epithelial-to-mesenchymal transition (EMT) (Xie et al., 2010). It is tempting to speculate that the DAB2IP/PP2A/GSK3β complex may be involved in the regulation of other GSK3β targets, with a role in a wide spectrum of cellular processes, including glycogen metabolism (e.g. Inhibitor-2 Glycogen Synthase), transcription (e.g c-Myc and c-Jun), insulin signaling (e.g. insulin receptor

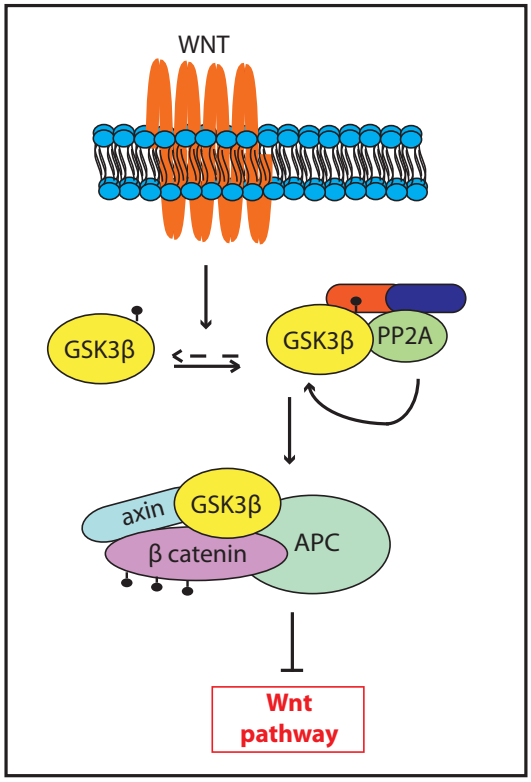

substrate 1), translation, cytoskeletal regulation, intracellular vesicular transport, cell cycle progression, and apoptosis (Doble and Woodgett, 2003).

Negative modulation of the PI3K-AKT axis

DAB2IP can regulate PI3K (phosphoinositide 3-kinase)/PKB (protein kinase B)-Akt, by directly acting on the two key factors of the pathway (Xie et al., 2009). This pathway is highly conserved, and its activation is tightly controlled via a multistep process. It transmits signals from ligand-stimulated receptor kinases (RTKs) to effector molecules that control metabolism, proliferation, cell size, survival, and motility (Guertin and Sabatini, 2007). In cancer, this pathway is frequently hyperactivated as a result of activation of RTKs by mutation (EGF) or gene amplification (HER2), activating mutations of components of the pathway, such as PI3K or Akt, and the deletion or decreased function of tumor suppressor PTEN (Fruman and Rommel, 2014). The PR and PER domains of DAB2IP are important for modulating PI3K-Akt activity (Table 1.1); DAB2IP binds p85 and affects PI3K-p85 relocation from the cytoplasm to the membrane, a necessary step for PI3K activation. Moreover, DAB2IP reinforces this inhibitory effect by directly binding AKT (Xie et al., 2009). Thus, DAB2IP has a key tumor-suppressive function as a negative regulator of the PI3K-AKT axis.

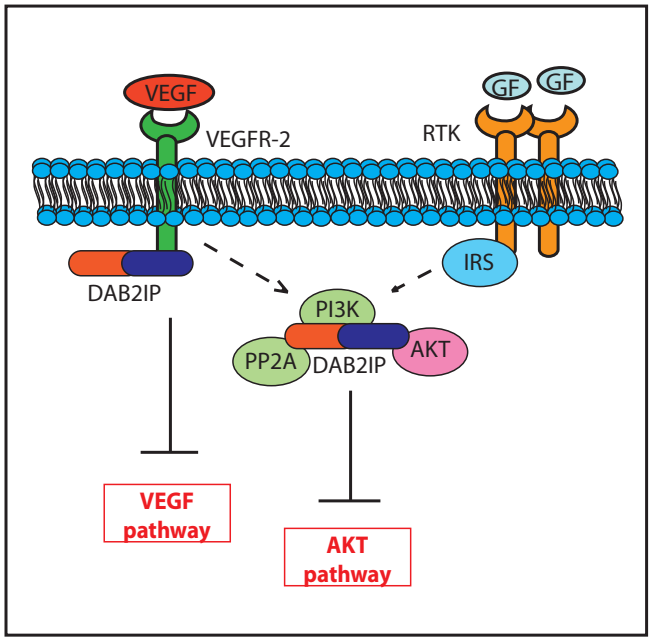

Negative modulation of VEGFR signaling

Vascular endothelial growth factor (VEGF) is a key regulator of angiogenesis during embryogenesis, skeletal growth and reproductive functions (Ferrara et al., 2003). The biological effects of VEGF are mediated by two receptor tyrosine kinases, VEGFR-1 and VEGFR-2, which differ considerably in signaling properties. VEGF primarily utilizes its VEGFR-2 to induce angiogenic response by activating a variety of signaling cascades, such as PI3K-Akt, PLC-γ-PKC, and MAPK (Ferrara et al., 2003). VEGF is also implicated in pathological angiogenesis associated with tumors and other disorders. Importantly, VEGF function in cancer is not limited to angiogenesis and vascular permeability; this signaling contributes to key aspects of tumorigenesis, such as the function of cancer stem cells, tumor initiation, and metastasis (Goel

and Mercurio, 2013). DAB2IP functions as endogenous inhibitor of adaptive angiogenesis, in part by binding to the VEGFR-2-PI3K (Zhang et al., 2008). DAB2IP binds VEGFR-2 with its C2 domain (Table 1.1), counteracting VEGF-induced activation of PI3K (Zhang et al., 2008). DAB2IP-KO mice show normal vascular development, but develop dramatically enhanced inflammatory angiogenesis. Consistent with this, VEGF-induced neovascularization is greatly increased in these mouse models (Zhang et al., 2008). In *in vitro* experiments, DAB2IP depletion augments VEGF-induced endothelial cells migration (Zhang et al., 2008). Notably, a global or vascular endothelial-specific depletion of DAB2IP augments tumor growth and metastasis in melanoma and breast cancer mouse models (Ji et al., 2015). A DAB2IP-deficient vascular environment not only enhances tumor neovascularization and increases secretion of EMT-promoting factors, but also increases pre-metastatic niche formation (Ji et al., 2015). These effects are associated with augmented VEGFR-2 activity and can be abrogated by systemic administration of VEGFR-2 kinase inhibitor (Ji et al., 2015).

Intriguingly, DAB2IP KO mice exhibit also reduced retinal angiogenesis, delayed developmental lymphangiogenesis in neonatal skin, and show weaker VEGF-C-induced corneal lymphangiogenesis, correlated with reduced expression of VEGFR-3 (Zhou et al., 2014b). Mechanistically, DAB2IP depletion increases the levels of miR-1236, a microRNA known to target VEGFR-3 mRNA (Zhou et al., 2014b). The authors reported also that DAB2IP binds directly VEGFR-3, modulating its surface expression and facilitating its recycling or/and delaying its trafficking to lysosomes. However, the mechanism that regulates this process is not completely understood (Zhou et al., 2014b). In summary, through a direct modulation of VEGF signaling, DAB2IP can regulate inflammatory-induced angiogenesis and the milieu of tumor microenvironment, dramatically affecting tumor growth and metastasis.

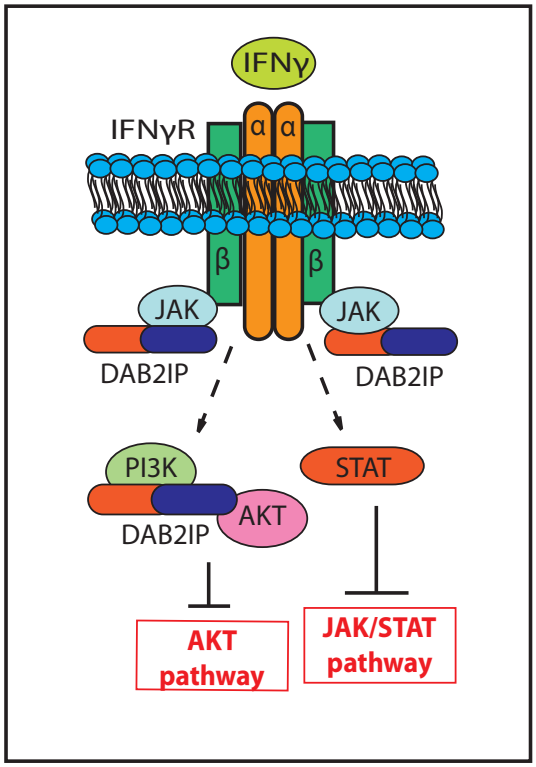

Inhibition of JAK2-STAT1/3 activation

DAB2IP directly binds to JAK2 through its N-terminal domain (Table 1.1), and inhibits JAK kinase activity, thus limiting JAK-dependent STAT1/3 and PI3K/Akt phosphorylation and

activation in vascular smooth muscle cells (VSMC). This DAB2IP functions strongly reduces proliferation and migration of VSMCs, two critical steps in neo-intima formation (Min and Pober, 2011; Yu et al., 2011). Notably, an association of DAB2IP with JAK2 is not detected in resting VSMC, but is strongly induced by IFN-γ, underlining again the important role of DAB2IP as a modulator of response to extracellular stimuli (Min and Pober, 2011). This suggests that DAB2IP may be important to inhibit intimal formation in graft arteriosclerosis, a pathological status characterized by diffuse, concentric arterial intimal hyperplasia composed of infiltrating host T cells, macrophages, and predominantly graft-derived smooth muscle-like cells that proliferate and elaborate extracellular matrix, resulting in luminal obstruction and allograft ischemia (Yu et al., 2011). In non-muscle invasive bladder cancer (NMIBC), the DAB2IP-dependent inhibition of the transactivation of STAT3 suppresses also the expression of Twist1 and its target gene P-glycoprotein, crucial factors for pirarubicin (THP) chemoresistance (Wu et al., 2015a). Accordingly, DAB2IP loss increases STAT3 transcriptional activity and the *in vivo* orthotopic tumor growth after intravescical THP treatment, supporting a role of DAB2IP in modulating chemosensitivity and recurrence of high-grade NMIBC (Wu et al., 2015a). It is tempting to speculate that DAB2IP might negatively regulate JAK-dependent activation of STAT3 in other cell types, including cancer, adding to its tumor-suppressive activities.

1.2.4 DAB2IP inactivation fosters tumor progression

Different studies describe the important role of DAB2IP in maintaining cell balance upon stress in different tissues, in the regulation of cell differentiation and tissue development. For example, three recent studies explore DAB2IP role in regulating neurogenesis, where DAB2IP drives neuronal differentiation of human mesenchymal stem cells (Chang et al., 2013) (Lee et al., 2012) (Qiao et al., 2013). Notably, DAB2IP KO mice are viable, show normal tissue development, but exhibit dramatically enhanced ischemia and inflammatory angiogenesis.

Importantly for this thesis, DAB2IP is a fundamental checkpoint to dampen multiple oncogenic pathways. Therefore, it is a bona-fide tumor suppressor and, in agreement with this role, its expression is frequently impaired in human tumors. However, loss of DA2IP expression does not induce cancer formation *per se*, since DAB2IP KO mice models do not display increased tumor incidence.

Therefore, DAB2IP inactivation is probably not a driver event in tumorigenesis. Rather, the loss-of-function of this modulator can strongly support cell transformation induced by several different possible driver mutations. Indeed, the role of DAB2IP in the multiple signaling

pathways summarized above has strong implications in various aspects of cancer formation and progression.

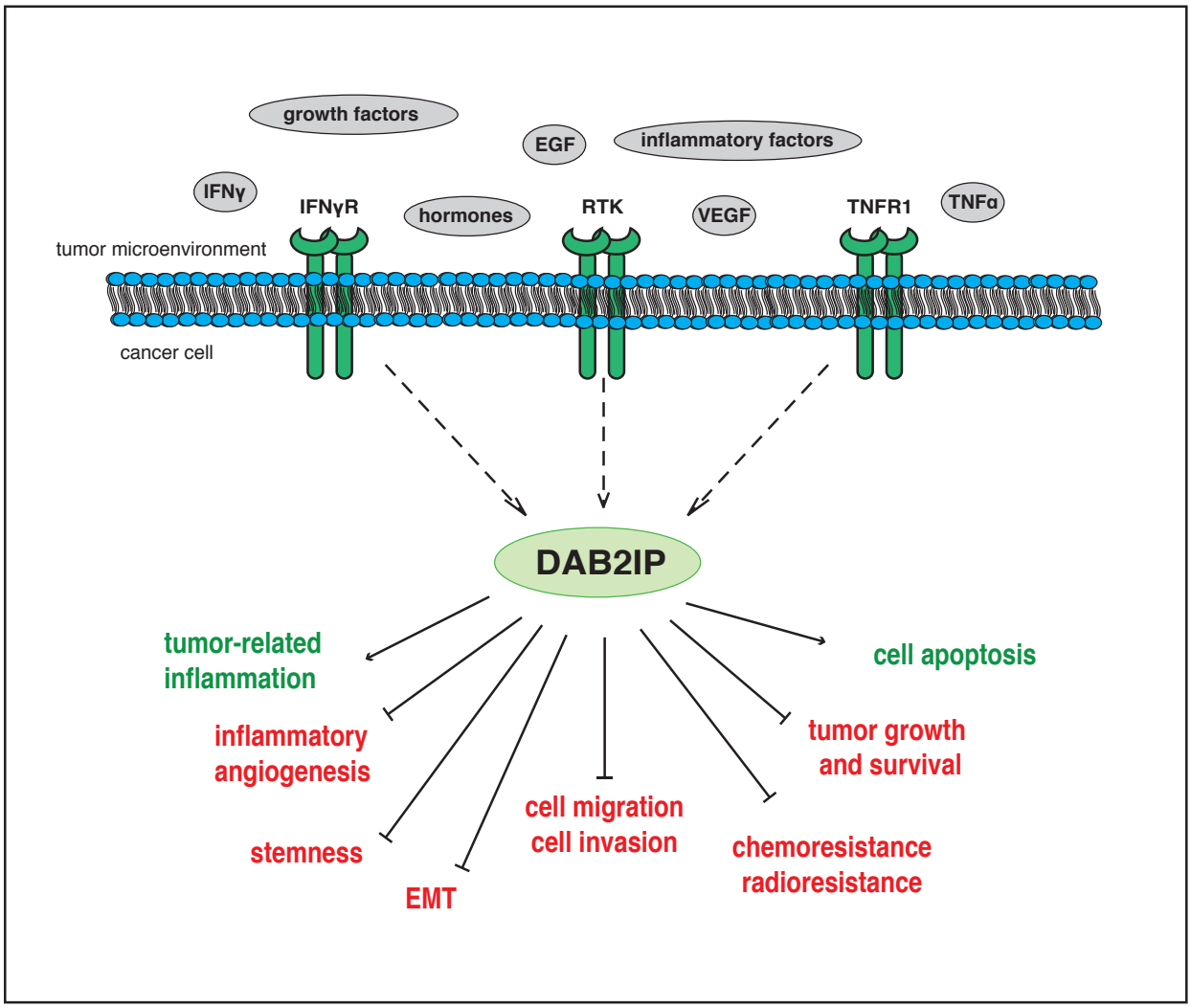

Figure 1.2: DAB2IP influences the cancer cell's response to a plethora of extracellular stimuli.
DAB2IP protein modulates different cytoplasmic signaling pathways, regulating cancer cell response to inflammatory cytokines, growth factors and hormones that are present in the tumor microenvironment and are secreted from stromal and immune cells, and the tumor cell itself. DAB2IP sustains cell apoptosis counteracting tumor growth and survival, stemness, induction of EMT and cell migration and invasion. Recent evidences demonstrate also that this tumor suppressor can impact tumor-related inflammation. See text for details.

DAB2IP and tumor survival and growth

The most fundamental trait of cancer cells involves their ability to sustain chronic proliferation. Normal tissues carefully control the production and release of growth-promoting signals, thereby ensuring a homeostasis of cell number, and thus maintenance of normal tissue architecture. Cancer cells acquire the capability to escape this control in a number of alternative ways.

Inactivation of Ras inhibitors, such as in the case of DAB2IP, has been reported to strongly sustain tumor growth (Calvisi et al., 2011; Duan et al., 2013; Wang et al., 2002). In the absence

of Ras mutation, down-regulation of DAB2IP levels is found in human liver or pancreatic cancer cells, and the expression of this protein is lower in patients with more advanced stage of disease (Duan et al., 2013).

Effects of DAB2IP perturbation in Ras-induced tumor growth have been recapitulated elegantly by Cichowski and colleagues (Min et al., 2010). They demonstrated that mice injected with prostatic cancer cells expressing H-Ras or depleted for DAB2IP develop highly proliferative tumors, which grow with similar kinetics and to a similar maximum size (Min et al., 2010). Notably, wild-type DAB2IP expression significantly blocked tumor development, whereas expression of the catalytically inactive RasGAP mutant (DAB2IP-R289L) was unable to suppress tumor growth (Min et al., 2010).

Similarly to Ras pathway activation, hyper-activation the PI3K/Akt signaling is frequently detected in tumors (Hanahan and Weinberg, 2011). Notably, DAB2IP-depleted prostate cells injected in mice, develop tumors with strong PI3K/Akt pathway activation (Xie et al., 2009); this signaling is also hyper-activated in hyperplastic prostate epithelium of DAB2IP KO mice (Xie et al., 2009). Increase in cell proliferation markers (i.e. cyclins and Ki67) in *in vitro and in vivo* models has been correlated to abrogation of DAB2IP inhibitory functions on this pathway (Xie et al., 2009).

Programmed cell death by apoptosis serves as a natural barrier to cancer development. However, apoptosis is attenuated in those tumors that progress to high-grade malignancy and develop resistance to therapy (Hanahan and Weinberg, 2011). Physiologically, DAB2IP promotes apoptosis in response to multiple stimuli, by directly sustaining ASK1/JNK activation. In various models of DAB2IP down-regulation, decrease in ASK1 dependent apoptosis has been appreciated (Luo et al., 2008; Xie et al., 2009; Zhang et al., 2007; Zhang et al., 2004).

In conclusion, DAB2IP represents a signaling platform that controls the balance between cell growth and apoptosis, which characterizes different types of normal or cancer cells. Based on these outcomes, DAB2IP function may dictate the effects of chemotherapy on cancer cell death. Therefore restoring DAB2IP expression in target tissue by either a genetic or inductive approach is expected to increase the therapeutic index of these agents, concomitantly affecting the activation of anti-proliferative and pro-apoptotic pathways.

DAB2IP and cell migration and metastasis

Metastasis is a multistep process whereby tumor cells disseminate from the primary tumor and colonize distant organs. Metastatic disease is the major cause of death from cancer (Bravo-Cordero et al., 2012; Kitamura et al., 2015). Tumor epithelial cells are converted in migratory

and invasive cells by epithelial to mesenchymal transition (EMT), a process controlled by a variety of regulatory circuits (De Craene and Berx, 2013). DAB2IP has a heavy impact on EMT; DAB2IP levels have been inversely correlated with expression of EMT markers in melanoma, bladder, prostate, colorectal and breast cancer. In particular, reduced DAB2IP levels correlate with increased vimentin (mesenchymal marker) and reduced E-cadherin (epithelial marker) expression (Ji et al., 2015; Marian et al., 2011; Min et al., 2015; Min et al., 2010; Shen et al., 2014; Wang et al., 2015; Xie et al., 2010). DAB2IP loss or inactivation initiates EMT in both human normal prostate epithelial and prostate carcinoma cell lines, inducing changes in cell morphology and biomarker expression, including decreased E-cadherin expression and augment vimentin, twist and fibronectin levels (Marian et al., 2011; Min et al., 2010; Xie et al., 2010). DAB2IP loss affects the migratory and invasive capability of tumor cells: orthotopic prostate and colorectal cancer xenografts showed that mice injected with DAB2IP-depleted cells have a dramatic increase in the incidence of lymph-node metastases (Min et al., 2015; Min et al., 2010; Xie et al., 2010).

Notably, increased DAB2IP levels revert EMT: overexpression of DAB2IP can restore E-cadherin levels in metastatic prostate and colorectal cancer cells (Min et al., 2010; Xie et al., 2010).

Finally, in bladder cancer, DAB2IP down-regulation promotes cell proliferation, migration and invasion together with the activation of ERK and Akt pathways (Shen et al., 2014).

DAB2IP can control EMT and cell migration and invasion by finely coordinating the WNT/βcatenin and NF-κB pathways. Cichowski and colleagues demonstrated that a point mutation in the period-like domain of DAB2IP, that prevents TRAF2 binding, renders the protein defective in suppressing xenograft dissemination in vivo, despite retaining its RasGAP activity - thus showing that NF-κB activation has an important role in mediating metastasis (Min et al., 2010). Similar results were recently obtained by Xie and colleagues in colorectal cancer (Min et al., 2015). In addition to its inhibitory activity on NF-κB, DAB2IP modulates GSK3β/βcatenin signaling in EMT; indeed, GSK3β phosphorylation is higher in $DAB2IP^{-/-}$ than in $DAB2IP^{+/+}$ mice, and βcatenin overexpression can reverse DAB2IP-mediated MET (mesenchymal-to-epithelial transition) (Xie et al., 2010).

To conclude, a large part of DAB2IP literature describes its role in modulating EMT and metastasis. Therefore, although depletion of this protein does not induce cancer by itself, DAB2IP loss can greatly increase cancer cell migration and invasion, especially in response to

extracellular inputs. Indeed, DAB2IP knockout mice have aberrantly dilated colonic crypts with altered monolayer epithelial arrangement (Min et al., 2015), and exhibit mesenchymal characteristic in the prostate gland and prostatic hyperplasia (Xie et al., 2010).

DAB2IP in stemness

Cancer stem cells (CSCs) are tumor cells that have the principal properties of self-renewal, tumor initiation capacity, and clonal long-term repopulation potential. They have been proposed as the driving force of tumorigenesis and the seed of metastases (Medema, 2013). A strong connection between EMT and CSCs properties exists, as they are sustained in human cancer by the same gene expression programs (Brabletz et al., 2005).

Two recent works describe a role of DAB2IP in modulating CSCs properties. One study reported that DAB2IP suppresses transcription of stem cell factor receptor CD117, by interacting with GATA-1 on a silencer element on its gene (Yun et al., 2015). Notably, this is the first – and only - evidence of a possible nuclear localization for DAB2IP, and of its potential direct role in modulating gene transcription. The authors also demonstrate that DAB2IP, through the inhibition of PI3K/Akt/mTOR signaling, activates c-myc-dependent ZEB1 expression, leading to elevated CSC phenotype (Yun et al., 2015). Indeed, DAB2IP KO prostate cancer cells increase sphere-formation activity *in vitro*, and augment tumorigenic potential in mice (Yun et al., 2015).

Another study reported that in human colorectal cancer (CRC), DAB2IP inhibition of NF-κB pathway can suppress EMT induction and CSC features (Min et al., 2015). The absence of DAB2IP in CRC cells increases sphere formation in soft agar, and expression of EMT and stem cell markers; reduced DAB2IP levels in CRC patients correlates with increased number of $CD133^+$ cells and faster tumor progression (Min et al., 2015).

DAB2IP and cancer-related inflammation

Inflammation plays a decisive role in cancer development and progression, including metastasis formation and response to therapy. Chronic inflammation associated with infection or immune diseases increases cancer risk, and can contribute to it by inducing oncogene mutations, genomic instability, enhanced angiogenesis, and metastasis (Colotta et al., 2009; Grivennikov et al., 2010). Later on, in the formed tumor microenvironment, cancer cells engage a continuous crosstalk with infiltrating immune and stromal cells; and a variety of cytokines, chemokines, prostaglandins, growth factors, and reactive oxygen-species are mediators of this dynamic crosstalk (Grivennikov et al., 2010).

Given its inhibitory role on NF-κB and STAT3 inflammatory pathways, DAB2IP functions as an anti-inflammatory protein, especially in vascular endothelial cells. Indeed, DAB2IP knockout mice show dramatically enhanced inflammation in models of ischemic hindlimb, graft arteriosclerosis and inflammatory angiogenesis (Huang et al., 2013; Min and Pober, 2011; Yu et al., 2011; Zhang et al., 2008). Mechanistically, DAB2IP represents a fundamental modulator of signal transduction in response to inflammatory mediators, including TNFα, IFN-γ, TLR4 and IL-1β (Di Minin et al., 2014; Wan et al., 2010; Yu et al., 2011; Zhang et al., 2003).

More importantly, various studies show that DAB2IP modulates secretion of inflammatory mediators in endothelial and cancer cells, and the recruitment of immune cells. In hyperlipidemic ApoE-/- mice, DAB2IP knockdown increases secretion of inflammatory cytokines (IL-12, IL-6, RANTES, TNF, MCP-1 and CX3CL1) and augments macrophage infiltration, thereby promoting increased endothelial dysfunction and early phases of atherosclerosis (Huang et al., 2013).

Evidences indicate DAB2IP as an important anti-inflammatory molecule, which can strongly affect the behavior of immune cells and the response to inflammatory mediators. Nevertheless, we still have little information about its potential role in modulating the inflammatory component of the tumor microenvironment, and this aspect deserves a deeper investigation.

DAB2IP in chemo- and radio- resistance

Resistance to chemotherapeutic drugs and radiotherapy is a significant barrier to cure cancer. Multiple molecular mechanisms are involved in chemo- and radio-resistance, including alteration in drugs metabolisms, the activation of survival signaling pathways, and evasion from death signals. Moreover, the tumor microenvironment can also dramatically influence the cancer cell response to drugs. DAB2IP has been linked to sensitivity to radiation in prostate tumors: loss of DAB2IP sustains more efficient DNA repair, resistance to apoptosis, and robust control of cell cycle checkpoint in prostate cancer cells exposed to ionizing radiation (IR) (Kong et al., 2010).

Similarly, DAB2IP loss in prostate cancer cells was shown to enhance chemoresistance by up-regulation of the anti-apoptotic protein clusterin (Wu et al., 2013). Accordingly, DAB2IP overexpression sensitizes prostate cancer cells to various chemotherapeutic agents (Wu et al., 2013). Finally, loss of DAB2IP augments STAT3 activation, increasing chemoresistance to pirarubicin in bladder cancer (Wu et al., 2015a; Zhou et al., 2015).

Notably, such evidences suggest that DAB2IP reactivation may be a potential approach for developing combined and more efficacious therapy.

1.2.5 Escaping DAB2IP mediated control in cancer

Despite its multiple tumor-suppressive functions, DAB2IP is only rarely mutated in human cancers. In contrast, a consistent body of literature reports the epigenetic inactivation of DAB2IP by promoter methylation in various tumors and tumor-derived cell lines (see below). More recently, alternative mechanisms for DAB2IP inactivation in cancer have been described, or suggested, uncovering an interesting scenario where tumor cells arising with very different genetic backgrounds may employ different means to disable such a unique "modulator" of multiple signaling pathways.

DAB2IP promoter methylation mediated by EZH2

The best characterized mechanism to inactivate DAB2IP is by epigenetic silencing. As already mentioned, the gene is complex and contains multiple CpG islands. A number of studies have described aberrant methylation of the gene in lung, breast, prostate, and gastrointestinal cancer (Chen et al., 2003; Dote et al., 2005; Dote et al., 2004; Yano et al., 2005). Main factor controlling DAB2IP methylation is the complex PRC2 (polycomb-repressive complex-2)/EZH2 (Enhancer of Zeste homolog)(Chen et al., 2003). The high level of di- and tri- methyl H3-Lys27 in DAB2IP promoter is modulated by EZH2: EZH2 recognizes and binds specific GpG island in DAB2IP promoter, leading the recruitment of the PRC2 protein complex and the histone deacetylase HDAC1/2 (Chen et al., 2005) (Wang et al., 2015) (Smits et al., 2012). Recently, it has been demonstrated that Snail transcription factor is required for the repressive function of EZH2 on DAB2IP in colon cancer. A positive feedback loop established between Snail and DAB2IP promotes metastasis in colon-rectal cancer (Wang et al., 2015).

DAB2IP post-transcriptional regulation mediated by microRNAs

Another mechanism that might contribute to reduce DAB2IP levels in cancer cells is post-transcriptional silencing by microRNAs (miRNAs). DAB2IP has a relatively long 3' UTR sequence, and is therefore a good candidate for miRNAs activity. Up to now, three studies have reported miRNAs able to target DAB2IP.

miR-338 was reported to reduce DAB2IP levels in neurons (Barik, 2008). miR-338 is located within the eighth intron of the Apoptosis-Associated Tyrosine Kinase (AATK) gene. AATK protein plays an essential role in promoting neuronal differentiation. miR-338 cooperates with AATK through suppression of the translation of a selected group of mRNAs whose protein products are negative regulators of neurite growth and neural differentiation - including DAB2IP. However, the study does not address the specific role of DAB2IP in this scenario, and

does not discuss the potential role of miR-338-dependent DAB2IP down-regulation in tumors (Barik, 2008).

miR-889 targets and down-regulates DAB2IP protein levels in esophageal squamous cell carcinoma (ESCC), sustaining cell proliferation in *in vitro* and *in vivo* experiments (Xu et al., 2015b). Notably, DAB2IP overexpression can subvert this phenotype. However, authors do not analyze the effects of the miR-889-mediated down-regulation of DAB2IP on other DAB2IP dependent phenotypes, including migration or invasion of ESCC cells. The levels of miRNA-889 and DAB2IP inversely correlated in ESCC tissue samples, where low DAB2IP correlates with poor differentiation and high tumor size (Xu et al., 2015b).

Finally, **miR-32** was shown to target DAB2IP in prostate cancer (Liao et al., 2015). The authors demonstrated that miR-32, a known onco-miRNA, is well paired with the 3'UTR of DAB2IP. They showed that prostate cancer cells depleted for DAB2IP by miR-32 action are more resistant to ionizing radiation treatment, with augmented cell proliferation and reduced cell apoptosis (Liao et al., 2015).

These three studies demonstrate that DAB2IP is a target for miRNAs-mediated regulation, and give a preliminary hint of the broad potential impact that this regulatory circuit may have in cancer, where miRNA expression is often deregulated (see below).

DAB2IP protein degradation mediated by FBW7 and Skp2

Recently, two studies have analyzed post-translational turnover of the DAB2IP protein, identifying two SCF E3 ubiquitin ligases that promote its degradation.

A recent study demonstrated that FBW7-containing SCF complexes can bind and degrade DAB2IP (Dai et al., 2014). A putative phospho-degron motif, commonly recognized by Fbw7 for substrate recruitment to the SCF protein complex, has been identified in DAB2IP. In line with this model, a putative CK1 phosphorylation site controls the efficiency of DAB2IP turnover (Dai et al., 2014).

A second study showed that DAB2IP can be poly-ubiquitinated by Skp2-containing SCF complexes. Specifically, the GAP domain of DAB2IP contains three putative sites for Skp2-elicited ubiquitination (Tsai et al., 2014). Notably, in prostate cancer cells, DAB2IP promotes Skp2 degradation, possibly by the inhibition of AKT. This reciprocal interaction may be involved in the regulation of cell growth and proliferation; however, an inverse correlation between the two proteins has not been clearly demonstrated (Tsai et al., 2014).

No studies have carefully analyzed DAB2IP protein stability and turnover under multiple different conditions, and it is plausible that other ubiquitin-ligases might be involved in its regulation.

Other post-translational modifications: role of Akt

A recent report suggests that DAB2IP can be phosphorylated by AKT1 (but not AKT2) on Ser-847, within the proline-rich domain. In transient overexpression experiments, mutation of serine 847 to Aspartic (to mimic constitutive phosphorylation) moderately reduced DAB2IP interaction with Ras and TRAF2; accordingly, mutation to Alanine increased DAB2IP interaction with both proteins. These results suggest that phosphorylation by endogenous kinases might interfere with DAB2IP activity (Dai et al., 2014). In support of a model whereby phosphorylation at Ser-847 inhibits DAB2IP functions, authors observed that overexpression of the phospho-mimetic DAB2IP (S847D) mutant had no effect on Ras-dependent p-ERK levels (Dai et al., 2014). Intriguingly, these data suggest an existing feedback regulatory loop between AKT and DAB2IP. Additional studies are required to confirm these observations, and to determine if Ser-847 phosphorylation might affect other important DAB2IP functions - first of all modulation of ASK1 and NF-κB signaling.

AIM OF THE THESIS

An intricate network of signals is continuously established among tumor cells and their microenvironment, and the traffic of information among distinct cells within a tumor strongly contributes to cancer development and progression. The tumor suppressor DAB2IP plays a fundamental role in this context, since it modulates signal transduction by multiple extrinsic inputs, including inflammatory cytokines, growth factors and hormones in the tumor microenvironment, affecting the behavior of tumor cells. As detailed above, multiple studies have begun to uncover molecular mechanisms through which DAB2IP tumor-suppressive functions can be inhibited in cancer. The simple block of DAB2IP activity can indeed permit tumor cell to simultaneously activate multiple oncogenic signals in response to extracellular stimuli, thereby augment tumor transformation and fostering the acquisition of oncogenic features.

Therefore, increasing our knowledge on mechanisms of DAB2IP regulation could strongly improve our possibilities to interfere with these cellular processes, eventually developing approaches to counteract them, with possible implication for cancer therapy. We think that increasing DAB2IP protein levels in tumor cells, or restoring its compromised oncosuppressive functions, would coordinately dampen multiple pro-survival pathways and, at the same time, activate cell death signaling, effectively reducing tumor growth, metastasis, and resistance to therapy. In this Thesis I explored two mechanisms through which tumor cells can counteract DAB2IP activity.

The first one is based on protein-protein interaction (Part 2 of this Thesis). In the host laboratory DAB2IP was recently cloned as a novel interactor of p53-family proteins (Lunardi et al., 2010). Later, we observed that DAB2IP is efficiently bound by mutant p53 proteins (mutp53). Expression of mutant p53 is a significant factor in cancer development and progression (Kim et al., 2015). Missense mutations of p53 not only induce loss of its tumor suppressive functions, but also confer to the protein new oncogenic properties (as detailed in Chapter 2.1). Notably, mutant p53 fosters tumor progression and invasion by reinforcing and up-regulating multiple oncogenic pathways including RAS, PI3K-Akt, βcatenin, and NF-κB (Dong et al., 2009; Muller et al., 2009; Sauer et al., 2010; Weisz et al., 2007). As mentioned above, all these pathways are coordinately antagonized by DAB2IP.

We therefore decided to study the role of mutant p53/DAB2IP interaction in cell transformation. Specifically, we hypothesized that some gain-of-function properties of mutant p53 might depend on sequestration and functional inactivation of DAB2IP, particularly in the context of TNF-

induced cell migration and invasion. We demonstrated that, blocking DAB2IP inhibitory activity on NF-κB pathway, mutant p53 reprograms TNFα dependent transcriptional response, promoting the invasive ability of tumor cells in response to inflammation, and counteracting the apoptotic response induced by TNF. Intriguingly, the displacement of mutp53/DAB2IP interaction subverts aggressive tumor phenotypes in *in vitro* and *in vivo* experiments.

The second mechanism is based on post-transcriptional inhibition by microRNAs (Part 3 of this Thesis).

MicroRNAs are small non-coding RNAs involved in the control of translation of a multitude of cellular proteins, and are implicated in the regulation of multiple biological processes, including cell proliferation, survival, migration and invasion (detailed in Chapter 3.1). Intriguingly, DAB2IP has a long 3'UTR that is heavily conserved among vertebrates, and is therefore a likely miRNAs target. Up to now, three miRNAs regulating DAB2IP (miR-32, miR-889 and miR-338) have been reported (Barik, 2008; Liao et al., 2015; Xu et al., 2015b). We decided to identify and characterize additional miRNAs targeting DAB2IP, and to explore their oncogenic role in cancer. Given the moderate reliability of software prediction tools, we decided to perform a high-throughput functional screening.

Considering the fundamental role of DAB2IP as modulator of multiple extrinsic inputs, aim of this study was also to characterize the implications of miRNA-mediated down-regulation of DAB2IP on the cancer cell's response to extracellular stimuli, especially inflammatory mediators such as TNFα.

Finally, a long-term aim of this work is the possible development of miRNA inhibitors as therapeutics to increase DAB2IP levels and/or restore DAB2IP tumor suppressive functions in cancer, with potential clinical impact.

PART 2: CYTOPLASMIC GAIN OF FUNCTION MUTANT p53 CONTRIBUTES TO INFLAMMATION-ASSOCIATED CANCER

In this part I describe studies on the functional aspects of mutant p53/DAB2IP binding in cancer progression, especially in the context of tumor inflammation. The interaction with mutant p53 represents an innovative mechanism of DAB2IP inhibition in tumor cells and exerts a strong impact in modulation of cancer cell response to inflammatory stimuli from the tumor microenvironment.

2.1 MUTANT p53 AS A DRIVER FORCE IN TRANSFORMATION

Wild type p53 (wt) is a transcription factor (Laptenko and Prives, 2006) with strong tumor suppressive activities that identify it as the "guardian of the genome" and label it as one of the most important players in cancer biology (Freed-Pastor and Prives, 2012). In normal cells, p53 activity is low, but in response to numerous stress signals, including DNA damage, oncogenes activation and hypoxia, p53 levels rise dramatically and result in the transcription of hundreds of genes with important roles in cell cycle arrest, senescence, apoptosis, DNA repair, metabolism, autophagy and differentiation (Meek, 2009). Notably, the TP53 gene is the most frequent target for mutation in human cancer: 96% in ovarian serous carcinoma, 54% in invasive breast carcinoma, and 75% in pancreas cancer (Kim et al., 2015). There are now strong evidences that mutation not only abrogates p53 tumor-suppressive functions, but also endows mutant proteins with novel oncogenic activities.

2.1.1 Pro-oncogenic roles of mutant p53

Alterations of p53 have been found in every region of the protein, but only a handful of the most frequently occurring mutations have been studied in depth for their contribution to cancer progression. Frameshift or nonsense mutations result in the loss of p53 protein expression, as seen with other tumor suppressor, including PTEN and Rb (Kim et al., 2015). However, approximately 75% of all tumor-associated p53 alterations result in missense mutation, leading to the substitution of a single amino acid in the p53 protein that can be stably expressed in the tumor cell (Kim et al., 2015; Muller and Vousden, 2014). These substitutions occur throughout the p53 protein, but most commonly cluster within the DNA binding region (in about 90% of cases) (Kim et al., 2015). Six "hotspot" residues are the most frequently substituted. These missense mutations lead to the production of full-length mutant p53 proteins with a prolonged half-life (Freed-Pastor and Prives, 2012) (Figure 2.1).

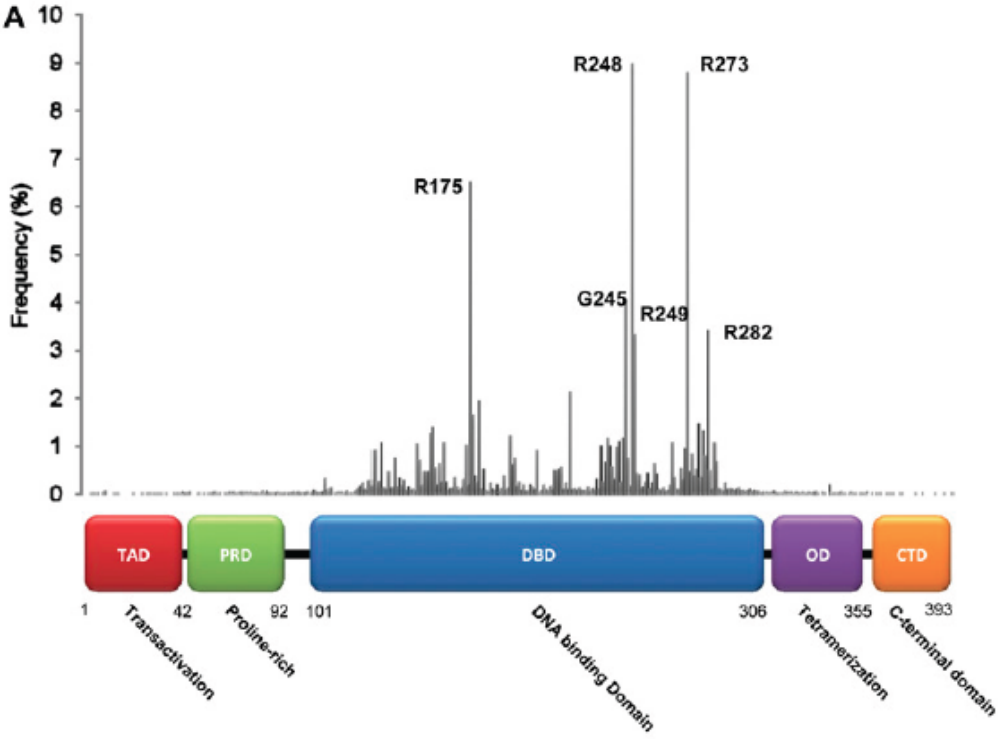

Figure 2.1: TP53 mutational spectrum in human cancer. Schematic representation of the p53 protein with domains structure illustrated: TAD: transactivation domain; PRD: proline-rich-domain; DBD: DNA-binding domain; OD: oligomerization domain (also contains a nuclear export signal); CTD: C-terminal regulatory domain (also contains three nuclear localization signals). The six hotspot mutations are highlighted: R175 and R273 are DNA-contact mutations, G256 and R249 are locally distorted mutants, R175 and R282 are globally denatured mutants. Figure reproduced from (Freed-Pastor and Prives, 2012).

The nature of these mutations provides several clues as to how p53 role is affected. DNA-binding domain activity is the critical function that is altered, suggesting that changes in transcriptional targets could be key to the activity of mutant p53. However, the mutations in the structured core of p53 can also have significant consequences to the folding of p53 and to the capability to establish new interactions. Therefore, the hotspot changes in p53 are traditionally classified as "conformational mutants" (or structural mutants) that can cause unfolding of the p53 protein, and "DNA contact mutants" that change amino acid critical for DNA binding (Muller and Vousden, 2013). They generally lead to a loss or diminution of the wild-type activity of p53, and because p53 normally acts as a tetramer, these mutant proteins may also function as dominant negative inhibitor over any remaining allele (Muller and Vousden, 2014). More important, the changes in p53 structural stability may be crucial to the acquisition of new oncogenic properties, known as Gain of Function or GOF (Muller and Vousden, 2013).

Gain of Function (GOF)

Single amino acid changes in the p53 gene may result in profound alteration to protein functions,

affecting diverse aspects of tumorigenesis. These include DNA synthesis, cell survival and proliferation, abnormal centrosomes and spindle checkpoints, somatic cell reprograming and stem cell characteristics, disruption of tissue architecture, invasion and metastasis, as well as increased angiogenesis, tumor-promoting inflammation and Warburg effect (Freed-Pastor and Prives, 2012; Muller and Vousden, 2014; Sabapathy, 2015).

GOF properties were better studied with the generation of the p53 mutant knock-in mice. The initial data demonstrated that the p53 R172H mice (equivalent to human R175H) were more tumor prone with more carcinomas. Further studies have cemented this finding: the presence of the R172H mutant p53 protein confers significant growth and metastatic propensity, compared to the loss of p53, in a variety of tumor types such as lung and pancreatic ductal adenocarcinomas (Caulin et al., 2007; Morton et al., 2010). Moreover, in knock-in mice, mutant p53-mediated prolonged activation of NF-κB pathway increases cytokines expression, inducing inflammation and tissue damage that strictly correlates with tumor growth (Cooks et al., 2013). Angiogenesis was also shown to be enhanced, through the activation of the DNA-binding protein inhibitor ID4 expression in cell culture studies (Fontemaggi et al., 2009).

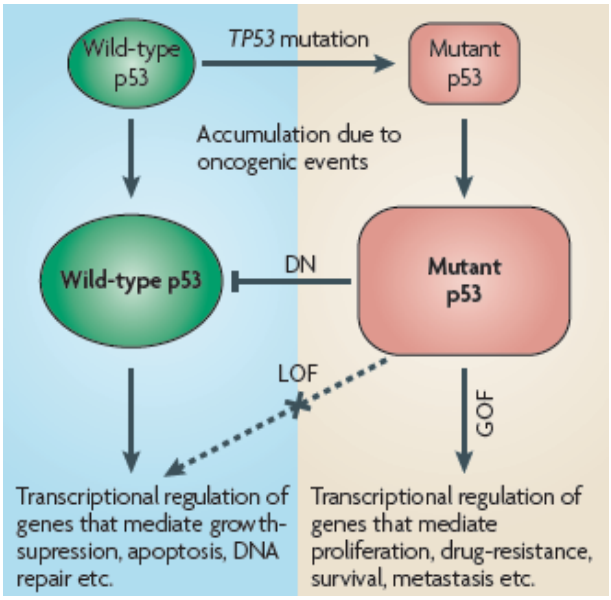

Figure 2.2: The phenotypic effects of TP53 mutations can be classified into three non-mutually exclusive groups. First Loss of Function (LOF), that abrogates or attenuates the binding of p53 to its consensus DNA sequence, and impedes the transcriptional activation of p53 target genes; second, the ability of mutant o53 to inhibit the function of the wtp53 proteins, forming a heterotetramer (Dominant Negative-DN). Finally, mutants p53 can aquire new oncogenic properties known as Gain of Function (GOF). Taken from (Brosh and Rotter, 2009).

Intriguingly, tumor cells carrying mutations of TP53 become addicted to the mutant p53 GOF. Indeed *in vitro* and mice studies demonstrated that tumor cells with accelerated growth and acquired migratory/invasive ability are strongly compromised upon mutant p53 abrogation (Adorno et al., 2009; Bossi et al., 2006; Bossi et al., 2008; Freed-Pastor et al., 2012; Girardini et al., 2011) (Alexandrova et al., 2015). The exact point at which cancer cells get addicted to mutant p53 is not understood. It is expected this happens at the point in time of loss of the remaining wild type p53 allele; however, it is likely that further events are required for this phenomenon (Sabapathy, 2015).

2.1.2 Mechanism and mediators of mutant p53 gain of function

There are multiple proposed mechanisms that account for mutant p53 gain of function. These include both transcriptional and non-transcriptional mechanisms. In the first case, they reflect alterations in the DNA-binding ability of mutant p53 (Figure 2.3, model 1). In the second case, gain of function involves changes in the interaction of mutant p53 with other proteins, including transcription factors (Figure 2.3, model 2 and 3) or proteins not directly related to the regulation of gene expression (Figure 2.3, model 4) (Freed-Pastor and Prives, 2012; Muller and Vousden, 2013).

Mutant p53 binds DNA to alter gene expression

Since tumor-derived mutants p53 retain the N-terminal transcriptional transactivation domains, much of the gain of function activity of these proteins has been related to a direct or indirect ability to regulate gene expression (Freed-Pastor and Prives, 2012). The amino acid substitutions within the DNA-binding domain of the majority of the p53 mutants may change, rather than abolish, sequence-specific DNA binding; this aspect mainly characterizes the concept of loss of function (Muller and Vousden, 2013). However, it is certainly true that mutant p53 has DNA-binding activity (Thukral et al., 1995), raising the possibility that some mutant p53 proteins may recognize a unique mutant p53 response element (Figure 2.3, model 1). Nevertheless, a consensus for mutant p53-specific binding has so far not been identified (Muller and Vousden, 2013).

Mutant p53 and transcription factor regulation

The best-characterized transcriptional function of mutant p53 is its ability to interact with other transcription factors and modulate the expression of their targets genes (Figure 2.3, model 2 and 3) (Freed-Pastor and Prives, 2012). In some cases, mutant p53 increases their transcriptional activity. p53 mutants have been demonstrated to transactivate MYC, CXCL1, PCNA, CDK1, IGF1R and EGFR, all of which can promote proliferation of cancer cells (Deb et al., 1992; Di Agostino et al., 2008; Frazier et al., 1998; Ludes-Meyers et al., 1996; Werner et al., 1996; Yan and Chen, 2009).

Additionally, mutant p53 can up-regulate genes that inhibit apoptosis or promote chemoresistance. For example, p53 mutants can transactivate BCL2L1 (also known as Bcl-xL) to sustain an anti-apoptotic response, and thus favor tumor growth (Bossi et al., 2008).

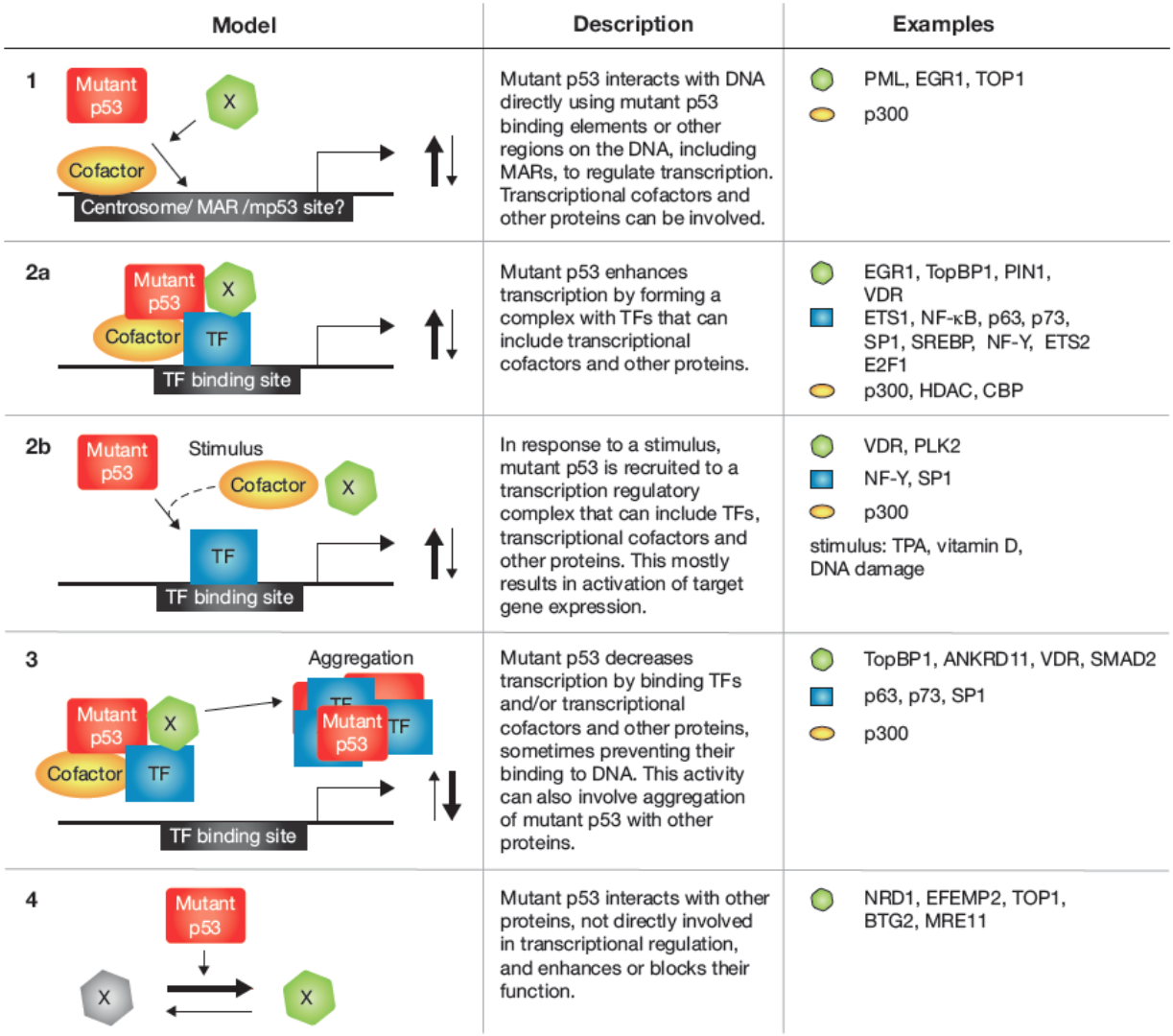

Figure 2.3: Model of mechanisms through which mutant p53 functions. As part of its gain of function mutant p53 interacts with different proteins, to enhance or inhibit their activities. Illustration taken from (Muller and Vousden, 2013). See text for the details.

In other cases, mutant p53 increases the activity of other transcription factors, with further complexity added by the role of cellular stimuli, transcriptional cofactors, and other proteins. For example, the interaction of mutant p53 with the nuclear factor Y (NF-Y) deregulates the cell cycle checkpoint following the induction of low levels of DNA damage. Under these conditions, DNA topoisomerase 2-binding protein 1 (TopBP1) recruits mutant p53 and the transcriptional cofactor p300, to mediate their binding with NF-Y, and induce the transcription of genes involved in the regulation of cell proliferation and chemoresistance (Di Agostino et al., 2006; Liu et al., 2011). Mutant p53 binding with p300 and NF-Y is also stimulates by mutant p53 phosphorylation mediated by PLK2 kinase (Valenti et al., 2011). Additionally, tumor-derived mutant p53 can enhance the transcriptional activity of NF-κB in response to TNF, partially

through a physical interaction with p65 (Cooks et al., 2013; Dell'Orso et al., 2011; Weisz et al., 2007). Mutant p53 has also been shown to transcriptionally regulate the expression of mevalonate pathway genes, through an interaction with SREBP family of transcription factors, allowing cells to make de novo cholesterol and other key metabolism (Freed-Pastor et al., 2012).

Mutant p53 activity on p63 and p73

Notably, the interaction of mutant p53 with transcription factors can also be inhibitory (Figure 2.3, model 3). Probably, the best understood example of this phenomenon is the inhibitory role that mutant p53 exerts on the transcriptional activity of the other members of the p53 family, p63 and p73. (Muller and Vousden, 2013).

Recent work has found that mutant p53 frequently binds DNA through p63 interaction, even though at sites distinct from those that p63 would normally bind, thus preventing normal p63 functions (Martynova et al., 2012). For example, p63 normally inhibits the activation of RCP (Rab coupling protein), through transcriptional targets that are still unknown, to prevent α5β1 integrin and EGFR recycling to the plasma membrane. Upon expression of mutant p53, p63 transcriptional activity is suppressed, resulting in enhanced RCP-driven recycling of α5β1 integrin and EGFR. This activates Rho and PKB/Akt to promote cell migration and invasion (Muller et al., 2009). The ability of mutant p53 to bind and inhibit p63 it itself regulated at various levels, with the involvement of additional partners, intrinsic and extrinsic signals. For example, in response to TGF-β treatment, the protein SMAD2 promotes the interaction between mutant p53 and p63, leading to the inhibition of p63-driven gene expression: two important suppressor of metastasis, Sharp1 and cyclin G2 are so less expressed, leading to an increased invasive capability of tumor cells (Adorno et al., 2009).

On the other hand, mutant p53 binding of p73 protects cells from chemotherapeutic agents, inducing less favorable response to chemo/radio- therapy in patients with head and neck cancer (Li and Prives, 2007). A recent work elegantly has showed how mutant p53, through the disruption of the p73/NF-Y complex can transcriptionally up-regulate the platelet-derived growth factor receptor b (PDGFR b), thus maintain a pro-metastatic phenotype of a murine models of pancreatic cancer (Weissmueller et al., 2014).

The evidence that both $p53^{+/-}/p63^{+/-}$ and $p53^{+/-}/p73^{+/-}$ double-mutant mice display an altered tumors spectrum and a more metastatic phenotype, if compared with mutant p53 knock-in models is in line with all these study (Flores et al., 2005).

Mutant p53 interaction patterns

Some of the known gain of function activities of mutant p53 are mediated by its ability to form aberrant protein complexes with several interacting partners not involved in gene transcription. The interaction with mutant p53 can enhance or inhibit their functions (Figure 2.3, model 4)(Muller and Vousden, 2013). For example, by interacting with MRE11, a DNA nuclease required for DNA repair, mutant p53 impairs homologous recombination and causes accumulation of unrepaired DNA breaks, thus promoting genetic instability in tumors and pre-tumorigenic lesions in mouse models (Song et al., 2007). Another example is represented by the cytoplasmic interaction between mutant p53 and AMPK (adenosine monophosphate -AMP-activated protein kinase), an important energy sensor in cells that regulates the balance between anabolism and catabolism. Under stress conditions, mutant p53, but not wild-type p53, preferentially binds to the AMPKα subunit and inhibits AMPK activation, leading to impaired metabolic checkpoint and increased anabolic tumor growth and progression (Zhou et al., 2014a). Other examples of this mechanism of GOF will be described below.

2.1.3 Mutant p53 oncogenic properties

Regulation of cell fate

The best-defined feature of mutant p53 is its ability to reprogram cell fate. Indeed, the first studies describing mutant p53 GOF, analyzed its role in preventing p53-independent apoptosis, especially in response to DNA damaging drugs, including doxorubicin or cisplatin (Li et al., 1998). Later, it was demonstrated that mutant p53 protects cells from other apoptosis inducers, such as TNFα and vitamin D (Stambolsky et al., 2010; Weisz et al., 2007). Mutant p53 has been also shown to accelerate cell proliferation by cooperating with Ras, E2F, PCNA and c-myc (Deb et al., 1992; Frazier et al., 1998; Sauer et al., 2010; Scian et al., 2005). Finally, numerous recent works demonstrated that depletion of mutant p53 strongly reduces proliferation and survival of tumor cells in various cellular contexts and under different cell treatments and stimulations, suggesting that cancer cells become somehow “addicted” to mutp53 oncogenic properties (Ali et al., 2013; Braicu et al., 2013; Zhu et al., 2011; Zhu et al., 2013b).

Genomic instability

In mutant p53 knock-in mice, several hot spot mutations were reported to disrupt the DNA damage response, through different mechanisms, including an inhibitory activity against ATM, leading to genomic instability (Liu et al., 2010; Song et al., 2007). In addition, mutant p53 can attenuate base excision repair (Offer et al., 1999) and, by binding topoisomerase I, induce

aberrant homologous DNA recombination events, and mutagenic DNA rearrangements (Albor et al., 1998; Restle et al., 2008).

Supporting these evidences, mutant p53 was found to induce genomic instability in mouse models of breast and prostate cancer (Caulin et al., 2007; Hingorani et al., 2005).

Somatic cell reprogramming and stem cells characteristic

Mutant p53 can interfere with cell differentiation (Matas et al., 2004), by promoting the reverse process of de-differentiation. In breast, lung and prostate tumors, an ESC (embryonic stem cell) gene signature was found to correlate with mutant p53 status (Markert et al., 2011; Mizuno et al., 2010). Moreover, tumors with p53 mutation and a stem cells transcription signature, and phenotype, have the worst outcome. Mouse embryonic fibroblast (MEF) cells co-expressing mutant p53 and Oct4 or Sox2, exhibit an enhanced cell reprogramming and a reduced differentiation capacity, if compared with p53 knockout MEF reprogrammed with Oct4 and Sox2 overexpression alone (Sarig et al., 2010).

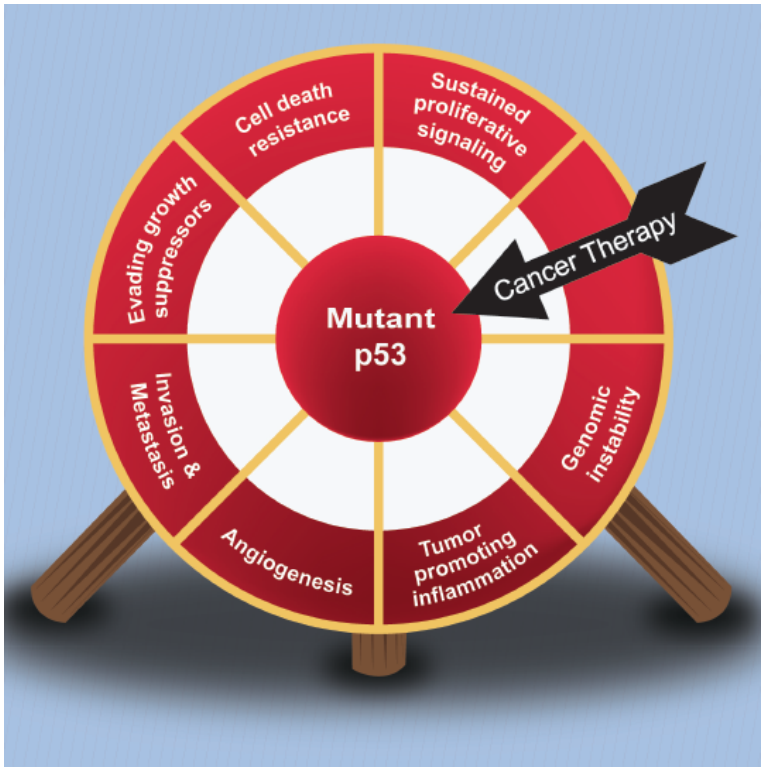

Figure 2.4: Mutant oncogenic activities integrated with the hallmarks of cancer. The hallmarks of cancer describe the events that compromise tumorigenic process. Mutant p53 was found to be involved in almost each of the described events (see the text for details). Thus, mutant p53 has been proposed has a promising target for cancer therapy. Figure taken from (Solomon et al., 2011).

Disruption of tissue architecture/migration/invasion

Normally, wt p53 maintains a transcriptional program to prevent EMT, and the loss of this suppression may contribute to the induction of an EMT-like phenotype in p53-null cells, together with tumor's invasive and metastatic potential (Muller et al., 2011). However, the novel properties acquired by mutant p53 are the main force driving migration and invasion (Solomon et al., 2011). The strongest support for the mutp53 GOF role in metastasis formation comes

from mouse models (Doyle et al., 2010; Heinlein et al., 2008; Lang et al., 2004; Olive et al., 2004; Weissmueller et al., 2014). Mutant p53 was found to facilitate tumor cell migration and invasion by enhancing the activation of EGFR/integrin signaling by a mechanism involving p63 inhibition (Muller et al., 2009). In another study, the prolyl-isomerase Pin1 was found to transduce oncogenic signals on mutant p53 to activate transcription of a specific set of pro-invasive and pro-migratory genes (Girardini et al., 2011).

Intriguingly, mutant p53 can also enhance invasion and metastasis mediating the cancer cells' crosstalk with the tumor microenvironment. This protein can up-regulate platelet-derived growth factor receptor b (PDGFR b) expression (Weissmueller et al., 2014), or reprograms the response of the cancer to cell to extrinsic inputs (i.e. TGF-β) (Adorno et al., 2009). Moreover a mechanistic link between mutant p53 GOF and chemokines secretion was proposed in enhanced cell motility (Yeudall et al., 2012).

Tumor microenvironment and tumor –related inflammation

Normally, wild type p53 protects against multiple inflammatory stress, including reactive oxygen and nitrogen species (ROS and RNS), viral infection, and cytokines (Figure 2.5) (Cooks et al., 2014). Emerging evidences suggest that mutant p53 oncogenic properties are deeply involved in the modulation of cancer cell crosstalk with immune cell population in the tumor microenvironment. The most convincing is a study on a mouse model of bowel disease, reporting that mutant p53 enhances the cell response to an inflammatory microenvironment and amplifies NF-κB activation, leading to an increase in the rate of transformation (Figure 2.5) (Cooks et al., 2013). In addition to favoring inflammation-induced transformation, mutant p53 was found to cooperate with NF-κB and enhance its transcriptional functions in response to TNFα in already transformed cancer cells (Weisz et al., 2007). Notably, analysis of human head and neck tumors, lung cancer, sporadic colorectal carcinoma, and human colitis-associated cancer revealed a close correlation between p53 mutation and activation of NF-κB (Cooks et al., 2013; Schwitalla et al., 2013; Weisz et al., 2007). Finally, it has been observed that hot-spot mutants sustain expression of a transcriptional signature enriched for inflammatory-related genes in tumor cells (Solomon et al., 2012; Yeudall et al., 2012).

Therefore mutant p53 has been shown to cooperate with NF-κB, and to amplify pro-inflammatory microenvironment. However, data regarding mutant p53 involvement in the upstream events of NF-κB pathway activation, and in the response to inflammation, are largely incomplete.

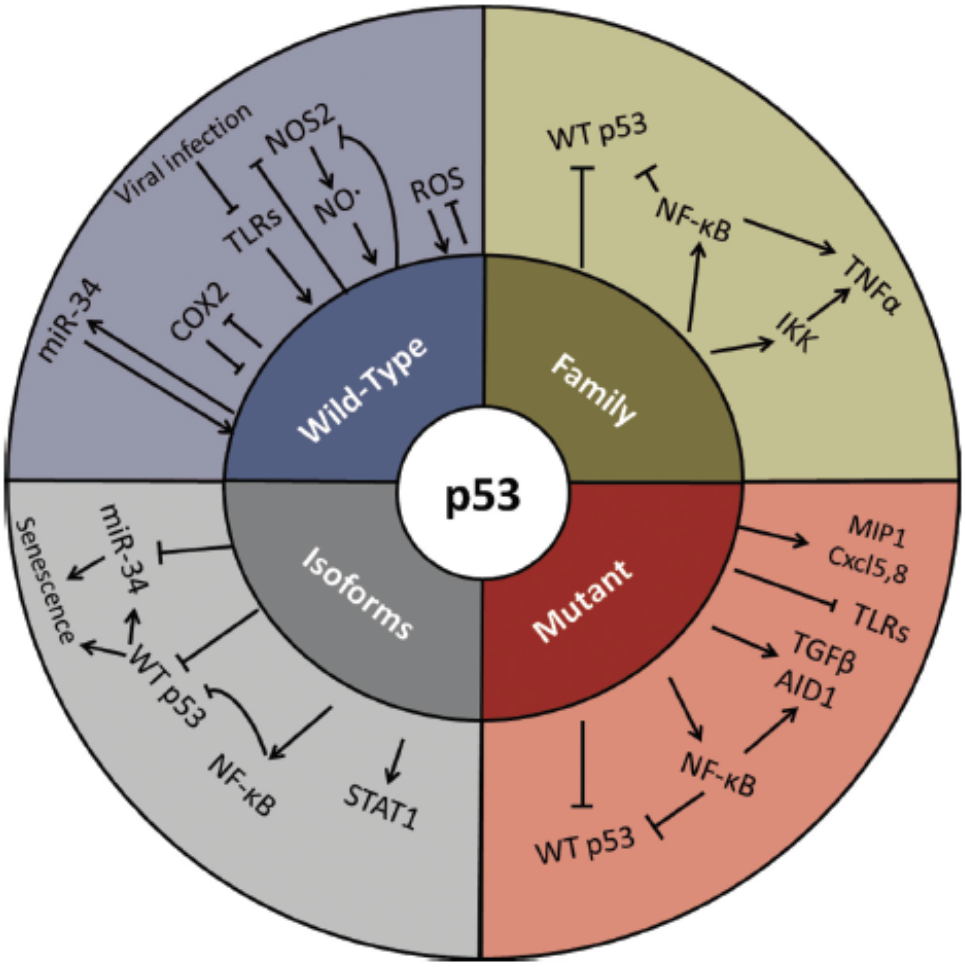

Figure 2.5: The p53 family in tumor-related inflammation. p53 pathway and other family members display a broad interaction with inflammatory elements such as reacitve oxigen and nitrogen species (ROS and RNS), cytokines, infection agents and pro-inflammatory NF-κB pathway. This complex crosstalk is higly dependent on p53 status, as different p53 isoforms and p53 mutants can mediate different responses and even promote chronic inflammation and associated cancer, acting in the tumor cells as well as in the stromal and immune compartments. Illustration taken from (Cooks et al., 2014).

2.2 CANCER-RELATED INFLAMMATION

The presence of leukocytes within the tumor, observed in the 19th century by Rudolf Virchow, provided the first evidence of a possible link between inflammation and cancer (Grivennikov et al., 2010). Nowadays, it has become clear that an inflammatory microenvironment is an essential component of all tumors, including those not causally related to an obvious inflammatory process (Elinav et al., 2013; Grivennikov et al., 2010).

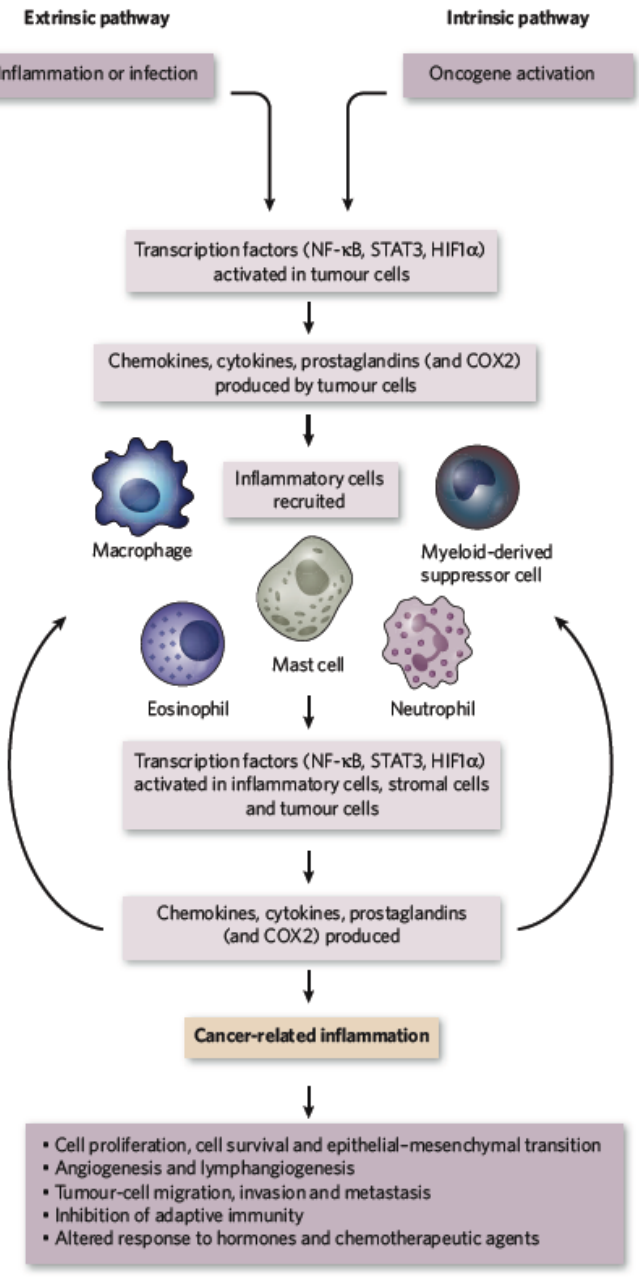

Figure 2.6: Signaling network that connects inflammation and cancer. In the intrinsic pathway, transformed cells produce inflammatory mediators, thereby generating an inflammatory microenvironment. In the extrinsic pathway inflammatory or infectious conditions augment the risk of developing cancer. The two pathways converge, resulting in the activation of pro-inflammatory ongogenic signaling in tumor cells, that coordinates the production of inflammatory mediators. These molecules modulate the behaviour of immune cells in the tumor microenvironment and activate the same key transcription factors in inflamamtory, stormal and tumor cells, resulting in a more inflammatory milieu. Image taken from (Mantovani et al., 2008).

Some forms of chronic inflammation can be clearly linked to cancer susceptibility. For example, persistent *Helicobacter pylori* infection is associated with gastric cancer and MALT (mucosa-associated lymphoid tissue) lymphoma, while infections with hepatitis B (HBV) or C (HCV) viruses increase risk of hepatocellular carcinoma, likewise papilloma virus for cervical carcinoma (Grivennikov et al., 2010). Chronic inflammation can be also caused by dietary factors, including obesity. Evidences of a relationship between obesity and different forms of cancer, including lymphoma, prostate, breast and endometrial cancer have been recently added to the previous evidence of a key role of obesity in liver and pancreas tumorigenesis (Wolin et al., 2010). Autoimmune diseases (e.g. inflammatory bowel disease for colon

carcinoma) and inflammatory conditions of uncertain origin (e.g. prostatitis for prostate cancer) can also promote carcinogenesis (Colotta et al., 2009).

In summary, inflammation can promote cancer development and progression (Grivennikov et al., 2010). The identification of molecular and cellular circuits linking inflammation and cancer, allowed the description of two distinct paths. In the intrinsic pathway, genetic events causing neoplasia initiate the expression of inflammatory-related factors the drive the construction of an inflammatory microenvironment within the tumor tissue. In the extrinsic pathway, the inflammatory condition associated to a particular disease state or environmental condition facilitates cancer development (Colotta et al., 2009) (Figure 2.6).

2.2.1 Inflammation and tumor initiation and promotion

Inflammation-induced tumor promotion may occur early or late, and can lead to activation of pre-malignant lesions that were dormant for many years. The mechanisms through which inflammation affects tumor promotion are numerous and in addition to increase proliferation and enhanced survival, can also sustain the angiogenic switch, EMT, invasion and metastasis (Grivennikov et al., 2010).

Inflammation may have a prominent role in initiating neoplastic transformation by increasing the rate of DNA damage and compromising DNA repair mechanisms (Grivennikov et al., 2010). In fact, ROS and RNS that are released by tissue macrophages and neutrophils, or that are induced in pre-malignant cells by inflammatory cytokines, cause DNA breaks, single base mutations or more complex DNA lesions (Colotta et al., 2009; Elinav et al., 2013; Grivennikov et al., 2010). Interestingly, inflammation may also augment cellular susceptibility to mutagenesis and indirectly increase genomic destabilization by counteracting DNA repair machinery and disrupting cell cycle checkpoints, which leads to the accumulation of random genetic alteration (Colotta et al., 2009; Elinav et al., 2013; Grivennikov et al., 2010).

Another important pathway through which inflammation sustains tumor development and progression is NF-κB signaling. Activated NF-κB has been detected in the majority of human malignancies (Ben-Neriah and Karin, 2011). It triggers the transcription of genes than control cell survival, proliferation, growth, as well as angiogenesis, invasion and chemokine and cytokines production, acting as key coordinators of innate immunity and inflammation (Figure 2.6) (Grivennikov et al., 2010). For example, NF-κB promotes the expression of multiple pro-survival and anti-apoptotic proteins, such as Bcl-2 and Bcl-xL, as well as c-IAP1 and c-IAP2, Mcl-1, c-FLIP, and survivin (Grivennikov et al., 2010). Interestingly, senescence state is reinforced by a senescence-associated secretory phenotype, (that include IL-1, IL-6 and

chemoattractants, such as IL-8), induced by NF-κB. Intriguingly, recent work demonstrates that loss of wt p53 induces a senescence-associated low grade inflammation in stressed colonic epithelial cell, promoting tumorigenesis (Pribluda et al., 2013).

Recent studies observed the involvement of inflammation also in prostate cancer (PCa) (Sfanos and De Marzo, 2012). Accordingly, the long-term use of aspirin decreases risk of PCa in men (Vidal et al., 2015).

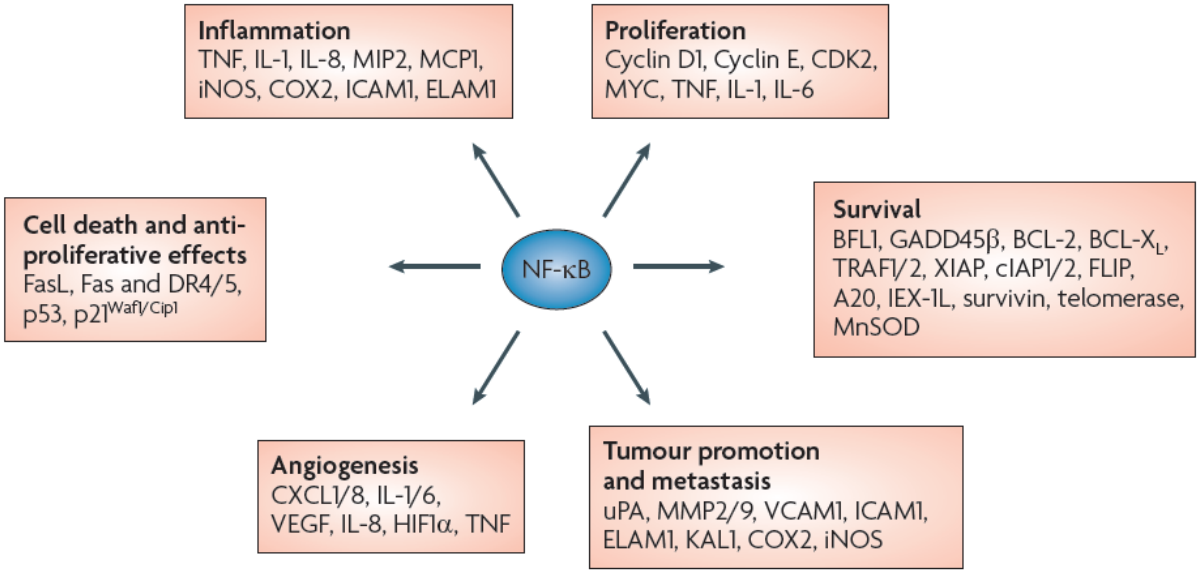

Figure 2.7: NF-κB regulated processes. NF-κB activation affects six hallmarks of cancer, through the transcription of genes involved in proliferation, survival, metastasis and invasion, angiogenesis, cell death and inflammation. Taken from (Baud and Karin, 2009).

Notably, it is well known that besides NF-κB, other inflammatory mediators contribute to metastasis of tumor cells. TGFβ, TNF, IL-6 and IL-1 enhance EMT by down-regulating the expression of epithelial markers (e.g. E-cadherin) and up-regulating the expression and activity of metalloproteins (Adorno et al., 2009; Bates and Mercurio, 2003; Sullivan et al., 2009; Voronov et al., 2003; Wu et al., 2009). Myeloid-derived monocytes and macrophages strongly facilitate tumor cell invasion, extravasation, and metastatic outgrowth (Elinav et al., 2013). Inflammation promotes the intravasation of cancer cells into blood vessel and lymphatics, through a crosstalk between tumor-associated macrophages (TAMs) and tumor cells (Grivennikov et al., 2006). Inflammatory mediators enhance the survival of circulating metastatic cells and promote their extravasation by up-regulating adhesions molecules. For example, CC- and CXC-chemokine and their receptors, (e.g. CCR1, CCR4, CCR7, CCR9,

CCR10, CXCR1-5 and CXCR7) are expressed by malignant cells from various tissues in response to cytokines; they direct the organ-specific migration of cancer cells (Grivennikov et al., 2010). Similarly, CCL18 and CCL2 promote mammary tumor migration by enhancing the adherence of metastatic cells to the extracellular matrix (Chen et al., 2011a; Qian et al., 2011; Wolf et al., 2012).

Importantly, inflammatory processes that accompany carcinogenesis can also exert an anti-tumor action that can be stimulated by multiple cytokines and accomplished by infiltrating immune cells. Indeed, various chemokines are associated with generating an anticancer immune contexture in various type of malignances (Bindea et al., 2013; Chew et al., 2012; Hirano et al., 2007; Kondo et al., 2006; Kunz et al., 1999; Rody et al., 2011). Therefore, a fine balance is generated within the tumor microenvironment between inflammatory mediators that are involved in attracting immune cells and modulating their activity, and those regulating cancer cell survival and acquisition of a more aggressive phenotype. An imbalance in this complex network of signals can skew the anti-tumor response of immune system to an anti-inflammatory process that sustain and enhance carcinogenesis.

2.2.2 Immune modulation by cancer (crosstalk between cancer and immune system)

One of the most important aspects of the inflammatory tumor microenvironment is the ability of cancer cells to interfere with every step of the antitumor inflammation response. Tumor cells act both in the recruitment and in the activation of adaptive and innate immunity.

They can reprogram the acquired T cells response from the pro-inflammatory and anti-tumoral Th1 cell subset, to the pro-tumorigenic Th2 type. Moreover, they can skew the phenotype of macrophages and neutrophils to a type 2 differentiation state through the secretion of IL-4, IL-13, TGFβ and IL-10, and sustain induction of myeloid-derived suppressor cells (MDSCs) (Elinav et al., 2013; Grivennikov et al., 2010). For example, in a mouse model of pancreatic ductal adenocarcinoma, it was recently shown that tumor-derived GM-CSF (granulocyte-macrophage colony stimulating factor) promotes the recruitment of $(GR1)^{+}CD11b^{+}$ myeloid cells that suppress antigen-specific T cells activity at the site of the tumor (Bayne et al., 2012). Moreover cancer cells actively recruit T_{reg} in the site of tumor (Facciabene et al., 2011).

However, cancer cells can also secrete mediators that are associated with an anti-tumor immune response. For example, in large cohorts of colorectal tumors, high expression of CX3CL1 (also known as fractalkine), CXCL9 and CXCL10, was associated with the infiltration of memory and effector T cells, particularly Th1 cells - and was strongly correlated with prolonged disease-free survival (Mlecnik et al., 2010).

A complex interplay of immune and tumor cells, both of which express inflammatory mediators and growth factors, builds the architecture on the immune context in tumors. The coordination of this complex network of information is essential to control a tumor. Subtle modification of this architecture, provoked by changes in the tumor cells or in the host immune system, or in the chemokine milieu of the local microenvironment, may weaken immune control of the tumor, with a good opportunity to augment tumor aggressiveness.

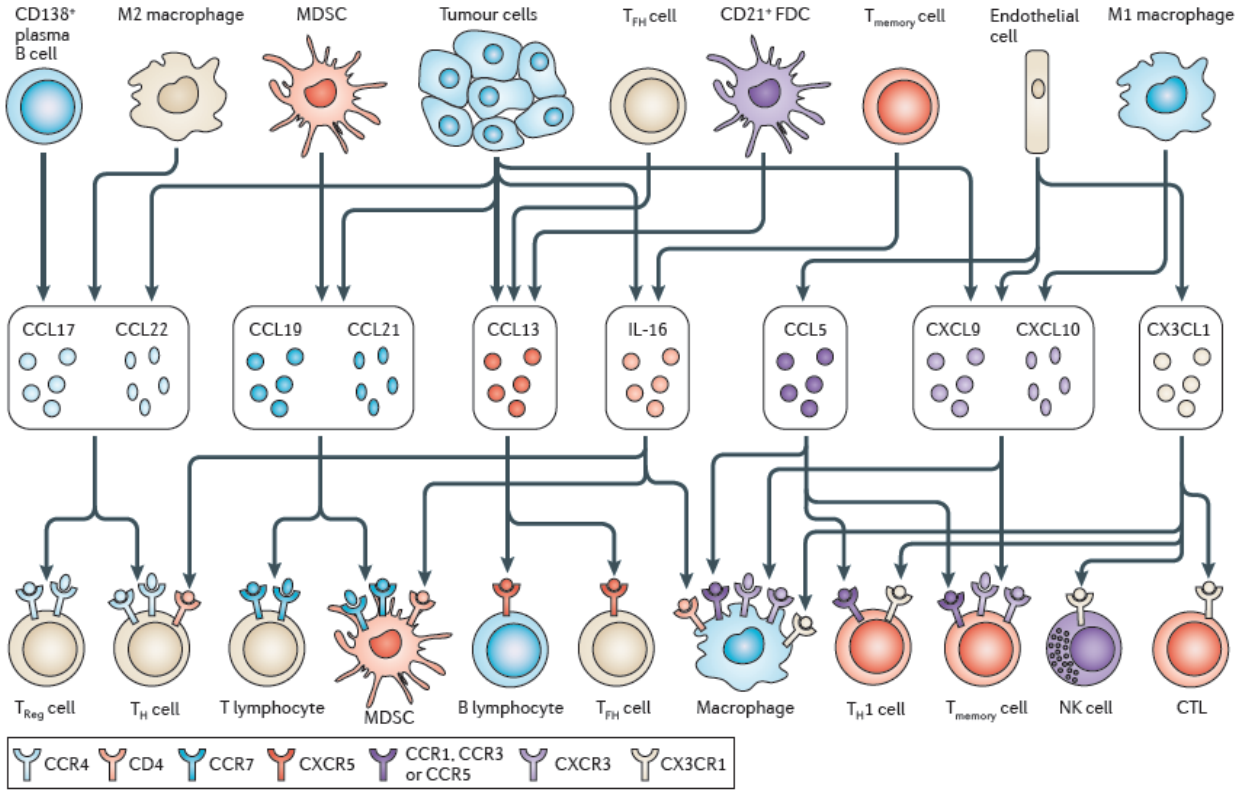

Figure 2.8: Cells and chemokines that coordinate the cancer cell-mediated immune modulation. The tumor microenvironment is characterized by the recruitment of multiple immune cells through the secretion of cytokines and chemokines by tumor cells and other infiltrating immune cells. CTL: cytotoxic T lymphocyte; FDC: follicular dendritic cell; MDSC: myeloid-derived suppressor cell; NK: natural killer; T_{fh}cell: T follicular helper cell; T_h:T helper; T_{reg}: regulatory T cell . Image taken from (Fridman et al., 2012).

2.2.3 TNFα signaling

The principal sources of TNF are activated immune cells, especially macrophages and T-cells, but TNF can be efficiently produced by other cell types, including fibroblasts and tumor cells (Wajant et al., 2003). TNF binds two distinct receptors, TNFR1 e TNFR2. This interaction results in the recruitment of the death domain-containing serine-threonine kinase RIP and the death-domain-containing adapter protein TRADD that, in turn, mediates the recruitment of

TRAF2 (Complex I). This protein complex recruits and activates the multi-protein cytoplasmic IKK, responsible for the inhibitory phosphorylation of IκB at two conserved serine residues in N-terminal regulatory domain. Once phosphorylated, IκB almost immediately undergoes polyubiquitination and degradation by proteasome, releasing p65/p50 from the inhibitory binding and leading to NF-κB activation (Figure 2.9) (Perkins, 2007; Wajant et al., 2003). Activation of NF-κB, mediates pro-tumorigenic activities of TNF.

TRAF2 and RIP also mediate activation of JNK and p38 MAP kinase cascade, stimulating programed cell death (Figure 2.9) (Wajant et al., 2003). TNFR1 can induce cell death by other two distinct processes. First, it induces necrosis, which is mediated by RIP- and TRAF2- driven excessive generation of ROS and subsequent prolonged JNK signaling (Lin et al., 2004). Second, TNRF1 induces caspase-mediated apoptosis, which involves the death domain contained in TRADD and FADD (Fas-associated death domain) and activation of the initiator caspase-8 (Complex II- Figure 2.9) (Wajant, 2009).

Notably, in some cases, TNF secretion in the microenvironment can exert an anti-tumor effect, inducing hyper-permeability in tumor-associated vessels, thus facilitating tumor entry of blood cells, and their cytotoxic properties. TNF can also stimulate the activity of antigen presenting cells (APC), promoting the immune response (Wajant, 2009).

However the finding that TNF depletion in mice protects from skin cancer development offered incontrovertible genetic evidence of its pro-tumor function (Moore et al., 1999).

In fact, tumor promotion mediated by TNF involves different strategies: TNF enhances tumor growth and invasion, leukocyte recruitment, especially those not related with cytotoxic activity, angiogenesis and facilitates EMT (Colotta et al., 2009; Wajant, 2009). TNF secreted by TAMs promotes Wnt/βcatenin signaling, through the inhibition of GSK3β, contributing to tumor development in gastric mucosa (Oguma et al., 2008). In breast cancer cells, TNF secretion in the tumor microenvironment establishes a crosstalk between tumor cells, immune cells and CAF, strongly sustaining invasiveness of breast cancer cells (Hagemann et al., 2004; Stuelten et al., 2005; Wang et al., 2005). Finally, TNF, together with IL-1 and IL-8 (also known as CXC-chemokine ligand 8), is also involved in prostate cancer initiation and progression, where its expression is also an indicator of worst prognosis, increased bone metastasis and shorter time to castration resistance and overall survival (Kea et al., 2013; Sharma et al., 2014; Wang et al., 2013).

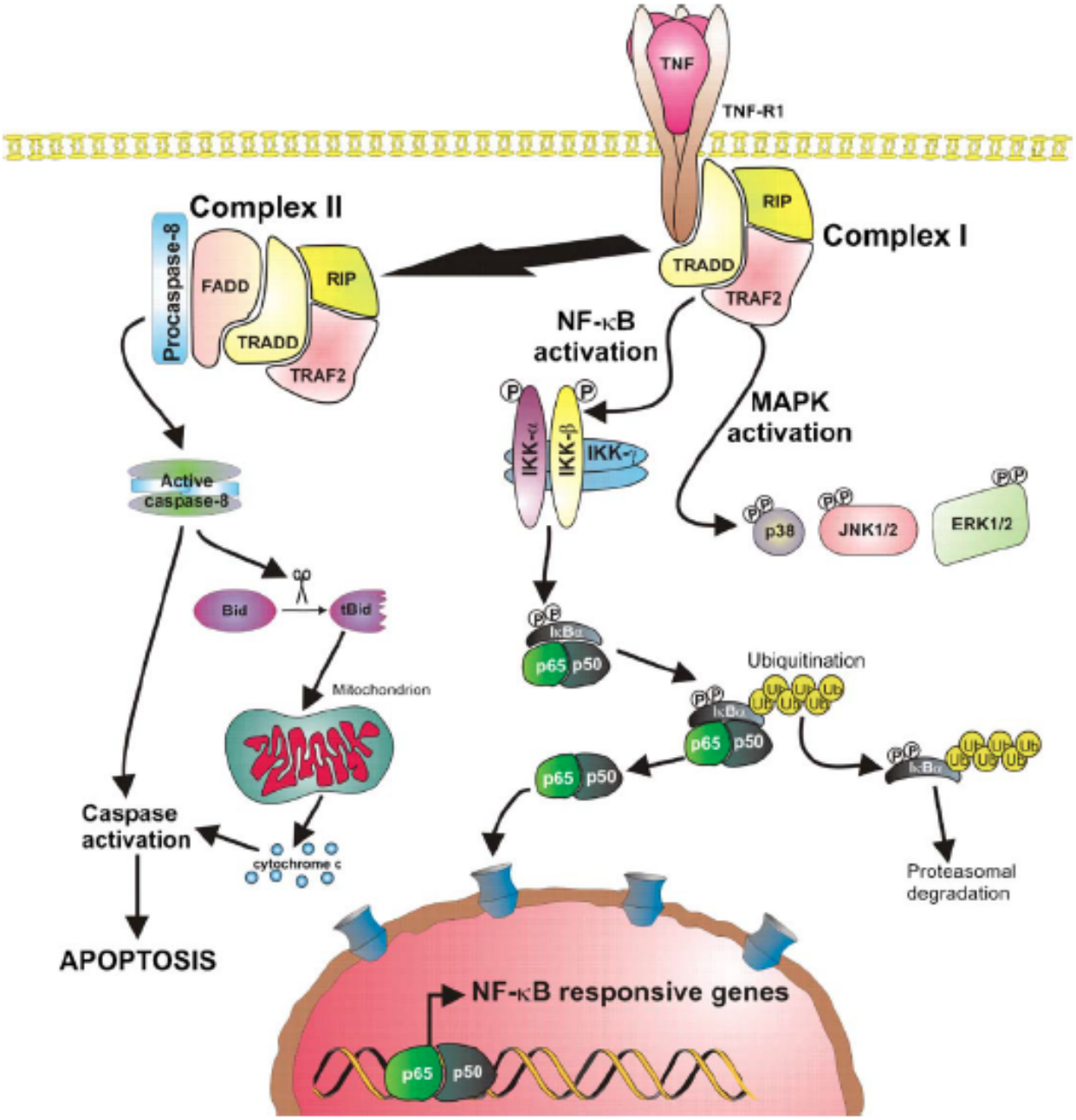

Figure 2.9: TNFR1 induces TNF signaling activation by protein complex I and II. TNFR1 is obquitiosly expressed in all cell types and can sustain directly the activation of pro-apototic pathways (JNK/p38MAP kinase and caspase 8 signaling) and pro-survival and pro-cell motility signals (NF-κB). Illustration taken from (Wullaert et al., 2006) (see the text for details).

Molecular Cell
Article

Mutant p53 Reprograms TNF Signaling in Cancer Cells through Interaction with the Tumor Suppressor DAB2IP

Giulio Di Minin,[1,7] Arianna Bellazzo,[1,2,7] Marco Dal Ferro,[1,2] Giulia Chiaruttini,[3] Simona Nuzzo,[4] Silvio Bicciato,[4] Silvano Piazza,[1] Damiano Rami,[2] Roberta Bulla,[2] Roberta Sommaggio,[5] Antonio Rosato,[5,6] Giannino Del Sal,[1,2] and Licio Collavin[1,2,*]

[1]Laboratorio Nazionale CIB (LNCIB), AREA Science Park, 34149 Trieste, Italy
[2]Dip. Scienze della Vita, Università degli Studi di Trieste, 34127 Trieste, Italy
[3]International Centre for Genetic Engineering and Biotechnology (ICGEB), AREA Science Park, 34149 Trieste, Italy
[4]Center for Genome Research, Dip. Scienze della Vita, Università degli Studi di Modena e Reggio Emilia, 41121 Modena, Italy
[5]Dip. Scienze Chirurgiche Oncologiche e Gastroenterologiche, Università degli Studi di Padova, 35128 Padova, Italy
[6]Istituto Oncologico Veneto IOV-IRCCS, 35128 Padova, Italy
[7]Co-first author
*Correspondence: collavin@lncib.it
http://dx.doi.org/10.1016/j.molcel.2014.10.013

SUMMARY

Inflammation is a significant factor in cancer development, and a molecular understanding of the parameters dictating the impact of inflammation on cancers could significantly improve treatment. The tumor suppressor p53 is frequently mutated in cancer, and p53 missense mutants (mutp53) can acquire oncogenic properties. We report that cancer cells with mutp53 respond to inflammatory cytokines increasing their invasive behavior. Notably, this action is coupled to expression of chemokines that can expose the tumor to host immunity, potentially affecting response to therapy. Mechanistically, mutp53 fuels NF-κB activation while it dampens activation of ASK1/JNK by TNFα, and this action depends on mutp53 binding and inhibiting the tumor suppressor DAB2IP in the cytoplasm. Interfering with such interaction reduced aggressiveness of cancer cells in xenografts. This interaction is an unexplored mechanism by which mutant p53 can influence tumor evolution, with implications for our understanding of the complex role of inflammation in cancer.

INTRODUCTION

Inflammation is tightly linked to cancer, but a mechanistic comprehension of this complex relationship remains elusive. In the tumor stroma inflammatory chemokines and cytokines, such as Tumor Necrosis Factor alpha (TNFα), modulate the activity of infiltrating immune cells and also the behavior of cancer cells, influencing tumor growth, dissemination, and response to therapy (Grivennikov et al., 2010). Molecular studies aimed at defining the impact of inflammation on specific tumors could thus provide novel prognostic markers and therapeutic strategies.

Expression of mutant p53 isoforms (mutp53) is another significant factor in cancer development, since tumor-associated p53 mutants can actively promote transformation through oncogenic gain-of-function (GOF) activities (Muller and Vousden, 2013; Oren and Rotter, 2010; Walerych et al., 2012).

Various evidences suggest that mutp53 oncogenic properties are deeply connected to tumor inflammation (Solomon et al., 2011, 2012; Yeudall et al., 2012). Perhaps the most convincing is a recent study on a mouse model of inflammatory bowel disease, reporting that mutp53 amplifies and sustains the proinflammatory microenvironment, leading to an increase in the rate of transformation (Cooks et al., 2013).

In addition to favoring inflammation-induced cell transformation, mutp53 may have an unexplored role in shaping the response to inflammation of already transformed cancer cells. In fact, a large proportion of tumors undergo p53 mutation at a later stage of transformation, when an inflammatory microenvironment has been established within the growing tumor mass. The recognition and molecular understanding of a potential mutp53 GOF in inflammation-driven tumor progression and metastasis is therefore of primary interest.

In the recent past, we identified 37 novel interactors of p53 family members (Lunardi et al., 2010). Among them, the RasGAP Disabled2 Interacting Protein (DAB2IP), also called ASK1 Interacting Protein (AIP1), stands out for its role in signaling by growth factors and inflammatory cytokines. Modulating the cell response to multiple potentially oncogenic signals, DAB2IP is a bona fide tumor suppressor and is frequently silenced by promoter methylation in aggressive human tumors (Dote et al., 2004; Qiu et al., 2007). Nonetheless, in many tumors DAB2IP is not methylated, and alternative mechanisms might exist to interfere with its functions.

In the present study, we find that DAB2IP can be functionally inactivated by physical interaction with mutant p53 proteins, with implications for the response of cancer cells to inflammatory cytokines.

RESULTS

Mutant p53 Increases the Invasive Behavior of Cancer Cells Exposed to Inflammatory Cytokines and Specifically TNFα

To explore the role of p53 mutation in the response of cancer cells to inflammation, we performed invasion assays with human breast cancer cell lines bearing mutant p53. To mimic the cytokine milieu of the tumor microenvironment, we used culture medium conditioned by LPS-activated murine dendritic cells (dendritic cell-conditioned medium [DCCM]). The cell lines used are metastatic and thus penetrate matrigel, but DCCM caused a significant increase in such behavior. Under these conditions, p53 depletion abrogated the effect of DCCM, indicating that mutp53 is required for this phenotype (Figures 1A, S1A, and S1B available online).

We performed the same experiments with Ras-trasformed embryonic fibroblasts (MEFs) derived from p53 knockout or p53(R172H) knockin mice; DCCM triggered a greater increase in invasion in mutp53 than in p53 null MEFs (Figure S1D), indicating that this phenotype represents a mutp53 gain of function.

Activated dendritic cells secrete a variety of cytokines and growth factors, including TNFα and TGFβ (Moustakas et al., 2002). Mutant p53 can form a complex with activated Smad2 and p63 in cancer cells, driving metastasis in response to TGFβ (Adorno et al., 2009); a specific TGFβ inhibitor had no impact on the proinvasive response to DCCM, thus excluding this aspect of the mutp53/p63 axis in the phenotype. In contrast, a TNFα blocking antibody efficiently suppressed the increase in invasion induced by DCCM (Figure 1B), indicating that TNFα is the main mediator of this effect.

Mutant p53 Increases Cell Invasion and Protects from Apoptosis in Response to TNFα

We thus repeated the above experiments using recombinant human TNFα, confirming that TNFα increases cell invasion in a mutp53-dependent manner (Figures 1C and S1C). This result was confirmed in a pancreatic cancer cell line with the p53(R273H) mutation (PANC-1), so it is not restricted to mammary cells (Figure S7A).

To verify whether mutp53 is sufficient for this phenotype, we introduced mutant p53 in a nontransformed mammary epithelial cell line. We used MCF-10A stably silenced for endogenous wild-type (WT) p53 (MCF-10A shp53) to generate a panel of mutp53 knockin cell lines (Figure 1D). Notably, TNFα treatment rendered mutp53 knockin cells significantly more invasive than p53 knockdown cells (Figures 1E and S1E). We conclude that mutp53 is sufficient to mediate this response in nontransformed cells.

We also analyzed the death-inducing effects of TNFα on breast cancer cell lines before and after mutant p53 knockdown. With the exception of MDA-MB-231, which underwent a partial G2 arrest (Figure S1F), mutp53 depletion sensitized cells to TNF-induced cell death (Figures 1F and 1G), indicating that mutant p53 restrains TNF-induced activation of proapoptotic pathways. This effect was confirmed also in PANC-1 cells (Figure S7B).

Mutant p53 Modulates TNF-Induced Transcription toward a Proinvasive and Immunogenic Gene Expression Program

To gain a molecular insight on this phenotype, we used microarrays to analyze the transcriptional profile of MDA-MB-231 treated with TNFα for 20 hr, with or without mutp53 silencing. Mutp53 depletion had a broad impact on transcription, independently of TNFα (Figure S2A), so we examined TNF-responsive genes, defined as the union of genes up- or downregulated by TNFα in control and/or mutp53-depleted cells (Table S1). Gene ontology (GO) enrichment analysis revealed that TNF-repressible genes are mostly related to the mitotic cell cycle. In contrast, TNF-inducible genes display a much broader spectrum of biological functions, including cell migration, apoptosis, and inflammatory and immune response (Table S2). Since in our cell models mutant p53 sustains invasion and survival, we focused our analysis on TNF-inducible genes and identified those less expressed (TNF-upsiC) or more expressed (TNF-upsip53) after mutp53 knockdown (Figure 2A).

Microarrays were validated by RT-qPCR on a selection of genes belonging to the TNF-upsiC and TNF-upsip53 groups, confirming their mutp53-dependent regulation (Figures 2C–2D and S2B). We also analyzed public breast cancer data sets with information on p53 status (Curtis et al., 2012; Miller et al., 2011) and verified that the TNF-upsiC metagene is more expressed in tumors with mutp53 (Figure S2C).

We noticed a specific enrichment for the processes "immune response," "cytokine production," and "positive regulation of cell migration" in TNF-upsiC genes (Figure 2B), suggesting that mutp53 modulates a transcriptional response to TNFα that can be proinvasive but also immunogenic. Indeed, TNF-upsiC genes include secreted proteins that can stimulate cell migration and metastasis (e.g., CA12, MMP9, and CXCL10) (Bjordahl et al., 2013; Muthuswamy et al., 2012; Xin et al., 2005), but also chemokines that may control recruitment of lymphocytes (e.g., CXCL10, CX3CL1, and LTB) (Duffy et al., 2000; Hsieh et al., 2010; Shin et al., 2010). To verify this last point, we asked whether medium conditioned by TNFα-treated MDA-MB-231 cells could attract lymphocytes from peripheral blood. We observed chemotaxis of T lymphocytes, cytotoxic T lymphocytes (CTL), and Natural Killer cells. Importantly, this activity was reduced by mutp53 knockdown (Figure S2D). Therefore, mutp53 can affect both cell-autonomous and non-cell-autonomous responses to TNFα.

Mutant p53 Coordinately Modulates TNF-Dependent Activation of Both NF-κB and JNK Pathways

Many of the genes identified are direct NF-κB targets (Table S1), yet they display a striking difference in mutp53 dependency. In addition to NF-κB, TNFα can trigger activation of ASK1/JNK kinases, and these two signaling axes have a complex reciprocal interaction that can affect gene expression (Wajant et al., 2003). We used inhibitors to selectively block either branch of the pathway and analyzed TNF-responsive genes differently affected by mutp53: MMP9 (TNF-upsiC group) and IL1B (TNF-upsip53 group). Not surprisingly, induction of both genes was impaired by the NF-κB inhibitor BAY (BAY11-7082), confirming that they are NF-κB targets (Figure 2E). However, there were

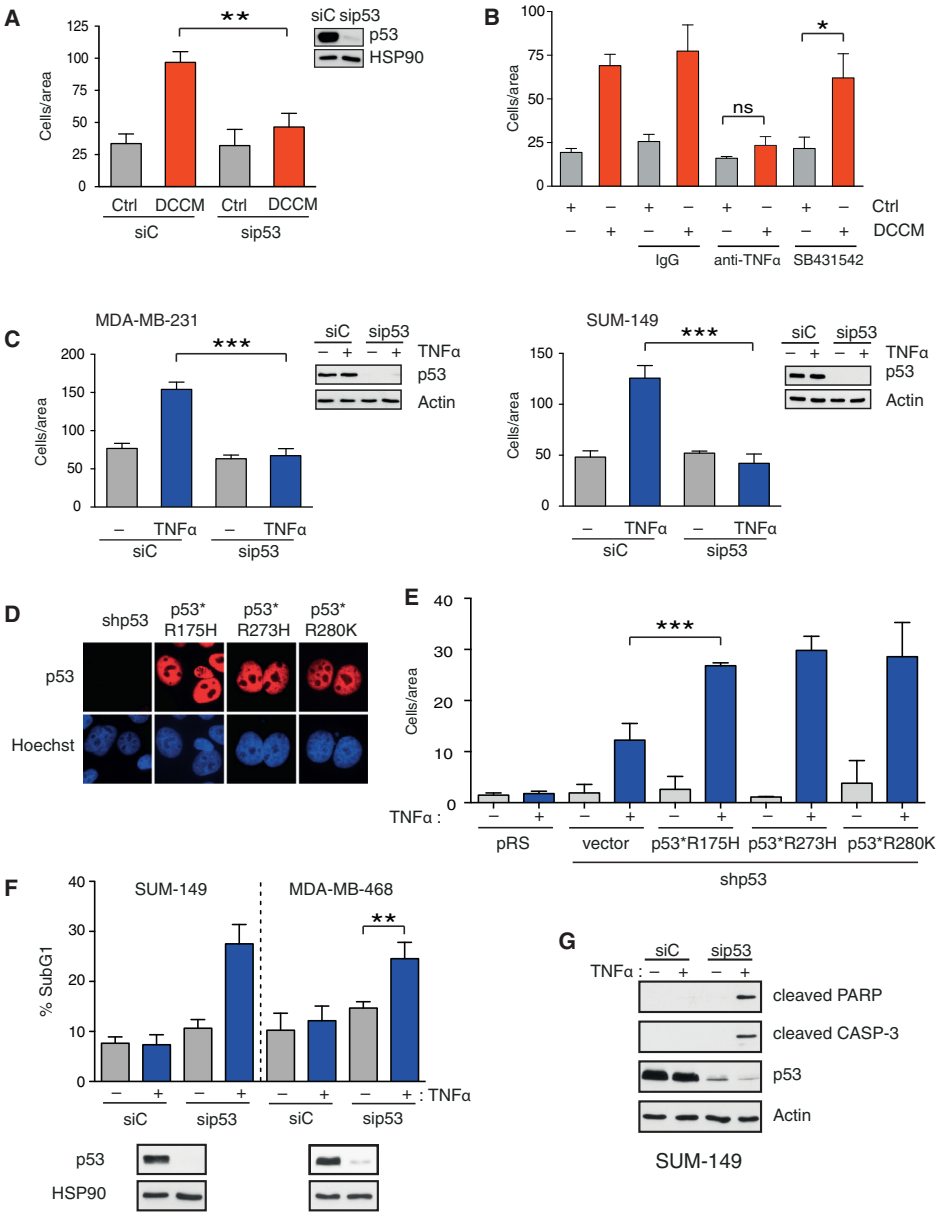

Figure 1. Mutant p53 Amplifies the Aggressive Behavior of Cancer Cells Exposed to Inflammatory Cytokines and TNFα

(A) Mutp53 drives inflammation-induced invasion. MDA-MB-231 cells were transfected with control (siC) or p53 (sip53) siRNAs; invasion assays were performed with medium conditioned by activated dendritic cells (DCCM). Graph summarizes migrated cells per area (mean ± SD; n = 3; **p < 0.01). Mutp53 depletion was checked by western blot. Representative images of migrated cells are shown in Figure S1A.

(B) Invasion assays with MDA-MB-231 were performed as in (A). Rabbit IgG (10 μg/ml), TNFα blocking antibody (10 μg/ml), or TGFβ inhibitor SB431542 (10 μM) were added to the medium as indicated (mean ± SD; n = 3; *p < 0.05).

(C) Invasion assays with indicated cell lines were performed in low serum plus 10 ng/ml TNFα (mean ± SD; n = 3; ***p < 0.001). Representative images of migrated cells are shown in Figure S1C.

(D and E) Mutp53 is sufficient for TNF-induced invasion. MCF-10A cells stably silenced for endogenous WT p53 (shp53) were infected with retroviruses expressing shRNA-resistant (*) p53 mutants. (D) Immunofluorescence of exogenous p53 mutants. Immunoblots are shown in Figure S1E. (E) Transwell migration assays (mean ± SD; n = 3; ***p < 0.001).

(F and G) Mutp53 depletion sensitizes cancer cells to TNF-induced cell death. (F) Indicated cells were treated with TNFα (10 ng/ml) for 48 hr. DNA content was analyzed by flow cytometry (mean ± SD; n = 3; **p < 0.01). Mutp53 depletion was checked by immunoblotting (bottom). (G) SUM-149 cells were treated with TNFα for 24 hr and analyzed by western blot to detect cleaved PARP and CASP-3.

See also Figure S1.

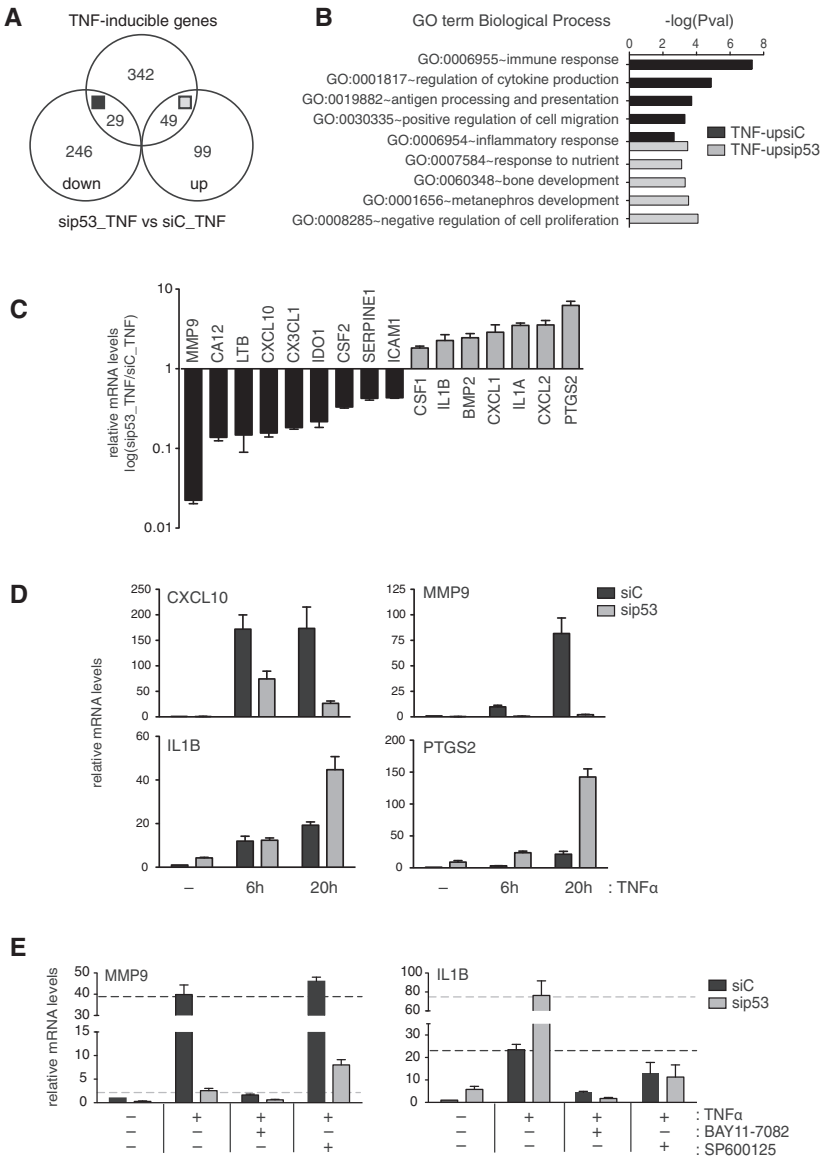

Figure 2. Mutant p53 Modulates the TNF-Induced Transcriptional Landscape

(A) MDA-MB-231 cells were treated with TNFα for 20 hr and analyzed by Illumina microarray. TNF-inducible genes less expressed (TNF-upsiC, black) or more expressed (TNF-upsip53, gray) in mutp53-depleted cells were selected. See also Table S1.

(B) Representative Gene Ontology terms specifically enriched in TNF-upsiC or TNF-upsip53 genes. See also Table S2.

(C) Expression of selected TNF-upsiC (black) or TNF-upsip53 (gray) genes was validated by RT-qPCR. Bars indicate differential expression in sip53_TNF versus siC_TNF samples (mean ± SD; n = 3). Values are normalized to histone H3 and compared to untreated siC-transfected samples.

(D) Expression of selected genes at 6 hr or 20 hr of TNFα treatment. Corresponding p53 immunoblot is shown in Figure S2B.

(E) Mutp53 sustains NF-κB and counteracts JNK-dependent transcription. MDA-MB-231 cells were stimulated with TNFα for 20 hr and treated with the NF-κB inhibitor BAY11-7082 (1 μM) or the JNK inhibitor SP600125 (10 μM) as indicated. Expression of MMP9 and IL1B mRNAs was measured by RT-qPCR as in (C). Dashed lines mark TNF-induced expression levels without inhibitors. See also Figure S2.

interesting differences in the response to the JNK inhibitor SP (SP600125). TNF-dependent induction of IL1B was reduced by SP treatment, indicating that both NF-κB and JNK positively regulate this gene. In contrast, induction of MMP9 was unaffected by SP in control cells but was amplified by SP in p53-depleted cells, suggesting that JNK represses this gene in the absence of mutp53. Identical results were obtained with CXCL10 and PTGS2 (Figure S2E). Transient knockdown of p65 RelA or JNK by siRNA produced similar outcomes (Figure S2F), confirming the direct involvement of these factors.

Together, the data are consistent with a model in which mutp53 sustains activation of NF-κB while counteracts activation of JNK in response to TNFα (Figure S2G). In line with this concept, predicted JUN/AP-1 consensus elements are enriched in the promoters of genes selectively upregulated by TNFα in mutp53-depleted cells (Figure S2H).

Mutant p53 Interacts with the Tumor Suppressor DAB2IP in the Cytoplasm

To unveil the mechanism of this mutp53 action, we searched for a potential target with a role in TNF signaling. We focused on the tumor suppressor DAB2IP, a protein that promotes activation of ASK1/JNK and inhibits activation of NF-κB in response to TNFα (Zhang et al., 2003, 2004).

We had previously found that DAB2IP can bind p53 family proteins (Lunardi et al., 2010); using coaffinity purification assays, we verified that DAB2IP can interact with hot-spot missense p53 mutants, with no evident bias for contact or conformational alterations (Figure 3A). Using deletion constructs, we mapped the reciprocal binding to the C2 domain of DAB2IP and the core domain of different p53 mutants (Figures 3B–3C and Figures S3A and S3B). This suggests that interaction does not involve p53 structural elements required for binding to DNA. This also implies that most p53 mutants can potentially bind DAB2IP.

DAB2IP is a cytoplasmic protein, so interaction with mutp53 must occur in the cytosol. Using fractionation, we verified that mutp53 is present in sizeable amounts in the cytoplasm of metastatic breast cancer cell lines (Figures 3D and S3F). The same was observed with p53 mutants expressed in nontransformed

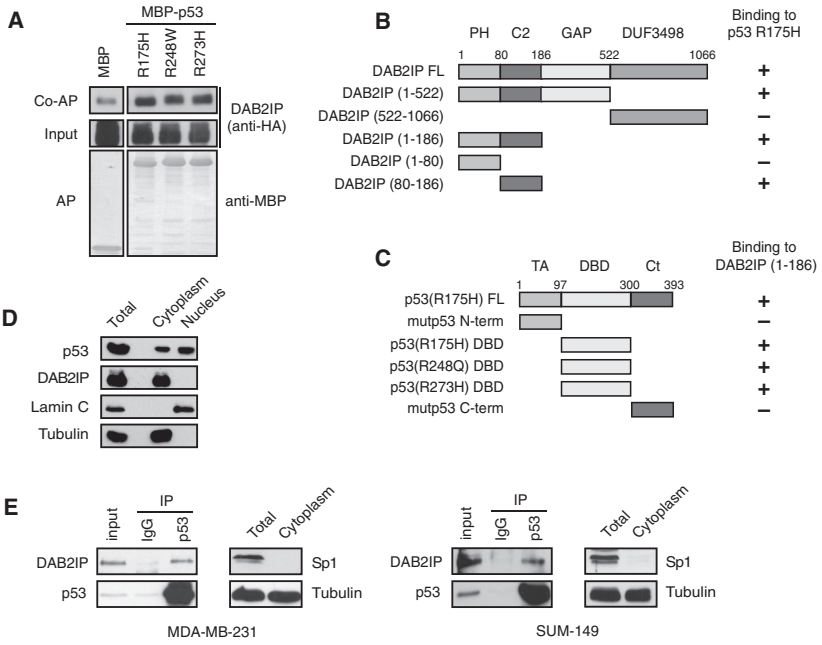

Figure 3. Mutant p53 Interacts with DAB2IP in the Cytoplasm

(A) DAB2IP binds hot-spot p53 mutants. We co-transfected 293T cells with HA-DAB2IP together with plasmids expressing p53 mutants fused to MBP. After purification on amylose resin, HA-DAB2IP bound to mutp53 was detected by western blot (top). Middle: DAB2IP in the lysate (1/40 inputs). Both panels are from the same autoradiography film (i.e., have the same exposure). Bottom: MBP-p53 fusion proteins (baits) after affinity purification.

(B) DAB2IP binds mutp53 through the C2 domain. Schematic representation of DAB2IP deletions used (PH, pleckstrin homology domain; C2, synGAP-like C2 domain; GAP, Ras-GTPase activating domain; DUF3498, domain of unknown function). Binding to MBP-p53(R175H) is indicated.

(C) p53 mutants bind DAB2IP through the DNA binding domain (DBD). Schematic representation of mutant p53 deletions used (TA, transactivation; Ct, oligomerization/C-terminal regulatory). Their interaction with HA-DAB2IP(1-186) is indicated.

(D) Cytoplasmic localization of mutant p53. MDA-MB-231 cells were subjected to fractionation to separate cytoplasm and nuclei. Equal fractions of each sample were analyzed by western blot. Tubulin (cytoplasmic) and Lamin C (nuclear) were blotted as controls.

(E) Endogenous p53(K280R) and p53(M237I) mutants were immunoprecipitated respectively from the cytoplasmic fraction of MDA-MB-231 and SUM-149 cells. Coprecipitated endogenous DAB2IP was detected by western blot. Sp1 was blotted to confirm cytoplasm purity. Input is 1/100 of the cytoplasmic fraction. See also Figure S3.

cells (Figure S3D). Using coimmunoprecipitation, we proved interaction between endogenous DAB2IP and mutp53 in the cytosolic fraction of MDA-MB-231, SUM-149, and PANC-1 cell lines (Figures 3E, S3F, and S7C), with different p53 mutants. No interaction was detected between endogenous DAB2IP and p53 in the cytosolic fraction of cells with wild-type p53 (Figure S3E). Thus, mutant p53 could affect TNF-induced activation of NF-κB and JNK by binding DAB2IP and interfering with its functions.

Inhibition of DAB2IP Defines a Cytoplasmic Gain of Function of mutp53

The above hypothesis implies that mutp53 should affect upstream events of the TNFα transduction cascade (Zhang et al., 2004). We analyzed TNF-induced IKBα and JNK phosphorylation as readouts of NF-κB and ASK1 signaling branches, respectively. In the absence of mutp53, phosphorylation and turnover of IKBα were significantly reduced, indicating less efficient activation (Figures 4A and S7D). Accordingly, nuclear translocation and activation of p65 RelA was also reduced (Figures 4C–4D and S3G).

Depletion of WT p53 had no impact on TNF-induced IKBα phosphorylation and p65 nuclear translocation in HCT116 cells (Figures S3H and S3I), supporting the notion that this phenotype is specific for mutant p53.

Oppositely, phosphorylation of JNK was increased and longer lasting in the absence of mutp53 (Figure 4B), as was phosphorylation of p38 MAPK, another ASK1 downstream kinase (Figure S3J). Together, these effects are consistent with mutp53 inhibiting DAB2IP and provide a mechanistic explanation for the coordinated impact of mutp53 on TNF-induced NF-κB and JNK activation.

The above hypothesis also implies that mutant p53 nuclear activities should not be required for the phenotype. To test this, we replaced the endogenous mutp53 of MDA-MB-231 cells with the same p53 mutant (R280K) deprived of nuclear localization signals (NLSs). Strikingly, expression of mutp53(ΔNLS) efficiently restored TNF-induced invasion in mutp53-depleted MDA-MB-231 cells (Figure 4E). The same was recapitulated in MCF-10A nontransformed cells; replacement of endogenous WT p53 with a cytoplasmic p53 mutant was sufficient to amplify TNF-induced migration (Figure 4F).

We conclude that this specific GOF of mutant p53, i.e., increased invasion triggered by inflammatory cytokines, is largely mediated by its cytoplasmic fraction.

The Effects of mutp53 in Modifying the Response to TNFα Depend on Its Binding to DAB2IP

To assess their functional relationship, we tested whether depletion of DAB2IP could rescue the effects of mutp53 knockdown in our cell models.

Silencing of DAB2IP restored TNF-induced invasion in mutp53-depleted MDA-MB-231 cells (Figures 5A and S4A). Similarly, DAB2IP knockdown protected mutp53-depleted SUM-149 cells from TNF-induced apoptosis (Figure 5B). The same relationship was confirmed in modulation of TNF-dependent

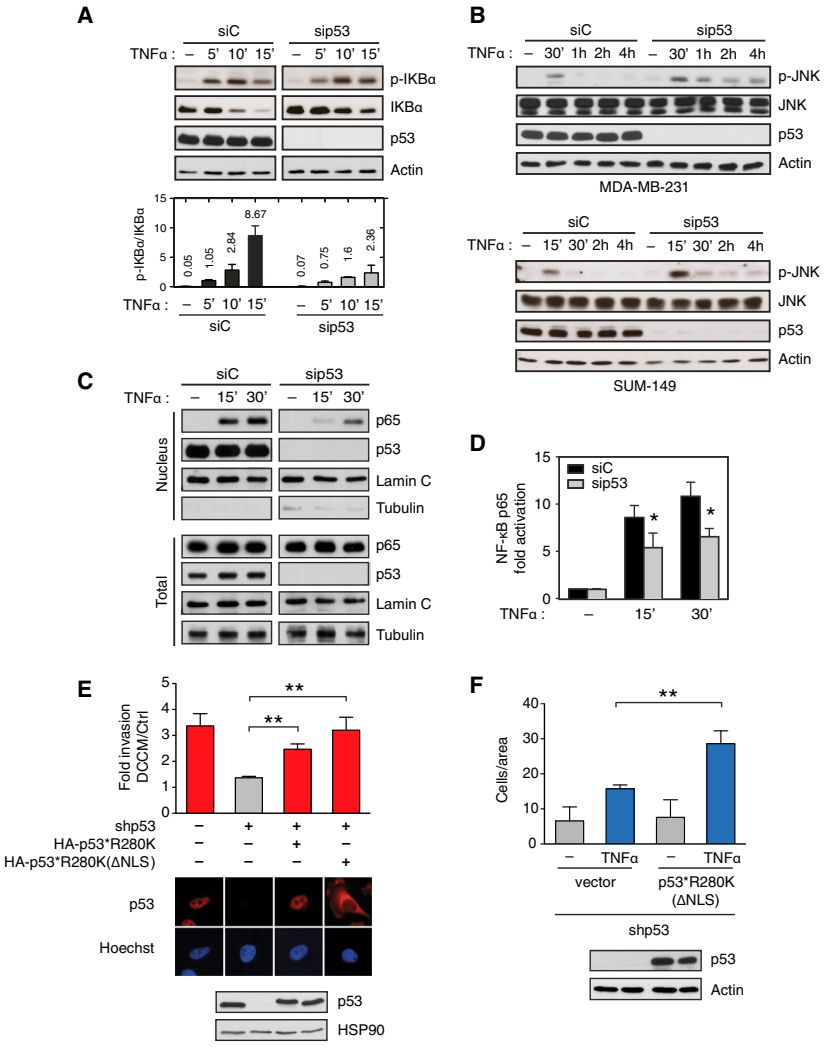

Figure 4. Cytoplasmic Gain of Function of Mutant p53 in the Response to TNFα

(A) Mutant p53 sustains TNF-induced phosphorylation and degradation of IKBα. MDA-MB-231 cells were silenced with indicated siRNAs, serum starved, and treated with TNFα (10 ng/ml). Phosphorylated and total IKBα were measured by immunoblotting. Bottom: the ratio of phosphorylated over total IKBα measured by densitometry on autoradiography films (mean ± SD; n = 3).

(B) Depletion of mutant p53 increases JNK activation by TNFα. Cells were treated as in (A). Phosphorylated and total JNK were analyzed by immunoblotting.

(C and D) Mutant p53 sustains TNF-induced nuclear translocation and activation of p65 RelA. (C) Cells were treated as in (A). At the indicated times cells were subjected to biochemical fractionation to separate cytoplasm and nuclei. Tubulin (cytoplasmic) and Lamin C (nuclear) were blotted as controls. (D) Sequence-specific DNA binding of p65 RelA was measured by ELISA in cells treated as in (A) (mean ± SEM; n = 4; *p < 0.02). Control immunoblots are shown in Figure S3G.

(E and F) Cytoplasmic mutant p53 promotes inflammation-driven invasion. (E) MDA-MB-231 cells stably silenced for mutp53 (shp53) were infected with retroviruses encoding shRNA-resistant (*) versions of p53(R280K) or its cytoplasmic variant p53(R280K)ΔNLS. Matrigel invasion assays with DCCM were done as in Figure 1A. Bars indicate the fold increase in migrated cells in DCCM versus Ctrl medium (mean ± SD; n = 3; **p < 0.01). Localization of mutp53 proteins (red) was verified by immunofluorescence. Expression levels were checked by western blot (bottom). (F) MCF-10A cells stably silenced for WT p53 (shp53) were infected with p53(R280K)ΔNLS retrovirus as in (E). Transwell migration assays with TNFα were performed as in Figure 1E (mean ± SD; n = 3; **p < 0.01). Expression of p53 was checked by western blot (bottom).

See also Figure S3.

transcription, whereby knockdown of DAB2IP strikingly reverted the effects of mutp53 depletion (Figures 5C, S4B, and S7E).

Finally, depletion of DAB2IP restored to normal the kinetics of TNF-induced IKBα, JNK, and p38 phosphorylation (Figures 5D–5F and S4C), as well as p65 nuclear translocation (Figure 5E), in mutp53 knockdown cells. In all these experiments, depletion of DAB2IP had a negligible impact on TNF-induced phenotypes in the presence of mutp53, strongly supporting an epistatic relationship between the two proteins.

Consistently, DAB2IP overexpression abolished the proinvasive behavior of MDA-MB-231 cells in response to inflammatory cytokines. Of note, escalating mutp53 levels in the cytoplasm, by overexpression of p53(R280K)ΔNLS, fully restored inflammation-induced invasion in DAB2IP-overexpressing cells (Figure 6A), strongly suggesting that mutp53 interferes with DAB2IP metastasis-suppressive functions.

DAB2IP interaction with the protein kinase ASK1 is required to funnel TNF-signaling toward the JNK pathway (Min et al., 2008; Zhang et al., 2003, 2004). In transient overexpression, we verified that increasing amounts of p53(R280K) caused a progressive reduction in the fraction of DAB2IP bound to ASK1 (Figures 6B and S5A). Analyzing endogenous proteins, we observed that depletion of mutant p53 in MDA-MB-231 cells increased the fraction of DAB2IP coimmunoprecipitated with ASK1 (Figure 6C). Together, these data indicate that mutp53 can compete with DAB2IP physiological interactors and in particular ASK1.

Disruption of the mutp53-DAB2IP Interaction Reduces the Invasive Behavior of Cancer Cells Exposed to Inflammation

We found that mutp53 binds to the N terminus of DAB2IP. To interfere with this interaction, we constructed a chimeric protein in which the first 186 amino acids of DAB2IP are fused to GFP. Since the C2 domain of DAB2IP is also involved in interaction with ASK1, we introduced a mutation that specifically prevents ASK1 binding (KA2, Figures S5B and S5C) (Zhang et al., 2003).

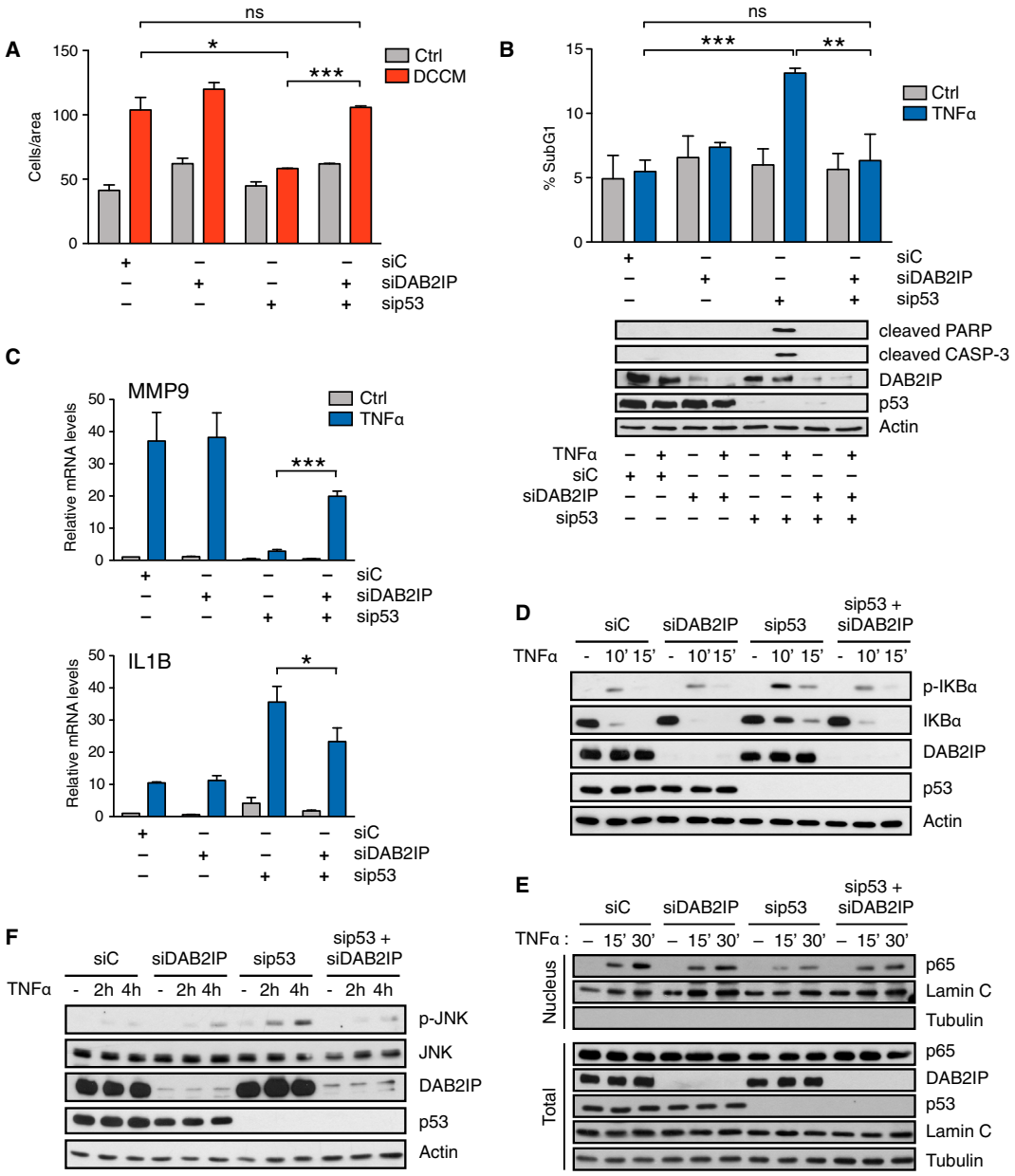

Figure 5. Functional Interaction between Mutant p53 and DAB2IP in the Response of Cancer Cells to Inflammatory Cytokines

(A) MDA-MB-231 were silenced for DAB2IP and/or mutp53 as indicated. Invasion assays were performed with DCCM as in Figure 1A (mean ± SD; n = 2; *p < 0.05; ***p < 0.001). Control immunoblot in Figure S4A.

(B) SUM-149 were silenced for DAB2IP and/or mutp53, serum starved, and treated with TNFα (10 ng/ml) for 24 hr. The fraction of cells in SubG1 was measured by flow cytometry (mean ± SD; n = 3; **p < 0.01; ***p < 0.001). The same cells were analyzed by western blot to detect cleaved PARP and CASP-3 (bottom).

(C) MDA-MB-231 were silenced for DAB2IP and/or mutp53. Expression of MMP9 and IL1B was measured by RT-qPCR after 20 hr of TNFα as in Figure 2 (mean ± SD; n = 3; *p < 0.05; ***p < 0.001). Control immunoblot in Figure S4B.

(D) MDA-MB-231 were silenced for DAB2IP and/or mutp53, and treated with TNFα as in Figure 4A. Phosphorylated and total IKBα were detected by immunoblotting.

(E) Cells treated as in (D) were subjected to biochemical fractionation to separate cytoplasm and nuclei. Tubulin (cytoplasmic) and Lamin C (nuclear) were blotted as controls.

(F) MDA-MB-231 were silenced for DAB2IP and/or mutp53 and treated with TNFα as in (D). Phosphorylated and total JNK were analyzed by immunoblotting.

See also Figure S4.

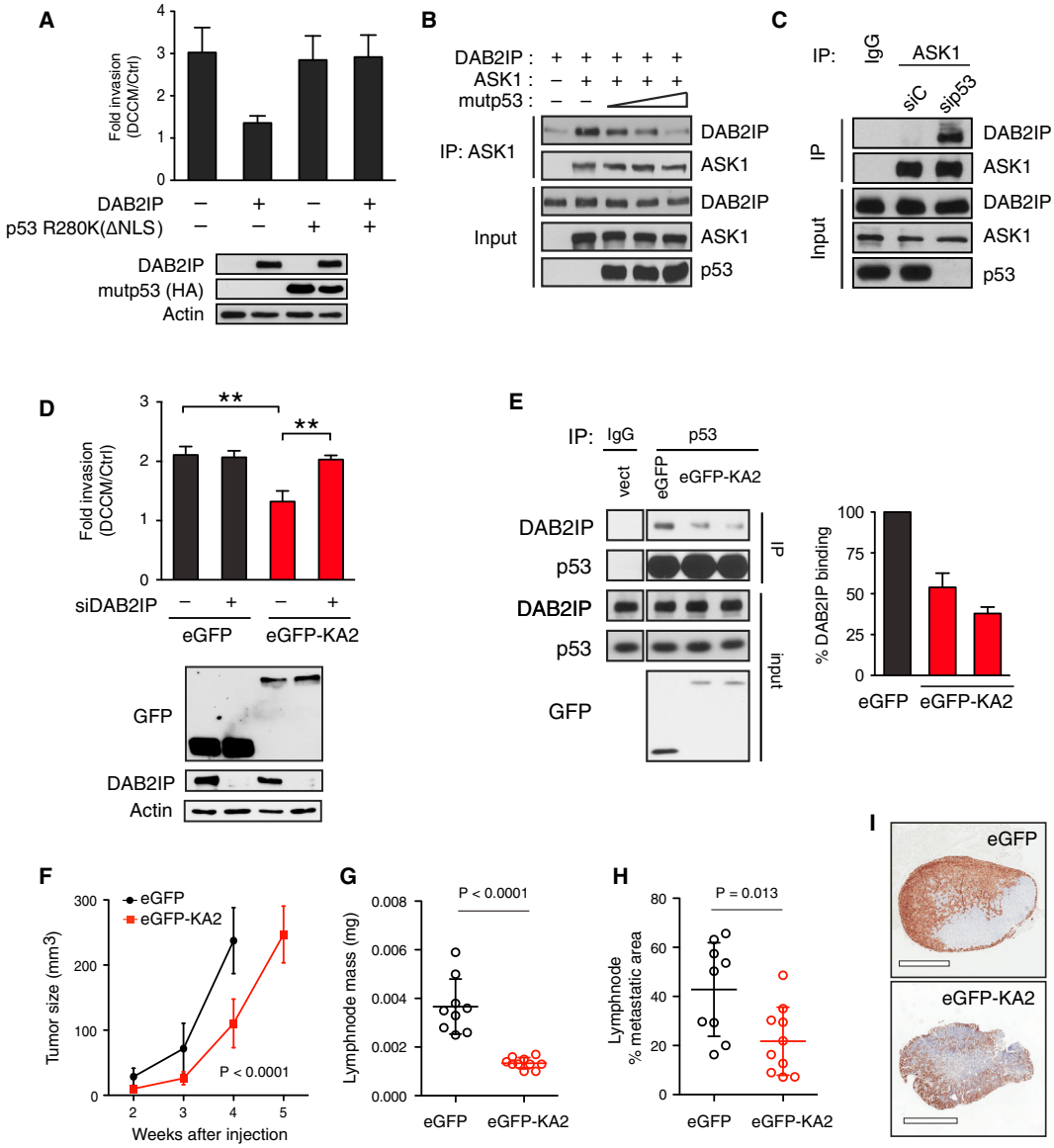

Figure 6. The mutp53-DAB2IP Interaction Is Required for the Invasive Response of Cancer Cells to Inflammation

(A) MDA-MB-231 cells stably overexpressing DAB2IP were infected with a retrovirus expressing HA-p53(R280K)ΔNLS or an empty retrovirus as a control. Invasion assays with DCCM were done as in Figure 1A; bars indicate the increase in cells migrated in DCCM versus Ctrl medium (mean ± SD; n = 3). Protein levels were checked by western blot (bottom).

(B) H1299 cells were cotransfected with plasmids expressing DAB2IP, HA-ASK1, and increasing amounts of p53(R280K). The fraction of DAB2IP bound to ASK1 was analyzed by western blot of ASK1 immunoprecipitates. Quantification is reported in Figure S5A.

(C) MDA-MB-231 cells were transfected with control or p53 siRNA. Endogenous DAB2IP bound to ASK1 was analyzed by coimmunoprecipitation with anti-ASK1 antibody.

(D) MDA-MB-231 cells were stably transduced with retroviruses expressing eGFP-DAB2IP$_{1\text{-}186}$KA2 fusion protein (eGFP-KA2) or eGFP alone, with or without DAB2IP siRNA as indicated. Invasion assays were performed as in (A) (**p < 0.01). Expression of eGFP proteins and endogenous DAB2IP was analyzed by western blot (bottom).

(E) Endogenous mutp53 was immunoprecipitated from MDA-MB-231 cells stably expressing eGFP or eGFP-KA2 (two lines derived from independent infections); coprecipitated endogenous DAB2IP was analyzed by western blot. Specificity was checked using unrelated IgG (panels are from the same autoradiography). The fraction of DAB2IP bound to mutp53 was quantified by densitometry; bars represents the DAB2IP$_{(co\text{-}IP)}$/DAB2IP$_{(input)}$ ratio, normalized to the eGFP sample (mean ± SD; n = 3).

(F–I) Expression of DAB2IP$_{1\text{-}186}$KA2 reduces growth and dissemination of cancer cells in immunocompromised mice. MDA-MB-231 cells stably expressing eGFP or eGFP-KA2 were injected in the mammary fat pad of SCID mice and different parameters of tumor progression were evaluated. (F) Kinetics of primary tumor

(legend continued on next page)

Invasion assays were performed with MDA-MB-231 expressing the eGFP-DAB2IP(1-186)KA2 fusion protein. The KA2 decoy protein had no obvious effects on cell growth and motility, but clearly reduced invasion triggered by inflammatory cytokines; notably, this effect requires DAB2IP (Figures 6D and S5D). The inhibitory action of the KA2 peptide was also verified in PANC-1 cells (Figure S7F).

Mechanistically, overexpression of the KA2 decoy significantly diminished the amount of endogenous DAB2IP coimmunoprecipitated with mutp53 (Figure 6E), confirming that reduced invasion might be due to an increase in "free" DAB2IP protein.

We next extended these experiments to an in vivo model. When injected orthotopically in the fat pad of nude mice, MDA-MB-231 cells expressing the KA2 fusion protein formed smaller tumors than control eGFP-expressing cells (Figure 6F), indicating reduced aggressiveness. To evaluate metastatic dissemination, homolateral axillary lymph nodes were collected and screened for invading human cells when the primary tumors reached a similar size. Gross weight and immunohistochemistry (Figures 6G–6I and S5E) confirmed that KA2-expressing cells were less abundant in lymph nodes than eGFP-expressing controls, clearly indicating reduced metastasis. Importantly, analysis of primary tumors confirmed that mutp53 levels were not affected (Figure S5F).

Implications of the mutp53/DAB2IP Interaction in Breast Cancer: A Meta-analysis

To explore the potential clinical impact of this molecular axis, we analyzed public gene expression data sets. We focused on basal-like triple negative breast cancers (TNBCs) that have a high frequency of p53 mutation and are an outstanding challenge for clinical management (Carey et al., 2010; Foulkes et al., 2010; Walerych et al., 2012).

We used a large metadata set of 19 independent studies, consisting of 3,254 individuals (see Supplemental Information) (Rustighi et al., 2014), and stratified patients based on expression of the mutp53-dependent TNF-inducible genes that were identified in MDA-MB-231 cells (Figure 2). To minimize cell line bias, we selected a subset of these genes consistently coexpressed in mutp53-enriched breast cancers (upsiC10, Figure S6A). The upsiC10 signature was not prognostic on the entire data set, but correlated with prolonged disease-free survival (DFS) in basal/TNBC patients (Figure 7A). We next restricted our analysis to data sets with information on p53 status. Notably, the upsiC10 metagene was predictive of survival specifically in patients with mutant p53 (Figure 7B). Similar results were obtained using all genes in the TNF-upsiC group (Figure S6B and Table S3).

Since mutp53 makes cancer cells more invasive in response to inflammation in vitro, the improved patients' survival suggests a host interaction effect. We noticed that genes associated to the TNFα/mutp53 axis include powerful chemokines that can promote recruitment of immune cells (Figures 2 and S2D), and an increased B and T cell infiltrate has been correlated to prolonged DFS in breast cancer (Finak et al., 2008; Fridman et al., 2012). We thus analyzed expression of immune-specific gene signatures as a proxy to infer amount and composition of infiltrating lymphocytes in tumor samples. We used previously published metagenes already validated in colon (Bindea et al., 2013) and breast cancer (Rody et al., 2009, 2011).

Within our cohort of basal breast cancers, lymphocyte metagenes were significantly more expressed in tumors with higher expression of the upsiC10 signature (Figures 7C and S6C), indicative of increased infiltration. Intriguingly, we found higher expression of cytotoxic (CTL+NK) and Th1, but not Th2, metagenes, suggesting that infiltrating T cells might be preferentially polarized toward a proinflammatory phenotype.

In line with studies by others (Rody et al., 2009, 2011), high expression of immune metagenes (with the remarkable exception of Th2 cells) correlated with prolonged DFS in basal/TNBC patients (Figures 7D and S6D). Strikingly, expression of immune metagenes correlated with better DFS specifically in tumors with mutant p53 (Figure 7E and Table S3).

Together, these observations suggest that mutp53 reprograms inflammatory signaling toward a gene expression profile that increases cell motility and survival but also promotes activation of tumor immune cells, potentially affecting clinical outcome.

DISCUSSION

Various evidences, including our work, indicate that mutation of p53 plays a primary role in the relationship between inflammation and cancer, suggesting that mutp53 may shift the effects of inflammation toward oncogenic outcomes. A recent study showed that p53 missense mutation can be a driver in inflammation-induced cancer formation (Cooks et al., 2013). Here, we demonstrate that mutp53 can also drive inflammation-induced cancer progression.

We observed that mutant p53 can influence multiple downstream molecular pathways activated by the TNF receptor. While confirming that mutp53 sustains TNF-induced activation of NF-κB, as previously reported by others (Cooks et al., 2013; Schneider et al., 2010; Weisz et al., 2007), we demonstrated that mutp53 also dims TNF-induced activation of ASK1/JNK. This dual effect is translated in a characteristic gene expression profile, with strong activation of a group of NF-κB target genes, but reduced or no activation of another group of NF-κB target genes.

Previous studies reported that mutp53 is recruited to κB sites on the promoters of inflammatory genes in response to TNFα (Cooks et al., 2013; Schneider et al., 2010; Weisz et al., 2007). We discovered that mutp53 also acts upstream, shifting the balance between activation of the NF-κB and ASK1/JNK pathways in response to TNFα. Mechanistically, a fraction of

growth. eGFP, black (n = 10); eGFP-KA2, red (n = 10). (G) Weight of homolateral lymph nodes when primary tumors reached similar size. eGFP, black, 4 weeks (n = 9); eGFP-KA2, red, 5 weeks (n = 10). (H) Percentage of area occupied by invading cells in lymph nodes, quantified by immunohistochemistry of human cytokeratin. (I) Representative sections of lymph nodes stained for human cytokeratin (bar = 1 mm).
See also Figure S5.

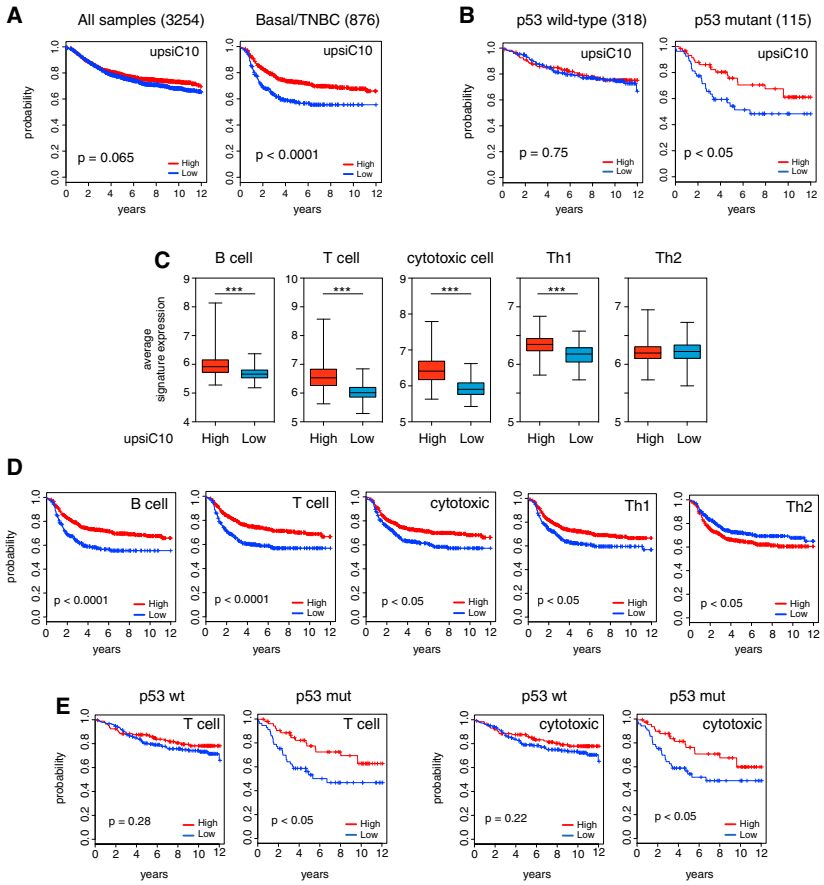

Figure 7. In Silico Analysis Reveals a Potential Impact of the TNF/mutp53 Axis in the Clinical Outcome of Breast Cancer

(A) Kaplan-Meier (K-M) survival curves for high or low expression of the upsiC10 signature in a large breast cancer metadata set and basal-like/TNBC samples (see Supplemental Information for details).

(B) K-M survival curves for high or low expression of the upsiC10 signature in breast cancers with known p53 status.

(C) Expression of metagenes identifying specific immune cell populations (Bindea et al., 2013) in basal-like/TNBC breast cancers divided according to high or low expression of the upsiC10 signature (***$p < 0.0001$).

(D) K-M survival curves for high or low expression of immune metagenes in basal-like/TNBC breast cancers.

(E) K-M survival curves for high or low expression of T cell and cytotoxic cell metagenes in breast cancers with known p53 status.

See also Figure S6 and Table S3.

mutp53 binds DAB2IP in the cytoplasm, interfering with formation of TNF-induced signaling complexes that activate the ASK1/JNK axis, thereby promoting activation of NF-κB.

DAB2IP is a tumor suppressor protein that is rarely mutated in cancer but is often silenced by promoter methylation (Dote et al., 2004; Qiu et al., 2007). Our data indicate that binding by mutp53 is an alternative means to inactivate DAB2IP functions in cancer. Notably, experiments with nuclear-excluded p53 mutants indicate that this activity may be sufficient to mediate the invasive response triggered by inflammatory cytokines in cancer cells. So, this is a bona fide cytoplasmic gain of function of mutp53.

In addition to funneling TNFα signals toward growth-restraining activation of ASK1, DAB2IP negatively modulates multiple oncogenic signaling pathways: most notably Ras and Akt (Min et al., 2010; Xie et al., 2009, 2010). It is quite possible that the mutp53/DAB2IP interaction in cancer cells may have broader effects than promoting inflammation-induced invasion. For instance, a role of mutant p53 has been described in sustaining Ras (Sauer et al., 2010) as well as Akt activation (Dong et al., 2009), but a convincing mechanism has not been described. It is possible that the mutp53/DAB2IP interaction might partially explain those observations as well.

DAB2IP can bind also WT p53, at least in vitro and in transient overexpression (Lunardi et al., 2010), raising interesting questions on whether such interaction can occur physiologically. In normal conditions, WT p53 concentration in the cytoplasm is very low, and we could not detect binding of the endogenous proteins. Accordingly, WT p53 depletion had no impact on DAB2IP-dependent TNF signaling steps (Figure S3), strongly indicating that the phenotypes described here are peculiar to mutant p53. Nonetheless, it is tempting to speculate that binding with DAB2IP can occur upon specific stress conditions that increase cytoplasmic p53, thus potentially linking p53 to nontranscriptional modulation of multiple signaling pathways. Additional work will be required to explore this possibility and its implications.

Our finding that tumor-derived p53 mutants can bind DAB2IP in the cytoplasm, competing with functionally relevant DAB2IP protein partners, provides striking evidence that mutant p53 can gain oncogenic functions by making nonphysiological interactions with other proteins—not necessarily transcription factors—and interfering with their function (Muller and Vousden, 2013; Oren and Rotter, 2010).

We tested the above principle by designing a fusion protein that can interfere with mutp53-DAB2IP binding. Notably, expression of such decoy abolished TNF-induced invasion in vitro, and xenograft growth and dissemination in vivo, confirming that this interaction is functionally relevant. These results provide a crucial proof of principle that peptide or nucleotide aptamers designed to interfere with the mutp53/DAB2IP interaction might have a potential application in targeted therapy of mutp53 cancers. Future work in this direction is warranted.

Various studies described WT p53 as an important mediator in the crosstalk between inflammatory microenvironment and cell behavior. In a complex interplay with NF-κB, p53 modulates expression of immune-response and inflammation genes; such

secretory phenotypes can contribute to tumor suppression in a non-cell-autonomous manner, for instance, controlling the inflammatory microenvironment and promoting macrophage M1- versus M2-type polarization (Lowe et al., 2013; Lujambio et al., 2013; Schwitalla et al., 2013). Loss of p53 can thus affect inflammatory pathways, eventually contributing to tumor formation.

In this study, we provide compelling evidence that mutation of p53, compared to its loss, confers additional properties to cancer cells, making them more aggressive in response to inflammatory cytokines and in particular TNFα. Intriguingly, our data also indicate that cancer cells with mutant p53 respond to TNFα by expressing secreted molecules that promote recruitment of immune cells, a phenomenon that can be tumor restraining (Fridman et al., 2012; Galon et al., 2013). We think this is a sort of "Achilles' heel" of mutp53 cancers; in response to inflammation, mutp53-modulated activation of NF-κB conveys powerful proinvasive and prosurvival activities but, at the same time, triggers expression of chemokines that can recruit leukocytes and modulate their functions within the tumor. Increased recruitment of B and T cells is associated with longer relapse-free survival in breast and other cancers (Fridman et al., 2012; Lee et al., 2013; Schmidt et al., 2008). Accordingly, our in silico studies indicate that cancers with mutant p53 have a better outcome if they express a gene signature linked to the mutp53/TNFα axis. These observations suggest that a relatively simple standard clinical-pathological parameter such as quantity and quality of infiltrating immune cells—i.e., the immunoscore (Galon et al., 2013)—may improve prediction of the clinical outcome of mammary tumors with mutant p53.

EXPERIMENTAL PROCEDURES

Cell Lines and Treatments

The following human cell lines were used: MDA-MB-231 (p53R280K), MDA-MB-468 (p53R273H), SUM-149 (p53M237I), PANC-1 (p53R273H), MCF-10A (p53 wild-type), HCT116 (p53 wild-type), and U2OS (p53 wild-type).

For gene expression analysis, cells were treated with recombinant human TNFα (10 ng/ml) in low serum (0.1% FBS) for the indicated times. When necessary, JNK (SP600125) and NF-κB (BAY11-7082) inhibitors were added to the medium 2 hr before TNFα. For analysis of IKBα, p38, and JNK phosphorylation, cells were serum starved for 24 hr before TNFα (10 ng/ml) addition.

Migration and Invasion Assays

For transwell migration assays, cells (0.5–1 × 10^5) were plated on 24-well PET inserts (8.0 μm pore size, Falcon). For invasion assays, cells (0.5–1 × 10^5) were plated on 24-well PET inserts (8.0 μm pore size, Falcon) coated with BD Matrigel (BD Bioscience). Cells that passed through the filter were fixed, stained, and counted after 16 hr or 18 hr, respectively. For invasion assays using DCCM, cells were seeded in 10% FBS on the upper chamber, while the lower chamber was filled with DCCM or control medium.

For invasion or transwell assays using recombinant TNFα, cells were pretreated with the cytokine; specifically, cells were kept in low (0.1%) serum with or without TNFα (10 ng/ml) for 24 hr. Subsequently, cells were trypsinized, counted, and reseeded on filters in low serum, with or without TNFα. The lower chamber was filled with high serum medium without TNFα.

Gene Expression Analysis

Total RNA was extracted with QIAzol (QIAGEN). For RT-qPCR, 1 μg of total RNA was reverse transcribed with QuantiTect Reverse Transcription kit (QIAGEN). Real-time PCR was performed using SsoAdvanced SYBR Green Master Mix (Biorad) on a CFX96 Real-Time PCR System (Biorad). Primer sequences are listed in Supplemental Experimental Procedures.

For microarrays, three biological replicates for each group (siC, siC_TNF, sip53, sip53_TNF) were hybridized on HumanHT-12-v4-BeadChip (Illumina). Processing and analysis of the data are described in detail in Supplemental Experimental Procedures.

In Vivo Tumorigenicity and Metastasis Assays

For xenografts, cells (1 × 10^6) were resuspended in 100 μl of DMEM and injected into the mammary fat pad of previously anesthetized 6-week-old SCID female mice. Tumor growth at the injection site was monitored by caliper measurements. For metastasis evaluation, animals were anesthetized and sacrificed at times when tumors were of similar size. Primary tumors were extracted and directly frozen in liquid nitrogen for molecular analyses. Lymph nodes were excised, weighted, formalin fixed, and paraffin embedded for hematoxylin-eosin staining and Cytokeratin 7 immunohistochemistry.

ACCESSION NUMBERS

The MDA-MB-231 expression array experiment was deposited in GEO with accession number GSE53153.

SUPPLEMENTAL INFORMATION

Supplemental Information includes Supplemental Experimental Procedures, seven figures, and three tables and can be found with this article online at http://dx.doi.org/10.1016/j.molcel.2014.10.013.

AUTHOR CONTRIBUTIONS

G.D.M. and A.B. designed and performed most experiments and contributed equally to this work. M.D.F., G.C., D.R., and R.S. performed in vitro and in vivo experiments. S.N., S.P., and L.C. did bioinformatics analyses. R.B., A.R., S.B., and G.D.S. supervised experiments and discussed and interpreted results of the study. G.D.M., A.B., and L.C. conceptualized the work and wrote the manuscript. L.C. supervised the project.

ACKNOWLEDGMENTS

We thank Karen H. Cichowski for providing DAB2IP expression constructs. We thank Federica Benvenuti and Miguel Mano for sharing reagents and occasional use of their equipment. We thank Dawid Walerych for plasmids encoding shRNA-resistant p53 mutants, Valeria Capaci and Alice Grison for help with microscopy, and Ramiro Mendoza for help with fractionations. We thank Giada Pastore for assistance with tissue culture. We acknowledge Andrea Lunardi, who did the very first mutp53-DAB2IP interaction assay. This work was supported by grants from AIRC (Italian Association for Cancer Research, IG 9208 and IG 14173) and Università degli Studi di Trieste (FRA 2012) to L.C. This work was also supported by grants from AIRC Special Program Molecular Clinical Oncology "5 per mille," and by MIUR (Italian Ministry for University and Research, PRIN2009) to G.D.S. G.D.M. was supported by a FIRC (Fondazione Italiana Ricerca sul Cancro) postdoctoral fellowship.

Received: January 8, 2014
Revised: July 16, 2014
Accepted: October 9, 2014
Published: November 13, 2014

REFERENCES

Adorno, M., Cordenonsi, M., Montagner, M., Dupont, S., Wong, C., Hann, B., Solari, A., Bobisse, S., Rondina, M.B., Guzzardo, V., et al. (2009). A Mutant-p53/Smad complex opposes p63 to empower TGFbeta-induced metastasis. Cell *137*, 87–98.

Bindea, G., Mlecnik, B., Tosolini, M., Kirilovsky, A., Waldner, M., Obenauf, A.C., Angell, H., Fredriksen, T., Lafontaine, L., Berger, A., et al. (2013).

Spatiotemporal dynamics of intratumoral immune cells reveal the immune landscape in human cancer. Immunity *39*, 782–795.

Bjordahl, R.L., Steidl, C., Gascoyne, R.D., and Ware, C.F. (2013). Lymphotoxin network pathways shape the tumor microenvironment. Curr. Opin. Immunol. *25*, 222–229.

Carey, L., Winer, E., Viale, G., Cameron, D., and Gianni, L. (2010). Triple-negative breast cancer: disease entity or title of convenience? Nat. Rev. Clin. Oncol. *7*, 683–692.

Cooks, T., Pateras, I.S., Tarcic, O., Solomon, H., Schetter, A.J., Wilder, S., Lozano, G., Pikarsky, E., Forshew, T., Rosenfeld, N., et al. (2013). Mutant p53 prolongs NF-κB activation and promotes chronic inflammation and inflammation-associated colorectal cancer. Cancer Cell *23*, 634–646.

Curtis, C., Shah, S.P., Chin, S.-F., Turashvili, G., Rueda, O.M., Dunning, M.J., Speed, D., Lynch, A.G., Samarajiwa, S., Yuan, Y., et al.; METABRIC Group (2012). The genomic and transcriptomic architecture of 2,000 breast tumours reveals novel subgroups. Nature *486*, 346–352.

Dong, P., Xu, Z., Jia, N., Li, D., and Feng, Y. (2009). Elevated expression of p53 gain-of-function mutation R175H in endometrial cancer cells can increase the invasive phenotypes by activation of the EGFR/PI3K/AKT pathway. Mol. Cancer *8*, 103.

Dote, H., Toyooka, S., Tsukuda, K., Yano, M., Ouchida, M., Doihara, H., Suzuki, M., Chen, H., Hsieh, J.T., Gazdar, A.F., and Shimizu, N. (2004). Aberrant promoter methylation in human DAB2 interactive protein (hDAB2IP) gene in breast cancer. Clin. Cancer Res. *10*, 2082–2089.

Duffy, M.J., Maguire, T.M., Hill, A., McDermott, E., and O'Higgins, N. (2000). Metalloproteinases: role in breast carcinogenesis, invasion and metastasis. Breast Cancer Res. *2*, 252–257.

Finak, G., Bertos, N., Pepin, F., Sadekova, S., Souleimanova, M., Zhao, H., Chen, H., Omeroglu, G., Meterissian, S., Omeroglu, A., et al. (2008). Stromal gene expression predicts clinical outcome in breast cancer. Nat. Med. *14*, 518–527.

Foulkes, W.D., Smith, I.E., and Reis-Filho, J.S. (2010). Triple-negative breast cancer. N. Engl. J. Med. *363*, 1938–1948.

Fridman, W.H., Pagès, F., Sautès-Fridman, C., and Galon, J. (2012). The immune contexture in human tumours: impact on clinical outcome. Nat. Rev. Cancer *12*, 298–306.

Galon, J., Angell, H.K., Bedognetti, D., and Marincola, F.M. (2013). The continuum of cancer immunosurveillance: prognostic, predictive, and mechanistic signatures. Immunity *39*, 11–26.

Grivennikov, S.I., Greten, F.R., and Karin, M. (2010). Immunity, inflammation, and cancer. Cell *140*, 883–899.

Hsieh, M.J., Chen, K.S., Chiou, H.L., and Hsieh, Y.S. (2010). Carbonic anhydrase XII promotes invasion and migration ability of MDA-MB-231 breast cancer cells through the p38 MAPK signaling pathway. Eur. J. Cell Biol. *89*, 598–606.

Lee, H.J., Seo, J.-Y., Ahn, J.-H., Ahn, S.-H., and Gong, G. (2013). Tumor-associated lymphocytes predict response to neoadjuvant chemotherapy in breast cancer patients. J. Breast Cancer *16*, 32–39.

Lowe, J., Shatz, M., Resnick, M., and Menendez, D. (2013). Modulation of immune responses by the tumor suppressor p53. BioDiscovery *8*, 2, http://dx.doi.org/10.7750/BioDiscovery.2013.8.2.

Lujambio, A., Akkari, L., Simon, J., Grace, D., Tschaharganeh, D.F., Bolden, J.E., Zhao, Z., Thapar, V., Joyce, J.A., Krizhanovsky, V., and Lowe, S.W. (2013). Non-cell-autonomous tumor suppression by p53. Cell *153*, 449–460.

Lunardi, A., Di Minin, G., Provero, P., Dal Ferro, M., Carotti, M., Del Sal, G., and Collavin, L. (2010). A genome-scale protein interaction profile of Drosophila p53 uncovers additional nodes of the human p53 network. Proc. Natl. Acad. Sci. USA *107*, 6322–6327.

Miller, T.W., Balko, J.M., Ghazoui, Z., Dunbier, A., Anderson, H., Dowsett, M., González-Angulo, A.M., Mills, G.B., Miller, W.R., Wu, H., et al. (2011). A gene expression signature from human breast cancer cells with acquired hormone independence identifies MYC as a mediator of antiestrogen resistance. Clin. Cancer Res. *17*, 2024–2034.

Min, W., Lin, Y., Tang, S., Yu, L., Zhang, H., Wan, T., Luhn, T., Fu, H., and Chen, H. (2008). AIP1 recruits phosphatase PP2A to ASK1 in tumor necrosis factor-induced ASK1-JNK activation. Circ. Res. *102*, 840–848.

Min, J., Zaslavsky, A., Fedele, G., McLaughlin, S.K., Reczek, E.E., De Raedt, T., Guney, I., Strochlic, D.E., Macconaill, L.E., Beroukhim, R., et al. (2010). An oncogene-tumor suppressor cascade drives metastatic prostate cancer by coordinately activating Ras and nuclear factor-kappaB. Nat. Med. *16*, 286–294.

Moustakas, A., Pardali, K., Gaal, A., and Heldin, C.H. (2002). Mechanisms of TGF-beta signaling in regulation of cell growth and differentiation. Immunol. Lett. *82*, 85–91.

Muller, P.A.J., and Vousden, K.H. (2013). p53 mutations in cancer. Nat. Cell Biol. *15*, 2–8.

Muthuswamy, R., Berk, E., Junecko, B.F., Zeh, H.J., Zureikat, A.H., Normolle, D., Luong, T.M., Reinhart, T.A., Bartlett, D.L., and Kalinski, P. (2012). NF-κB hyperactivation in tumor tissues allows tumor-selective reprogramming of the chemokine microenvironment to enhance the recruitment of cytolytic T effector cells. Cancer Res. *72*, 3735–3743.

Oren, M., and Rotter, V. (2010). Mutant p53 gain-of-function in cancer. Cold Spring Harb. Perspect. Biol. *2*, a001107.

Qiu, G.-H., Xie, H., Wheelhouse, N., Harrison, D., Chen, G.G., Salto-Tellez, M., Lai, P., Ross, J.A., and Hooi, S.C. (2007). Differential expression of hDAB2IPA and hDAB2IPB in normal tissues and promoter methylation of hDAB2IPA in hepatocellular carcinoma. J. Hepatol. *46*, 655–663.

Rody, A., Holtrich, U., Pusztai, L., Liedtke, C., Gaetje, R., Ruckhaeberle, E., Solbach, C., Hanker, L., Ahr, A., Metzler, D., et al. (2009). T-cell metagene predicts a favorable prognosis in estrogen receptor-negative and HER2-positive breast cancers. Breast Cancer Res. *11*, R15.

Rody, A., Karn, T., Liedtke, C., Pusztai, L., Ruckhaeberle, E., Hanker, L., Gaetje, R., Solbach, C., Ahr, A., Metzler, D., et al. (2011). A clinically relevant gene signature in triple negative and basal-like breast cancer. Breast Cancer Res. *13*, R97.

Rustighi, A., Zannini, A., Tiberi, L., Sommaggio, R., Piazza, S., Sorrentino, G., Nuzzo, S., Tuscano, A., Eterno, V., Benvenuti, F., et al. (2014). Prolyl-isomerase Pin1 controls normal and cancer stem cells of the breast. EMBO Mol Med *6*, 99–119.

Sauer, L., Gitenay, D., Vo, C., and Baron, V.T. (2010). Mutant p53 initiates a feedback loop that involves Egr-1/EGF receptor/ERK in prostate cancer cells. Oncogene *29*, 2628–2637.

Schmidt, M., Böhm, D., von Törne, C., Steiner, E., Puhl, A., Pilch, H., Lehr, H.A., Hengstler, J.G., Kölbl, H., and Gehrmann, M. (2008). The humoral immune system has a key prognostic impact in node-negative breast cancer. Cancer Res. *68*, 5405–5413.

Schneider, G., Henrich, A., Greiner, G., Wolf, V., Lovas, A., Wieczorek, M., Wagner, T., Reichardt, S., von Werder, A., Schmid, R.M., et al. (2010). Cross talk between stimulated NF-kappaB and the tumor suppressor p53. Oncogene *29*, 2795–2806.

Schwitalla, S., Ziegler, P.K., Horst, D., Becker, V., Kerle, I., Begus-Nahrmann, Y., Lechel, A., Rudolph, K.L., Langer, R., Slotta-Huspenina, J., et al. (2013). Loss of p53 in enterocytes generates an inflammatory microenvironment enabling invasion and lymph node metastasis of carcinogen-induced colorectal tumors. Cancer Cell *23*, 93–106.

Shin, S.Y., Nam, J.S., Lim, Y., and Lee, Y.H. (2010). TNFα-exposed bone marrow-derived mesenchymal stem cells promote locomotion of MDA-MB-231 breast cancer cells through transcriptional activation of CXCR3 ligand chemokines. J. Biol. Chem. *285*, 30731–30740.

Solomon, H., Madar, S., and Rotter, V. (2011). Mutant p53 gain of function is interwoven into the hallmarks of cancer. J. Pathol. *225*, 475–478.

Solomon, H., Buganim, Y., Kogan-Sakin, I., Pomeraniec, L., Assia, Y., Madar, S., Goldstein, I., Brosh, R., Kalo, E., Beatus, T., et al. (2012). Various p53 mutant proteins differently regulate the Ras circuit to induce a cancer-related gene signature. J. Cell Sci. *125*, 3144–3152.

Wajant, H., Pfizenmaier, K., and Scheurich, P. (2003). Tumor necrosis factor signaling. Cell Death Differ. *10*, 45–65.

Walerych, D., Napoli, M., Collavin, L., and Del Sal, G. (2012). The rebel angel: mutant p53 as the driving oncogene in breast cancer. Carcinogenesis *33*, 2007–2017.

Weisz, L., Damalas, A., Liontos, M., Karakaidos, P., Fontemaggi, G., Maor-Aloni, R., Kalis, M., Levrero, M., Strano, S., Gorgoulis, V.G., et al. (2007). Mutant p53 enhances nuclear factor kappaB activation by tumor necrosis factor alpha in cancer cells. Cancer Res. *67*, 2396–2401.

Xie, D., Gore, C., Zhou, J., Pong, R.C., Zhang, H., Yu, L., Vessella, R.L., Min, W., and Hsieh, J.T. (2009). DAB2IP coordinates both PI3K-Akt and ASK1 pathways for cell survival and apoptosis. Proc. Natl. Acad. Sci. USA *106*, 19878–19883.

Xie, D., Gore, C., Liu, J., Pong, R.C., Mason, R., Hao, G., Long, M., Kabbani, W., Yu, L., Zhang, H., et al. (2010). Role of DAB2IP in modulating epithelial-to-mesenchymal transition and prostate cancer metastasis. Proc. Natl. Acad. Sci. USA *107*, 2485–2490.

Xin, H., Kikuchi, T., Andarini, S., Ohkouchi, S., Suzuki, T., Nukiwa, T., Huqun, Hagiwara, K., Honjo, T., and Saijo, Y. (2005). Antitumor immune response by CX3CL1 fractalkine gene transfer depends on both NK and T cells. Eur. J. Immunol. *35*, 1371–1380.

Yeudall, W.A., Vaughan, C.A., Miyazaki, H., Ramamoorthy, M., Choi, M.-Y., Chapman, C.G., Wang, H., Black, E., Bulysheva, A.A., Deb, S.P., et al. (2012). Gain-of-function mutant p53 upregulates CXC chemokines and enhances cell migration. Carcinogenesis *33*, 442–451.

Zhang, R., He, X., Liu, W., Lu, M., Hsieh, J.T., and Min, W. (2003). AIP1 mediates TNF-alpha-induced ASK1 activation by facilitating dissociation of ASK1 from its inhibitor 14-3-3. J. Clin. Invest. *111*, 1933–1943.

Zhang, H., Zhang, R., Luo, Y., D'Alessio, A., Pober, J.S., and Min, W. (2004). AIP1/DAB2IP, a novel member of the Ras-GAP family, transduces TRAF2-induced ASK1-JNK activation. J. Biol. Chem. *279*, 44955–44965.

Molecular Cell, Volume *56*
Supplemental Information

Mutant p53 Reprograms TNF Signaling in Cancer Cells through Interaction with the Tumor Suppressor DAB2IP

Giulio Di Minin, Arianna Bellazzo, Marco Dal Ferro, Giulia Chiaruttini, Simona Nuzzo, Silvio Bicciato, Silvano Piazza, Damiano Rami, Roberta Bulla, Roberta Sommaggio, Antonio Rosato, Giannino Del Sal, and Licio Collavin

Figure S1 (related to Fig 1) - Di Minin et al., Collavin

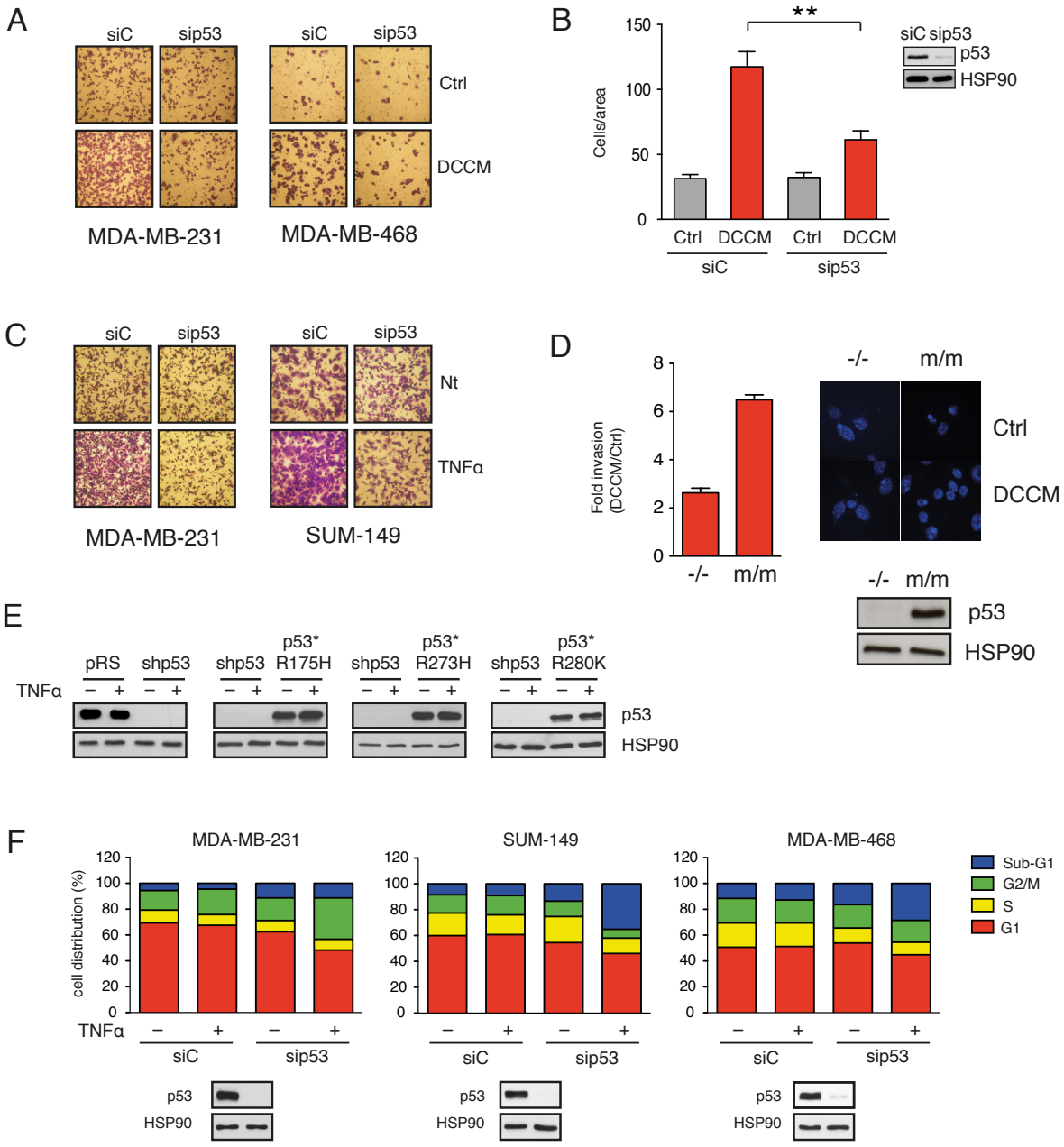

Figure S2 (related to Figure 2) - Di Minin et al., Collavin

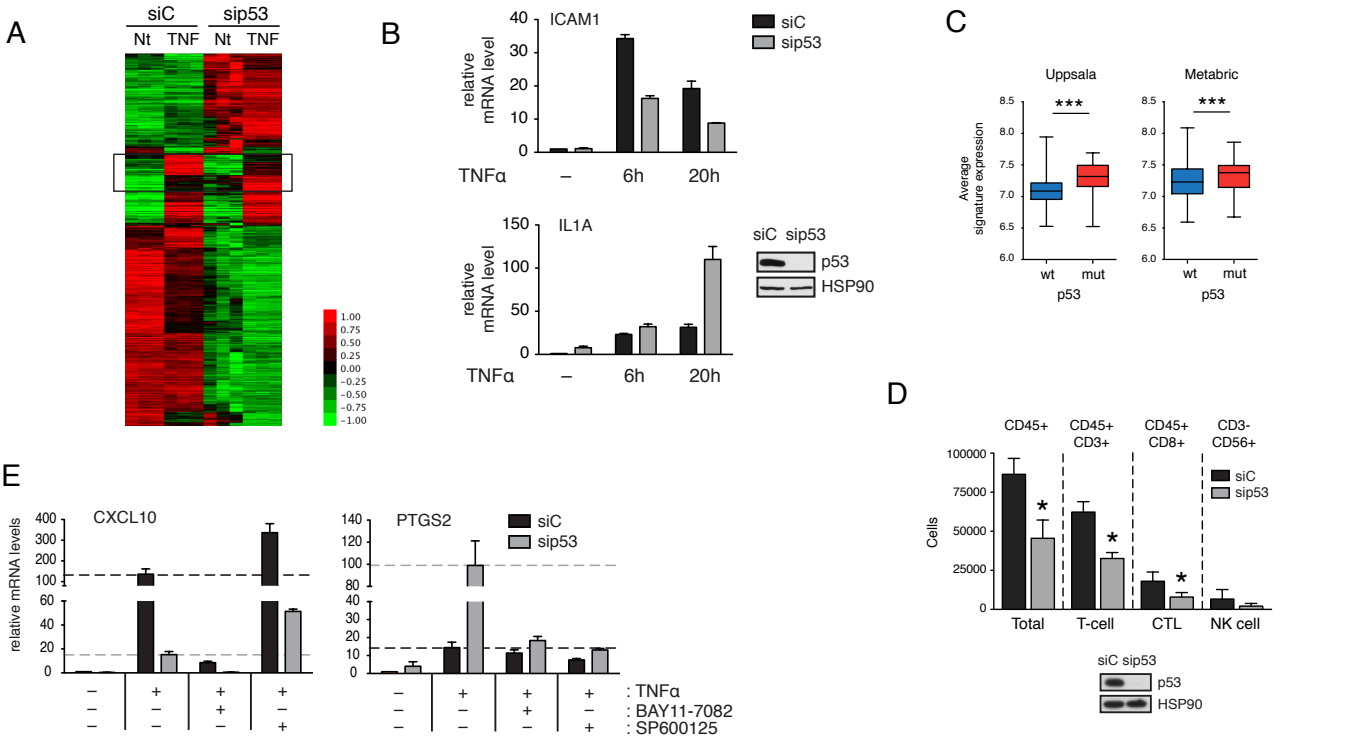

■ siC only

Gene symbol	Matrix name	Yes (sites/1000bp)	Yes/No	P-value
TP53, TP63, TP73	V$P53_02	2	1.679	0.0003
NFKB1, NFKB2, RELA	V$NFKB_Q6_01	1.7778	1.7111	0.0005
R	V$R_01	0.2222	6.3532	0.0007
SRF	V$SRF_C	0.2222	3.9842	0.0056
HIC1	V$HIC1_03	1	1.5176	0.0269

□ sip53 only

Gene symbol	Matrix name	Yes (sites/1000bp)	Yes/No	P-value
ALX1	V$CART1_01	0.5093	2.9745	0.0019
v-Jun	V$VJUN_01	0.1852	7.251	0.0033
NKX2-5	V$NKX25_Q5	0.5556	2.3033	0.0083
FOS, JUN	V$AP1_Q2_01	1.1111	1.7249	0.0095
FOS, JUN	V$AP1_Q4_01	1.0185	1.7566	0.0105
ARID5B	V$MRF2_01	0.3704	2.5262	0.0175
IRF7-9, STAT1-2	V$ISRE_01	0.3704	2.3588	0.0248
NFYA, NFYB, NFYC	V$NFY_Q6_01	0.6481	1.7304	0.0392

□ common

Gene symbol	Matrix name	Yes (sites/1000bp)	Yes/No	P-value
NFKB1, NFKB2, RELA	V$NFKB_Q6_01	2.21	2.13	9.50E-10
ZBTB16	V$PLZF_02	1.80	1.72	3.10E-05
HOXA9, MEIS1	V$MEIS1BHOXA9_02	1.72	1.60	3.30E-04
GATA1-6	V$GATA_Q6	1.41	1.57	1.50E-03
IRF1-9, STAT1-2	V$IRF_Q6	0.23	2.69	9.20E-03
BCL6	V$BCL6_Q3	0.86	1.57	1.10E-02
IRF7-9, STAT1-2	V$ISRE_01	0.34	2.16	1.10E-02
MEF2A, MEF2C-D	V$MEF2_Q6_01	0.21	2.56	1.80E-02
LEF1, TCF3, TCF7	V$TCF4_Q5	0.57	1.58	3.00E-02
ALX1	V$CART1_01	0.31	1.81	4.30E-02

Figure S3 (related to Figures 3 and 4) - Di Minin et al., Collavin

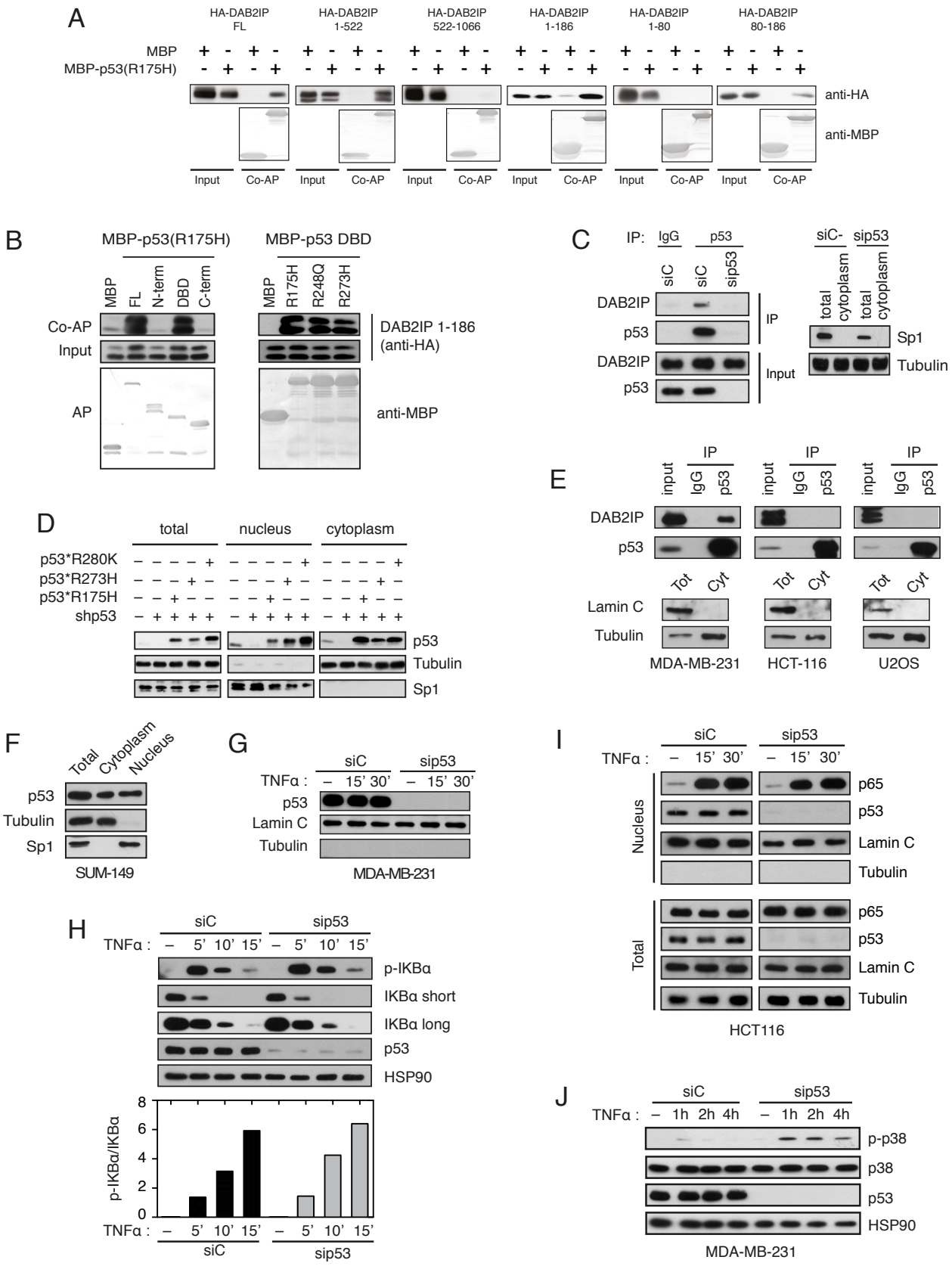

Figure S4 (related to Figure 5) - Di Minin et al., Collavin

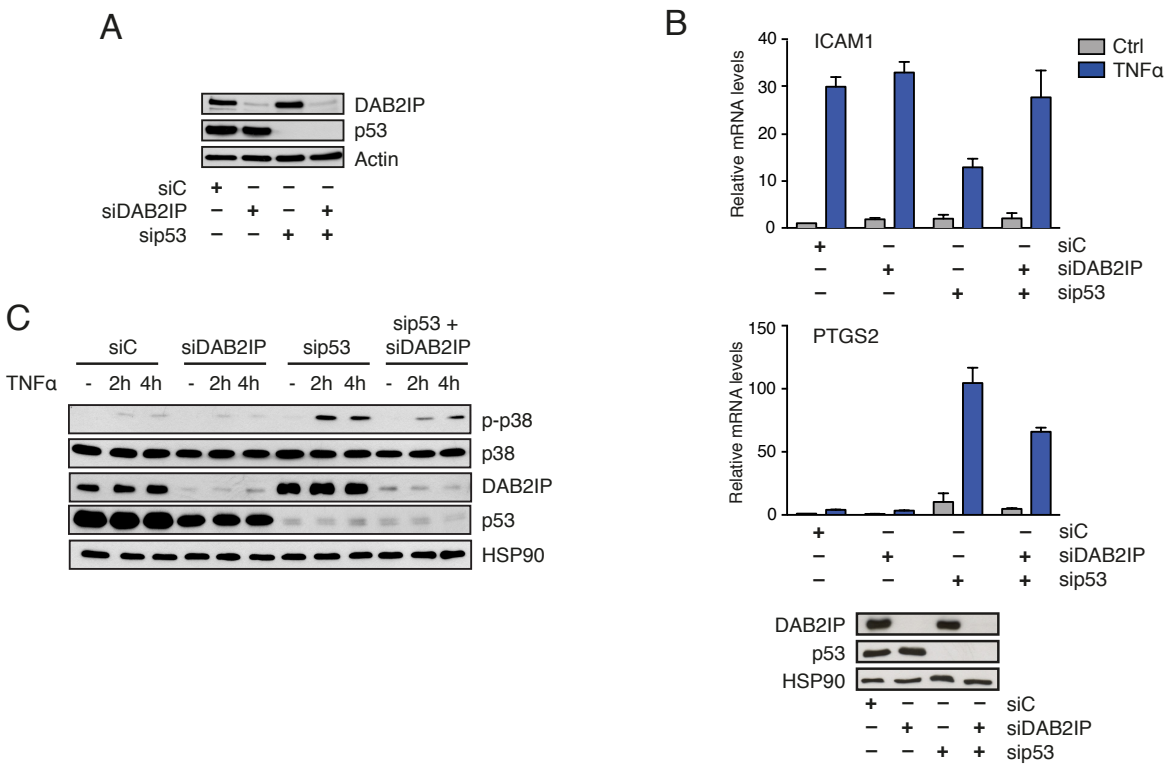

Figure S5 (related to Figure 6) - Di Minin et al., Collavin

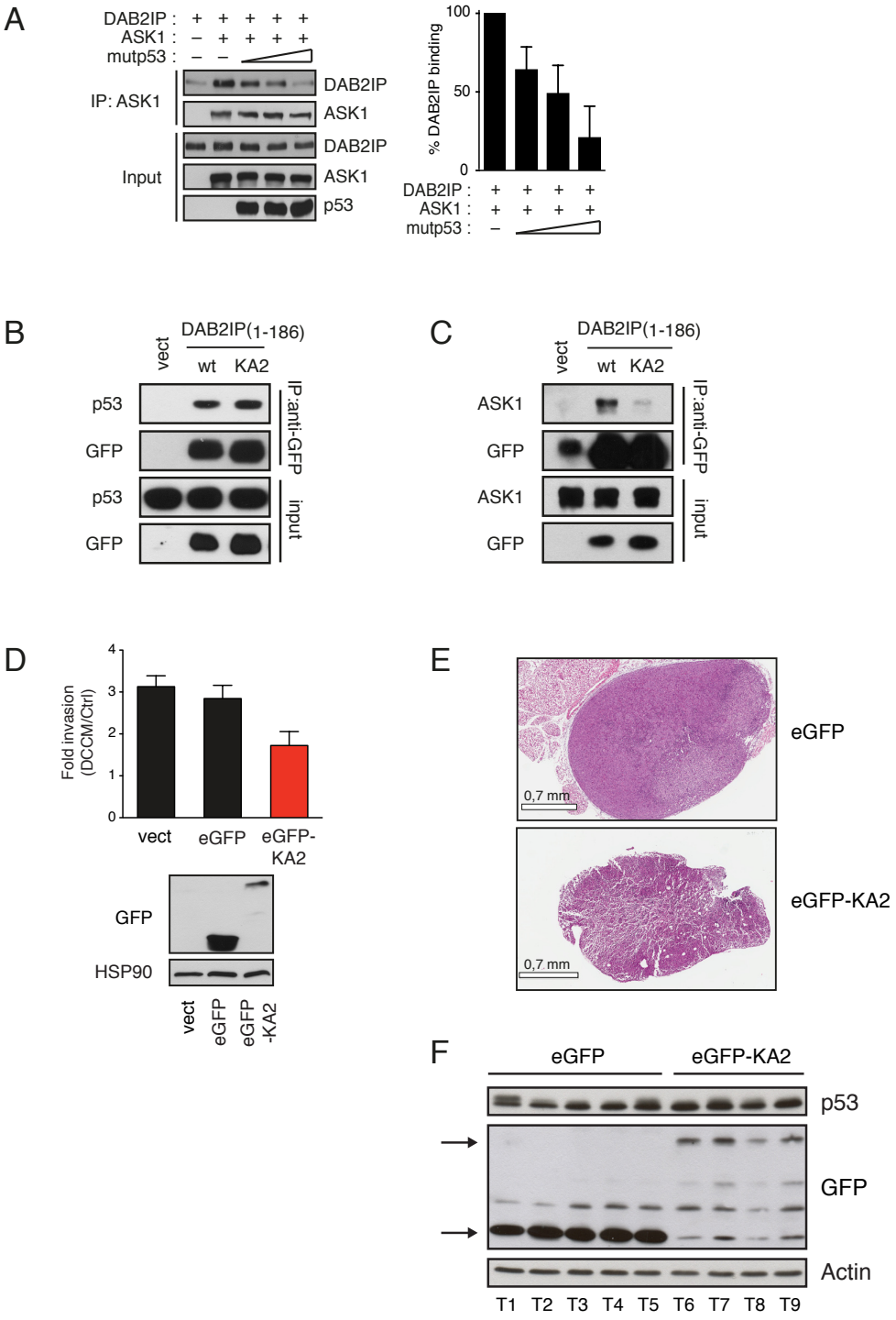

Figure S6 (related to Figure 7) - Di Minin et al., Collavin

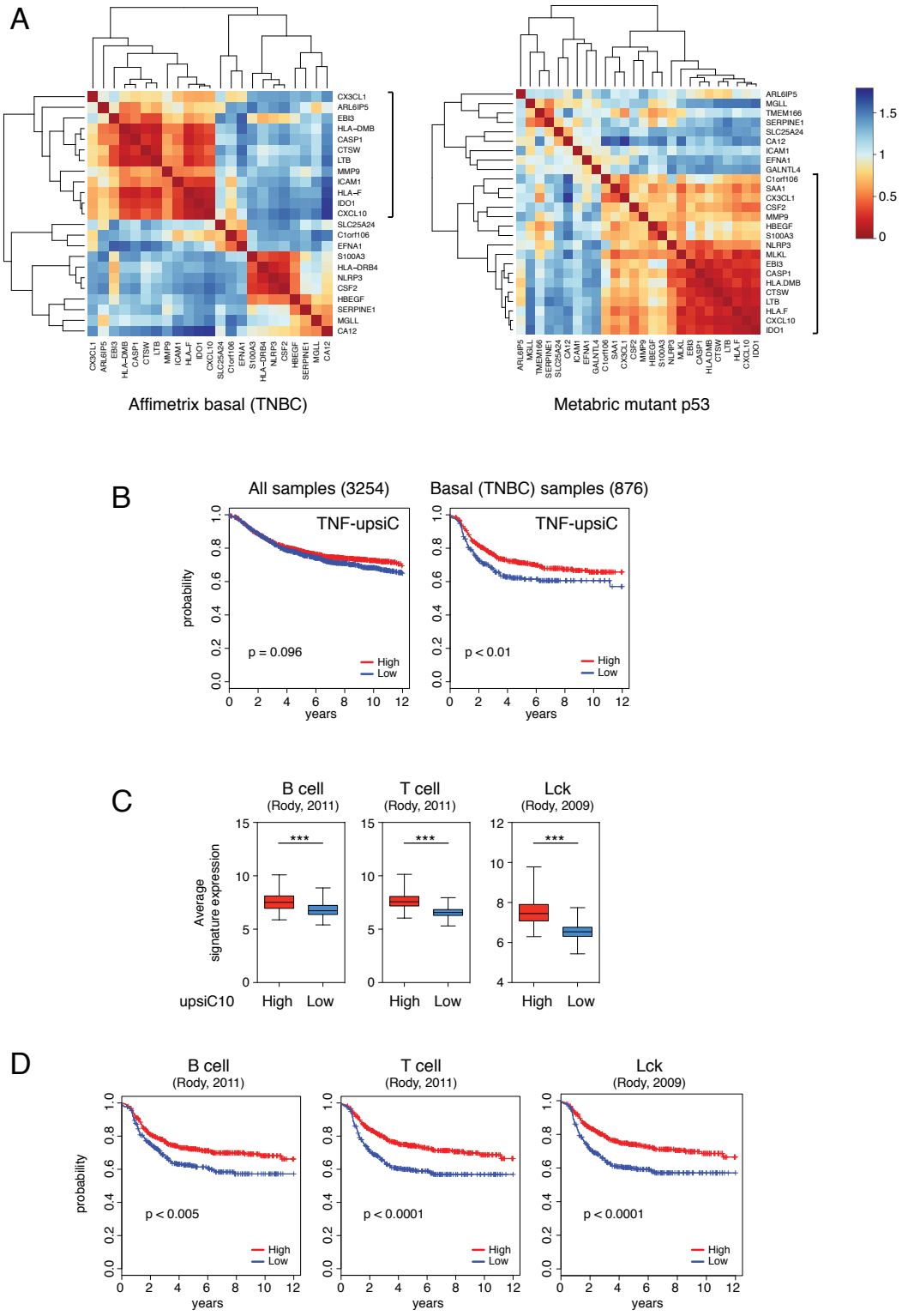

Figure S7 - Di Minin et al., Collavin

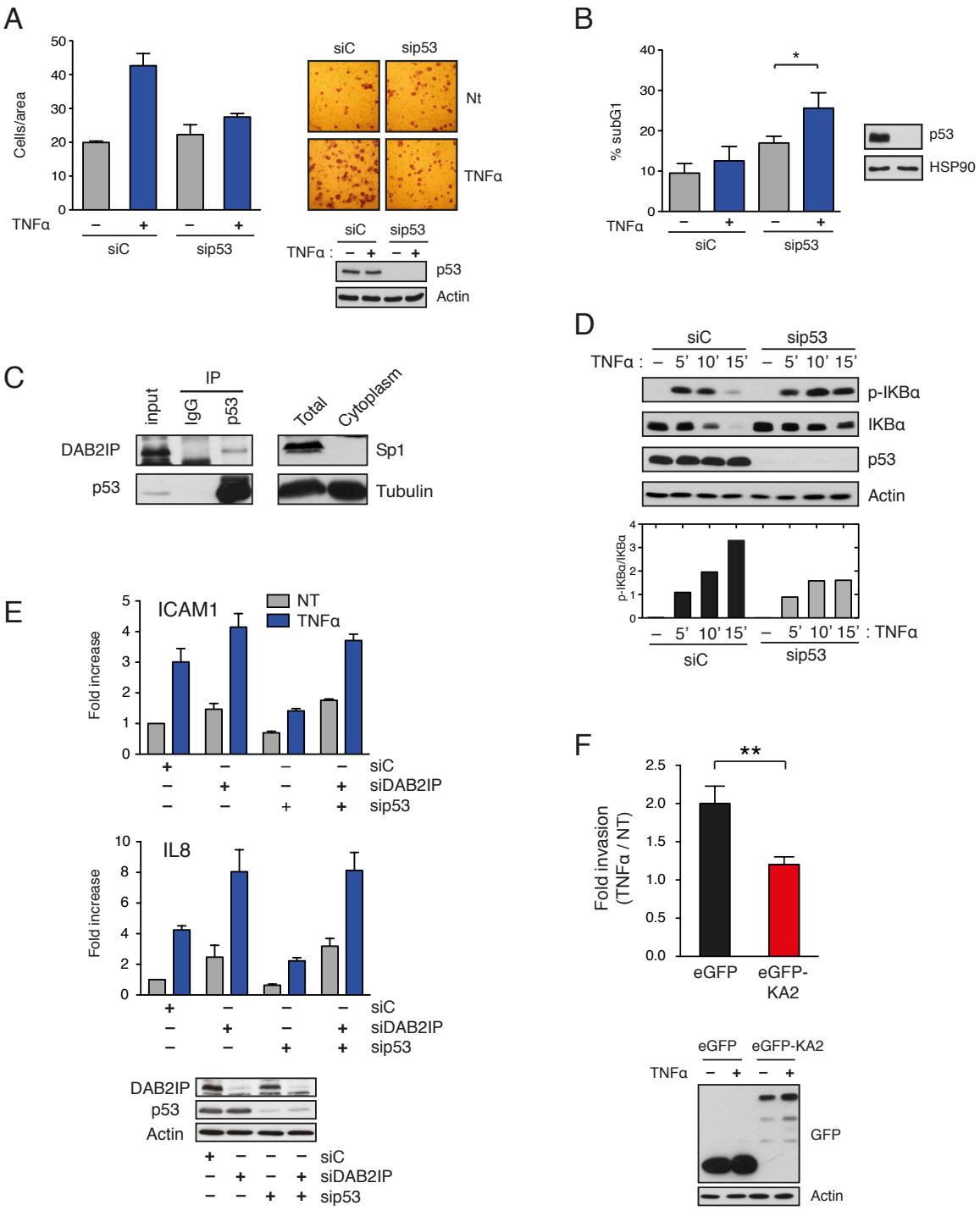

SUPPLEMENTAL FIGURE LEGENDS

Figure S1 (related to Figure 1): Mutant p53 promotes cell invasion and protects from apoptosis in response to TNFα.

(A) Mutp53 drives inflammation-induced invasion. Representative images of migrated MDA-MB-231 and MDA-MB-468 cells from the experiment described in Figure 1A and Figure S1B. Cells were fixed and detected by Crystal Violet staining.

(B) Mutp53 drives inflammation-induced invasion. MDA-MB-468 were transfected with control (siC) or p53 (sip53) siRNAs; invasion assays were performed in the presence of medium conditioned by activated dendritic cells (DCCM) or control medium (Ctrl). Bars indicate the average number of migrated cells per area. Mutp53 depletion was checked by western blot of the same cells.

(C) Mutp53 is necessary for TNF-induced invasion. Representative images of migrated cells from TNF invasion experiments in Fig 1C.

(D) Mutp53 drives inflammation-induced invasion. Ras-transformed mouse embryo fibroblasts (MEF) derived from p53-null (-/-) or p53R172H knock-in (m/m) mice were used for invasion assays as in B. Migrated cells were fixed and detected by Hoechst staining. Bars indicate the average fold increase in cells migrated in DCCM vs Ctrl medium (mean ± SD; n=3). Representative images of migrated cells are shown. Endogenous p53 was checked by western blot (bottom panels).

(E) Mutp53 is sufficient for TNF-induced invasion. Representative immunoblots of mutp53 expression in the cell lines used for the transwell experiments reported in Fig 1E.

(F) Depletion of mutant p53 sensitizes cancer cells to the cytotoxic effect of TNFα. MDA-MB-231, SUM-149, and MDA-MB-468 cell lines were transfected with control (siC) or p53 (sip53) siRNAs and treated with TNFα (10 ng/ml) for 48 hr. DNA content was analyzed by flow cytometry after Propidium Iodide (PI) staining. Graphs summarize percent distribution of the cells in various phases of the cell cycle, as well as cells with sub-G1 DNA content (mean of 3 independent experiments). p53 was blotted in the same cells to control knockdown efficiency.

Figure S2 (related to Figure 2): Mutant p53 modulates the TNF-induced transcriptional landscape of MDA-MB-231 cells

(A) Unsupervised hierarchical clustering of all genes of the filtered microarray expression matrix, excluding features with low standard deviations (<0.4). Red - increased expression, green - decreased expression relative to average levels of signals (log 2 scale). Genes differentially regulated by TNFα in control vs sip53 treated cells are boxed.

(B) Validation of microarray results. Expression of ICAM1 (belonging to the TNF-upsiC group) and IL1A (belonging to the TNF-upsip53 group) were measured by RT-qPCR at 6 or 20 hr of TNFα treatment in MDA-MB-231 cells. Data are normalized to H3 gene, and compared to expression levels of untreated cells transfected with siC. Depletion of endogenous mutant p53 was checked by immunoblotting (panel on the right).

(C) The mutp53-dependent TNF-inducible genes identified by microarray in MDA-MB-231 cells are more expressed in primary breast cancers with mutant p53.
Expression of the TNF-upsiC metagene in tumors with wild-type or mutant (missense) p53 from the Uppsala (Miller et al., 2011) and Metabric (Curtis et al., 2012) datasets. Significance was calculated by unpaired t-test (*** P<0.0001).
(D) Mutp53 sustains a secretory phenotype that stimulates lymphocyte chemotaxis. Peripheral blood mononuclear cells (PBMCs) from anonymous healthy blood donors were isolated from buffy coats. Transwell migration assays were performed for 45 min in the presence or absence of conditioned medium from mutant (siC) or p53 silenced (sip53) MDA-MB-231 cells treated with TNFα for 20 hr in low serum. The total number of cells migrated to the lower side of the inserts was counted, and differences in population distribution were evaluated by flow cytometry after labeling with specific fluorescent antibody. The histogram summarizes the number of migrated cells accordingly to the different immune subtypes analyzed (mean ± SD; n=4; * P<0.05): Total (Lympho-monocytes: CD45+), T-cell (T lymphocytes: CD45+/CD3+), CTL (Cytotoxic T Lymphocytes: CD45+/CD8+), NK cell (Natural Killer cells: CD3-/CD56+). Efficiency of mutant p53 depletion was controlled by immunoblotting (bottom panel).
(E) Mutp53 sustains NF-κB and counteracts JNK-dependent transcription. MDA-MB-231 cells were silenced with control (siC) or p53 (sip53) siRNAs, and treated with TNFα for 20 hr. Cells were also treated with the NF-κB inhibitor BAY11-7082 (1μM) or the JNK inhibitor SP600125 (10μM). Expression of CXCL10 and PTGS2 was measured by RT-qPCR as in B (mean ± SD; n=3). Dashed lines provide a reference for TNF-induced expression of each gene - with or without mutp53 silencing - in the absence of inhibitors.

(F) MDA-MB-231 cells were silenced with control (siC) or p53 (sip53) siRNAs. Where indicated, cells were also transfected with siRNA against p65 (sip65) and JNK (siJNK). Subsequently, cells were treated with TNFα (10ng/ml) for 20 hr. Expression of MMP9, CXCL10, IL1B and PTGS2 mRNA was measured by RT-qPCR. Efficiency of p53, p65 and JNK knockdown was confirmed by western blot (panel on the right).

(G) A model derived from the observed impact of mutp53 depletion on TNF-induced transcription of different NF-κB target genes.

(H) In silico analysis reveals enrichment of predicted JUN/AP1 transcription factor binding sites in the promoters of TNF-inducible genes upregulated by depletion of mutant p53 in our microarray. Genes induced by TNFα by at least two-fold were divided in three groups: those induced only in the presence of mutant p53 (siC only, black) those induced only after mutant p53 knockdown (sip53 only, grey), and those that are induced in either condition (common, white). The genes were analyzed using ExPlain (http://www.biobase-international.com) to identify enrichment for predicted transcription factor binding sites in their upstream genomic sequences. The table summarizes the top scoring results. In the tables are indicated the transcription factor (Gene symbol), the binding site code (Matrix name), the frequency of the binding site in the promoter of analyzed genes (Yes-sites/1000bp), the enrichment with respect to the background (Yes/No), and the significance of this enrichment (P-value); data are sorted according to P-value.

Figure S3 (related to Figures 3 and 4): Physical and functional interaction between DAB2IP and mutant or wild-type p53

(A) Mutp53 binds the C2 domain of DAB2IP. HEK-293T cells were co-transfected with the indicated HA-tagged DAB2IP deletion constructs, together with a plasmid expressing the p53(R175H) hot-spot mutant fused to MBP. After purification with amylose resin, samples were analyzed by western blot. Input lanes correspond to 1/40 of the lysate used for Co-AP. Bottom panels show the MBP-fusion proteins (baits) after purification.

(B) Mutp53 binds to DAB2IP through the DNA binding (DBD) domain. Interaction between the DAB2IP 1-186 fragment and various mutp53 deletions fused to MBP was analyzed by Co-AP as above. The input is 1/40 of the lysate. The two upper panels are from the same autoradiography (i.e. have the same exposure). The bottom panels show MBP-fusion proteins (baits) after purification.

(C) Mutp53 and DAB2IP interact in the cytoplasm. MDA-MB-231 cells were silenced with control (siC) or p53 (sip53) siRNAs. Endogenous mutp53 was immunoprecipitated from the cytoplasmic fraction of transfected cells. Co-precipitated endogenous DAB2IP was detected by western blot. Sp1 was blotted to confirm cytoplasm purity. Input corresponds to 1/100 of the cytoplasmic fraction used for immunoprecipitation.

(D) Cytoplasmic localization of exogenous p53 mutants in infected MCF-10A cells. MCF-10A cell lines used in Figure 1D-E were subjected to biochemical fractionation to separate cytoplasm and nuclei. Equal fractions of each sample were analyzed by western blot. Tubulin (cytoplasmic) and Sp1 (nuclear) were blotted as controls.

(E) Wild-type p53 and DAB2IP do not interact in the cytoplasm. Endogenous mutant p53 and wt p53 were immunoprecipitated respectively from the cytoplasmic fraction of HCT116 and U2OS cells. Co-precipitated endogenous DAB2IP was detected by western blot. Lamin C was blotted to confirm cytoplasm purity (absence of nuclei). Input corresponds to 1/100 of the cytoplasmic fraction used for immunoprecipitation.

(F) Cytoplasmic localization of endogenous mutant p53 in SUM-149 breast cancer cells. Cells were fractionated and analyzed as in D.

(G) Mutant p53 sustains TNF-induced activation of p65 RelA. Representative western blot of nuclear fractions of MDA-MB-231 cells used for the ELISA experiments in Figure 4D.

(H) Wild-type p53 has no impact on TNF-induced phosphorylation and degradation of IKBα. HCT116 cells were silenced with control (siC) or p53 siRNAs (sip53), serum starved, and treated with TNFα (10ng/ml) for the indicated times. Phosphorylated and total IKBα were detected by immunoblotting. Lower panel shows the ratio of phosphorylated IKBα over IKBα in this representative experiment, measured by densitometry on autoradiographic films.

(I) Wild-type p53 has no impact on TNF-induced nuclear translocation of p65 RelA. HCT116 cells were treated as in H. At the indicated time-points cells were subjected to biochemical fractionation to separate cytoplasm and nuclei. Total cell lysate and purified nuclei were analyzed by western blot. Tubulin (cytoplasmic) and Lamin C (nuclear) were blotted as controls.

(J) Depletion of mutant p53 increases p38 MAPK activation by TNFα. MDA-MB-231 cells were silenced with control (siC) or p53 siRNAs (sip53), serum starved, and treated with TNFα (10ng/ml) for the indicated times. Phosphorylated and total p38 were analyzed by immunoblotting.

Figure S4 (related to Figure 5): Functional interaction between mutant p53 and DAB2IP in the response of cancer cells to inflammatory cytokines

(A) DAB2IP knockdown restores inflammation-driven invasion in mutp53-depleted cancer cells. MDA-MB-231 were treated with siRNAs against p53 or DAB2IP, alone or in combination, as indicated. Shown is a representative western blot of cells used for invasion assays in Figure 5A.

(B) DAB2IP knockdown restores the transcriptional response to TNFα in mutp53-depleted cancer cells. MDA-MB-231 cells were silenced for DAB2IP and/or mutp53 as indicated. Expression of ICAM1 and PTGS2 was measured by RT-qPCR after 20 hr of TNFα (10 ng/ml) treatment as in Figure 5C. DAB2IP and/or mutp53 depletion was checked by western blot (bottom panel).

(C) DAB2IP knockdown counteracts increased TNF-induced phosphorylation of p38 MAPK in mutp53-depleted cancer cells. MDA-MB-231 cells were silenced for DAB2IP and/or mutp53, and treated with TNFα as in Figure 5F. Phosphorylated and total p38 were analyzed by immunoblotting.

Figure S5 (related to Figure 6): The mutp53-DAB2IP interaction is required for the invasive response of cancer cells to inflammation.

(A) Overexpression of mutp53 interferes with DAB2IP binding to ASK1. H1299 cells were co-transfected with plasmids expressing DAB2IP, HA-ASK1, and increasing amounts of p53(R280K), as indicated. The fraction of DAB2IP bound to ASK1 was analyzed by western blotting of ASK1 immunoprecipitates, and quantified by densitometry on autoradiography films; bars represent the $DAB2IP_{(co\text{-}IP)}/DAB2IP_{(input)}$ ratio, normalized to the sample without mutp53 (mean ± SD; n=3).

(B) The $DAB2IP_{1\text{-}186}$ KA2 peptide binds mutp53. MDA-MB-231 cells were stably transduced with retroviruses expressing GFP-$DAB2IP_{1\text{-}186}$ wt, GFP-$DAB2IP_{1\text{-}186}$ KA2 or with an empty vector. Cell lysates were immunoprecipitated with an anti-GFP antibody, and endogenous mutp53 associated to $DAB2IP_{1\text{-}186}$ variants was analyzed by western blot.

(C) The $DAB2IP_{1\text{-}186}$ KA2 peptide has negligible binding to ASK1. Cells transduced as above were subjected to biochemical fractionation to separate the cytoplasmic and nuclear proteins. GFP-fusion proteins were immunoprecipitated from the cytoplasmic fraction, and co-immunoprecipitated endogenous ASK1 was analyzed by western blot. Input and IP panels are from the same film (i.e. have the same exposure).

(D) Overexpression of the p53-binding domain of DAB2IP reduces inflammation-driven invasion. MDA-MB-231 cells were stably transduced with retroviruses expressing the eGFP-$DAB2IP_{1\text{-}186}$KA2 fusion protein (eGFP-KA2), eGFP alone, or an empty vector as further control. Invasion assays were performed as in Fig. 6D. Expression of eGFP proteins and endogenous DAB2IP was checked by western blot (bottom).

(E) Expression of DAB2IP$_{1-186}$KA2 reduces the metastatic potential of cancer cells injected in the fat pad of immunocompromised mice. Representative sections of lymph nodes from mice injected with eGFP or eGFP-KA2 expressing cells, stained with Hematoxylin and Eosin.

(F) Primary tumors generated by MDA-MB-231 cells stably expressing eGFP or eGFP-KA2 were collected from the mammary pads, snap-forzen in liquid nitrogen, and stored at -80°C. Tumors were mechanically disrupted, homogenized in lysis buffer, and analyzed by western blot for expression of eGFP fusion proteins and endogenous mutant p53.

Figure S6 (related to Figure 7): In silico analysis reveals a potential impact of the TNF α /mutp53 axis in the clinical outcome of breast cancer

(A) A subset of genes correlated to the TNFα/mutp53 axis is reproducibly co-expressed in breast cancers with mutp53. Heat maps of 1-Pearson correlation coefficients of the 29 mutp53-dependent TNF-inducible genes derived from our microarray in MDA-MB-231 cells. Two independent sets of tumors were analyzed: the basal/TNBC samples of the Affymetrix breast cancer metadataset (left) and the mutant p53 samples of the Metabric breast cancer dataset (right). Genes robustly co-regulated in both sets of tumors (black bar) define the upsiC10 signature.

(B) Genes linked to the TNFα/mutp53 axis correlate with prolonged metastasis-free survival in basal/TNBC breast cancer patients. Kaplan-Meier survival curves for high or low expression of the TNF-upsiC signature in the entire breast cancer metadataset, or in the basal/TNBC subset.

(C) Expression of metagenes identifying specific immune cells subpopulations (Rody et al., 2009; Rody et al., 2011) in basal-like/TNBC breast cancer samples stratified according to high or low expression of the upsiC10 signature.

(D) Higher expression of lymphocyte markers correlates with prolonged metastasis-free survival in basal/TNBC breast cancer patients. Kaplan-Meier survival curves for high (red) or low (blue) expression of immune metagenes from Rody et al. (2009) and Rody et al. (2011) in basal-like/TNBC breast cancer patients.

Figure S7 (related to Figures 1, 3, 4, 5 and 6): The mutp53/DAB2IP axis modulates the response to TNFα in the pancreatic cancer cell line PANC-1.

(A) Mutp53 drives TNF-induced invasion. PANC-1 cells were transfected with control (siC) or p53 (sip53) siRNAs. Invasion assays were performed in low serum plus TNFα (10ng/ml). Mutp53 depletion was checked by western blot of the same cells (lower panel). Representative images of migrated cells are also shown. Bars indicate the average number of cells per area (mean ± SD; n=3).

(B) Mutp53 depletion sensitizes cells to TNF-induced cell death. PANC-1 cells were transfected with control (siC) or p53 (sip53) siRNAs and treated with TNFα (10ng/ml) for 48 hr. DNA content was analyzed by flow cytometry after Propidium Iodide (PI) staining. The histogram summarizes the fraction of cells in SubG1 (mean ± SD; n=3). Mutp53 depletion was checked by western blot of the same cells (left panel).

(C) Mutp53 and DAB2IP interact in the cytoplasm. Endogenous mutp53 was immunoprecipitated from the cytoplasmic fraction of PANC-1 cells. Co-precipitated endogenous DAB2IP was detected by western blot. Sp1 was blotted to confirm cytoplasm purity. Input corresponds to 1/100 of the cytoplasmic fraction used for immunoprecipitation.

(D) Mutp53 depletion reduces TNF-induced phosphorylation and degradation of IKBα. PANC-1 cells were silenced with control (siC) or p53 siRNAs (sip53), serum starved, and treated with TNFα (10ng/ml) for the indicated times. Phosphorylated and total IKBα were measured by immunoblotting. Lower panel shows the ratio of phosphorylated IKBα over IKBα in this representative experiment, measured by densitometry on autoradiographic films.

(E) DAB2IP knockdown restores the transcriptional response to TNFα in mutp53-depleted cancer cells. PANC-1 cells were silenced for DAB2IP and/or mutp53 as indicated. Expression of ICAM1 and IL8 was measured by RT-qPCR after 20 hr of TNFα (10 ng/ml) treatment. DAB2IP and/or mutp53 depletion was checked by western blot (bottom panel).

(F) Overexpression of the p53-binding domain of DAB2IP reduces TNF-driven invasion. PANC-1 cells were stably transduced with retroviruses expressing the eGFP-DAB2IP$_{1-186}$KA2 fusion protein (eGFP-KA2), or eGFP alone. Invasion assays were performed in low serum plus TNFα (10ng/ml). Graph shows the increase in invasion triggered by TNF (mean ± SD; n=3; ** $P < 0.005$). Expression of eGFP proteins was analyzed by western blot (bottom panel).

Table S1. Listing of TNF-responsive genes differentially expressed in sip53 versus siC transfected MDA-MB-231 cells.

Table S2. Output of GO term enrichment analysis performed using the DAVID 6.7 release (http://david.abcc.ncifcrf.gov/sevice) on the indicated groups of TNF-responsive genes identified in MDA-MB-231 cells.

Table S3. Univariate Cox regression analysis of the expression of various metagenes in relation to disease free survival (DFS) in breast cancer patients stratified according to the status of p53.

Metagene	*Tumor samples*[§]	*Hazard Ratio (95% CI)*	*P-value*
Upsic10	TP53 wt	1 (0.7982, 1.253)	0.999
	TP53 mut	**0.575** (0.3697, 0.895)	0.0141 *
TNF-upsiC	TP53 wt	0.911 (0.589, 1.407)	0.673
	TP53 mut	**0.333** (0.164, 0.676)	0.0023 **
Bindea et al., 2013			
B_cells	TP53 wt	0.9103 (0.7565, 1.095)	0.32
	TP53 mut	**0.7228** (0.5229, 0.9992)	0.0494 *
T_cells	TP53 wt	0.9709 (0.8062, 1.169)	0.775
	TP53 mut	**0.6612** (0.4708, 0.9287)	0.017 *
CTL	TP53 wt	0.9665 (0.8189, 1.141)	0.687
	TP53 mut	**0.6286** (0.4343, 0.9098)	0.0138 *
NK	TP53 wt	0.9605 (0.8073, 1.143)	0.649
	TP53 mut	**0.675** (0.4578, 0.9952)	0.0472 *
Th1	TP53 wt	0.9271 (0.7436, 1.156)	0.501
	TP53 mut	**0.6461** (0.448, 0.9318)	0.0194 *
Th2	TP53 wt	0.765 (0.5082, 1.152)	0.199
	TP53 mut	0.8319 (0.442, 1.566)	0.568
Rody et al., 2011			
B_cells	TP53 wt	0.8935 (0.7084, 1.127)	0.342
	TP53 mut	**0.6798** (0.4626, 0.999)	0.0494 *
T_cells	TP53 wt	0.9704 (0.8091, 1.164)	0.746
	TP53 mut	**0.5585** (0.3854, 0.8094)	0.0021 **
Rody et al., 2009			
Lck	TP53 wt	0.9566 (0.7941, 1.152)	0.64
	TP53 mut	**0.5349** (0.3642, 0.7855)	0.0014 **

§ Samples from the CRCM cohort (Sabatier et al., 2011): p53wt (n=125), p53 mutant (n=68); and the Uppsala cohort (Miller et al., 2005): p53wt (n=189), p53 missense (n=47).

** P<0.05; ** P<0.01*

SUPPLEMENTAL EXPERIMENTAL PROCEDURES

Cell Culture, Transfections, Retroviral Transductions and treatments. MDA-MB-231 (p53R280K), MDA-MB-468 (p53R273H), PANC-1 (p53R273H), 293T, 293GP, HCT116 (wt-p53), U2OS (wt-p53) and MEF (Mouse Embryonic Fibroblasts) were cultured in DMEM medium (Sigma) supplemented with 10% FCS (ECS0180L, Euroclone), and antibiotics (DE17-602E, Lonza). H1299 cells were cultured in RPMI medium (Sigma) supplemented with 10% FBS and antibiotics. SUM-149 (p53M237I) cells were cultured in DMEM:F12 Ham's medium 1:1, supplemented with 10% FCS and antibiotics. MCF10A cells were maintained in DMEM:F12 Ham's medium 1:1, supplemented with 5% horse serum, insulin (10 μg/ml), hydrocortisone (0.5 μg/ml) and epidermal growth factor (EGF 20 ng/ml).

All human mammary cell lines were subjected to STR genotyping with PowerPlex 18D System and confirmed in their identity comparing the results to reference cell databases (DMSZ, ATCC, and JCRB databases), where possible.

MEFs were generated by crossing mice of the appropriate genotype, and collecting cells from 13.5 d.p.c. embryos. MEF p53KO and MEF KI p53R172H were immortalized through retroviral transduction of H-RasV12 (Girardini et al., 2011).

HEK293T or 293GP were transfected using calcium-phosphate. Transfections of H1299 were performed with Lipofectamine 2000 (Invitrogen), following manufacturer's instructions. For siRNA transfections, cells were transfected with 50 nM siRNA oligonucleotides using Lipofectamine RNAiMax (Invitrogen), following manufacturer's instructions. After 48 hr of silencing, cells were subsequently processed.

siRNAs used in this work are listed in the following table:

siRNA	Sequence	Purchase from/ Reference
Control siRNA (siC)	Unknown	All star negative control (1027281,Qiagen)
sip53 ORF	GACUCCAGUGGUAAUCUAC	Eurofins MWG
siDAB2IP A	GGAGCGCAACAGUUACCUG	Eurofins MWG
siDAB2IP B	GGUGAAGGACUUCCUGACA	Eurofins MWG
siDAB2IP 3'UTR	GUAAUGUAACUAUCUCACC	Eurofins MWG
siJNK1/2 A	AAAGAAUGUCCUACCUUCU	Eurofins MWG

siJNK1/2 B	AGAAGGUAGGACAUUCUUU	Eurofins MWG
sip65	GCCCUAUCCCUUUACGUCA	Eurofins MWG

For retroviruses production, low confluent HEK 293GP packaging cells were transfected by calcium phosphate precipitation. After 48–72 hr the virus-containing medium was filtered and added to target cells. Cells were selected with blasticidin (2 μg/ml) and/or puromycin (0.5 μg/ml) and kept under selection for the entire experiment.
Human TNFα was purchased from Invitrogen (PHC3015); TGF-β inhibitor SB431542 (S4317), JNK inhibitor SP600125 (S5567), and NF-κB inhibitor BAY11-7082 (B556) were purchased from Sigma. Mouse TNFα blocking antibody was purchased from BD Pharmigen (#558415).
For gene expression analysis, cells were treated with recombinant TNFα (10ng/ml) in low serum (0.1% FBS) for the indicated times. When necessary, JNK (SP600125) and NF-κB (BAY11-7082) inhibitors were added to low serum medium 2 hr before addition of TNFα. For analysis of p-IKBα and p-JNK, cells were serum starved for 24 hr and subsequently TNFα (10ng/ml) was added for the indicated times.

Plasmids.

pCS2-HA-DAB2IP FL and deletions were generated by cloning PCR products generated using specific primers; mouse DAB2IP was amplified from pLENTI-DAB2IP (kindly provided by K. Cichowski) with AccuPrime™ Taq DNA Polymerase High Fidelity (Invitrogen), following manufacturer's instructions. pLPC-DAB2IP and pLPC-p53R175H, -p53R273H, -p53R280K were obtained by cloning respectively DAB2IP and p53R175H, p53R273H, p53R280K coding region into pLPC empty vector. pLPC-p53*R175H, -p53*R273H, -p53*R280K were generated introducing silent mutations in the region targeted by p53 siRNA by site directed mutagenesis in pLPC-p53R175H, -p53R273H, -p53R280K respectively. pLPC-p53*R280K ΔNLS was obtained starting from pcDNA3-p53 ΔNLS (kindly provided by U. Moll): R280K mutation and subsequently silent mutations in the region targeted by p53 siRNA were introduced by site directed mutagenesis and then subcloned in pLPC vector.

pLPC-DAB2IP$_{1-186}$wt was obtained by cloning DAB2IP$_{1-186}$ coding region from pCS2-DAB2IP$_{1-186}$ to pLPC; pLPC-DAB2IP$_{1-186}$KA2 was generated mutating lysine residues by site directed mutagenesis (Zhang et al., 2003).
pcDNA3-MBP and MBP-p53 wt were described previously (Lunardi et al., 2010); the full-length coding sequences and various deletions of p53 hot-spot mutants were PCR amplified from corresponding expression plasmids and cloned in frame with MBP in the pcDNA3-MBP vector. pcDNA3HA-ASK1 was kindly provided by L. Schmitz. pSR-shp53 plasmid was previously described (Drost et al., 2010). pLKO-shDAB2IP plasmid was generated by cloning in the pLKO lentiviral vector a double stranded oligo corresponding to siDAB2IP A (described above).

Cell manipulation and Western blot analysis. Total cell extracts were prepared in RIPA buffer without SDS (150mM NaCl, 50mM Tris-HCl pH8, 1mM EDTA, 1% NP-40, 0.5% Na-deoxycholate) supplemented with 1 mM PMSF, 5 mM NaF, 1 mM Na_3VO_4, 10μg/ml CLAP, 1μM TSA and 5μM nicotinamide. Protein concentration was determined with Bio-Rad Protein Assay Reagent (#500-0006, Bio-Rad). Lysates were resolved by SDS/PAGE and transferred to nitrocellulose (Millipore).
Nucleus-cytoplasm fractionation. Cells were scraped in PBS and washed two times. The pellet obtained after the last centrifugation was resuspended in Cytoplasmic-buffer (10mM HEPES pH7.9, 1.5mM $MgCl_2$, 10mM KCl, 0.5mM DTT, 0.1% NP-40) supplemented with inhibitors (1mM PMSF, 5mM NaF, 10mg/ml CLAP, 1mM Na3VO4); lysis was obtained gently pipetting a couple of times. After 3' in ice, lysates were centrifuged at 2500g for 5' at 4°C; the supernatant was collected as the cytoplasmic fraction. The pellet was washed twice in Wash-buffer (10mM HEPES pH7.9, 1.5mM $MgCl_2$, 10mM KCl, 0.5mM DTT) and then Nuclei in the pellet were resuspended in Nuclear-buffer (20mM HEPES pH7.9, 1.5mM $MgCl_2$, 420mM NaCl, 0.2mM EGTA, 0.5mM DTT, 25% glycerol) supplemented with inhibitors (1mM PMSF, 5mM NaF, 10mg/ml CLAP, 1mM Na3VO4); nuclear extract was recovered by centrifugation at 15000g for 15' at 4°C. To evaluate DAB2IP and p53 cellular localization, nuclear and cytosolic fractions were also prepared using the ProteoExtract® Subcellular Proteome Extraction Kit, following the manufacturer's instructions.

Western blot analysis was performed according to standard procedures using the following primary antibodies:

Target	**Antibody**
p-JNK (Thr183/Tyr185)	#9251 (Cell Signaling)
JNK	sc-571 (Santa Cruz)
HA	12CA5 hybridome
p-IKBα (Ser32/36)	#9246 (Cell Signaling)
IKBα	#9242 (Cell Signaling)
HSP90	sc-13119 (Santa Cruz)
Actin	#A9718 (Sigma)
Cleaved Caspase-3	#9664 (Cell Signaling)
PARP p85 fragment	TB273 (Promega)
p53 (DO1)	sc-126 (Santa Cruz)
DAB2IP	A302-440A (Bethyl)
Tubulin	T5168 (Sigma)
SP1	sc-59 (Santa Cruz)
MBP	home-made rabbit polyclonal
ASK1 (F-9)	sc-5294 (Santa Cruz)
ASK1 (H-300)	sc-7931 (Santa Cruz)
GFP	home-made rabbit polyclonal
p65 RelA	sc-372X (Santa Cruz)
Lamin A/C	sc-6215 (Santa Cruz)
p-p38 MAPK (Thr180/Tyr182)	#9216 (Cell Signaling)
p38 MAPK	#9212 (Cell Signaling)

Protein Interaction studies

Coaffinity purification. Co-AP experiments were performed as described in Lunardi et al. (2010), with minor changes. Plasmids were transfected in human 293T cells. 48 hr after transfection cells were lysed in coaffinity purification buffer (50 mM Tris·HCl pH8, 150 mM NaCl, 1 mM EDTA pH8, 1 mM DTT, 5% glycerol, protease inhibitors (Sigma), 1 mM PMSF, 5 mM NaF, 1 mM beta-glycerolphosphate) for 30 min on ice and cleared by centrifugation for 30 min at 13000g at 4 °C, and protein complexes were collected on amylose beads. After extensive washes, purified complexes were separated by SDS/PAGE, detected by immunoblotting, and visualized by ECL (Amersham). Purified MBP baits were visualized by DAB staining (Sigma).

Co-immuno precipitation. Co-IP experiments with endogenous proteins were performed using Co-IP buffer (NaCl 120mM, Tris-HCl pH8 20mM, EDTA 1mM, NP40 0.5%) with protease inhibitors. Samples were cleared by centrifugation for 30 min at 13000g at 4 °C and incubated for 2 hr at 4 °C with specific antibody. After 1 hr incubation with protein G-Sepharose (GE Healthcare), immunoprecipitates were washed three times in Co-IP buffer, resuspended in sample buffer, and analyzed by immunoblotting. For Co-IP of endogenous DAB2IP and mutp53, p53DO1 (sc-126) was used for immunoprecipitation, and mouse purified IgGs as negative control. For Co-IP of endogenous DAB2IP and ASK1, anti-ASK1 (sc-7931) was used for immunoprecipitation, and mouse IgGs as negative control. Anti-GFP antibody (home-made rabbit polyclonal) was used to immunoprecipitate GFP-DAB2IP$_{1\text{-}186}$KA2 to study differential interaction with endogenous p53 and ASK1 proteins. Anti-HA (12CA5) was used to immunoprecipitate ASK1 in transfected H1299 cells.

Immunofluorescence. Cells were fixed in 4% paraformaldehyde at room temperature, and permeabilized in PBS plus 0.1% Triton X-100. Permeabilized cells were incubated with primary antibodies, followed by Alexa Flour® 568, 488 conjugated secondary antibodies (Life Technologies). Images were captured using a Leica DM4000B epifluorescence microscope.

Nuclear extract preparation and NF-κB transcription factor activation assay. Nuclear protein extract from MDA-MB-231 were prepared using Active Motif Nuclear Extract Kit. NF-κB p65 activation was measured through its ability to bind a specific DNA consensus site with TransAM Chemi NF-κB p65 ELISA (Active Motif) according to the manufacture's instructions. 2ug of nuclear protein extract were analyzed in each point. The chemiluminescent signal was read on an EnSpire Multimode Plate Reader (PerkinElmer).

RNA extraction and RT-qPCR. Total RNA was extracted with QIAzol (Qiagen) following manufacturer's instructions. 1μg of total RNA was reverse-transcribed with QuantiTect Reverse Transcription (Qiagen). Real-time qPCR was performed using

SsoAdvanced™SYBR® Green Master Mix (Biorad) on a CFX96™ Real-Time PCR System (Biorad). List of primers used:

Target	Sequence
DAB2IP	Fw: 5'CACATCACCAACCACTAC3' Rev: 5'TCCACCTCTGACATCATC3'
p53	Fw: 5'CTCCTCTCCCCAGCCAAAGA3' Rev: 5'GGAACATCTCGAAGCGCTCA3'
CA12	Fw: 5'CAGTTTTCCGAAACCCCGTG3' Rev: 5'TGCCGCAGTACAGACTTGC3'
MMP9	Fw: 5'GCCTTTGGACACGCACGACGT3' Rev: 5'GCAGGACGGGAGCCCTAGTC3'
LTB	Fw: 5'AGGGAGGACTGGTAACGGAG3' Rev: 5'GAAACGCCTGTTCCTTCGTC3'
CXCL10	Fw: 5'TGGCATTCAAGGAGTACCTCTC3' Rev: 5'TGATGGCCTTCGATTCTGGA3'
SERPINE1	Fw: 5'GACCGCAACGTGGTTTTCTC3' Rev: 5'GCCATGCCCTTGTCATCAAT3'
CX3CL1	Fw: 5'ACGGTGTGACGAAATGCAAC3' Rev: 5'TTGACCCATTGCTCCTTCGG3'
CSF2	Fw: 5'AATGTTTGACCTCCAGGAGCC3' Rev: 5'TCTGGGTTGCACAGGAAGTT3'
IDO-1	Fw: 5'GCAAGAACGGGACACTTTGC3' Rev: 5'GCCTTTCCAGCCAGACAAAT3'
ICAM1	Fw: 5'GGGCATAGAGACCCCGTTGCCT3' Rev: 5' GGGTGCCAGTTCCACCCGTTC3'
CXCL1	Fw: 5'TTGCCTCAATCCTGCATCCC3' Rev: 5'TTGGATTTGTCACTGTTCAGCA3'
CSF1	Fw: 5'TCCAGCCAAGATGTGGTGAC3' Rev: 5'AGTTCCCTCAGAGTCCTCCC3'
IL1B	Fw: 5'GCCTGAAGCCCTTGCTGTAGT3' Rev: 5'GCGGCATCCAGCTACGAA3'
BMP-2	Fw: 5'AGACCTGTATCGCAGGCACT3' Rev: 5'CGGGTTGTTTTCCCACTCGT3'
CXCL2	Fw: 5'TCACAGTGTGTGGTCAACAT3' Rev: 5'ACACAGAGGGAAACACTGCAT3'
IL1A	Fw: 5'TAAGCTGCCAGCCAGAGAGGGA3' Rev: 5'AGCCTTCATGGAGTGGGCCATAGC3'
IL8	Fw: 5'GGCAGCCTTCCTGATTTCTG3' Rev: 5'CTTGCCAAAACTGCACCTTCA3'
PTGS2	Fw: 5'GTTCCACCCGCAGTACAGAA3' Rev: 5'AGGGCTTCAGCATAAAGCGT3'
Actin	Fw: 5'CGCCGCCAGCTCACCATG3' Rev: 5'CACGATGGAGGGGAAGACGG3'

H3	Fw: 5'GAAGAAACCTCATCGTTACAGGCCTGGT3' Rev: 5'CTGCAAAGCACCAATAGCTGCACTCTGGAA 3'
GAPDH	Fw: 5'CATGCCATCACTGCCACCC3' Rev: 5'ACCTGGTCCTCAGTGTAGC 3'
18S	Fw: 5'GTAACCCGTTGAACCCCATT3' Rev: 5'CCATCCAATCGGTAGTAGCG3'

Cell cycle and FACS analysis. For FACS analysis, adherent and floating cells were harvested, permeabilized with 0.1% NP-40 in PBS containing RNase A (200 μg/ml) and then stained with 50 μg/ml Propidium Iodide (#P4865, Sigma). At least $2x10^4$ cells were counted in each experiment, using a FACSCalibur flow cytometer (Becton-Dickinson). Cell cycle analysis was performed with FlowJo software (http://www.flowjo.com/).

Migration and invasion assays. For transwell migration assays, cells ($0.5\text{-}1x10^5$) were plated on 24 well PET inserts (8.0 μm pore size, Falcon). After 16 hr, cells that passed through the filter were fixed in 4% PFA, stained with 0.05% crystal violet (or Hoechst, as indicated) and counted.

For invasion assays, cells ($0.5\text{-}1x10^5$) were plated on 24 well PET inserts (8.0 μm pore size, Falcon) coated with BD Matrigel™ (BD Bioscience). Cells that passed through the matrigel-coated filter were fixed, stained, and counted after 18 hr.

For invasion assays using DCCM, cells were seeded in 10% FBS on the upper chamber, while the lower chamber was filled with DCCM or control medium. After 18 hr cells were fixed as previously described. For invasion or transwell assays using recombinant TNFα, cells were pre-treated with the cytokine; specifically, cells were kept in low (0.1%) serum with or without TNFα (10ng/ml) for 24 hr. Subsequently, cells were trypsinized, counted, and re-seeded on filters in low serum, with or without TNFα. The lower chamber was filled with high serum medium without TNFα. Cells were fixed as previously described.

DCCM media preparation. Precursor cells were extracted from C57BL/6 mice bone marrow and grown in IMDM (Iscove's Modified Dulbecco's Medium, GIBCO) supplemented with 10% fetal bovine serum (FBS, GIBCO), primocin (Invivogen), and beta-mercaptoethanol 50μM (Sigma-Aldrich). The cells were induced to differentiate

through addiction of 30% GM-CSF (Granulocyte-macrophage colony-stimulating factor), produced harvesting the conditioned culture media of J558 cells. Dendritic cells were maintained in IMDM medium for 7-8 days. Subsequently, they were stimulated O/N with LPS (1μg/ml). The supernatant was then harvested and centrifuged to remove cells in suspension. DCCM was aliquoted and stored at -80°C.

***In vivo* Tumorigenicity and Metastasis assays.** For xenograft studies, $1x10^6$ of MDA-MB-231_GFP or MDAMB231_eGFP-DAB2IP$_{1-186}$KA2 were resuspended in 100 μl of DMEM, injected into the mammary fat of previously anesthetized 6 weeks old SCID female mice (1-3% isoflurane, Merial). The mice were used and housed in a specific pathogen-free (SPF) animal facility. Procedures involving animals and their care were in conformity with institutional guidelines (D.L. 116/92 and subsequent complementing circulars) and all experimental protocols were approved by the ethical Committee of the University of Padua (CEASA). Tumor growth at the injection site was monitored by repeated caliper measurements. Tumor volume was calculated using the formula: tumor volume (mm^3) = $D \times d^2/2$, where D and d are the longest and the shortest diameters, respectively. After 21 days the animals from MDA-MB-231_GFP group were anesthetized and the primary tumors were extracted and directly frozen in liquid nitrogen to perform molecular analyses. The mice from MDAMB231_eGFP-DAB2IP$_{1-186}$KA2 group were sacrificed when the tumor reached the same volume of the control group, at day 25. For metastasis studies the lymph nodes were excised and formalin-fixed and paraffin-embedded (Diapth) for hematoxylin-eosin staining and human Cytokeratin 7 (Cell Marque, OV-TL12/30) staining.
All *in vivo* tumor growth experiments were conducted according to the UK Coordinating Committee on Cancer Research (UKCCCR) guidelines 1989 for the welfare of animals in experimental neoplasia. During *in vivo* experiments, animals in all experimental groups were examined daily for a decrease in physical activity and other signs of disease.

Peripheral blood mononuclear cells (PBMCs) chemoattractant assay.
Peripheral blood mononuclear cells (PBMCs) from healthy blood donors were isolated from anonymous buffy coats, kindly provided by the local blood bank (Dipartimento

Immunotrasfusionale, Ospedale Maggiore, Trieste, Italy) using Ficoll-PaqueTM PLUS density gradient (GE Healthcare) as previously described (Spessotto et al., 1995). PBMCs (9 x 10^5 cells/ml), resuspended in DMEM with 0.1% FBS, were added to the upper compartment of the polycarbonate insert of a 6-well Transwell system (24 mm diameter, 8μm pores; Corning Costar). PBMCs were left to migrate for 45 min at 37°C and 5% CO_2 in MDA-MB-231 cells conditioned medium (CM), added to the lower chamber as a chemoattractant for PBMCs. The number of cells transmigrated to the lower side of the insert was evaluated by Coulter Counter® Analyzers (Coulter Electronics). PBMCs migrated were fixed with FIX & PERM® cell fixation and permeabilization kit (Società Italiana Chimici) according to the manufacturer's instructions. A total number of 5×10^5 cells were incubated on shaking at 800 rpm O/N at 4°C with PE- or FITC-conjugated mouse monoclonal antibody (mAb) specific to human CD3 (clone MEM-57), CD8 (clone MEM-31), CD45 (clone MEM-28), CD56 (clone MEM-188) (ImmunoTools GmbH) and IgG1 and IgG2a (ImmunoTools GmbH) isotype controls. Cells were fixed with 1% PFA (Sigma-Aldrich) and analyzed for fluorescence with a FACSCalibur flow cytometer (BD Falcon) using CellQuest software.

Statistical Analysis

In all graphs data are expressed as mean ± SD of three independent experiments, except when otherwise indicated. Differences were analyzed by Student's t test using Prism 5 (GraphPad). P-values < 0.05 were considered significant.

Microarray Hybridization and Analysis

For gene profiling, we used the Illumina HumanHT-12-v4-BeadChip (Illumina), which includes a bead pool of more than 48,000 unique bead types corresponding to 40,876 transcripts. Total RNA (2μg) isolated from MDA-MB-231 cells expressing siRNA control (siC) and siRNA for TP53 (sip53), treated with or without TNFα were reverse transcribed and amplified according to standard protocols and in vitro transcription was then carried out to generate cRNA. cRNA was hybridized onto each array (three replicates for each condition) and then labeled with Cy3-streptavidin (Amersham Biosciences). The array was then scanned using a BeadStation 500 system (Illumina).

The full data set was submitted to Gene Expression Omnibus under accession number GSE53153. The probe intensities were calculated and normalized using GenomeStudio Data Analysis Software's Gene Expression Module (GSGX) Version 1.9 (Illumina). Further data processing was performed in the R computing environment (http://www.r-project.org/) version 2.15, with BioConductor packages (http://www.bioconductor.org/). Statistical analysis for differentially expressed genes was performed with *limma* (Smyth, 2004). P-values were adjusted for multiple testing using Benjamini and Hochberg's method to control the false discovery rate (Hochberg and Benjamini, 1990).

Cluster analysis

Starting from the normalized annotated expression matrix, after gene mean centering, features whose standard deviation was less than 0.5 were filtered out. Unsupervised hierarchical cluster analysis (average-linkage method) was performed using Cluster software (EisenLab). Cluster results were then visualized using Java TreeView software.

Definition of TNF-inducible genes

We selected differentially expressed probes with greater than 1.5 fold change in siC_TNF vs siC and/or in sip53_TNF vs sip53 contrasts. One of the 3 replicates of sip53 untreated cells was slightly more variable than the others, so we used a less selective P value cutoff in sip53-transfected samples (adjusted P value < 0.05 in sip53 versus adjusted P value <0.005 in siC transfected samples). We defined TNF-inducible genes as the union of genes differentially induced by TNFα in each contrast (420 genes, Figure 2A).
To obtain TNF-inducible genes specifically affected by mutant p53 depletion, we first identified genes differentially expressed in the siC_TNF vs sip53_TNF contrast by FC>=2, generating two lists: genes downregulated in sip53_TNF samples (275 genes, up_siC) and genes upregulated in sip53_TNF samples (148 genes, up_sip53). Next, we intersected both lists with the list of TNF-inducible genes (Figure 2A), obtaining TNF-inducible genes differentially expressed in control or sip53-depleted cells after TNF-treatment (Table S1).

Gene Ontology (GO) term enrichment analysis

Differentially expressed gene lists were analyzed for functional associations. Data were analyzed through DAVID Bioinformatics Resources v6.7 (Dennis et al., 2003; Huang da et al., 2009) using standard parameters and the Illumina HumanHT-12_V3_0_R2_11283641_A gene set as background population (Table S2).

ExPlain analysis

To analyze enrichment in predicted transcription factor binding sites, we used the ExPlain 3.1 package of the Biobase suite (Kel et al., 2008).

We focused on genes differentially expressed by FC >= 2 in siC_TNF vs siC and in sip53_TNF vs sip53, and generated three lists: 1) genes induced by TNFα only in control cells; 2) genes induced by TNFα only in sip53-transfected cells; 3) genes induced by TNFα in both. We analyzed predicted transcription factor binding sites in the genomic region spanning -500 to +100 nucleotides of the genes in the three lists. As control background population we used a set of 3000 genes showing no change upon TNF-treatment in our microarrays (-0.02 < logFC > 0.02).

Breast cancer datasets and meta-analysis

We used a meta-dataset comprising 3254 unique samples from 19 independent studies comprising microarray data of breast cancer samples and annotations on patients' clinical outcome. Generation and normalization of the meta-dataset, together with the list of datasets included, are described in detail in Rustighi et al. (2013).

A total of 876 basal/TNBC samples has been defined using Subtype Clustering Model and ESR1, ERBB2 and AURKA gene modules as implemented in the *scmod2.robust* function of the *genefu* Bioconductor package (Wirapati et al., 2008).

To identify two groups of tumor samples with either high or low levels of a given gene signature, we used the classifier described in Adorno et al. (2009). Briefly, we defined a classification rule based on summarizing the standardized expression levels of each gene in a signature into a combined score with zero mean. Tumors were then classified as signature Low if the combined score was negative and as signature High if the combined

score was positive. This classification was applied to log2 expression values obtained using RMA on the meta-dataset described above.
The same classification was used for analysis of average expression of various signatures in the affimetrix meta-dataset as well as in the Uppsala (Miller et al., 2011) and Metabric (Curtis et al., 2012) datasets.
The upsiC10 signature includes the following genes: MMP9, LTB, CXCL10, HLA-DMB, CX3CL1, EBI3, CASP1, HLA-F, IDO1, CTSW.

Survival analysis

To evaluate the prognostic value of genes signatures, we estimated, using the Kaplan-Meier method (Kalbfleisch and Prentice, 2002), the probabilities that patients would remain disease free (DFS). Kaplan-Meier curves were compared using the log-rank test (Harrington and Fleming). P-values were calculated according to the standard normal asymptotic distribution. Survival analysis and Kaplan-Meier plots were obtained using R *survcomp* package. Kaplan-Meyer curves were compared using the log-rank test of the *surv_test* function (*coin* R package).

To evaluate the prognostic value of gene signatures in datasets with known p53 status, we collected the only available public datasets with known p53 status and reliable information on disease-free (or relapse-free) survival: these are the Uppsala (Miller et al., 2005) and CRCM (Sabatier et al., 2011) studies.
The Uppsala dataset contains information on p53 sequence. In this dataset, 189 samples are annotated as “wt”, and 58 samples as “mutant” p53. Among the latter, 11 samples have nonsense or frameshift mutations in the first half of the p53 sequence, and therefore are predicted to express no p53 protein: these samples were manually annotated as p53-null (ko). All other mutants are predicted to encode translatable p53 proteins with various structural alterations (37 are missense). The CRCM dataset contains information on the immunohistochemical (IHC) detection of p53: a weak or null IHC signal is annotated as “wt” and a strong IHC signal is annotated as “mutant” p53. Therefore, CRCM samples annotated as “mutant” are conceptually similar to samples annotated as “mutant” in the manually edited Uppsala dataset.

We used the two datasets to analyze disease-free survival by univariate Cox regression using the *coxph* function (*survival* R library), merging the results to calculate the hazard ratio (HR) for expression of various metagenes (Table S3).

SUPPLEMENTAL REFERENCES

Adorno, M., Cordenonsi, M., Montagner, M., Dupont, S., Wong, C., Hann, B., Solari, A., Bobisse, S., Rondina, M.B., Guzzardo, V.*, et al.* (2009). A Mutant-p53/Smad complex opposes p63 to empower TGFbeta-induced metastasis. Cell *137*, 87-98.

Curtis, C., Shah, S.P., Chin, S.-F., Turashvili, G., Rueda, O.M., Dunning, M.J., Speed, D., Lynch, A.G., Samarajiwa, S., Yuan, Y.*, et al.* (2012). The genomic and transcriptomic architecture of 2,000 breast tumours reveals novel subgroups. Nature *486*, 346-352.

Dennis, G., Jr., Sherman, B.T., Hosack, D.A., Yang, J., Gao, W., Lane, H.C., and Lempicki, R.A. (2003). DAVID: Database for Annotation, Visualization, and Integrated Discovery. Genome biology *4*, P3.

Drost, J., Mantovani, F., Tocco, F., Elkon, R., Comel, A., Holstege, H., Kerkhoven, R., Jonkers, J., Voorhoeve, P.M., Agami, R.*, et al.* (2010). BRD7 is a candidate tumour suppressor gene required for p53 function. Nat Cell Biol *12*, 380-389.

Girardini, J.E., Napoli, M., Piazza, S., Rustighi, A., Marotta, C., Radaelli, E., Capaci, V., Jordan, L., Quinlan, P., Thompson, A.*, et al.* (2011). A Pin1/mutant p53 axis promotes aggressiveness in breast cancer. Cancer Cell *20*, 79-91.

Hochberg, Y., and Benjamini, Y. (1990). More powerful procedures for multiple significance testing. Stat Med *9*, 811-818.

Huang da, W., Sherman, B.T., and Lempicki, R.A. (2009). Systematic and integrative analysis of large gene lists using DAVID bioinformatics resources. Nature protocols *4*, 44-57.

Kalbfleisch, J.D., and Prentice, R.L. (2002). The Statistical Analysis of Failure Time Data (Hoboken, NJ, USA: John Wiley & Sons, Inc.).

Kel, A., Voss, N., Valeev, T., Stegmaier, P., Kel-Margoulis, O., and Wingender, E. (2008). ExPlain: finding upstream drug targets in disease gene regulatory networks. SAR and QSAR in environmental research *19*, 481-494.

Lunardi, A., Di Minin, G., Provero, P., Dal Ferro, M., Carotti, M., Del Sal, G., and Collavin, L. (2010). A genome-scale protein interaction profile of Drosophila p53 uncovers additional nodes of the human p53 network. Proc Natl Acad Sci U S A *107*, 6322-6327.

Miller, T.W., Balko, J.M., Ghazoui, Z., Dunbier, A., Anderson, H., Dowsett, M., Gonzalez-Angulo, A.M., Mills, G.B., Miller, W.R., Wu, H.*, et al.* (2011). A Gene Expression Signature from Human Breast Cancer Cells with Acquired Hormone Independence Identifies MYC as a Mediator of Antiestrogen Resistance. Clinical Cancer Research *17*, 2024-2034.

Rustighi, A., Zannini, A., Tiberi, L., Sommaggio, R., Piazza, S., Sorrentino, G., Nuzzo, S., Tuscano, A., Eterno, V., Benvenuti, F.*, et al.* (2013). Prolyl-isomerase Pin1 controls normal and cancer stem cells of the breast. EMBO Molecular Medicine *DOI: 10.1002/emmm.201302909*.

Smyth, G.K. (2004). Linear models and empirical bayes methods for assessing differential expression in microarray experiments. Stat Appl Genet Mol Biol *3*, Article3.

Spessotto, P., Dri, P., Bulla, R., Zabucchi, G., and Patriarca, P. (1995). Human eosinophil peroxidase enhances tumor necrosis factor and hydrogen peroxide release by human monocyte-derived macrophages. Eur J Immunol *25*, 1366-1373.

Wirapati, P., Sotiriou, C., Kunkel, S., Farmer, P., Pradervand, S., Haibe-Kains, B., Desmedt, C., Ignatiadis, M., Sengstag, T., Schutz, F.*, et al.* (2008). Meta-analysis of gene expression profiles in breast cancer: toward a unified understanding of breast cancer subtyping and prognosis signatures. Breast Cancer Res *10*, R65.

Zhang, R., He, X., Liu, W., Lu, M., Hsieh, J.T., and Min, W. (2003). AIP1 mediates TNF-alpha-induced ASK1 activation by facilitating dissociation of ASK1 from its inhibitor 14-3-3. J Clin Invest *111*, 1933-1943.

PART 3: IDENTIFICATION OF microRNA TARGETING DAB2IP

In this part, I describe the results of a project aimed to identify and characterize microRNAs able to target and down-regulate DAB2IP in tumor cells. This could represent an important additional mechanism counteracting DAB2IP tumor suppressive functions in human malignancies, and may set the basis for a potential therapeutic strategy to restore DAB2IP levels and activity in cancers in which this protein is down-regulated.

3.1 microRNA

Currently, there are nearly 2000 annotated microRNA (miRNA) precursor genes in the human genome. They are processed into more than 2500 mature miRNA sequences, many of them with unknown functions (Adams et al., 2014). miRNAs show a crucial role in the regulation of gene expression. Indeed, it has been proposed that at least 50% of mammalian proteins are controlled by this kind of small non coding RNA (Krol et al., 2010). They are 20-22 nt –long and appear to be involved in the regulation of virtually all biological processes, including development, differentiation, apoptosis and proliferation. Notably, changes in their expression have been observed in multiple human pathologies, including cancer (Adams et al., 2014; Krol et al., 2010).

3.1.1 microRNA biogenesis

miRNA genes are transcribed by both RNA polymerase II (RNAPol II) and RNA polymerase III (RNAPol III) into a primary transcript (pri-miRNA) (Winter et al., 2009). More than half of miRNA loci are transcribed as clusters from polycistronic transcriptional units (Lee et al., 2002). They can be localized in intergenic regions, or be located within other genes, in intronic non-coding regions (40% of human miRNAs) or within exons (10% of human miRNAs).

While intergenic miRNAs are transcribed autonomously by RNA Pol II from their own specific promoter, intronic and exonic miRNAs are presumed to be transcribed with their host gene (Tessitore et al., 2014). In mammals, most miRNAs have multiple paralogs, likely derived from gene duplications, which share the same seed sequence and presumably target genes. However, differences in the 3' miRNA sequence may affect the miRNA-mRNA affinity, so that paralogous miRNAs may exert very distinct roles *in vivo* (Ventura et al., 2008).

Expression of miRNAs is under the same kind of control as protein-coding genes (Winter et al., 2009), and each miRNA located in a given genomic cluster can be transcribed and regulated independently (Song and Wang, 2008).

It should be considered that pri-miRNAs can be subjected to RNA editing; this process can change their sequence, affecting base-paring and structural properties, thus influencing their further processing as well as their target recognition abilities (Winter et al., 2009). Notably, miRNA editing has been shown to enhance miRNA processing by Drosha (Kawahara et al., 2008). The pri-miRNA folds into hairpins with two single-stranded flanking regions upstream and downstream. The double-stranded stem and the unpaired flanking regions are critical for DGCR8 binding and cleavage by the RNase-type III endonuclease Drosha (components of the nuclear Microprocessor complex) (Han et al., 2006; Zeng and Cullen, 2005). This cleavage occurs co-transcriptionally, preceding intron splicing (Morlando et al., 2008), and generates the pre-miRNA (Figure 3.1). After nuclear processing, the pre-miRNA is exported into the cytoplasm by Exportin-5 (Yi et al., 2003), in a manner not dependent on miRNA sequence or loop structure.

In the cytoplasm the pre-miRNA is processed by the RISC loading complex (RLC). The RNase-type III endonuclease Dicer, the double strand RNA-binding domain proteins TRBP (Tar RNA binding protein), PACT (protein activator of PKR) and the core component Argonate-2 (Ago-2) assemble this protein complex (Winter et al., 2009). Argonaute family contains four AGO proteins, AGO1 to AGO4. Their function in miRNA pathway is demonstrated with their ability to repress protein synthesis when artificially tethered to the mRNA 3'UTR (Filipowicz et al., 2008; Pillai et al., 2004). AGO1 is dedicated to the miRNA pathway, and AGO2 is the only one that functions in RNA interference processes (Peters and Meister, 2007). TRBP and PACT are not essential for the endonuclease activity of Dicer, but they can facilitate it, stabilizing Dicer protein (Krol et al., 2010; Winter et al., 2009). Moreover, they are important for the recruitment of AGO2 (MacRae et al., 2008). Dicer cleaves the loop of the pre-miRNA and generates a 22-ntmiRNA duplex with two nucleotides protruding as overhangs at each 3' end. This cleavage is essential for miRNA processing and has been observed in many organisms (Bernstein et al., 2001; Ketting et al., 2001). Deletion of Dicer decreases or totally abrogates the production of mature miRNAs in cells (Grishok et al., 2001; Hutvagner et al., 2001), while in mice, its loss is associated with lethality early in development, underlining its crucial role in miRNA processing, and the crucial role of miRNAs in embryogenesis (Bernstein et al., 2003). Intriguingly, for pre-miRNAs that display a high degree of complementary along the hairpin stem, an additional endonucleolytic cleavage mediated by Ago2 occurs before the Dicer-mediated one (Bernstein et al., 2003).

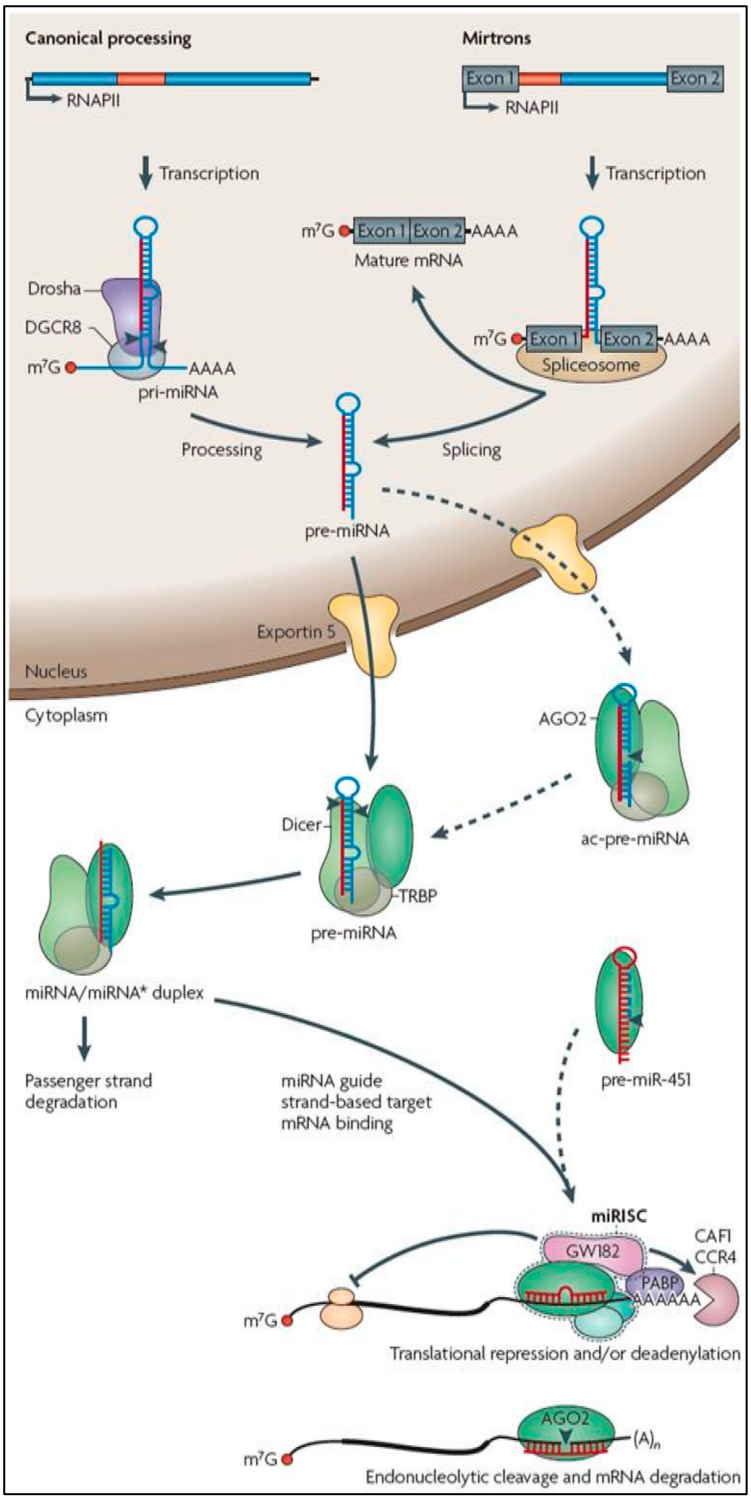

Figure 3.1: Biogensesis of miRNAs and their assembly into microribonucleoproteins. The pri-miRNAs are transcribed from independent miRNA gene or are portions of introns of protein-coding gene (mirtron). Pri-miRNA folds into hairpind structures containing imperfectly base-paired stems and are processed in two steps, catalysed by RNaseIII-type endonucleases Drosha and Dicer. These enzymes work together with accessory proteins containing a dsRNA-binding domain: DGR8 for Drosha and TRBP for Dicer. After Drosha-mediated cleavege, pre-miRNAs are transported in the cytoplasm by Exportin-5, where they are cleaved by Dicer to yield 20bp miRNA duplexes. In some cases a previous clevaged of pre-miRNA is mediated by AGO2. Then, one strand is selected to act as a mature miRNA, while the other one is generally degradeted. Occasionally, both arms of the duplex give rise to two guide miRNAs. Following their processing, miRNAs are assembled into miRNP (or miRISC) to mediate miRNA-specific translational repression. Figure taken from (Krol et al., 2010).

Dicer also participates in loading miRNAs into miRISC (miRNA-induced silencing complexes), also known as miRNP (micro-ribonucleoprotein–RNP-complex) (Krol et al., 2010; Winter et al., 2009). The mature miRISC complex is composed by a single strand RNA and one of the AGO proteins that harbors the silencer activity of the complex (Krol et al., 2010) (Winter et al., 2009) To form the active RISC complex involved in gene silencing, the functional guide strand,

complementary to the target mRNA, needs to be separated by the other strand in the duplex (the passenger strand). Apart from the AGO proteins, miRISC often comprises other proteins, which probably drive its assembly or regulation, or act as effectors (Peters and Meister, 2007).

The thermodynamic stability of the miRNA duplex ends defines which strand, miRNA-3p or miRNA-5p, is preferentially loaded on miRISC. Notably, cleavage heterogeneity can affect the stability of the hairpin ends, and thus influence strand selection (Krol et al., 2010). In addition, the identity of the 5'-terminal nucleotide may directly affect the efficiency of miRNA loading into miRISC, independent of duplex end stability (Frank et al., 2010).

Commonly, most miRNA genes produce one dominant mature miRNA; the passenger strand miRNA, also identified as miRNA*, is generally degraded once the guide strand is loaded on the RISC complex (Winter et al., 2009). However, passenger strand miRNAs* can also be loaded into RISC to function in gene regulation (Ghildiyal et al., 2010; Okamura et al., 2009).

Notably, the ratio of miRNA to miRNA* production and RISC loading can vary in different tissues or developmental stages; this probably depends on specific properties of the pre-miRNA duplex, or on the activity of different accessory factors (Krol et al., 2004; Zeng and Cullen, 2005). Notably, this ratio can be modulated also by the availability of the respective mRNA targets, as a results of enhanced destabilization of either miRNA or miRNA* occurring in the absence of respective complementary mRNA (Krol et al., 2010).

3.1.2 microRNAs mechanisms of action

In plants, miRNAs generally bind mRNA target with nearly perfect complementarity and trigger endonucleolytic mRNA cleavage by a RNAi-like mechanism (Filipowicz et al., 2008). In rare cases, this mechanism it applied also in mammals: perfect pairing of a miRNA with its target leads to endonucleolytic cleavage of the mRNA by Argonaute (Figure 3.2, model a) (Llave et al., 2002). However, most commonly, miRNAs bind imperfectly their targets, inducing a set of different processes that support the block of mRNA translation and impair protein synthesis (Filipowicz et al., 2008; Pasquinelli, 2012).

Partial pairing of the miRNA to the target 3'UTR sites can result in the deadenylation of the mRNA. The miRISC-associated GW182 protein mediates the recruitment of the CCR4-NOT deadenylating complex and the decapping proteins DCP1 and DCP2, which remove the poly(A) tail and make the mRNA susceptible to exonucleolytic degradation (Figure 3.2, model b) (Behm-Ansmant et al., 2006; Braun et al., 2011; Wu et al., 2006).

Partial pairing of the miRNA to the target 3'UTR sites can also cause reduction of protein, but not mRNA levels. This phenomenon can be explained by inhibition of translation initiation and

elongation, as well as by direct proteolysis of the peptide that is being synthesized (Behm-Ansmant et al., 2006; Filipowicz et al., 2008) (Figure 3.2). Factors bound at the 3'UTR of a mRNA-miRNA complex exert an inhibitory effect on translational initiation by the recruitment of proteins that interfere with the eIF4E and eIF4G interaction (one of the essential steps to catalyze initiation of translation) or bind directly to the mRNA cap. Both these mechanisms counteract the recruitment of the 40S ribosomal subunit and the formation of 40S initiation complex (Figure 3.2, model c).

The observation that miRNAs are associated with polysomes implies that translation can be repressed by the miRISC also after initiation, possibly by promoting ribosome drop-off, premature ribosome dissociation, or stimulating proteolysis of the nascent peptide (Filipowicz et al., 2008; Pasquinelli, 2012).

Intriguingly, under certain circumstances miRNAs have also been shown to up-regulate target mRNA expression. (Orom et al., 2008; Vasudevan et al., 2007).

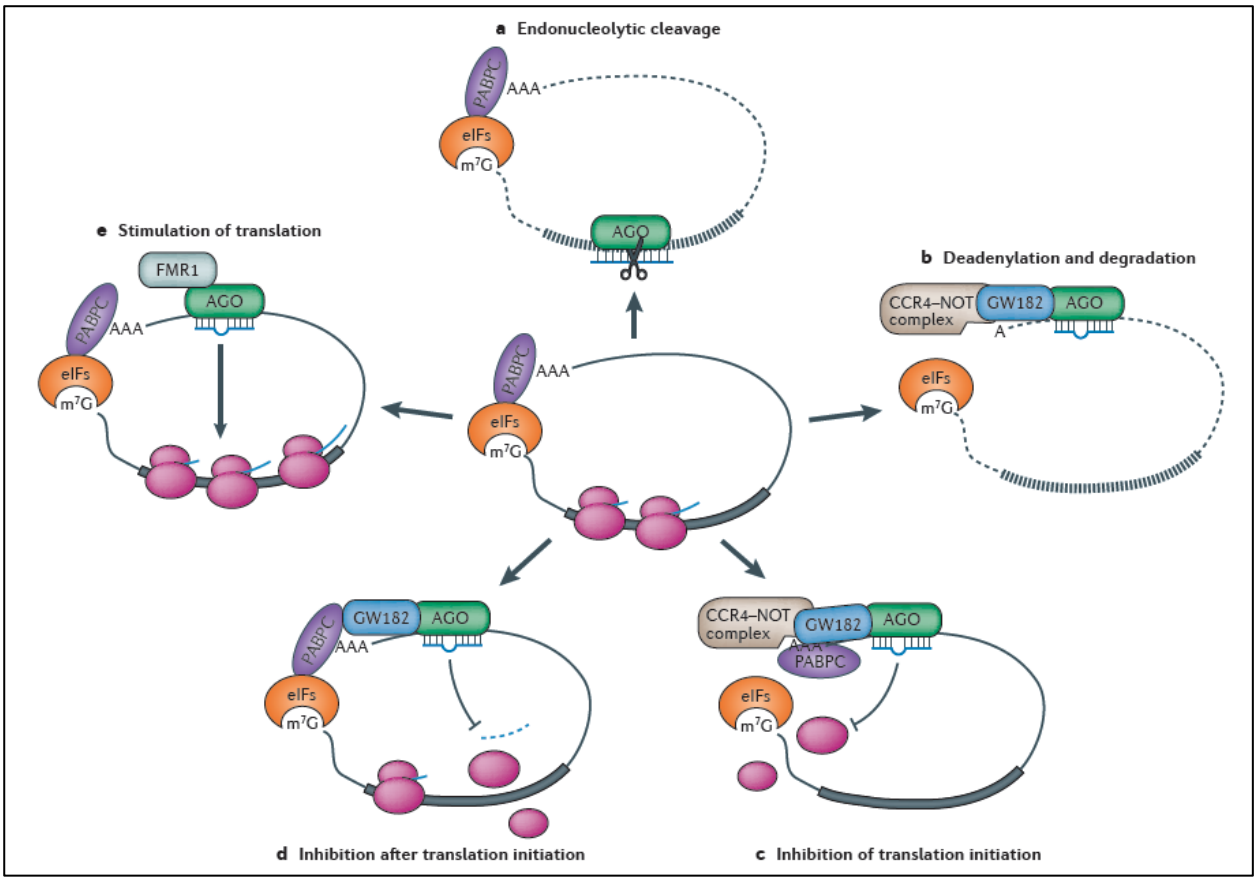

Figure 3.2: Possible mechanisms of microRNA-mediated post-transcriptional gene repression in mammals. A schematic representation of the better known mechanisms implicated in miRNA-mediated regulation of translation and protein production. Reproduced from (Pasquinelli, 2012). See text for details.

3.1.3 microRNAs in cancer

The first evidence of an association between miRNA deregulation and cancer was published in 2002: the loss of two miRNAs (miR-15 and miR-16), whose genes are localized into a chromosomal region frequently deleted in chronic lymphocytic leukemia (CLL), was correlated with the development of an indolent form of CLL (Calin et al., 2002). Progressively, various evidences showed how miRNAs are involved in the control of several cancer-relevant processes, such as proliferation, apoptosis, DNA damage, regulation of the tumor microenvironment, migration and invasion (Baranwal and Alahari, 2010; Chou et al., 2013; Hwang and Mendell, 2006; Jovanovic and Hengartner, 2006; Tessitore et al., 2014).

Abnormal expression of miRNAs has been observed in both solid and hematopoietic tumors (Calin and Croce, 2006; Lu et al., 2005). Thus, miRNA expression signatures distinguish cancerous tissues from normal tissue; these signatures are associated to diagnosis, staging, progression, prognosis and response to treatment in many cancer types. For instance, two large studies using various solid tumors and leukemias demonstrated that miRNA-expression profiles classify human cancers according to developmental lineage and differentiation stage, and that patterns of miRNAs expression for each tumor type reflect distinct mechanism of transformation (Lu et al., 2005; Volinia et al., 2006). Notably, these studies and other have individuated a group of miRNAs whose expression is commonly altered in tumors, involving common impaired regulatory pathways. For example miR-21, miR-17-92 cluster, and let-7 are often deregulated leading to the activation of important oncogenic pathways (Johnson et al., 2005; Mendell, 2008; Volinia et al., 2006).

miRNAs are not involved only in tumor development, but affect every step of carcinogenesis (Acunzo and Croce, 2015; Acunzo et al., 2015). For example, a pro-metastatic role has been observed for miR-10b in breast carcinoma. Expression of this miRNA is promoted by the EMT inducer Twist; miR-10b inhibits the translation of the homebox D10 (HOXD10) mRNA, releasing expression of the pro-metastatic gene RHOC (Ma et al., 2007). Conversely, members of the miR-200 family and miR-205 have been shown to decrease cell motility and invasiveness by targeting the ZEB transcription factor, a known EMT inducer, and protein kinase PKCγ (Gandellini et al., 2009; Gregory et al., 2008).

The miR-92a family is a group of highly conserved miRNAs, including miR-25, miR-92a-1, miR-92a-2, and miR-363, that share an identical seed region, and arise from three different paralogous clusters: miR-17-92, miR-106b-25 and miR-106a-363 (Li et al., 2014a). They are all known onco-miRNAs able to sustain proliferation, migration, and invasion of tumor cells. For example, miR-92a can directly target PHLPP2 (PH domain leucine-rich repeat protein

phosphatase), an important negative inhibitor of the PI3K/Akt/mTOR pathways; up-regulation of miR-92a can activate this signaling, inhibiting cell apoptosis induced by chemotherapy in mantle cell lymphoma (Rao et al., 2012). The family-member miR-25 targets the cell cycle inhibitor p21, the pro-apoptotic factor Bim, and the inhibitory Smad 7 directly, resulting in an increased level of TGF-β signaling, and TGF-β pathway-mediated tumor growth and invasion (Kan et al., 2009; Petrocca et al., 2008b; Smith et al., 2012).

In conclusion, there is now a vast literature in support of the major impact of miRNAs in cancer, so the mechanisms of their aberrant expression represent a crucial aspect of oncogenesis.

miRNA deregulation in cancer could be due to aberrant epigenetic changes in the methylation status of miRNA promoters (Fabbri et al., 2013). Notably, half of the known miRNAs reside in genomic regions that are reported to be prone to alterations in cancer, including minimal regions of amplification, which may contain oncogenes and onco-miRNAs, common breakpoint region in or near pro-oncogene or tumor suppressor genes and fragile site (Volinia et al., 2006).

Another mechanism involved in aberrant miRNA levels expression in cancer is the altered functions and/or activities of the enzymes implicated in miRNA biogenesis. For example, the expression of Drosha and Dicer is reduced in 39% of patients with ovarian cancer and in lung cancer (Karube et al., 2005; Merritt et al., 2008), while frameshift or nonsense mutations of Dicer were observed in other tumors, resulting in truncated proteins (Lin and Gregory, 2015). Three recurrent inactivating mutations of Exportin 5 were identified in sporadic colon, gastric and endometrial tumors, possibly resulting in a global reduction of mature miRNAs (Melo et al., 2010).

Clearly, activity of transcription factors is also a major player in the regulation of miRNA expression, with multifaceted and opposite roles. A very important example of this is the induction of miR-17-92 cluster transcription by the c-myc proto-oncogene (O'Donnell et al., 2005).

3.2 MicroRNA 149-3p (miR-149*)

In this Thesis, I describe functional studies regarding miR-149, so I summarize here the current knowledge about this molecule.

The human miRNA-149 gene localizes on chromosome 2q37.3, within the first intron of the glypican 1 (GPC1) gene, and encodes for two different miRNAs: miR-149-5p (miR-149, guide strand) and miR-149-3p (miR-149*, passenger strand). Both miRNAs are highly conserved among mammals (Chamorro-Jorganes et al., 2014; Jin et al., 2011).

There are studies indicating that both miR149 and miR-149* may have a role in tumors; however, the available information on their target identity, regulation, and possible involvement in oncogenic biological processes is limited and occasionally controversial. Moreover, there are very scarce data regarding their transcription and biosynthesis regulation.

miR-149 is an intronic miRNA, so its expression should be linked to that of its host gene, GPC1. Glypicans (GPCs) are glycosyl-phosphatidylinositol-anchored (GPI-anchored) heparan sulphate proteoglycans (HSPGs) (Fico et al., 2011). Together with syndecans, they are the major cell membrane HSPGs; their presence in extracellular matrix and in cell surface is crucial for the regulation of various biological processes, including cell proliferation, development and differentiation, blood coagulation, angiogenesis and tumor metastasis (Iozzo and Sanderson, 2011). Intriguingly, GPC1 is involved in angiogenesis and tumorigenesis; indeed, it is frequently overexpressed in multiple malignances, such as pancreatic carcinoma, breast cancer and glioma (Aikawa et al., 2008; Kleeff et al., 1998; Kleeff et al., 1999; Matsuda et al., 2001; Su et al., 2006). GPC1 has been shown to act as a co-receptor for FGF, enhancing FGF signaling, especially in endothelial cells, sustaining cell cycle progression and cell proliferation (Chamorro-Jorganes et al., 2014).

In contrast to what expected for an intronic miRNA, Chamorro-Jorganes and colleagues observed poor correlation in the expression pattern of miR-149 (including mature and primary miRNA analysis) and GPC1 in a panel of human tissues and cell lines. They concluded that this observation is indicative of independent transcriptional regulation (Chamorro-Jorganes et al., 2014). In support of their hypothesis, they identified a predicted transcription start site (TSS) located 3,1kb upstream of the miR-149 gene sequence. Looking for evidences of a putative promoter, they recognized three distinctive regions with various chromatin states in endothelial cells (EC). Notably, in other cell types the chromatin state of these regions were different, possibly justifying the differences in miR-149 expression among various cell lines (Chamorro-Jorganes et al., 2014). Treating endothelial cells with FGF2, the authors observed increased

levels of pri-miRNA and both mature miRNAs, suggesting that this growth factor may be involved in the regulation of the expression of miR-149 and miR-149*, at least in endothelial cells (Chamorro-Jorganes et al., 2014).

Notably, TNF signaling has been observed to negatively modulate miR-149 expression. TNFα treatment in endothelial cells down-regulates miR-149 levels specifically through p38MAPK signaling activation; no effect is mediated by TNF-induced JNK and Akt pathways (Palmieri et al., 2014). This study did not consider miR-149* expression.

Recently, Li et al. have observed that miR-149 is dramatically down-regulated in fibrosis and in gastric cancer associated fibroblasts (CAFs). Intriguingly, they observed that such down-regulation could be associated with hypermethylation of an H3K27ac-enriched area in a GC-rich region within -2.500 to 1500 base pair upstream of the putative miR-149 transcriptional star site (Li et al., 2015). They found that PGE2 (prostaglandin E2) treatment strongly induces DNA methylation of miR-149 gene and down-regulates miRNA-149 expression, while treatment with an inhibitor of DNA methylation abolishes this effect (Li et al., 2015). In normal fibroblasts, miR-149 down-regulates IL6-expression, maintaining these cells in an inactive state. Notably, the authors describe this regulatory circuit in the interaction between *H. pylori*-infected gastric epithelial cells and gastric CAFs: *H. pylori* infection induces the secretion of PGE2 by gastric epithelial cells; PGE2 silences miR-149 by hypermethylation of miR-149 gene, removing the suppression on IL-6 and EP2; the elevated levels of IL-6 stimulates the tumor-promoting ability of fibroblasts, which enhances EMT transition and stem-like properties of gastric cancer cells (Li et al., 2015). This work is a good example of a how miRNAs can modulate the behavior of immune cells in the tumor microenvironment, and how modification in their regulation and synthesis can affect tumor development and progression. However, as in previous work, this study did not consider miR-149* expression. It is tempting to speculate that TNF-mediated p38MAPK signaling, as well PGE2-mediated hypermethylation, could regulate miR-149* levels in cells, as has been observed for miR-149.

Interestingly, in one study focused on miR-149*, Jin et al. identified a putative p53-responsive element located 1.592 to 1.572 base pair upstream of the GPC1 translational star site. The p53 binding region is transcriptionally responsive to treatment with tunicamycin (TM), a drug that induces Endoplasmic Reticulum (ER) stress. They found that treatment with TM increases levels and transcriptional activity of p53, and augments miR-149* levels in melanoma cells. Notably, an increase of miR-149-5p has also been measured, although to less extent (Jin et al., 2011).

One interesting aspect that emerges from literature regarding miR-149/miR-149* is the involvement of both strands in the regulation of translation, so that this gene actually encodes two functional miRNAs. Chamorro-Jorganes and colleagues observed that the two miR-149 strands showed an overall different pattern of expression, which is in agreement with the idea of tissue-dependent mechanisms of strand selection (Chamorro-Jorganes et al., 2014).

Notably, in some cases they functionally cooperate; for instance, both miR-149 strands target the GPC1 and FGFR1 mRNAs, to control a complex signaling network in endothelial cells that have a role in proliferation, cell motility and angiogenesis (Chamorro-Jorganes et al., 2014).

Indeed, even though miR-149 and miR-149* do not have the same seed sequence, they share many predicted targets involved in multiple aspects of tumorigenesis, including angiogenesis, inflammation, proliferation, migration and invasion, as inferred by bioinformatics analysis (Chamorro-Jorganes et al., 2014). When both miRNAs are co-expressed in cells, this is likely to promote cooperative silencing, therefore reinforcing their activity.

In addition to common targets, miR-149 and miR-149* display also many different putative and validated targets, and are involved in the regulation of different biological processes, often with opposite results.

While miR-149 almost exclusively acts as a tumor suppressor miRNA (Bischoff et al., 2014; Chamorro-Jorganes et al., 2014; Chan et al., 2014; Fujii et al., 2015; Ke et al., 2013; Li et al., 2015; Luo et al., 2015; Palmieri et al., 2014; Wang et al., 2012; Xu et al., 2015a; Xue et al., 2015), two works indicate that miR-149* exerts mainly a pro-tumoral activity (Fan et al., 2016; Jin et al., 2011).

In particular, miR-149 has been observed to counteract EMT and cell migration and invasion in hepatocellular carcinoma and in breast, endothelial cell, colorectal, and non-small cell lung cancer (Palmieri et al., 2014) (Bischoff et al., 2014; Chan et al., 2014; Ke et al., 2013; Luo et al., 2015; Xu et al., 2015a). miR-149 was also reported to block cell proliferation and cell cycle progression in gastric and prostate cancer and glioma (Fujii et al., 2015; Wang et al., 2012; Xue et al., 2015). In these studies, miR-149 was shown to down-regulate various signaling proteins, growth factors, and cytokines, including IL-6, MMP9, IL-8, ZBTB2, FOXM1, actin–regulatory protein PPM1F, small GTPases Rap1a and Rap1b, and the kinase Akt.

On the contrary, miR-149* seems to be able to promote cell proliferation and suppress apoptosis in liquid ad solid tumors. In melanoma cells, under ER stress, p53 mediates a pro-survival pathway by up-regulation of miR-149*, that in turn targets glycogen synthase kinase-3α (GSK3α), eventually leading to stabilization of Mcl-1, an anti-apoptotic protein belonging to the Bcl-2 family (Jin et al., 2011). Inhibition of miR-149* results in marked retardation of tumor

initiation and growth in xenografts mouse models; this reduced tumor growth correlates with high GSK3α and low Mcl-1 levels, and increased caspase3/7 activity (Jin et al., 2011).
A recent work has shown that miR-149* is highly expressed in T-ALL lymphoblastic leukemia cell lines (Molt-4 and Jurkat) and in bone marrow cells from T-ALL patients (Fan et al., 2016). In this cell context miR-149* overexpression down-regulates JunB, a transcription factor downstream of JNK signaling, influencing cell cycle progression and survival (Fan et al., 2016). Interestingly, the authors have also observed that miR-149* overexpression down-regulates p21, cyclin D1, and downstream effectors of mTOR signaling (4EBP1 and p70s6k), extended the list of putative means through which miR-149* could sustain the development and the progression of T-ALL (Fan et al., 2016).

However, miR-149* has also been shown to act as a tumor suppressor miRNA in HeLa and BeC2 neuroblastoma cell lines. In these cells, miR-149* overexpression leads to down-regulation of Akt and E2F1 protein levels, and induction of apoptosis. The silencing of Akt and E2F1 recapitulate this phenotype, suggesting that the pro-apoptotic effects of miR-149* are exerted by repressing these two proteins (Lin et al., 2010).

To conclude, while the role of miR-149 is relatively well understood in tumorigenesis, and data indicate it is tumor suppressive in almost all condition studied, much less is known about miR-149*, its possible targets, and its role in tumorigenesis. Moreover, our knowledge about the mechanisms that control expression of the miR-149 gene in tumors is still very limited, and in particular we have absolutely no clues about the cellular processes or biological stimuli that dictate expression of the miR-149 or miR-149* strands in cancer cells.
Nevertheless, both microRNAs seem to be important in carcinogenesis, both because they control pathways and processes important in tumor development, such as cell migration and invasion, cell proliferation and apoptosis, and because their expression may be regulated by stress conditions, and by extracellular stimuli such as cytokines and growth factors from the tumor microenvironment.

3.3 RESULTS

3.3.1 Identification and validation of microRNAs targeting DAB2IP

To discover additional DAB2IP-targeting miRNAs, we employed a functional approach. In collaboration with dr. Miguel Mano (ICGEB, Trieste), using an automated high-throughput screening facility, we screened a collection of 879 human miRNA mimics using dual-Luciferase-based report gene system (psiCHECK). The 3'UTR of human DAB2IP was cloned downstream of Renilla Luciferase reporter gene in psiCHECK vector. This vector expresses another reporter gene, Firefly Luciferase, used to normalize the efficiency of transfection. We co-transfected psiCHECK-DAB2IP 3'UTR, or psiCHECK empty vector, together with a library of miRNA mimics in HeLa cells. After 48 hours we read the Renilla/Firefly luciferase activity ratio. The graph in Figure 3.3A reports the list of top miRNAs able to down-regulate the reporter, resulting after two rounds of primary screening. Among them, we identified miR-338-3p, previously reported to target DAB2IP 3'UTR (Barik, 2008), confirming the reliability of the assay.

Interestingly, our functional screening identified several miRNAs that specifically up-regulate the DAB2IP 3'UTR reporter, suggesting the existence of molecular circuits that could enhance DAB2IP mRNA translation or stability (Figure 3.3B).

Our experimental approach allowed the identification of miRNAs that are not detected by prediction algorithms (Target Scan, miRanda, miRDB, mirWalk, RNA22), or have a very low probability score. Below are Venn diagrams showing the overlap between miRNAs identified through high-throughput screening (Exp) and miRNAs suggested by at least one (Pred 1) or at least three (Pred 3) prediction programs.

miRNAs down-regulating DAB2IP 3'UTR reporter

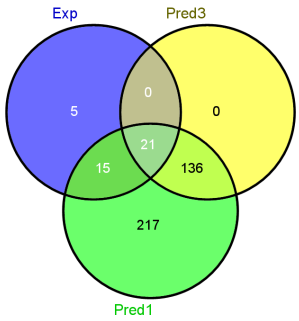

miRNAs up-regulating DAB2IP 3'UTR reporter

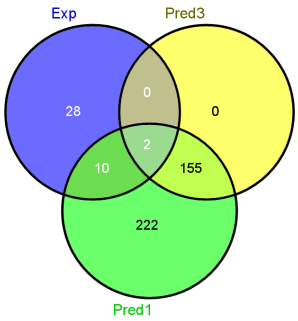

We next performed a secondary screening using the psiCHECK empty vector to expunge false positives. At the end of the screening, we identified 81 miRNAs that specifically target the

DAB2IP 3'UTR reporter with high confidence.

We focused on 41 miRNAs that repress DAB2IP 3'UTR reporter. Having a substantial number of hits, we selected the best candidates based on efficiency of inhibition on the DAB2IP 3'UTR reporter. Then, we performed a process of validation by measuring their effects on endogenous DAB2IP in multiple cell lines (HeLa, MCF-10A, SKOV-3, H1299, HCT-116, HePG2, PC-3 and LNCaP). We transfected miRNA mimics for 48 hours, and then did Western blots to evaluate DAB2IP protein levels. Representative blots relative to non-transformed mammary epithelial (MCF-10A) and prostate (PC-3) cancer cells are shown in Figure 3.3C. As can be seen, the majority of tested miRNAs reduced the protein levels of DAB2IP, at least in one cell line.

We next analyzed expression of positive miRNAs in these cell lines by RT-PCR (data not shown). We found that two top-scoring miRNAs were not expressed in our model cell lines: miR-555 and miR-582-5p. These were excluded from further study.

A heat map in Figure 3.3D summarizes the activity of 8 miRNAs tested in multiple cell lines. Some miRNAs exert different effects depending on the cell line. Notably, miR-744, miR-92a and miR-96 induced strong reduction of DAB2IP levels in at least four out of seven cell lines (Figure 3.3D). Intriguingly, among top hits there are two miRNAs that originate from the same precursor. miR-149 (miR-149-5p) is the guide strand, and has tumor suppressive functions in multiple human malignancies (Bischoff et al., 2014; Chamorro-Jorganes et al., 2014; Chan et al., 2014; Fujii et al., 2015; Ke et al., 2013; Li et al., 2015; Luo et al., 2015; Palmieri et al., 2014; Wang et al., 2012; Xu et al., 2015a; Xue et al., 2015). miR-149* (miR-149-3p) is the passenger strand, and its role in tumor progression is still unclear. Notably, miR-149* is able to induce robust DAB2IP reduction in all cell lines, while miR-149 has a weaker effect, although still detectable.

We therefore focused on miR-744, miR-92a, miR-96 and miR-149* in order to examine their ability to sustain oncogenic pathways activation, and promote and/or enhance the acquisition of aggressive phenotypes, possibly through the inhibition of DAB2IP translation.

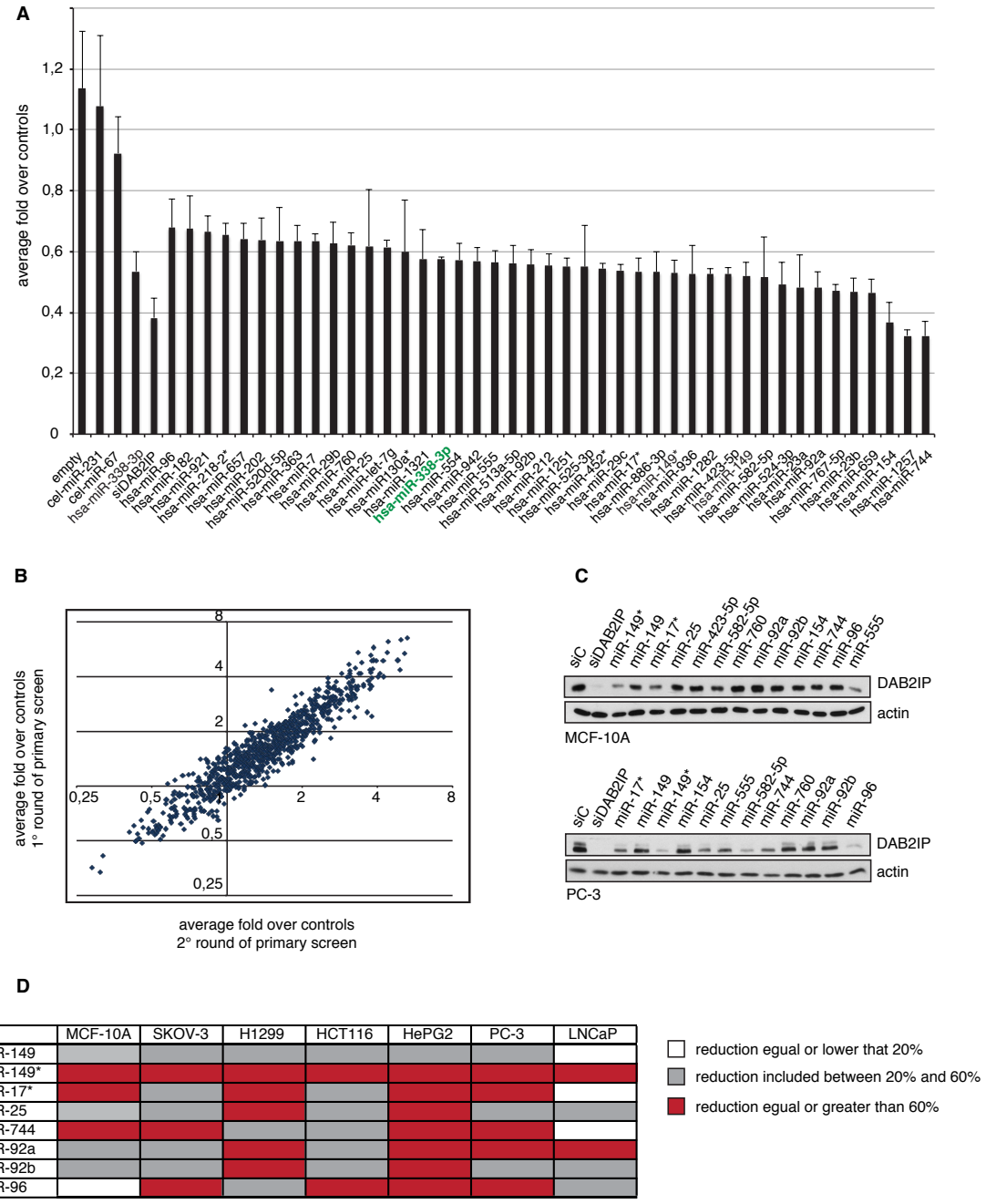

Figure 3.3: Identification of microRNAs targeting DAB2IP by high-throughput functional screening.
A-B) Results of the primary screening**. A)** HeLa cells were reverse-transfected with miRNA mimics; after 24 hours cells were transfected with psiCHECK2 DAB2IP 3'UTR vector. Dual-Luciferase assay was performed 48 hours later. The graph summarizes the results of two rounds of primary screen. The Y axis reports RLuc/FLuc ratio for each miRNA, normalized to the average of negative controls. Cel-miR-231 and cel-miR-67 were used as negative controls, while miR-338-3p mimic and a DAB2IP siRNA were transfected as positive controls (mean ± SD, n=2). In green, miR-338-3p, previously reported to target DAB2IP (Barik, 2008). **B)** The plot describes, for each microRNA, the reporter fold expression normalized to the average of all samples, in two independent screens. Values lower than 1 indicate specific repression; a significant number of samples have values greater than 2, corresponding to induction of the reporter. **C-D)** Top scoring miRNAs are able to reduce endogenous DAB2IP protein levels. **C)** A representative western blot of MCF-10A and PC-3 cells transfected with indicated miRNA mimics for 48 hours. DAB2IP siRNA (siDAB2IP) was used as positive control. Actin was used as loading control. **D**) The heat map summarizes the effects of the indicated miRNA mimics on endogenous DAB2IP protein levels in the indicated cell lines. Cells were treated as described in C. For quantitative evaluation, gel bands were quantified by densitometry on autoradiography films and normalized to control siRNA-transfected samples.

3.3.2 DAB2IP depletion strongly increases tumor cells motility

The choice of experimental assay and cellular context in which to perform the functional characterization of validated miRNAs should be based on the characteristic of each miRNA, its biological role (if known), and the kind of tumors in which it is mostly expressed. Finally, also the biological processes in which DAB2IP is involved must be considered.

Since DAB2IP is a powerful inhibitor of EMT induction, cell migration, and invasion, we evaluated the impact of DAB2IP knockdown on cell motility. We performed invasion and migration assays with several cell lines: PC-3, MCF-10A, SKOV-3 (ovarian cancer), HepG2 (hepatocellular carcinoma).

We found that DAB2IP silencing strongly increases matrigel invasion in PC-3, HepG2 and SKOV-3 cell lines (Figure 3.4A-C), and cell migration in MCF-10A (Figure 3.4D). We thus confirmed that cell migration/invasion is a cell phenotype linked to DAB2IP depletion.

Consistently, we observed that stable DAB2IP overexpression in PC-3 cells reduces vimentin (mesenchymal marker) expression, and matrigel invasion. We infected PC-3 cells with retroviral vectors encoding the two major DAB2IP isoforms (DAB2IP-long and DAB2IP-short); the encoded proteins differ at the N-terminus, where DAB2IP-long has additional 96 amino acids, allowing for a putative larger PH domain (Figure 1.1, Chapter 1.2). Notably, both isoforms reduced the expression of vimentin (Figure 3.4E), suggesting they are both involved in the regulation of pathways that control EMT. Curiously, we noticed that the short isoform of DAB2IP significantly reduced the motility of PC-3 cells (Figure 3.8B), in agreement with its ability to reduce vimentin expression. In contrast, the long DAB2IP isoform had a lesser impact on basal PC-3 invasion. We don't know the reason for the different effect exerted by the two isoforms. Immunoblotting and immunofluorescence confirmed high expression levels and cytoplasmic and membrane localization of both isoforms (Figure 3.4E).

In collaboration with dr. Luigi Marchionni at Johns Hopkins University of Baltimore (USA), we analyzed the correlation between DAB2IP mRNA levels and clinical parameters in public gene expression datasets. We focused on prostate cancer, a tumor in which the loss of DAB2IP often correlates with aggressive phenotype and metastasis formation (Kong et al., 2010; Min et al., 2010; Xie et al., 2010; Zhou et al., 2015). We analyzed the GSE21032 dataset, referring to a patient cohort in which data relative to mRNAs and miRNAs expression in primary tumors and metastases are available, along with clinical parameters (Taylor et al., 2010). In line with previous studies, DAB2IP levels are significantly reduced in primary tumors and metastasis, compared to normal tissue (Figure 3.4F).

Together, these observations suggest that DAB2IP inhibits cell invasion in various tumor contexts, especially in prostate cancer, and therefore migration/invasion is a cell phenotype that could be linked to DAB2IP depletion.

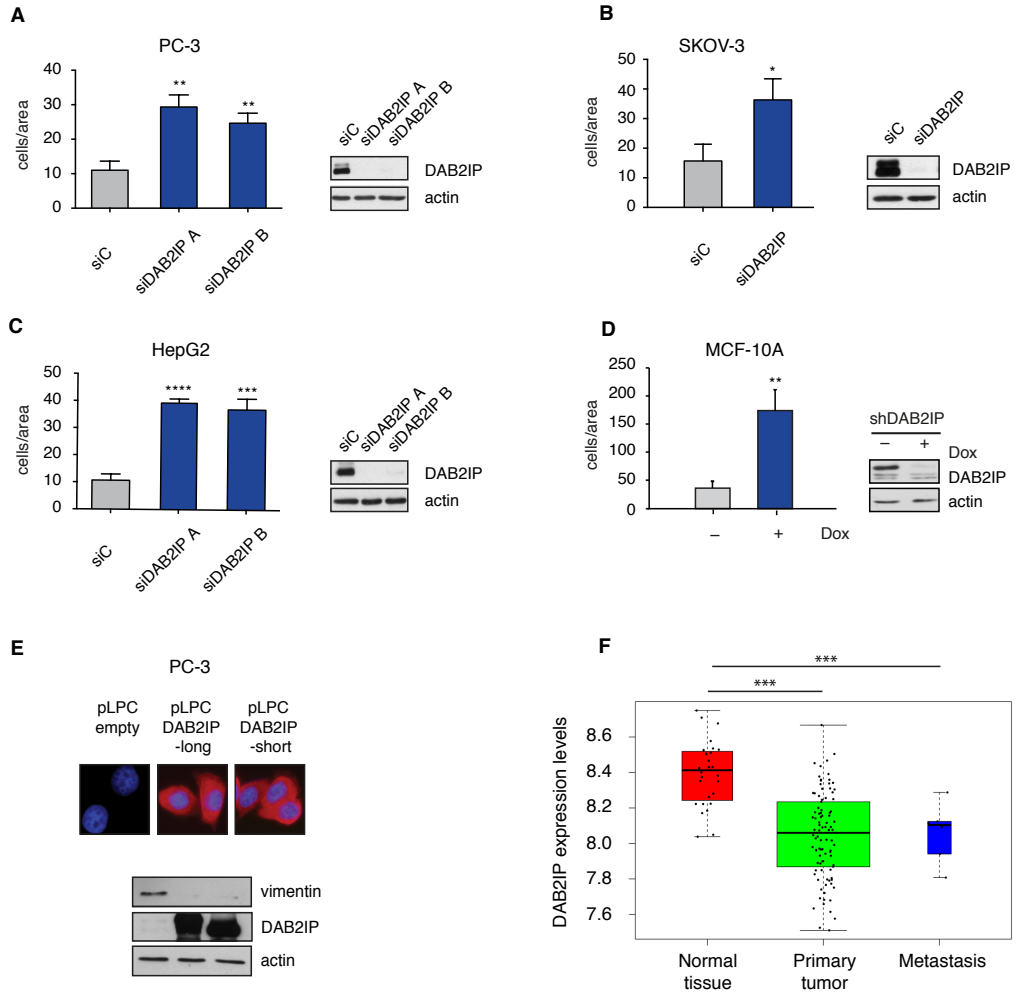

Figure 3.4: DAB2IP depletion increases cell motility and metastasis. A-D) DAB2IP silencing increases tumor cell invasion and migration. **A-C)** Indicated cells were transfected with DAB2IP (siDAB2IP) or control siRNAs (siC). After 48 hours, invasion assays were performed using matrigel-coated transwell filters under low serum conditions; the lower chamber was filled with high serum medium (10%FBS). Where indicated, two different DAB2IP siRNAs were used. Graphs summarize migrated cells per area (mean ± SD; n=3; ***P<0.001; **P<0.01; *P<0.05). DAB2IP depletion was checked by western blot, with actin as loading control. **D)** MCF-10A cells were infected with a lentivirus expressing an inducible shRNA targeting DAB2IP 3'UTR sequence (shDAB2IP). After 96 hours of doxycycline (dox) treatment (50ng/ml) to induce the expression of shRNA, migration assays were performed using transwell filters in low serum; the low chamber was filled with high serum medium. Graph summarizes migrated cells per area (mean ± SD; n=3; **P<0.01). Efficiency of DAB2IP depletion was confirmed by western blot of the same cells. **E)** Stable DAB2IP overexpression reduces vimentin expression. PC-3 cells were infected with retroviral constructs expressing two isoforms of DAB2IP (pLPC DAB2IP-long and pLPC DAB2IP-short). pLPC empty vector was used as control. Immunofluorescence and immunoblotting confirm DAB2IP overexpression and cytoplasmic localization. **F)** DAB2IP expression is significantly reduced in primary tumors and metastasis. Boxplot showing DAB2IP expression levels across normal prostate, primary cancers, and metastatic lesions from GSE21032 dataset (Taylor et al., 2010). Significance was calculated by Anova test (***P<0.001).

3.3.3 miR-96 and miR-149* enhance cancer cell invasivity

To infer the potential cancer relevance of positive miRNA hits, and in particular their impact on metastasis formation, we analyzed their expression in the GSE21032 prostate cancer dataset (Taylor et al., 2010).

As shown in Figure 3.5A, miR-96 is strongly expressed in primary tumors and metastases. This is in line with its known oncogenic role in various cancers. For example, in prostate carcinomas it has been observed that miR-96 targets FOXO1 to inhibit apoptosis and enhance proliferation (Fendler et al., 2013; Yu et al., 2014). This miRNA has been shown to sustain cell migration and invasion in breast, hepatocellular, non-small cell lung cancer, and tongue squamous cell carcinoma by the regulation of various proteins (Guo et al., 2014; Guo et al., 2015; Leung et al., 2015; Li et al., 2014b; Siu et al., 2015). Finally, in prostate cancer TGF-β can increase miR-96 levels that in turn sustains invasion through the up-regulation of mTOR signaling (Siu et al., 2015).

Also miR-92a is strongly expressed in metastatic lesions (data not shown). miR-92a belong to miR-17-92 cluster, and is a well known onco-miRNA. Its expression promotes cell proliferation, suppresses apoptosis of cancer cell and induces tumor angiogenesis and metastasis (Hayashita et al., 2005; Li et al., 2014a; Mendell, 2008; Rao et al., 2012). Both E2F1 and E2F3 can directly activate transcription of this miRNA, establishing a negative feedback loop (Petrocca et al., 2008a).

On the contrary, miR-744 is not differentially expressed in this dataset (not shown). In literature its role is still controversial. Some works describe it as an onco-miRNA whose serum levels have been proposed as non-invasive biomarkers for the detection of gastric cancer (Fang et al., 2015; Song et al., 2012; Tan et al., 2015). However, it has been also demonstrated that miR-744 targets and down-regulates oncogenes such as c-Myc in hepatocellular carcinoma, where reduced miR-744 expression increases cell proliferation (Lin et al., 2014).

Finally, miR-149* is strongly expressed in prostate tumor tissue, with even higher levels in metastatic lesions (Figure 3.5A).

For their strong correlation with metastasis in prostate cancer patients, we decided to further analyze the role of miR-149* and miR-96 in cell invasion mediated by DAB2IP down-regulation. To this aim, we transfected miR-149* and miR-96 mimics in PC-3 cells and performed invasion assays. Knockdown of DAB2IP by siRNAs provided a positive control. As shown in Figure 3.5B, both miRNAs are able to increase the invasive properties of this metastatic cell line, with similar, if not better, efficiency as DAB2IP depletion.

While miR-96 has known pro-oncogenic and pro-invasive activity in various malignances,

supported by multiple publications, the role miR-149* in tumorigenesis is not completely understood. In particular, evidences for miR-149* functions in migration and metastasis of cancer cells have not been reported yet. For this reason we decided to focus our attention on miR-149*, and tested if the observed phenotype could be extended to other cell models.

Overexpression of miR-149* clearly increased invasivity of metastatic prostate LNCaP and ovarian SKOV-3 cancer cell lines (Figure 3.5C-D). We then turned to MCF-7 breast cancer cells, which are not invasive and migrate poorly in trans-well assays. As shown in Figure 3.6C, DAB2IP depletion enhances the motility of these cells. Notably, miR-149* overexpression also efficiently increased MCF-7 cell migration, confirming that cell migration/invasion is a robust property of this miRNA (Figure 3.6C).

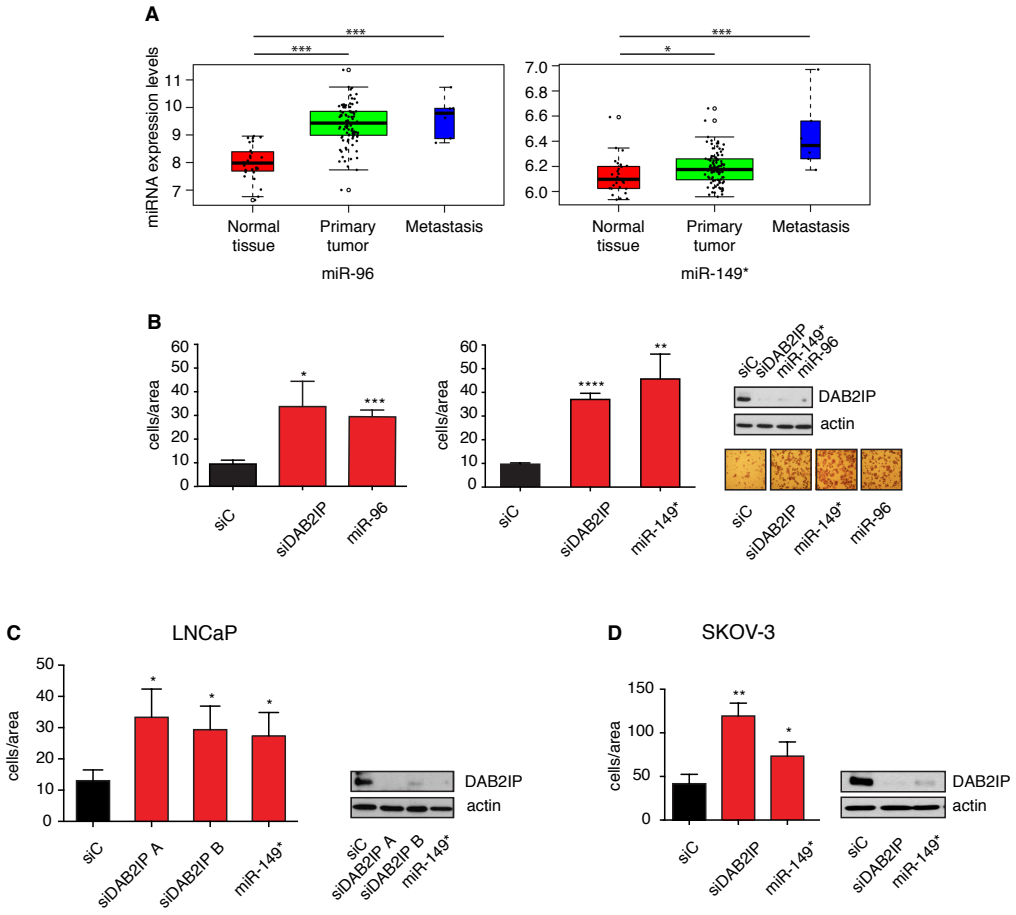

Figure 3.5: miR-149* and miR-96 increase tumor cells motility and metastasis.

A) miRNA-96 and miR-149* expression is significantly increased in primary tumor and metastasis. Boxplot showing miRNA expression levels across normal prostate, primary cancers, and metastatic lesions from GSE21032 data set (Taylor et al., 2010). Significance was calculated by Anova test. (***P<0,001; *P<0,05). **B)** miR-96 and miR-149* increase prostate cancer cells invasion. PC-3 cells were transfected with a mix of two DAB2IP siRNAs (siDAB2IP), with a control siRNA (siC), or with miRNA mimics (miR-96 and miR-149*) as indicated for 48 hours. Invasion assay was performed as in Figure 3.4A. Graph summarizes migrated cells per area (mean ± SD; n=3; ***P<0,001; **P<0,01; *P<0,05). DAB2IP depletion was checked by western blot, with actin as loading control. Representative images of migrated cells are shown. **C-D)** miR-149* increases invasion of LNCaP and SKOV-3 cells. Cells were transfected as indicated for 48 hours. Invasion assay was performed as in Figure 3.4A. Graph summarizes migrated cells per area (mean ± SD; n=3; **P<0,01; *P<0,05). DAB2IP depletion was checked by western blot.

3.3.4 miR-149* and miR-149, two sides of the same coin?

Our screening identified, among the validated hits, also miR-149 (miR-149-5p), encoded by the same precursor as miR-149*, but with a different seed sequence. Prediction analysis confirmed that target sites for miR-149 and miR-149* are present within the 3'UTR of human DAB2IP and indeed, at least in some cell types, miR-149 down-regulates DAB2IP protein levels (Figure 3.3C-D). We therefore analyzed expression and activity of miR-149 as described above for miR-149*. Interestingly, we found no evidence of differential miR-149 expression in prostate cancer samples from GSE21032 (Figure 3.6A), and we observed no relevant effects of its overexpression in cell invasion/migration assays in PC3 or MCF-7 cells, an effect correlated to a much less efficient depletion of endogenous DAB2IP protein (Figure 3.6B-C). Together, these data strongly suggest that the two miRNAs encoded by the miR-149 gene, despite sharing the potential to target DAB2IP, may have significantly different activities.

We used RT-qPCR to measure miR-149* and miR-149 levels in a panel of tumor and non-transformed cell lines (Figure 3.6D). The expression of miR-149* appears to be very similar in all cell lines, with comparable levels both in cancer (PC-3, LNCaP, MCF-7, MDA-231, MDA-468, SKOV-3, OVCAR-3, TOV112D, H1299, HCT116) and in non-transformed cell lines (PWRE, RWPE, MCF-10A). Instead, miR-149 shows a more variable pattern of expression, with lower levels in tumor than in non-transformed or less aggressive cell lines. For example, miR-149 is more expressed in non-transformed prostate epithelial cells (i.e. PWRE and RWPE), than in prostate cancer (PC-3 and LNCaP). This is in line with its described tumor suppressive activity (Bischoff et al., 2014; Chamorro-Jorganes et al., 2014; Chan et al., 2014; Fujii et al., 2015; Ke et al., 2013; Li et al., 2015; Luo et al., 2015; Palmieri et al., 2014; Wang et al., 2012; Xu et al., 2015a; Xue et al., 2015).

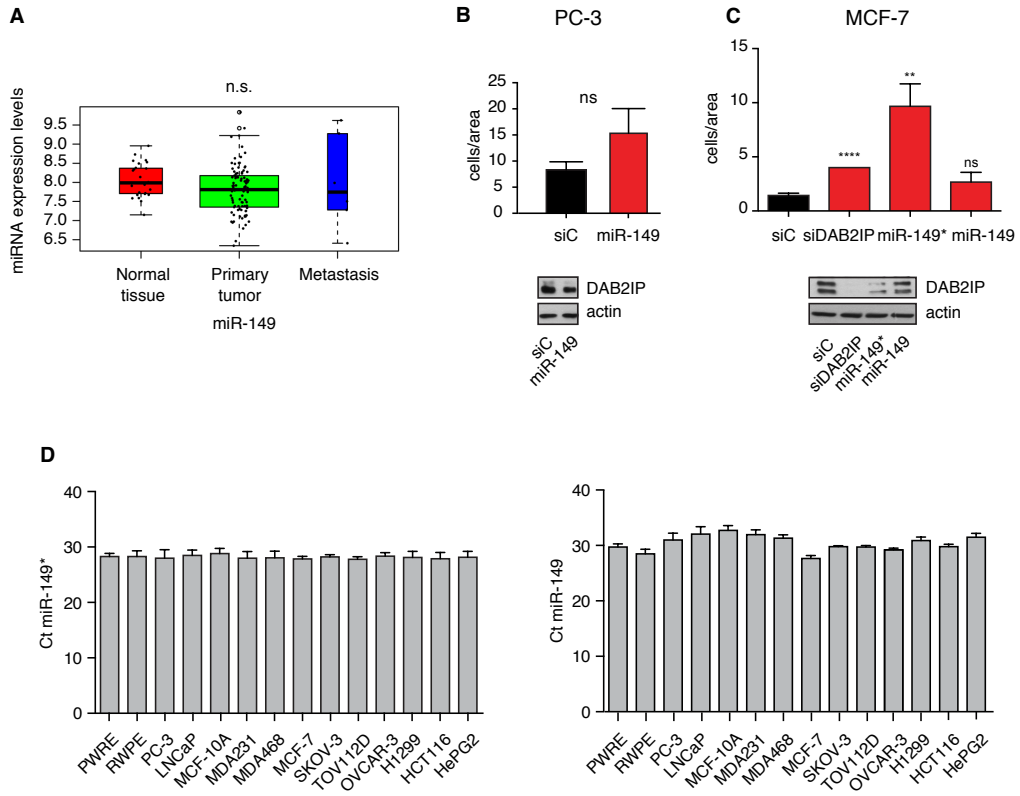

Figure 3.6: miR-149 and miR-149* sharing the potential to target DAB2IP, but with different effect on cell motility.

A) miRNA-149 is not differentially expressed in prostate cancer. Boxplot showing miRNA expression levels across normal prostate, primary cancers, and metastatic lesions from GSE21032 data set (Taylor et al., 2010). Significance was calculated by Anova test (ns = non significant). **B)** miR-149 does not induce a significant increase of cell invasion. PC-3 cells were transfected with miR-149 for 48 hours. Invasion assay was performed as in Figure 3.4A. Graph summarizes migrated cells per area (mean ± SD; n=3). DAB2IP depletion was checked by western blot, with actin as loading control. **C)** miR-149*, but not miR-149, increases migration of breast cancer cells. MCF-7 was transfected with mix of two DAB2IP siRNAs (siDAB2IP), control siRNAs (siC) or miRNA mimics as indicated for 48 hours. Migration assay was performed as described in Figure 3.4D. Graph summarizes migrated cells per area (mean ± SD; n=3; ***P<0,001; **P<0,01). DAB2IP depletion was checked by western blot. **D)** miR-149* and miR-149 are expressed in tumor and in non-transformed cell lines. The graphs summarize the expression of both miRNAs detected by RT-qPCR. The Y axis reports measured Ct of both miRNAs in each cell line. Error bars indicate standard deviation (n=3).

3.3.5 miR-149* inhibition increases DAB2IP protein levels and reduces prostate cancer cells invasion

miR-149* seems to be a potential onco-miRNA in prostate cancer, given its ability to sustain invasion (Figure 3.5B-C) and its increased expression in metastasis of prostate cancer patients (Figure 3.5A). To further validate the role of miR-149* in promoting invasion, we counteracted endogenous miR-149* activity using a specific miRNA inhibitor. We transfected miR-149* (inh 149*) or control inhibitors (inh C) in PC-3 and LNCaP cells, and performed matrigel invasion assays. The miR-149* inhibitor strongly reduced invasive capability of both PC-3 and LNCaP cells, simultaneously increasing DAB2IP protein levels (Figure 3.7A). This observation convince us of a powerful role of miR-149* in sustaining tumor cells invasion, at least in prostate cancer.

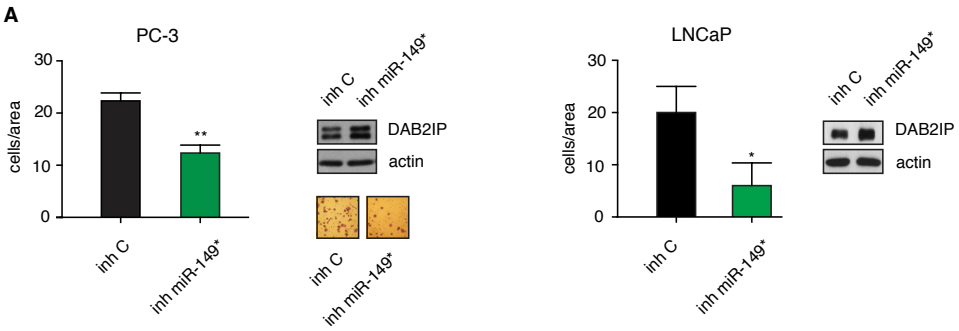

Figure 3.7: Endogenous miR-149* inhibition reduces prostate cancer cells invasion. A) Inhibition of endogenous miR-149* reduces tumor cells invasion and increases DAB2IP protein levels. PC-3 and LNCaP cells were transfected with miR-149* (inh miR-149*) or control hairpin inhibitors (inh C) for 24 or 48 hours, respectively. Invasion assay was performed as in Figure 3.4A. Graphs summarize migrated cells per area (mean ± SD; n=3; **P<0,01; *P<0,05). Western blot confirms increased expression of DAB2IP protein. Actin was used as loading control. Representative images of migrated PC-3 cells are shown.

3.3.6 miR-149* increases the invasive behavior of cancer cells through DAB2IP protein down-regulation

To asses if DAB2IP down-regulation mediated by miR-149* is the main driver for increased invasion in prostate cancer cells, we tested whether DAB2IP depletion might have additional effects on the pro-invasive phenotype induced by miR-149* overexpression. To this aim we co-transfected DAB2IP siRNAs with miR-149* mimic for 48 hours in PC-3 cells, and performed matrigel invasion assays. As shown in Figure 3.8A, overexpression of miR-149*, depletion of DAB2IP by siRNA, or co-transfection of both reagents gave a similar increase in cell invasion, supporting the notion that the impact of miR-149* on this specific phenotype is largely mediated by DAB2IP depletion.

To further confirm the epistasis between miR-149* and DAB2IP, we tested whether overexpression of DAB2IP could rescue the effects of miR-149* in our cell models. We transfected miR-149* or control siRNA in PC-3 cells overexpressing DAB2IP isoforms encoded by cDNA constructs lacking the 3'UTR sequences recognized by miR-149* (Figure 3.4E). As expected, miR-149* overexpression increased invasion of vector transfected PC-3 cells, but could not increase invasivity of DAB2IP overexpressing cells (Figure 3.8B). In other words, DAB2IP blocked miR-149* induced prostate cancer cell invasion, confirming their functional epistasis.

To confirm that miR-149*-induced invasion depends on its binding to the 3'UTR of DAB2IP mRNA, we used miRNA Target Protector technology. Target Protectors (TP) are innovative tools, designed to protect the miRNA-binding site of a specific target gene, blocking the access of a specific miRNA to its target site, and thus preventing protein down-regulation. The important advantage of these molecules is their ability to counteract the effects of a given miRNA on a specific target gene, without affecting its action on other cellular genes.

We designed target protectors for three putative miR-149* binding sites on human DAB2IP 3'UTR, as predicted by miRDB (www.mirdb.org/miRDB/) (Figure 3.8C).

The transfection of target protectors significantly increased DAB2IP protein levels in PC-3, similar to what observed with miR-149* inhibitor, thus confirming that endogenous miR-149* is active in these cells (Figure 3.8D). Quite robust results were obtained by combined transfection of the three target protectors (TPmix). Importantly, all three TPs could protect to some extent DAB2IP from downregulation by a miR-149* mimic (Figure 3.8D). This experiment confirms that miR-149* reduces DAB2IP protein levels by targeting its 3'UTR, and indicates that all three predicted binding sites on DAB2IP mRNA are functional targets of this microRNA.

We next investigated the effects of TPs on invasivity of prostate cancer cells, with or without miR-149* overexpression. We transfected PC-3 cells with miR-149*, with or without target protectors (TPmix), and performed matrigel invasion assays. In these conditions, target protectors increased DAB2IP protein levels and reduced invasion of PC-3 cells (Figure 3.8E), suggesting they counteract the activity of endogenous miR-149* in these cells. Moreover, TPmix reduced the invasivity of cells overexpressing the miR-149* mimic, partially protecting DAB2IP protein from miR-149* induced down-regulation (Figure 3.8E).

We conclude that miR-149* ability to increase invasion of prostate cancer cells is largely mediated by its ability to bind the 3'UTR of DAB2IP mRNA, and reduce expression of DAB2IP protein, and its tumor suppressive functions.

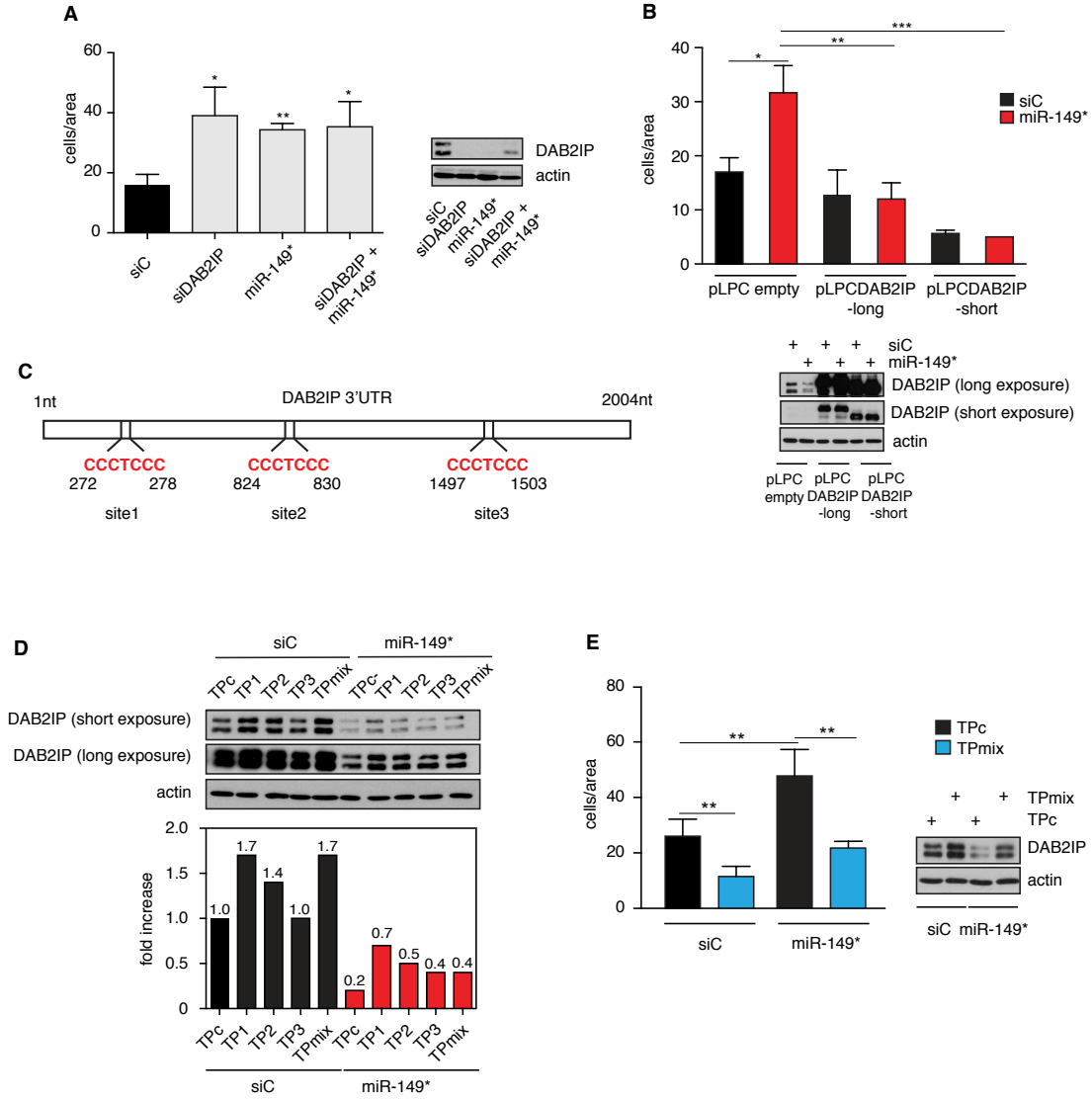

Figure 3.8: Functional interaction between miR-149* and DAB2IP in prostate cancer cells.

A) PC-3 cells were transfected with DAB2IP siRNAs (siDAB2IP), control siRNA (siC) or miR-149* mimic as indicated for 48 hours. Invasion assays were performed as in Figure 3.4A. Graph summarizes migrated cells per area (mean ± SD; n=3). Western blot confirmed DAB2IP silencing. **B)** PC-3 cells infected with retroviruses expressing DAB2IP-long or -short isoforms were transfected with miR-149* mimic (miR-149*) or control siRNA (siC) for 48 hours. Invasion assay was performed as in A. Graph summarizes migrated cells per area (mean ± SD; n=3; ***P<0,001; **P<0,01; *P<0,05). A control western blot of endogenous and exogenous DAB2IP proteins is shown. **C)** Schematic representation of the three putative miR-149* target sites on DAB2IP 3'UTR; in red miR-149* seed sequence. We designed three Target Protectors that bind specifically site 1 (TP1), site 2 (TP2) and site 3 (TP3). **D)** Target Protectors increase DAB2IP protein levels in untreated cells, and in cells transfected with miR-149*. PC-3 were co-transfected with three different target protectors (TP1, TP2, TP3) alone or in combination, with a non-targeting control (TPc), and either control siRNA (siC) or miR-149* mimic for 48 hours. DAB2IP protein levels were measured by western blot. Bottom: graph summarizes the fold increase over control (siC+TPc transfected sample) measured by densitometry of autoradiography films. **E)** Target protectors significantly reduce prostate cancer cells invasion. PC-3 cells were transfected with control siRNA (siC), miR-149* and target protectors mix (TPmix) or negative control (TPc) as indicated for 48 hours. Invasion assay was performed as in Figure 3.4A. Graph summarizes migrated cells per area (mean ± SD; n=3; **P<0,01). Control western blot was performed to detect endogenous DAB2IP protein levels. Actin was used as loading control.

3.3.7 miR-149*-mediated DAB2IP depletion induces an inflammatory, immunogenic, NF-κB-related gene expression program

To gain a molecular insight on the invasive phenotype, we used microarrays to analyze the transcriptional profile of PC-3 cells transfected with miR-149* mimic, or with DAB2IP specific siRNAs. We observed that overexpression of miR-149* had a much broader impact on transcription than DAB2IP knockdown, probably reflecting its nature of pleiotropic modulator of translation. Gene Set Enrichment Analysis (GSEA) revealed that genes down-regulated by miR-149* or DAB2IP siRNA are not involved in the modulation of cell motility and/or EMT, and in general are not associated to biological processes that could be linked to the phenotypes under analysis (data not shown). On the contrary, genes up-regulated by miR-149* or DAB2IP siRNA (miR-149*_UP and siDAB2IP_UP) revealed enrichment for relevant biological functions, including hypoxia, inflammatory and immune response, apoptosis, and EMT. Moreover, up-regulated genes were enriched in hallmarks of relevant signaling pathways such as TNF via NF-κB, mTORC1, and IL6-STAT3 (Figure 3.9A-B). Not surprisingly, miR-149* up-regulated genes are also enriched for additional biological processes, including glycolysis, response to estrogen, and Heme metabolism, that are not detected in genes up-regulated by DAB2IP depletion (Figure 3.9A). These could be connected to biological functions mediated by miR-149* in a DAB2IP-independent mechanism. Notably, one of the hallmarks with strongest enrichment in both conditions was "TNF signaling via NF-κB", a pathway which is related to EMT and cell motility (Figure 3.9C).

To define pathways and processes activated by miR-149* in a manner strictly dependent on DAB2IP inhibition, we focused on common genes up-regulated by DAB2IP siRNA and by miR-149* mimics transfection (Figure 3.9D); GSEA confirmed a specific enrichment for hallmarks of NF-κB signaling. Among NF-κB target genes common in the miR-149*_UP and siDAB2IP_UP genesets, we identified some chemokines and cytokines, including CCL20, IL8 (CXCL8), and CSF2 (GM-CSF). These inflammatory factors are involved in the regulation of immune cells recruitment and activity; however, studies *in vitro* and *in vivo* demonstrated that they are also fundamental regulators of EMT and cell motility in tumor microenvironment (Cheng et al., 2014; Gales et al., 2013; Park et al., 2007; Roberti et al., 2012; Rudisch et al., 2015; Zeng et al., 2014).

We conclude that miR-149*-mediated reduction of DAB2IP sustains a transcription program that supports cell motility and inflammatory response, and defines NF-κB signaling activation.

Microarrays were validated by RT-qPCR on a selection of genes belonging to the intersection of miR-149*_UP and siDAB2IP_UP genesets, confirming their regulation (Figure 3.9E).

To further validate these results, we transfected PC-3 cells with a miR-149* inhibitor, and performed RT-qPCR of selected target genes. The inhibition of miR-149* significantly reduced CCL20, CSF2 and PTX3 expression, confirming their positive regulation by miR-149*, possibly through inhibition of DAB2IP (Figure 3.9F).

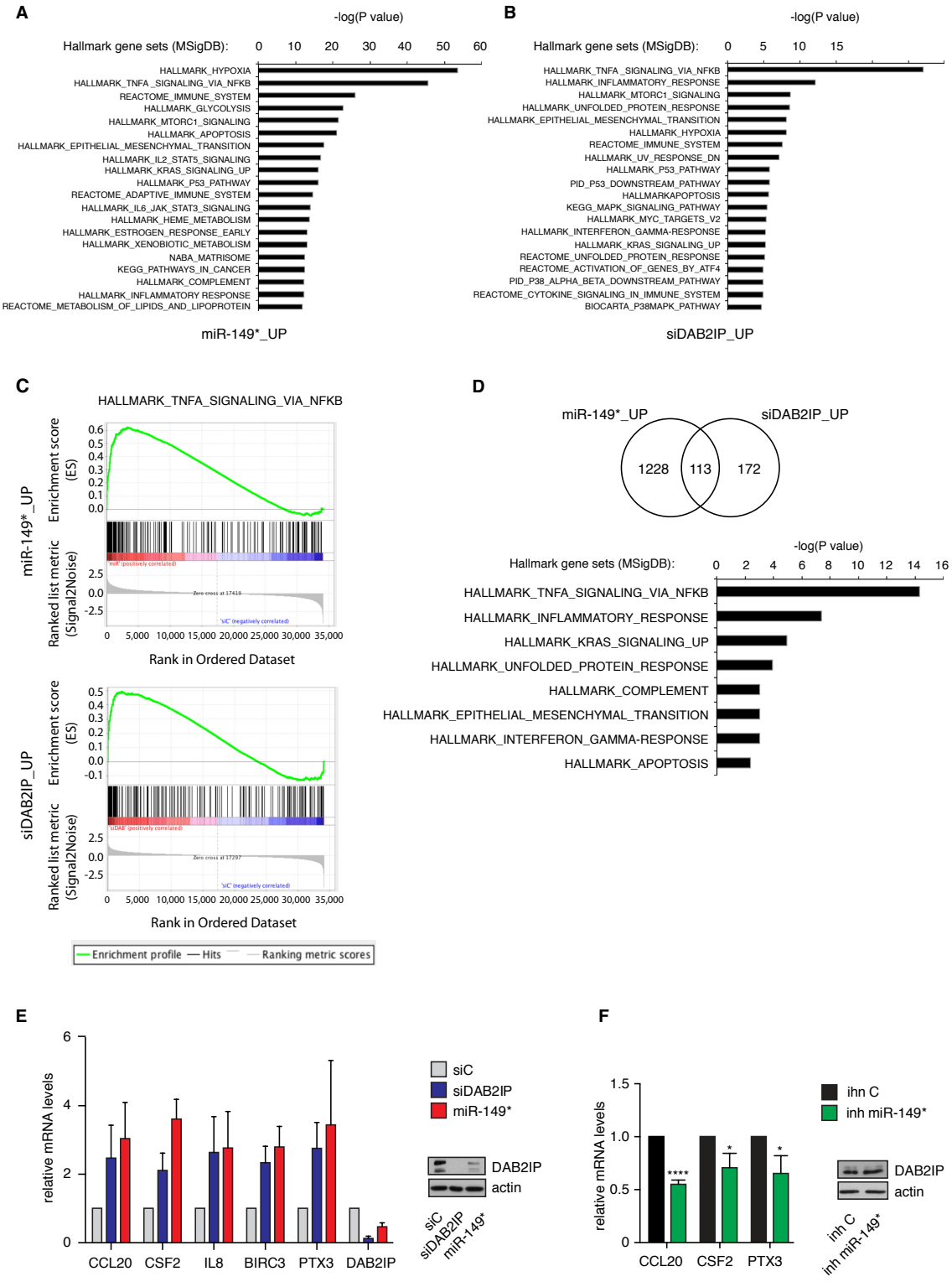

Figure 3.9: miR-149*-mediated DAB2IP reduction modulates prostate cancer cells transcription program.
A-B) PC-3 cells were transfected with DAB2IP siRNA mix (siDAB2IP), control siRNA (siC) and miRNA-149* mimic for 48 hours and analyzed by Illumina microarray. Up-regulated genes were selected and analyzed by Gene Set Enrichment Analysis (GSEA) tool. Top GSEA hallmarks specifically enriched in miR-149*_UP or siDAB2IP_UP are shown. (MSigDB= Molecular Signature Data Base). **C)** GSEA enrichment plots for the "TNF signaling via NF-κB" hallmark. **D)** Venn diagram shows the intersection of miR-149*_UP and siDAB2IP_UP gene

sets. Graph summarizes the top enriched hallmarks in common up-regulated genes. **E)** Expression of selected genes identified in miR-149*_UP and siDAB2IP_UP was validated by RT-qPCR. Values are normalized to histone H3 and compared to siC samples (mean ± SD; n=4). A control western blot is shown on the right. **F)** Basal expression of validated common genes depends on miR-149*. miR-149* or control inhibitors were transfected in PC-3 cells for 48 hours. Expression of indicated genes was measured by RT-qPCR. Values are normalized to histone H3 and compared to inh C samples (mean ± SD; n=3). A control western blot is shown on the right.

3.3.8 miR-149* sustains cell invasion through increased activation of NF-κB signaling

The hallmark most enriched upon DAB2IP depletion and miR-149* overexpression is TNF signaling via NF-κB, and many validated genes are NF-κB targets (CCL20, IL8, CSF2, BIRC3 and PTX3). Several studies indicate that DAB2IP is a fundamental inhibitor of NF-κB signaling, and demonstrate that this inhibitory activity reduces EMT and restrains cell motility in various cancer models (Min et al., 2015; Min et al., 2010). We therefore evaluated the nuclear localization of transcription factor NF-κB by immunoblotting on purified nuclear and cytoplasmic fractions of transfected PC-3 cells. An increased nuclear localization of p65 RelA was observed in cells transfected with miR-149* mimic, or DAB2IP siRNA as a positive control (Figure 3.10A).

We used a specific siRNA against p65 RelA to evaluate the relevance of NF-κB activation in the increased invasion observed upon miR-149* overexpression. As shown in Figure 3.10B, the transient knockdown of p65 RelA totally blocked the invasiveness of PC-3 cells induced by miR-149* overexpression, or by DAB2IP depletion. Curiously, depletion of NF-κB does not affect the basal invasive behavior of this metastatic cell line (Figure 3.10B). This observation suggests that NF-κB signaling is fundamental for the increase in invasivity triggered by miR-149* overexpression; it is possible that other pathways (i.e. PI3K/Akt or Wnt/βcatenin) are involved in the maintenance of basal invasive features of PC-3 cells.

These experiments demonstrate that NF-κB signaling is the main pathway involved in the invasive phenotype observed in prostate cancer cells upon miR-149*-dependent DAB2IP reduction.

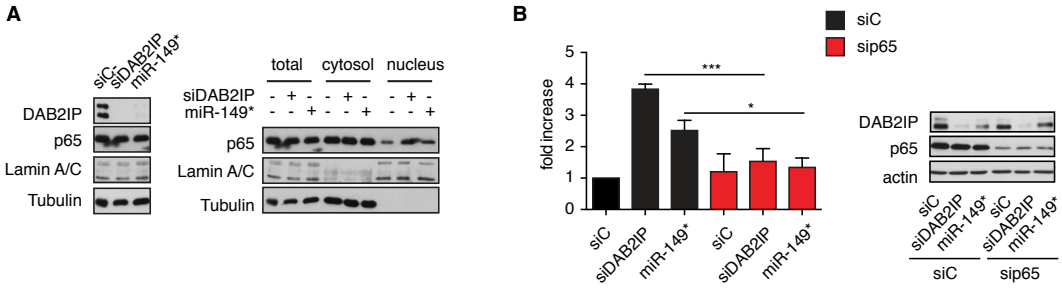

Figure 3.10: NF-κB pathway activation mediates miR-149* induced cell invasion. A) Overexpression of miR-149* or siRNA-mediated DAB2IP depletion increase nuclear localization of p65 RelA. PC-3 cells were transfected as described in Figure 3.5 and subjected to biochemical fractionation to purify nuclei from cytoplasm. Tubulin (cytoplasmic) and Lamin A/C (nuclear) were blotted as controls. DAB2IP depletion was checked by western blot of total samples (left panel). **B)** Depletion of p65 RelA blocks miR-149*-induced cell invasion. PC-3 cells were co-transfected with a DAB2IP siRNAs mix (siDAB2IP), miR-149* mimic, a siRNA to p65 RelA (sip65) or a control siRNA (siC), as indicated. After 48 hours, invasion assay was performed as in Figure 3.4A (mean ± SD; n=3; ***P<0,001; *P<0,05). Western blot confirmed DAB2IP and p65 RelA silencing. Actin was used as loading control.

3.3.9 miR-149* affects TNF-induced transcription

Many genes up-regulated upon miR-149* overexpression, or DAB2IP depletion, are cytokines and chemokines downstream of TNFα signaling via NF-κB (Figure 3.9A-C). To evaluate the role of miR-149* in the response to TNFα, we transfected PC-3 cells with a miR-149* inhibitor for 48 hours, and then treated cells with this cytokine for 20 hours. TNFα up-regulated the expression of CCL20 and IL8, while transfection of a miR-149* inhibitor counteracted this phenotype (Figure 3.11A). This preliminary observation suggests that miR-149* - likely by reducing DAB2IP levels – can modulate NF-κB signaling upon inflammatory stimuli, in particular TNFα, with implications for oncogenic behavior of tumor cells exposed to inflammation. By affecting TNFα signaling, therefore, miR-149* can control inflammation-induced invasion, proliferation, or survival of tumor cells. Further experiments are needed to better characterize this aspect.

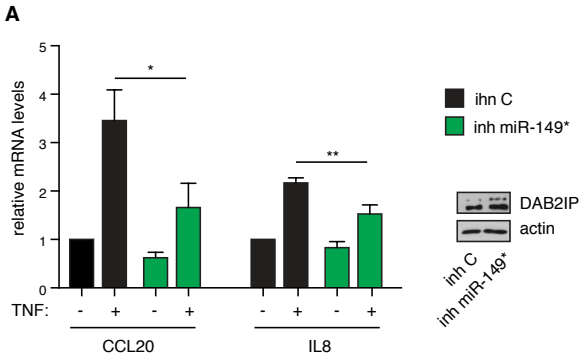

Figure 3.11: miR-149* inhibition modulates TNF-induced transcription. A) PC-3 cells were transfected with miR-149* or control inhibitors as described in Figure 3.9F. Cells were serum starved and treated with TNFα (10 ng/ml) for 20 hours. Expression of CCL20 and IL8 was measured by RT-qPCR. Values are normalized to histone H3 and compared to inh C samples (mean ± SD; n=3; **P<0,01; *P<0,05). A control western blot is shown on the right.

3.3.10 Implications of miR-149* in cancer: analysis of TCGA dataset

To explore the potential clinical impact of this molecular axis, with the help of Denis Torre (University of Trieste) we analyzed the expression of both miR-149 (miR-149-5p) and miR-149* in public gene expression datasets from TCGA (The Cancer Genome Atlas). In particular, we analyzed miR-149 expression levels in breast cancer (BRCA), prostate adenocarcinoma (PRAD), and lung squamous cell carcinoma (LUSC). We performed two different analyses, comparing paired samples (tumor versus normal tissues of the same patient) and unpaired samples (all tumors versus all normal).

Notably, miR-149 (hsa-miR-149, mature) is easily and better detected in tumors and normal tissues with respect to the passenger strand (hsa-miR-149, star), suggesting it is expressed at higher levels. However, miR-149* is clearly overexpressed in breast cancer samples with respect to their corresponding paired normal tissues (Figure 3.12A), in line with its oncogenic effect in tissue culture experiments.

In unpaired analyses, both miR-149 and miR-149* resulted to be overexpressed in breast, prostate, and lung squamous cell carcinomas (Figure 3.12B), with absolute miR-149 expression levels consistently higher than those of miR-149*. The higher expression of miR-149* in breast, prostate and lung cancer correlates with its pro-metastatic role described previously (Figure 3.5). In contrast, cancer overexpression of miR-149-5p appears in conflict with its reported tumor suppressive activity. However, it should be considered that miRNA activity does not depend only on expression levels in cells and tissues, but also on the biological context, abundance of mRNA target, and regulation of its biogenesis and function.

Together, these preliminary analyses suggest that miR-149* is overexpressed in prostate, breast, and lung squamous cell cancers, in agreement with is oncogenic ability to sustain invasion through the reduction of DAB2IP levels and the increase of NF-κB activity, most likely in response to inflammatory stimuli, including TNF.

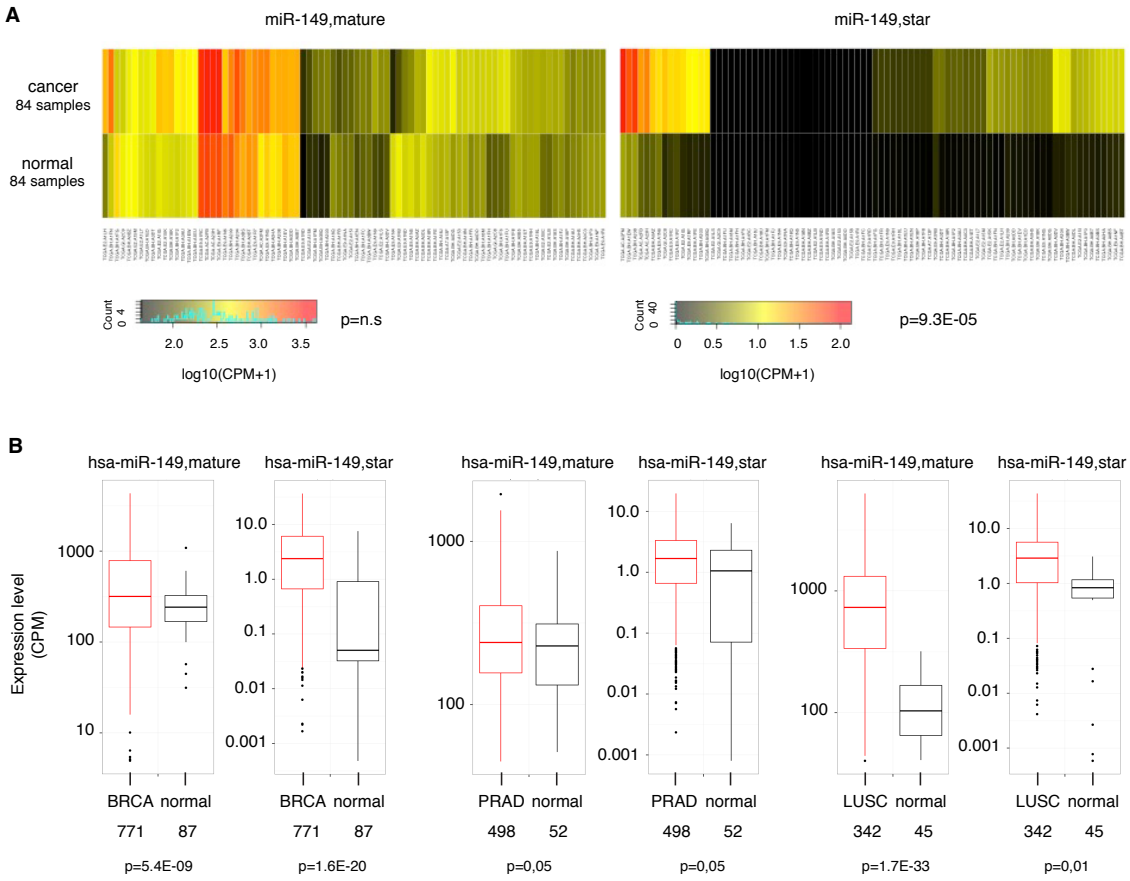

Figure 3.12: miR-149* is differentially expressed in breast, prostate, and squamous cell lung carcinoma.
A) Expression of miR-149 (miR-149, mature) and miR-149* (miR-149, star) in 84 paired breast tissue samples (tumor versus normal tissue of the same patient) from TCGA. Significance was calculated with Wilcoxon test (p= FDR). **B)** Expression of miR-149 (miR-149, mature) and miR-149* (miR-149, star) in unpaired breast, prostate, and lung cancers from TCGA. Significance was calculated with non-parametric Mann-Whitney test (p= FDR).
BRCA= breast cancer; PRAD= prostate adenocarcinoma; LUSC= lung squamous cell carcinoma.

3.4 DISCUSSION

The tumor suppressor DAB2IP is emerging as a fundamental factor to maintain physiological control of signaling pathways, to counteract acquisition of oncogenic properties, and to modulate the crosstalk with immune and stromal cells in the microenvironment. For this reason DAB2IP tumor suppressive activities are disabled in human malignancies through multiple mechanisms, including the inhibitory binding with the oncogenic mutant p53 protein, as described in Part 2 of this Thesis. Since DAB2IP has a rather long 3'UTR, it is a good candidate miRNA target. Three miRNAs have been described to down-regulate DAB2IP in various tissue or cancer types (Barik, 2008; Liao et al., 2015; Xu et al., 2015b). We performed a high-throughput screening and identified 81 additional miRNAs able to target and modulate - either negatively or positively - a reporter with the DAB2IP 3'UTR (Figure 3.3).

Importantly, this screen identified miRNAs that escaped available prediction algorithms. For example, miR-555 was not identified by these tools, and miR-17-3p and miR-96 are predicted only by a few engines, and with a very low score. However, we confirmed by western blot that miR-555, miR-17-3p and miR-96 significantly down-regulate DAB2IP endogenous proteins in various cell lines (Figure 3.3C- D).

Intriguingly, this screen also identified a consistent number of miRNAs that can up-regulate the DAB2IP 3'UTR reporter. We have not studied these miRNAs, but the robustness of the effect suggests that at least some of them can actually increase DAB2IP mRNA stability or translation.

Examples of miRNAs able to up-regulate target mRNA translation have been reported (Orom et al., 2008; Vasudevan et al., 2007). For example, miRNA-369-3 directs the association between Ago and fragile X mental retardation-related protein 1 (FXR1) with AU-rich elements (AREs) to activate translation of its target mRNA (Vasudevan et al., 2007). AREs have been shown to bind specific proteins to regulate mRNA stability or translation in response to external and internal stimuli. An analogous process was observed for miR-let-7, and for a synthetic microRNA called miRcxc-4 (Vasudevan et al., 2007). It is therefore possible that similar mechanisms may be involved in positive regulation of DAB2IP translation by some of these miRNAs. It is also possible that miRNAs can up-regulate the DAB2IP 3'UTR reporter through indirect mechanisms; for example they may down-regulate proteins that bind the 3' UTR to inhibit translation or stability, or they may block expression or activity of other microRNAs targeting DAB2IP. Characterization of the identified miRNAs potentially able to up-regulate DAB2IP may represent an interesting future development of this project.

Focusing on miRNAs that down-regulate DAB2IP, we found some known onco-miRNAs, including miR-96 (Chen et al., 2015; Fendler et al., 2013; Guo et al., 2014; Guo et al., 2015; Leung et al., 2015; Li et al., 2014b; Siu et al., 2015; Wu et al., 2015b; Xia et al., 2014; Yu et al., 2014), and members of the miR-17-92 cluster and its paralogs, such as miR-25 and miR-92a (Kan et al., 2009; Li et al., 2014a; Petrocca et al., 2008b; Smith et al., 2012). Down-regulation of DAB2IP could thus represent an additional means through which these oncogenic miRNAs promote proliferation, survival, and especially motility of cancer cells. Indeed, we experimentally confirmed that overexpression of miR-96 down-regulates DAB2IP and increases prostate cancer cells invasion (Figure 3.5).

However, we also identified tumor suppressor miRNAs; for instance miR-29c (Ding et al., 2011; Liu et al., 2013; Wang et al., 2011), miR-744 (Fang et al., 2015; Song et al., 2012; Tan et al., 2015), miR-154 (Xin et al., 2014; Zhu et al., 2013a; Zhu et al., 2014), and miR-149 (Bischoff et al., 2014; Chamorro-Jorganes et al., 2014; Chan et al., 2014; Fujii et al., 2015; Ke et al., 2013; Li et al., 2015; Luo et al., 2015; Palmieri et al., 2014; Wang et al., 2012; Xu et al., 2015a; Xue et al., 2015). Our data suggest that by targeting DAB2IP these miRNAs can potentially exert also pro-oncogenic functions; therefore, their contribution to tumor progression may depend on biological context and availability of targets.

In this Thesis, we validated and functionally characterized miR-149*. We demonstrated that this miRNA can significantly reduce DAB2IP protein levels by binding three specific regions in the 3'UTR (Figure 3.8C-D). According to our experiments, site 1 is the more important for miR-149* function; however, also sites 2 and 3 are involved in the process, indicative of functional redundancy.

We used miRNA inhibitor and target protectors (TPs) to inhibit miR-149* activity, and observed DAB2IP protein accumulation in prostate cancer cells (Figure 3.7A and 3.8D). Importantly, these approaches also strongly reduced matrigel invasion, indicating that endogenous miR-149* contributes to DAB2IP inactivation in PC-3 cells (Figure 3.7A and 3.8E).

Notably, our data do not demonstrate if miR-149* may have a driving role in cell transformation. To define its oncogenic potential, it will be necessary to overexpress miR-149* in non-transformed prostate and mammary epithelial cells. Our prediction is that forced miR-149* expression would promote, or facilitate, cancer development and progression. At the same time, stable expression of a "miRNA sponge" construct could be used to stably inhibit miR-149* in tumor cells. Long-term overexpression or inhibition of miR-149* could be used to investigate its role in the acquisition of mesenchymal features, in three-dimensional growth of prostate cancer

cells *in vitro* (prostate spheres), and eventually in tumor growth and dissemination *in vivo*, performing xenograft experiments in nude mice.

To infer oncogenic pathways or biological processes linked to miR-149*-induced invasive phenotype, we analyzed the transcriptional program of PC-3 cells overexpressing miR-149* or depleted for DAB2IP. A key involvement of NF-κB activity was predicted by this analysis (Figure 3.9). We experimentally confirmed that NF-κB is an essential player in increased invasion induced by miR-149* overexpression - or DAB2IP depletion (Figure 3.10).

Notably, the analysis of the transcriptional landscape of cells transfected with DAB2IP siRNA allowed us to identify other biological processes implicated in the acquisition of oncogenic features upon DAB2IP inactivation. This is the first study to examine the transcriptional program of tumor cells depleted for DAB2IP; we observed up-regulation of genes involved in the unfolded protein response (UPR), epithelial to mesenchymal transition (EMT), apoptosis, K-Ras, p38MAP kinase, and STAT signaling. Notably, these biological processes and pathways are known to be somehow regulated by DAB2IP (as described in Chapter 1.2). Interestingly, we also observed enrichment for genes implicated in hypoxia, inflammation, and immune system regulation; these are possibly liked to the already mentioned pathways, or may suggest DAB2IP implication in additional yet undefined molecular circuits. Importantly, these hallmarks are also enriched in the set of genes up-regulated by miR-149* overexpression, suggesting that miR-149* can affect these processes through inhibition of DAB2IP.

The role of DAB2IP in the modulation of cell response to inflammation has been described in endothelial cells (Huang et al., 2013; Wan et al., 2010; Yu et al., 2011), but not completely explored in the context of tumor development and progression. We have demonstrated that inhibition of DAB2IP by interaction with mutant p53 reprograms TNF-induced transcription, shifting the spectrum of cytokines and chemokines expressed by cancer cells from a tumor-promoting to a pro-inflammatory and anti-tumorigenic program (Part 2 of this Thesis). Another recent work described the effects of DAB2IP depletion on tumor microenvironment: DAB2IP loss in vascular endothelial cells subverts the secretion of EMT-promoting factors in the tumor niche, enhancing tumor vascularization, pre-metastatic niche formation, and augmenting tumor growth and metastasis in mouse models of breast cancer and melanoma (Ji et al., 2015).

Based on our data, we speculate that DAB2IP reduction mediated by miR-149* can also affect the inflammatory and immunogenic transcriptional program of tumor cells, in particular in response to inflammatory signals. We obtained results in line with this concept: expression of some inflammatory cytokines and chemokines (CCL20, IL8, PTX3 and CSF2) was induced in

PC-3 cells treated with miR-149*, both in basal conditions and after TNF-treatment (Figure 3.9 and Figure 3.11). These secreted factors are important inducer of tumor cells invasion, and often predict worst survival (Cheng et al., 2014; Frick et al., 2016; Gales et al., 2013; Park et al., 2007; Roberti et al., 2012; Rudisch et al., 2015; Zeng et al., 2014). In the tumor microenvironment, these secreted factors are principally pro-metastatic, pro-angiogenic, and pro-inflammatory. More importantly, these factors can affect tumor recruitment and activity of immune cells. For example, CCL20 is known to increase the recruitment of regulatory T cells (T_{reg}), Th17, and immature dendritic cells in various tumors, including hepatocellular carcinoma, cervical and breast cancer, sustaining escape of immune control and tumor progression (Chen et al., 2011b; Treilleux et al., 2004; Walch-Ruckheim et al., 2015).

If this model is true, we predict a positive correlation between expression of this group of genes (a molecular signature including CCL20, CSF2, PTX3, IL8, BIRC3) and levels of miR-149* in tumor samples; if this is confirmed, it would be interesting to correlate this pattern of expression with quantity and quality of the inflammatory infiltrate, and with patients' clinical survival. This model also predicts that prostate cancer cells expressing high miR-149* would secrete factors capable of affecting the recruitment of immune cells and modulation of their activity. Co-culture experiments and transwell migration assays to evaluate lymphocyte chemotaxis can be performed to test this hypothesis.

An important open question regards the mechanisms involved in miR-149* regulation. The evidence of p53-dependent regulation of miR-149* upon ER stress induction in melanoma cells has been described (Jin et al., 2011), as well as FGF2 dependent regulation of miR-149* in endothelial cells (Chamorro-Jorganes et al., 2014). We performed some experiments and observed that FGF2 treatment does not induce miR-149* expression in our cell models (data not shown), indicating that these circuits might be cell-type specific. We have not tested ER-stress in our cells yet.

miRNA-149 gene localizes within the very large first intron of the human glyplican-1 (GPC1) gene, in the same orientation. Interestingly, it is also within in the first intron of a long non-coding RNA that overlaps the GPC1 gene in the opposite orientation; no information is available on this lncRNA (LOC100130449) and on its possible regulatory interaction with its antisense overlapping host gene – or miRNA. I anticipate that this complex gene arrangement will eventually prove to have some important regulatory functions, at least in some tissues or conditions.

One study reported that miR-149 and miR-149* transcription is uncoupled from that of the host

GPC1 gene, and suggested the existence of a transcription start site (TSS) located within 3,1kb upstream of the miR-149 gene, also identifying three regions with various chromatin states indicative of gene regulatory regions (Chamorro-Jorganes et al., 2014). I think that additional specific studies are necessary to better characterize these regions, to confirm the existence of a miR-149 gene promoter within the GPC1 intron, and eventually to identify transcription factors potentially involved in its regulation.

Other works identified molecular circuits involved in the regulation of miR-149 transcription. TNF treatment negatively modulates miR-149 transcription in a P38 MAPK dependent mechanism (Palmieri et al., 2014). Hypermethylation of miR-149 promoter induced by PGE2 has been recently observed in gastric cancer associated fibroblast (Li et al., 2015). Finally a positive correlation between syndecan-1 and miR-149 has been detected in androgen-independent prostate cancer cell lines (i.e. PC-3) (Fujii et al., 2015).

Clearly, mechanisms controlling miR-149* expression, in particular in prostate cancer cells, are of great interest to understand its potential impact in cancer. I am particularly intrigued by the possibility of a negative feedback loop between TNFα and miR-149*, and DAB2IP, as this could strongly impact cell-autonomous and non-autonomous responses of cancer cells to inflammatory tumor microenvironment. Also PGE2 could be involved in this regulatory circuit, with strong impact on the crosstalk between tumor and stromal cells.

An intriguing aspect emerging from this study is the opposite effect observed for miR-149 and miR-149* in tumor cells. While miR-149 has tumor suppressive functions in multiple human malignancies, our work revealed novel tumorigenic properties for miR-149*. Notably, although both of the miRNAs can target DAB2IP, they have significantly different effects on cell motility. Indeed, miR-149 expression did not affect prostate and breast cancer cell invasion (Figure 3.6A-C) This may be explained by the fact that this miRNA has a weaker effect on DAB2IP levels reduction than miR-149* (Figure 3.3C-D and 3.6B-C). However, we should also consider that miR-149 can down-regulate various proteins controlling cell-migration in tumors (Bischoff et al., 2014; Chan et al., 2014; Ke et al., 2013; Luo et al., 2015; Xu et al., 2015a), and this could potentially counteract the metastatic phenotype triggered by DAB2IP depletion.

Together, these observations suggest that the miR-149 gene encodes two miRNAs that can have an opposite impact on cell behavior, potentially affecting tumor progression and aggressiveness.

Notably, the miR-149* levels in primary tumors and normal tissue is very low, if compared with the guide strand, which seems to be easily detected and highly expressed (Figure 3.12).

However, miR-149* is differentially expressed between normal and tumor tissue in prostate,

breast and lung squamous cell carcinoma (Figure 3.12). Data from the GSE21032 study (Taylor et al., 2010) confirmed these observations. In particular, the expression of miR-149* is strongly increased in metastatic lesions, at least in prostate cancer (Figure 3.5A). These data suggest that, where its expression and stability are augmented, miR-149* may promote acquisition of a more aggressive phenotype, increasing the metastatic potential of tumor cells - probably even better than miR-149 silencing or genetic deletion. This is an interesting hypothesis that will require further consideration, initially through the scrutiny of additional public gene expression datasets.

The molecular parameters controlling pri- and pre- miRNA processing, as well as co-factors involved in the assembly on miRISC, can deeply impinge on the choice between one strand and the other. It is possible that deregulation of these factors in human tumors can increase the stability of the oncogenic miR-149*, facilitating its loading on miRISC, while increasing the degradation of tumor-suppressive miR-149, dictating the acquisition of oncogenic features. A molecular understanding of the parameters involved in this aspect could significantly increase our comprehension of the role of miR-149/miR-149* on carcinogenesis.

To conclude, in this part of my PhD I identified and validated novel microRNAs able to target DAB2IP and modulate its expression levels in tumor cells. I collected convincing evidences for an oncogenic role of miR-149* in prostate cancer; I found that its overexpression in tumor and metastatic cells strongly augments invasive ability through the reduction of DAB2IP levels and the sustained activation of a specific NF-κB transcriptional program.

Importantly, I found that inhibition of endogenous miR-149* activity restores DAB2IP protein functions and counteracts invasivity in a prostate cancer cell line model, suggesting possible applications of this strategy in tumor therapy. Intriguingly, miR-149*-mediated DAB2IP reduction seems to be involved in the regulation of an inflammatory transcriptional program, which includes pro-angiogenic, pro-metastatic, and immunogenic factors. Expression and secretion of these inflammatory factors in the tumor microenvironment, sustained by miR-149*, could significantly affect the crosstalk between tumor and immune cells, with a possible relevant impact on tumor progressions and patient survival.

3.5 EXPERIMENTAL PROCEDURES

Cell Culture, Transfections, Retroviral Transductions and treatments

Cell Culture. PC-3, LNCaP, OVCAR-3, TOV112 and H1299 were cultured in RPMI medium (Sigma) supplemented with 10% FBS (ECS0180L, Euroclone), and antibiotics (ECB3001D, Euroclone). HeLa, SKOV-3, HCT116, MDA-MB-231, MDA-MB-468, were cultured in DMEM medium (Sigma) supplemented with 10% FBS, and antibiotics. HepG2 and MCF-7 were cultured in EMEM (Sigma) supplemented with MEM Non-essential Amino Acid Solution (Sigma), 10% FBS, and antibiotics. MCF10A cells were maintained in DMEM:F12 Ham's medium 1:1, supplemented with 5% horse serum (HS), insulin (10 μg/ml), hydrocortisone (0.5 μg/ml) and epidermal growth factor (EGF 20 ng/ml). PWRE and RWPE were cultured in Keratinocyte Serum Free Medium (K-SFM) (Invitrogen), supplemented with bovine pituitary extract (BPE 0.05 mg/ml) and epidermal growth factor (EGF 5 ng/ml). All human cell lines were subjected to STR genotyping with PowerPlex 18D System and confirmed in their identity comparing the results to reference cell databases (DMSZ, ATCC, and JCRB databases).

Transfections. For the high-throughput screening, miRIDIAN microRNA Library packaged in 96-well plates was purchased from Dharmacon. HeLa cells were plated in these 96-well plates; the day after they were transfected with Fugene (Promega), following manufacturer's instructions.

For siRNA, miRNAs, miRNA inhibitors and Target Protectors transfections, cells were plated and transfected the day after with 50 nM siRNA oligonucleotides, 3nM miRNAs mimics, 20nM miRNAs hairpin inhibitors and Target protectors, using Lipofectamine RNAiMax (Invitrogen), following manufacturer's instructions. After 48 hours of silencing, cells were processed.
siRNAs, used in this work are listed in the following table:

siRNA	Sequence	Purchase from/ Reference
Control siRNA (siC)	Unknown	All star negative control (1027281,Qiagen)
siDAB2IP A	GGAGCGCAACAGUUACCUG	Eurofins MWG
siDAB2IP B	GGUGAAGGACUUCCUGACA	Eurofins MWG
siDAB2IP 3'UTR	GUAAUGUAACUAUCUCACC	Eurofins MWG
sip65	GCCCUAUCCCUUUACGUCA	Eurofins MWG

Human miRNA mimics and Hairpin Inhibitors were purchased from Dharmacon.

Catalog Number	Mature Accession	Mature Name	Mature Sequence
C-301151-01	MIMAT0004609	hsa-miR-149-3p	AGGGAGGGACGGGGGCUGUGC
C-300486-05	MIMAT0000071	hsa-miR-17-3p	ACUGCAGUGAAGGCACUUGUAG
C-300498-05	MIMAT0000081	hsa-miR-25-3p	CAUUGCACUUGUCUCGGUCUGA
C-301089-01	MIMAT0004748	hsa-miR-423-5p	UGAGGGGCAGAGAGCGAGACUUU
C-300873-01	MIMAT0003219	hsa-miR-555	AGGGUAAGCUGAACCUCUGAU
C-300901-01	MIMAT0003247	hsa-miR-582-5p	UUACAGUUGUUCAACCAGUUACU
C-301251-01	MIMAT0004957	hsa-miR-760	CGGCUCUGGGUCUGUGGGGA
C-300510-05	MIMAT0000092	hsa-miR-92a-3p	UAUUGCACUUGUCCCGGCCUGU
C-300872-03	MIMAT0003218	hsa-miR-92b-3p	UAUUGCACUCGUCCCGGCCUCC
C-300514-07	MIMAT0000095	hsa-miR-96-5p	UUUGGCACUAGCACAUUUUUGCU
C-300631-07	MIMAT0000450	hsa-miR-149	UCUGGCUCCGUGUCUUCACUCCC
C-300633-03	MIMAT0000452	hsa-miR-154	UAGGUUAUCCGUGUUGCCUUCG
IH-301151-02-0002	MIMAT0004609	hsa-miR-149-3p	Unknown
IN-001005-01-05	Hairpin Inhibitor Negative Control		Unknown

miScript Target Protectors and negative control Target Protector were purchased from Qiagen.

Assay Name	Catalog Number	Target binding site sequence provide/Sequence:
Neg. Control Target Protector	MTP0000002	Unknown
Target Protector DAB2IP 1	MTP0076757	5'TGCTGGAGAAAGCCACGCCCTCCCTGCTAG 3'
Target Protector DAB2IP 2	MTP0076750	5'CTCTTCTCTCCCCAGCCCCCTCCCACCGCT3'
Target Protector DAB2IP 3	MTP0076743	5'TTCTGTAGCTTATCTGCCCCTCCCCCACTT3'

Retroviral Transductions. For retrovirus production, low confluence (≈20%) 293GP packaging cells, stably expressing retroviral gag and pol proteins, were transfected by calcium-phosphate precipitation. Briefly, cells were plated the day before the transfection in 10 cm^2 dishes in exactly 10 ml of medium. Each different virus was produced by co-transfection of 10 μg of the vector of interest and 5 μg of pEnv encoding vector. After 8 hours, medium was changed and cells were incubated at 37°C. After 48-72 hours the virus-containing medium was filtered (0.45 μm filter) and supplemented with 10% FBS and polybrene (8 ug/ml). The culture medium of target cells growing at low confluence (≈30-40%) was replaced by the appropriate viral supernatant and incubated at 37°C for 24 hours. Cells were selected with puromycin (0.5 μg/ml) and kept under selection for the entire experiment.

Lentiviral Transductions. For Lentivirus production HEK-293T cells were transfected with the packaging plasmids and the plasmid construct of interest, using standard calcium-phosphate method. After 8 hours, medium was changed and cells were incubated at 37°C. After 48 hours, the supernatants containing viral particles were filtered (0.45 μm filter), supplemented with 10% FBS and polybrene (8ug/ml). The culture medium of target cells growing at low confluence (≈30-40%) was replaced by the appropriate viral supernatant and incubated at 37°C for 24 hours. Cells were selected with puromycin (0.5 μg/ml) and kept under selection for the entire experiment. 50 ng/ml of Doxycycline has been used to induce shRNA expression and DAB2IP protein knockdown.

Treatments. Human TNFα was purchased from Invitrogen (PHC3015). Cells were treated with recombinant TNFα (10ng/ml) in low serum (0.1% FBS) for 20 hours.

Plasmids

psiCHECK2 DAB2IP 3'UTR was generated by amplifying DAB2IP 3'UTR (NM_032552.2) from genomic DNA extracted from H1299 cells and subsequently cloning it into psiCHECK2 (Promega) downstream of Renilla Luciferase reporter gene, between NotI and XhoI restriction sites.

pLKO-shDAB2IP plasmid was generated by cloning in the pLKO lentiviral vector a double stranded oligonucleotide corresponding to the sequence of siDAB2IP 3'UTR.

pLPC-DAB2IP-long was obtained by cloning mouse DAB2IP (mDAB2IP) transcript variant 1 (NM_001114125.1) into pLPC empty vector. pLPC-DAB2IP-short was generated by amplifying DAB2IP-long coding region using specific primers starting from nucleotide 404 of mDAB2IP transcript variant 1 sequence, and cloning it into pLPC empty vector.

Cell manipulation and Western blot analysis

Total cell extracts were prepared in RIPA buffer without SDS (150mM NaCl, 50mM Tris-HCl pH8, 1mM EDTA, 1% NP-40, 0.5% Na-deoxycholate) supplemented with 1 mM PMSF, 5 mM NaF, 1 mM Na_3VO_4, 10μg/ml CLAP, 1μM TSA and 5μM nicotinamide. Protein concentration was determined with Bio-Rad Protein Assay Reagent (#500-0006, Bio-Rad). Lysates were resolved by SDS/PAGE and transferred to nitrocellulose (Millipore).

Western blot analysis was performed according to standard procedures using the following primary antibodies:

Target	Antibody
Actin	#A9718 (Sigma)
DAB2IP	A302-440A (Bethyl)
Tubulin	T5168 (Sigma)
p65 RelA	sc-372X (Santa Cruz)
Lamin A/C	sc-6215 (Santa Cruz)
Vimentin	ab8069 ((Abcam)

Anti-goat, anti-mouse and anti-rabbit HRPO-conjugated (Sigma), were used as secondary antibodies.

Nucleus-cytoplasm fractionation

Cells were washed two times in PBS and scraped in Cytoplasmic-buffer (10mM HEPES pH7.9, 1.5mM $MgCl_2$, 10mM KCl, 0.5mM DTT, 0.1% NP-40) supplemented with inhibitors (1mM PMSF, 5mM NaF, 10mg/ml CLAP, 1mM Na3VO4); lysis was obtained gently pipetting a couple of times. After 3 minutes in ice, lysates were centrifuged at 2500g for 5 minutes at 4°C; the supernatant was collected as the cytoplasmic fraction. The pellet was washed twice in Wash-buffer (10mM HEPES pH7.9, 1.5mM $MgCl_2$, 10mM KCl, 0.5mM DTT) and then Nuclei in the pellet were resuspended in Nuclear-buffer (20mM HEPES pH7.9, 1.5mM $MgCl_2$, 420mM NaCl, 0.2mM EGTA, 0.5mM DTT, 25% glycerol) supplemented with inhibitors (1mM PMSF, 5mM NaF, 10mg/ml CLAP, 1mM Na3VO4); after 30 minutes of incubation in ice, nuclear extract was recovered by centrifugation at 15000g for 15 minutes at 4°C.

Immunofluorescence

Cells were washed two times with PBS and fixed in 4% paraformaldehyde at room temperature for 20 minutes. The fixed cells were then permeabilized in PBS plus 0.1% Triton X-100 at room temperature for 5 minutes. Permeabilized cells were incubated with primary antibodies for 1 hour at room temperature. The coverslip was then washed three times PBS before incubation with secondary antibodies (Alexa Fluor® 568, 488 conjugated secondary antibodies - Life Technologies) for 1 hour, and then incubated 5 minutes with Hoecst. Each coverslip was prepared for microscopic examination by applying mounting medium (ProLong Gold antifade reagent, Life Technologies). Images were captured using a Leica DM4000B epifluorescence microscope.

RNA extraction and RT-qPCR

Total RNA was extracted with QIAzol (Qiagen) following manufacturer's instructions.

For mRNA expression analysis, 1μg of total RNA was reverse-transcribed with QuantiTect

Reverse Transcription (Qiagen). DAB2IP, CCL20, IL8, PTX3, BIRC3, CSF2 and the housekeeping gene control H3 were amplified SsoAdvanced™SYBR® Green Master Mix (Biorad) on a CFX96™ Real-Time PCR System (Biorad).

For microRNAs expression analysis, 1ug of RNA was retro-transcribed with miScript PCR System (Qiagen). miR-149*, miR-149, the other microRNAs studied and the housekeeping gene control U6B and SNORD25 small nuclear RNAs were amplified with miScript SYBR Green PCR kits (Qiagen), following manufacturer's instructions on a CFX96™ Real-Time PCR System (Biorad).

List of primers used:

Target	Sequence
DAB2IP	Fw: 5'CACATCACCAACCACTAC3' Rev: 5'TCCACCTCTGACATCATC3'
CCL20	Fw: 5' CAGTGCTGCTACTCCACCTC3' Rev: 5' AAAGTTGCTTGCTGCTTCTGA3'
CSF2	Fw: 5'AATGTTTGACCTCCAGGAGCC3' Rev: 5'TCTGGGTTGCACAGGAAGTT3'
IL8	Fw: 5'GGCAGCCTTCCTGATTTCTG3' Rev: 5'CTTGCCAAAACTGCACCTTCA3'
PTX3	Fw: 5' GCGGTGCTAGAGGAGCTG3' Rev: 5' GCCTCATTGGTCTCACTGGA3'
BIRC3	Fw: 5' AGCTGAAGCTGTGTTATATGAGC3' Rev: 5' ACTGTACCCTTGATTGTACTCCT3'
H3	Fw: 5'GAAGAAACCTCATCGTTACAGGCCTGGT3' Rev: 5'CTGCAAAGCACCAATAGCTGCACTCTGGAA 3'

Assay Name	Official Symbol	Catalog Number	Purchase from
Hs_SNORD25_11	SNORD25	MS00014007	Qiagen
Hs_RNU6B_13	RNU6B	MS00014000	Qiagen
Hs_miR-149_1	MIR149	MS00003570	Qiagen
Hs_miR-149*_3	MIR149	MS00037702	Qiagen
Hs_miR-1282	MIR1282	MS00014462	Qiagen
Hs_miR-92b	MIR92B	MS00032144	Qiagen
Hs_miR-92_1	MIR92A1	MS00006594	Qiagen
Hs_miR-154_1	MIR154	MS00003598	Qiagen
Hs_miR-744	MIR744	MS00010549	Qiagen
Hs_miR-96_1	MIR96	MS00003360	Qiagen
Hs_miR-25_1	MIR25	MS00003227	Qiagen
Hs_ miR-555_1	MIR555	MS00004655	Qiagen
Hs_ miR-582_1	MIR582	MS00004844	Qiagen

Migration and invasion assays

For transwell migration assays, cells ($1x10^5$) were plated on 24 well PET inserts (8.0 μm pore size, Falcon). After 18 hours, cells that passed through the filter were fixed in 4% PFA, stained with 0.05% crystal violet and counted.

For invasion assays, cells ($0.5\text{-}1x10^5$) were plated on 24 well PET inserts (8.0 μm pore size, Falcon) coated with BD Matrigel™ (BD Bioscience). Cells that passed through the matrigel-coated filter were fixed, stained, and counted after 20 hours. Specifically, for both invasion and transwell migration assays, cells were seeded on filters in low serum (0.1% FBS); the lower chamber was filled with high serum medium (10% FBS). MCF-10A cells were seeded on filter in low serum (0.05% HS), with the addiction of insulin (10 μg/ml), hydrocortisone (0.5 μg/ml) and epidermal growth factor (EGF 20 ng/ml); the lower chamber was filled with high serum medium (5% HS), with the addiction of insulin (10 μg/ml), hydrocortisone (0.5 μg/ml) and epidermal growth factor (EGF 20 ng/ml).

Statistical Analysis

In all graphs data are expressed as mean ± SD of three independent experiments, except when otherwise indicated. Differences were analyzed by Student's t test using Prism 6 (GraphPad), except when otherwise indicated. P-values < 0.05 were considered significant.

Microarray Hybridization and Analysis

For gene profiling, we used the Illumina HumanHT-12-v4-BeadChip (Illumina), which includes a bead pool of more than 48,000 unique bead types corresponding to 40,876 transcripts. Total RNA (2μg) isolated from PC-3 cells expressing control siRNA (siC), siRNA for DAB2IP (siDAB2IP), or miR-149* mimic were reverse transcribed and amplified according to standard protocols and in vitro transcription was then carried out to generate cRNA. cRNA was hybridized onto each array (three replicates for each condition) and then labeled with Cy3-streptavidin (Amersham Biosciences). The array was then scanned using a BeadStation 500 system (Illumina). The probe intensities were calculated and normalized using GenomeStudio Data Analysis Software's Gene Expression Module (GSGX) Version 1.9 (Illumina). Further data processing was performed in the R computing environment (http://www.r-project.org/) version 3.2.2, with BioConductor packages (http://www.bioconductor.org/). Statistical analysis for differentially expressed genes was performed with *limma* (Smyth, 2004). P-values were adjusted

for multiple testing using Benjamini and Hochberg's method to control the false discovery rate (Hochberg and Benjamini, 1990).

Acunzo, M., and Croce, C.M. (2015). MicroRNA in Cancer and Cachexia--A Mini-Review. The Journal of infectious diseases *212 Suppl 1*, S74-77.

Acunzo, M., Romano, G., Wernicke, D., and Croce, C.M. (2015). MicroRNA and cancer--a brief overview. Advances in biological regulation *57*, 1-9.

Adams, B.D., Kasinski, A.L., and Slack, F.J. (2014). Aberrant regulation and function of microRNAs in cancer. Current biology : CB *24*, R762-776.

Adorno, M., Cordenonsi, M., Montagner, M., Dupont, S., Wong, C., Hann, B., Solari, A., Bobisse, S., Rondina, M.B., Guzzardo, V.*, et al.* (2009). A Mutant-p53/Smad complex opposes p63 to empower TGFbeta-induced metastasis. Cell *137*, 87-98.

Aikawa, T., Whipple, C.A., Lopez, M.E., Gunn, J., Young, A., Lander, A.D., and Korc, M. (2008). Glypican-1 modulates the angiogenic and metastatic potential of human and mouse cancer cells. The Journal of clinical investigation *118*, 89-99.

Albor, A., Kaku, S., and Kulesz-Martin, M. (1998). Wild-type and mutant forms of p53 activate human topoisomerase I: a possible mechanism for gain of function in mutants. Cancer research *58*, 2091-2094.

Alexandrova, E.M., Yallowitz, A.R., Li, D., Xu, S., Schulz, R., Proia, D.A., Lozano, G., Dobbelstein, M., and Moll, U.M. (2015). Improving survival by exploiting tumour dependence on stabilized mutant p53 for treatment. Nature *523*, 352-356.

Ali, A., Wang, Z., Fu, J., Ji, L., Liu, J., Li, L., Wang, H., Chen, J., Caulin, C., Myers, J.N.*, et al.* (2013). Differential regulation of the REGgamma-proteasome pathway by p53/TGF-beta signalling and mutant p53 in cancer cells. Nature communications *4*, 2667.

Baranwal, S., and Alahari, S.K. (2010). miRNA control of tumor cell invasion and metastasis. International journal of cancer Journal international du cancer *126*, 1283-1290.

Barik, S. (2008). An intronic microRNA silences genes that are functionally antagonistic to its host gene. Nucleic acids research *36*, 5232-5241.

Bates, R.C., and Mercurio, A.M. (2003). Tumor necrosis factor-alpha stimulates the epithelial-to-mesenchymal transition of human colonic organoids. Molecular biology of the cell *14*, 1790-1800.

Baud, V., and Karin, M. (2009). Is NF-kappaB a good target for cancer therapy? Hopes and pitfalls. Nature reviews Drug discovery *8*, 33-40.

Bayne, L.J., Beatty, G.L., Jhala, N., Clark, C.E., Rhim, A.D., Stanger, B.Z., and Vonderheide, R.H. (2012). Tumor-derived granulocyte-macrophage colony-stimulating factor regulates myeloid inflammation and T cell immunity in pancreatic cancer. Cancer cell *21*, 822-835.

Behm-Ansmant, I., Rehwinkel, J., Doerks, T., Stark, A., Bork, P., and Izaurralde, E. (2006). mRNA degradation by miRNAs and GW182 requires both CCR4:NOT deadenylase and DCP1:DCP2 decapping complexes. Genes & development *20*, 1885-1898.

Ben-Neriah, Y., and Karin, M. (2011). Inflammation meets cancer, with NF-kappaB as the matchmaker. Nature immunology *12*, 715-723.

Bernstein, E., Caudy, A.A., Hammond, S.M., and Hannon, G.J. (2001). Role for a bidentate ribonuclease in the initiation step of RNA interference. Nature *409*, 363-366.

Bernstein, E., Kim, S.Y., Carmell, M.A., Murchison, E.P., Alcorn, H., Li, M.Z., Mills, A.A., Elledge, S.J., Anderson, K.V., and Hannon, G.J. (2003). Dicer is essential for mouse development. Nature genetics *35*, 215-217.

Bindea, G., Mlecnik, B., Tosolini, M., Kirilovsky, A., Waldner, M., Obenauf, A.C., Angell, H., Fredriksen, T., Lafontaine, L., Berger, A.*, et al.* (2013). Spatiotemporal dynamics of intratumoral immune cells reveal the immune landscape in human cancer. Immunity *39*, 782-795.

Bischoff, A., Huck, B., Keller, B., Strotbek, M., Schmid, S., Boerries, M., Busch, H., Muller, D., and Olayioye, M.A. (2014). miR149 functions as a tumor suppressor by controlling breast epithelial cell migration and invasion. Cancer research *74*, 5256-5265.

Boguski, M.S., and McCormick, F. (1993). Proteins regulating Ras and its relatives. Nature *366*, 643-654.

Bossi, G., Lapi, E., Strano, S., Rinaldo, C., Blandino, G., and Sacchi, A. (2006). Mutant p53 gain of function: reduction of tumor malignancy of human cancer cell lines through abrogation of mutant p53 expression. Oncogene *25*, 304-309.

Bossi, G., Marampon, F., Maor-Aloni, R., Zani, B., Rotter, V., Oren, M., Strano, S., Blandino, G., and Sacchi, A. (2008). Conditional RNA interference in vivo to study mutant p53 oncogenic gain of function on tumor malignancy. Cell Cycle *7*, 1870-1879.

Brabletz, T., Jung, A., Spaderna, S., Hlubek, F., and Kirchner, T. (2005). Opinion: migrating cancer stem cells - an integrated concept of malignant tumour progression. Nature reviews Cancer *5*, 744-749.

Braicu, C., Pileczki, V., Irimie, A., and Berindan-Neagoe, I. (2013). p53siRNA therapy reduces cell proliferation, migration and induces apoptosis in triple negative breast cancer cells. Molecular and cellular biochemistry *381*, 61-68.

Braun, J.E., Huntzinger, E., Fauser, M., and Izaurralde, E. (2011). GW182 proteins directly recruit cytoplasmic deadenylase complexes to miRNA targets. Molecular cell *44*, 120-133.

Bravo-Cordero, J.J., Hodgson, L., and Condeelis, J. (2012). Directed cell invasion and migration during metastasis. Current opinion in cell biology *24*, 277-283.

Brosh, R., and Rotter, V. (2009). When mutants gain new powers: news from the mutant p53 field. Nature reviews Cancer *9*, 701-713.

Calin, G.A., and Croce, C.M. (2006). MicroRNA signatures in human cancers. Nature reviews Cancer *6*, 857-866.

Calin, G.A., Dumitru, C.D., Shimizu, M., Bichi, R., Zupo, S., Noch, E., Aldler, H., Rattan, S., Keating, M., Rai, K.*, et al.* (2002). Frequent deletions and down-regulation of micro- RNA genes miR15 and miR16 at 13q14 in chronic lymphocytic leukemia. Proceedings of the National Academy of Sciences of the United States of America *99*, 15524-15529.

Calvisi, D.F., Ladu, S., Conner, E.A., Seo, D., Hsieh, J.T., Factor, V.M., and Thorgeirsson, S.S. (2011). Inactivation of Ras GTPase-activating proteins promotes unrestrained activity of wild-type Ras in human liver cancer. Journal of hepatology *54*, 311-319.

Carpentier, I., Coornaert, B., and Beyaert, R. (2004). Function and regulation of tumor necrosis factor receptor type 2. Current medicinal chemistry *11*, 2205-2212.

Caulin, C., Nguyen, T., Lang, G.A., Goepfert, T.M., Brinkley, B.R., Cai, W.W., Lozano, G., and Roop, D.R. (2007). An inducible mouse model for skin cancer reveals distinct roles for gain- and loss-of-function p53 mutations. The Journal of clinical investigation *117*, 1893-1901.

Chamorro-Jorganes, A., Araldi, E., Rotllan, N., Cirera-Salinas, D., and Suarez, Y. (2014). Autoregulation of glypican-1 by intronic microRNA-149 fine tunes the angiogenic response to FGF2 in human endothelial cells. Journal of cell science *127*, 1169-1178.

Chan, S.H., Huang, W.C., Chang, J.W., Chang, K.J., Kuo, W.H., Wang, M.Y., Lin, K.Y., Uen, Y.H., Hou, M.F., Lin, C.M.*, et al.* (2014). MicroRNA-149 targets GIT1 to suppress integrin signaling and breast cancer metastasis. Oncogene *33*, 4496-4507.

Chang, S.L., Chou, R.H., Zeng, H.J., Lin, Y.H., Chiu, T.Y., Yang, D.M., Hung, S.C., Lai, C.H., Hsieh, J.T., Shyu, W.C.*, et al.* (2013). Downregulation of DAB2IP promotes mesenchymal-to-neuroepithelial transition and neuronal differentiation of human mesenchymal stem cells. PloS one *8*, e75884.

Chen, H., Karam, J.A., Schultz, R., Zhang, Z., Duncan, C., and Hsieh, J.T. (2006). Cloning of mouse Dab2ip gene, a novel member of the RasGTPase-activating protein family and characterization of its regulatory region in prostate. DNA and cell biology *25*, 232-245.

Chen, H., Pong, R.C., Wang, Z., and Hsieh, J.T. (2002). Differential regulation of the human gene DAB2IP in normal and malignant prostatic epithelia: cloning and characterization. Genomics *79*, 573-581.

Chen, H., Toyooka, S., Gazdar, A.F., and Hsieh, J.T. (2003). Epigenetic regulation of a novel tumor suppressor gene (hDAB2IP) in prostate cancer cell lines. The Journal of biological chemistry *278*, 3121-3130.

Chen, H., Tu, S.W., and Hsieh, J.T. (2005). Down-regulation of human DAB2IP gene expression mediated by polycomb Ezh2 complex and histone deacetylase in prostate cancer. The Journal of biological chemistry *280*, 22437-22444.

Chen, J., Yao, Y., Gong, C., Yu, F., Su, S., Chen, J., Liu, B., Deng, H., Wang, F., Lin, L.*, et al.* (2011a). CCL18 from tumor-associated macrophages promotes breast cancer metastasis via PITPNM3. Cancer cell *19*, 541-555.

Chen, K.J., Lin, S.Z., Zhou, L., Xie, H.Y., Zhou, W.H., Taki-Eldin, A., and Zheng, S.S. (2011b). Selective recruitment of regulatory T cell through CCR6-CCL20 in hepatocellular carcinoma fosters tumor progression and predicts poor prognosis. PloS one *6*, e24671.

Chen, S., Gulla, S., Cai, C., and Balk, S.P. (2012). Androgen receptor serine 81 phosphorylation mediates chromatin binding and transcriptional activation. The Journal of biological chemistry *287*, 8571-8583.

Chen, Y., Dong, X., Yu, D., and Wang, X. (2015). Serum miR-96 is a promising biomarker for hepatocellular carcinoma in patients with chronic hepatitis B virus infection. International journal of clinical and experimental medicine *8*, 18462-18468.

Cheng, X.S., Li, Y.F., Tan, J., Sun, B., Xiao, Y.C., Fang, X.B., Zhang, X.F., Li, Q., Dong, J.H., Li, M.*, et al.* (2014). CCL20 and CXCL8 synergize to promote progression and poor survival outcome in patients with colorectal cancer by collaborative induction of the epithelial-mesenchymal transition. Cancer letters *348*, 77-87.

Chew, V., Chen, J., Lee, D., Loh, E., Lee, J., Lim, K.H., Weber, A., Slankamenac, K., Poon, R.T., Yang, H.*, et al.* (2012). Chemokine-driven lymphocyte infiltration: an early intratumoural event determining long-term survival in resectable hepatocellular carcinoma. Gut *61*, 427-438.

Chou, J., Shahi, P., and Werb, Z. (2013). microRNA-mediated regulation of the tumor microenvironment. Cell Cycle *12*, 3262-3271.

Clarke, H.J., Chambers, J.E., Liniker, E., and Marciniak, S.J. (2014). Endoplasmic reticulum stress in malignancy. Cancer cell *25*, 563-573.

Clevers, H. (2006). Wnt/beta-catenin signaling in development and disease. Cell *127*, 469-480.

Colotta, F., Allavena, P., Sica, A., Garlanda, C., and Mantovani, A. (2009). Cancer-related inflammation, the seventh hallmark of cancer: links to genetic instability. Carcinogenesis *30*, 1073-1081.

Cooks, T., Harris, C.C., and Oren, M. (2014). Caught in the cross fire: p53 in inflammation. Carcinogenesis *35*, 1680-1690.

Cooks, T., Pateras, I.S., Tarcic, O., Solomon, H., Schetter, A.J., Wilder, S., Lozano, G., Pikarsky, E., Forshew, T., Rosenfeld, N.*, et al.* (2013). Mutant p53 prolongs NF-kappaB activation and promotes chronic inflammation and inflammation-associated colorectal cancer. Cancer cell *23*, 634-646.

Dai, X., North, B.J., and Inuzuka, H. (2014). Negative regulation of DAB2IP by Akt and SCFFbw7 pathways. Oncotarget *5*, 3307-3315.

Davis, R.J. (2000). Signal transduction by the JNK group of MAP kinases. Cell *103*, 239-252.

De Craene, B., and Berx, G. (2013). Regulatory networks defining EMT during cancer initiation and progression. Nature reviews Cancer *13*, 97-110.

Deb, S., Jackson, C.T., Subler, M.A., and Martin, D.W. (1992). Modulation of cellular and viral promoters by mutant human p53 proteins found in tumor cells. Journal of virology *66*, 6164-6170.

Dell'Orso, S., Fontemaggi, G., Stambolsky, P., Goeman, F., Voellenkle, C., Levrero, M., Strano, S., Rotter, V., Oren, M., and Blandino, G. (2011). ChIP-on-chip analysis of in vivo mutant p53 binding to selected gene promoters. Omics : a journal of integrative biology *15*, 305-312.

Di Agostino, S., Cortese, G., Monti, O., Dell'Orso, S., Sacchi, A., Eisenstein, M., Citro, G., Strano, S., and Blandino, G. (2008). The disruption of the protein complex mutantp53/p73 increases selectively the response of tumor cells to anticancer drugs. Cell Cycle *7*, 3440-3447.

Di Agostino, S., Strano, S., Emiliozzi, V., Zerbini, V., Mottolese, M., Sacchi, A., Blandino, G., and Piaggio, G. (2006). Gain of function of mutant p53: the mutant p53/NF-Y protein complex reveals an aberrant transcriptional mechanism of cell cycle regulation. Cancer cell *10*, 191-202.

Di Minin, G., Bellazzo, A., Dal Ferro, M., Chiaruttini, G., Nuzzo, S., Bicciato, S., Piazza, S., Rami, D., Bulla, R., Sommaggio, R.*, et al.* (2014). Mutant p53 reprograms TNF signaling in cancer cells through interaction with the tumor suppressor DAB2IP. Molecular cell *56*, 617-629.

Ding, D.P., Chen, Z.L., Zhao, X.H., Wang, J.W., Sun, J., Wang, Z., Tan, F.W., Tan, X.G., Li, B.Z., Zhou, F.*, et al.* (2011). miR-29c induces cell cycle arrest in esophageal squamous cell carcinoma by modulating cyclin E expression. Carcinogenesis *32*, 1025-1032.

Doble, B.W., and Woodgett, J.R. (2003). GSK-3: tricks of the trade for a multi-tasking kinase. Journal of cell science *116*, 1175-1186.

Dong, P., Xu, Z., Jia, N., Li, D., and Feng, Y. (2009). Elevated expression of p53 gain-of-function mutation R175H in endometrial cancer cells can increase the invasive phenotypes by activation of the EGFR/PI3K/AKT pathway. Molecular cancer *8*, 103.

Dote, H., Toyooka, S., Tsukuda, K., Yano, M., Ota, T., Murakami, M., Naito, M., Toyota, M., Gazdar, A.F., and Shimizu, N. (2005). Aberrant promoter methylation in human DAB2 interactive protein (hDAB2IP) gene in gastrointestinal tumour. British journal of cancer *92*, 1117-1125.

Dote, H., Toyooka, S., Tsukuda, K., Yano, M., Ouchida, M., Doihara, H., Suzuki, M., Chen, H., Hsieh, J.T., Gazdar, A.F.*, et al.* (2004). Aberrant promoter methylation in human DAB2 interactive protein (hDAB2IP) gene in breast cancer. Clinical cancer research : an official journal of the American Association for Cancer Research *10*, 2082-2089.

Doyle, B., Morton, J.P., Delaney, D.W., Ridgway, R.A., Wilkins, J.A., and Sansom, O.J. (2010). p53 mutation and loss have different effects on tumourigenesis in a novel mouse model of pleomorphic rhabdomyosarcoma. The Journal of pathology *222*, 129-137.

Duan, Y.F., Li, D.F., Liu, Y.H., Mei, P., Qin, Y.X., Li, L.F., Lin, Q.X., and Li, Z.J. (2013). Decreased expression of DAB2IP in pancreatic cancer with wild-type KRAS. Hepatobiliary & pancreatic diseases international : HBPD INT *12*, 204-209.

Elinav, E., Nowarski, R., Thaiss, C.A., Hu, B., Jin, C., and Flavell, R.A. (2013). Inflammation-induced cancer: crosstalk between tumours, immune cells and microorganisms. Nature reviews Cancer *13*, 759-771.

Esteller, M. (2011). Non-coding RNAs in human disease. Nature reviews Genetics *12*, 861-874.

Fabbri, M., Calore, F., Paone, A., Galli, R., and Calin, G.A. (2013). Epigenetic regulation of miRNAs in cancer. Advances in experimental medicine and biology *754*, 137-148.

Facciabene, A., Peng, X., Hagemann, I.S., Balint, K., Barchetti, A., Wang, L.P., Gimotty, P.A., Gilks, C.B., Lal, P., Zhang, L.*, et al.* (2011). Tumour hypoxia promotes tolerance and angiogenesis via CCL28 and T(reg) cells. Nature *475*, 226-230.

Fan, S.J., Li, H.B., Cui, G., Kong, X.L., Sun, L.L., Zhao, Y.Q., Li, Y.H., and Zhou, J. (2016). miRNA-149* promotes cell proliferation and suppresses apoptosis by mediating JunB in T-cell acute lymphoblastic leukemia. Leukemia research *41*, 62-70.

Fang, Y., Zhu, X., Wang, J., Li, N., Li, D., Sakib, N., Sha, Z., and Song, W. (2015). MiR-744 functions as a proto-oncogene in nasopharyngeal carcinoma progression and metastasis via transcriptional control of ARHGAP5. Oncotarget *6*, 13164-13175.

Feller, S.M., Ren, R., Hanafusa, H., and Baltimore, D. (1994). SH2 and SH3 domains as molecular adhesives: the interactions of Crk and Abl. Trends in biochemical sciences *19*, 453-458.

Fendler, A., Jung, M., Stephan, C., Erbersdobler, A., Jung, K., and Yousef, G.M. (2013). The antiapoptotic function of miR-96 in prostate cancer by inhibition of FOXO1. PloS one *8*, e80807.

Ferrara, N., Gerber, H.P., and LeCouter, J. (2003). The biology of VEGF and its receptors. Nature medicine *9*, 669-676.

Fico, A., Maina, F., and Dono, R. (2011). Fine-tuning of cell signaling by glypicans. Cellular and molecular life sciences : CMLS *68*, 923-929.

Filipowicz, W., Bhattacharyya, S.N., and Sonenberg, N. (2008). Mechanisms of post-transcriptional regulation by microRNAs: are the answers in sight? Nature reviews Genetics *9*, 102-114.

Flores, E.R., Sengupta, S., Miller, J.B., Newman, J.J., Bronson, R., Crowley, D., Yang, A., McKeon, F., and Jacks, T. (2005). Tumor predisposition in mice mutant for p63 and p73: evidence for broader tumor suppressor functions for the p53 family. Cancer cell *7*, 363-373.

Fontemaggi, G., Dell'Orso, S., Trisciuoglio, D., Shay, T., Melucci, E., Fazi, F., Terrenato, I., Mottolese, M., Muti, P., Domany, E.*, et al.* (2009). The execution of the transcriptional axis mutant p53, E2F1 and ID4 promotes tumor neo-angiogenesis. Nature structural & molecular biology *16*, 1086-1093.

Frank, F., Sonenberg, N., and Nagar, B. (2010). Structural basis for 5'-nucleotide base-specific recognition of guide RNA by human AGO2. Nature *465*, 818-822.

Frazier, M.W., He, X., Wang, J., Gu, Z., Cleveland, J.L., and Zambetti, G.P. (1998). Activation of c-myc gene expression by tumor-derived p53 mutants requires a discrete C-terminal domain. Molecular and cellular biology *18*, 3735-3743.

Freed-Pastor, W.A., Mizuno, H., Zhao, X., Langerod, A., Moon, S.H., Rodriguez-Barrueco, R., Barsotti, A., Chicas, A., Li, W., Polotskaia, A.*, et al.* (2012). Mutant p53 disrupts mammary tissue architecture via the mevalonate pathway. Cell *148*, 244-258.

Freed-Pastor, W.A., and Prives, C. (2012). Mutant p53: one name, many proteins. Genes & development *26*, 1268-1286.

Frick, V.O., Rubie, C., Keilholz, U., and Ghadjar, P. (2016). Chemokine/chemokine receptor pair CCL20/CCR6 in human colorectal malignancy: An overview. World journal of gastroenterology *22*, 833-841.

Fridman, W.H., Pages, F., Sautes-Fridman, C., and Galon, J. (2012). The immune contexture in human tumours: impact on clinical outcome. Nature reviews Cancer *12*, 298-306.

Fruman, D.A., and Rommel, C. (2014). PI3K and cancer: lessons, challenges and opportunities. Nature reviews Drug discovery *13*, 140-156.

Fujii, T., Shimada, K., Tatsumi, Y., Fujimoto, K., and Konishi, N. (2015). Syndecan-1 responsive microRNA-126 and 149 regulate cell proliferation in prostate cancer. Biochemical and biophysical research communications *456*, 183-189.

Gales, D., Clark, C., Manne, U., and Samuel, T. (2013). The Chemokine CXCL8 in Carcinogenesis and Drug Response. ISRN oncology *2013*, 859154.

Gandellini, P., Folini, M., Longoni, N., Pennati, M., Binda, M., Colecchia, M., Salvioni, R., Supino, R., Moretti, R., Limonta, P.*, et al.* (2009). miR-205 Exerts tumor-suppressive functions in human prostate through down-regulation of protein kinase Cepsilon. Cancer research *69*, 2287-2295.

Ghildiyal, M., Xu, J., Seitz, H., Weng, Z., and Zamore, P.D. (2010). Sorting of Drosophila small silencing RNAs partitions microRNA* strands into the RNA interference pathway. RNA *16*, 43-56.

Girardini, J.E., Napoli, M., Piazza, S., Rustighi, A., Marotta, C., Radaelli, E., Capaci, V., Jordan, L., Quinlan, P., Thompson, A.*, et al.* (2011). A Pin1/mutant p53 axis promotes aggressiveness in breast cancer. Cancer cell *20*, 79-91.

Goel, H.L., and Mercurio, A.M. (2013). VEGF targets the tumour cell. Nature reviews Cancer *13*, 871-882.

Gregory, P.A., Bert, A.G., Paterson, E.L., Barry, S.C., Tsykin, A., Farshid, G., Vadas, M.A., Khew-Goodall, Y., and Goodall, G.J. (2008). The miR-200 family and miR-205 regulate epithelial to mesenchymal transition by targeting ZEB1 and SIP1. Nature cell biology *10*, 593-601.

Grishok, A., Pasquinelli, A.E., Conte, D., Li, N., Parrish, S., Ha, I., Baillie, D.L., Fire, A., Ruvkun, G., and Mello, C.C. (2001). Genes and mechanisms related to RNA interference regulate expression of the small temporal RNAs that control C. elegans developmental timing. Cell *106*, 23-34.

Grivennikov, S.I., Greten, F.R., and Karin, M. (2010). Immunity, inflammation, and cancer. Cell *140*, 883-899.

Grivennikov, S.I., Kuprash, D.V., Liu, Z.G., and Nedospasov, S.A. (2006). Intracellular signals and events activated by cytokines of the tumor necrosis factor superfamily: From simple paradigms to complex mechanisms. International review of cytology *252*, 129-161.

Guertin, D.A., and Sabatini, D.M. (2007). Defining the role of mTOR in cancer. Cancer cell *12*, 9-22.

Guo, H., Li, Q., Li, W., Zheng, T., Zhao, S., and Liu, Z. (2014). MiR-96 downregulates RECK to promote growth and motility of non-small cell lung cancer cells. Molecular and cellular biochemistry *390*, 155-160.

Guo, Y., Ren, M.S., Shang, C., Zhu, L., and Zhong, M. (2015). MTSS1 gene regulated by miR-96 inhibits cell proliferation and metastasis in tongue squamous cellular carcinoma Tca8113 cell line. International journal of clinical and experimental medicine *8*, 15441-15449.

Hagemann, T., Robinson, S.C., Schulz, M., Trumper, L., Balkwill, F.R., and Binder, C. (2004). Enhanced invasiveness of breast cancer cell lines upon co-cultivation with macrophages is due to TNF-alpha dependent up-regulation of matrix metalloproteases. Carcinogenesis *25*, 1543-1549.

Han, J., Lee, Y., Yeom, K.H., Nam, J.W., Heo, I., Rhee, J.K., Sohn, S.Y., Cho, Y., Zhang, B.T., and Kim, V.N. (2006). Molecular basis for the recognition of primary microRNAs by the Drosha-DGCR8 complex. Cell *125*, 887-901.

Hanahan, D., and Weinberg, R.A. (2000). The hallmarks of cancer. Cell *100*, 57-70.

Hanahan, D., and Weinberg, R.A. (2011). Hallmarks of cancer: the next generation. Cell *144*, 646-674.

Hayashita, Y., Osada, H., Tatematsu, Y., Yamada, H., Yanagisawa, K., Tomida, S., Yatabe, Y., Kawahara, K., Sekido, Y., and Takahashi, T. (2005). A polycistronic microRNA cluster, miR-17-92, is overexpressed in human lung cancers and enhances cell proliferation. Cancer research *65*, 9628-9632.

Heinlein, C., Krepulat, F., Lohler, J., Speidel, D., Deppert, W., and Tolstonog, G.V. (2008). Mutant p53(R270H) gain of function phenotype in a mouse model for oncogene-induced mammary carcinogenesis. International journal of cancer Journal international du cancer *122*, 1701-1709.

Hingorani, S.R., Wang, L., Multani, A.S., Combs, C., Deramaudt, T.B., Hruban, R.H., Rustgi, A.K., Chang, S., and Tuveson, D.A. (2005). Trp53R172H and KrasG12D cooperate to promote chromosomal instability and widely metastatic pancreatic ductal adenocarcinoma in mice. Cancer cell *7*, 469-483.

Hirano, S., Iwashita, Y., Sasaki, A., Kai, S., Ohta, M., and Kitano, S. (2007). Increased mRNA expression of chemokines in hepatocellular carcinoma with tumor-infiltrating lymphocytes. Journal of gastroenterology and hepatology *22*, 690-696.

Hochberg, Y., and Benjamini, Y. (1990). More powerful procedures for multiple significance testing. Stat Med *9*, 811-818.

Homayouni, R., Magdaleno, S., Keshvara, L., Rice, D.S., and Curran, T. (2003). Interaction of Disabled-1 and the GTPase activating protein Dab2IP in mouse brain. Brain research Molecular brain research *115*, 121-129.

Hsu, H., Xiong, J., and Goeddel, D.V. (1995). The TNF receptor 1-associated protein TRADD signals cell death and NF-kappa B activation. Cell *81*, 495-504.

Huang, Q., Qin, L., Dai, S., Zhang, H., Pasula, S., Zhou, H., Chen, H., and Min, W. (2013). AIP1 suppresses atherosclerosis by limiting hyperlipidemia-induced inflammation and vascular endothelial dysfunction. Arteriosclerosis, thrombosis, and vascular biology *33*, 795-804.

Huarte, M., and Rinn, J.L. (2010). Large non-coding RNAs: missing links in cancer? Human molecular genetics *19*, R152-161.

Hutvagner, G., McLachlan, J., Pasquinelli, A.E., Balint, E., Tuschl, T., and Zamore, P.D. (2001). A cellular function for the RNA-interference enzyme Dicer in the maturation of the let-7 small temporal RNA. Science *293*, 834-838.

Hwang, H.W., and Mendell, J.T. (2006). MicroRNAs in cell proliferation, cell death, and tumorigenesis. British journal of cancer *94*, 776-780.

Iozzo, R.V., and Sanderson, R.D. (2011). Proteoglycans in cancer biology, tumour microenvironment and angiogenesis. Journal of cellular and molecular medicine *15*, 1013-1031.

Isono, K., Nemoto, K., Li, Y., Takada, Y., Suzuki, R., Katsuki, M., Nakagawara, A., and Koseki, H. (2006). Overlapping roles for homeodomain-interacting protein kinases hipk1 and hipk2 in the mediation of cell growth in response to morphogenetic and genotoxic signals. Molecular and cellular biology *26*, 2758-2771.

Jager, R., Bertrand, M.J., Gorman, A.M., Vandenabeele, P., and Samali, A. (2012). The unfolded protein response at the crossroads of cellular life and death during endoplasmic reticulum stress. Biology of the cell / under the auspices of the European Cell Biology Organization *104*, 259-270.

Ji, W., Li, Y., He, Y., Yin, M., Zhou, H.J., Boggon, T.J., Zhang, H., and Min, W. (2015). AIP1 Expression in Tumor Niche Suppresses Tumor Progression and Metastasis. Cancer research *75*, 3492-3504.

Ji, W., Li, Y., Wan, T., Wang, J., Zhang, H., Chen, H., and Min, W. (2012). Both internalization and AIP1 association are required for tumor necrosis factor receptor 2-mediated JNK signaling. Arteriosclerosis, thrombosis, and vascular biology *32*, 2271-2279.

Jiang, Y., Woronicz, J.D., Liu, W., and Goeddel, D.V. (1999). Prevention of constitutive TNF receptor 1 signaling by silencer of death domains. Science *283*, 543-546.

Jin, L., Hu, W.L., Jiang, C.C., Wang, J.X., Han, C.C., Chu, P., Zhang, L.J., Thorne, R.F., Wilmott, J., Scolyer, R.A., *et al.* (2011). MicroRNA-149*, a p53-responsive microRNA, functions as an oncogenic regulator in human melanoma. Proceedings of the National Academy of Sciences of the United States of America *108*, 15840-15845.

Johnson, S.M., Grosshans, H., Shingara, J., Byrom, M., Jarvis, R., Cheng, A., Labourier, E., Reinert, K.L., Brown, D., and Slack, F.J. (2005). RAS is regulated by the let-7 microRNA family. Cell *120*, 635-647.

Jovanovic, M., and Hengartner, M.O. (2006). miRNAs and apoptosis: RNAs to die for. Oncogene *25*, 6176-6187.

Kalliolias, G.D., and Ivashkiv, L.B. (2016). TNF biology, pathogenic mechanisms and emerging therapeutic strategies. Nature reviews Rheumatology *12*, 49-62.

Kan, T., Sato, F., Ito, T., Matsumura, N., David, S., Cheng, Y., Agarwal, R., Paun, B.C., Jin, Z., Olaru, A.V.*, et al.* (2009). The miR-106b-25 polycistron, activated by genomic amplification, functions as an oncogene by suppressing p21 and Bim. Gastroenterology *136*, 1689-1700.

Karube, Y., Tanaka, H., Osada, H., Tomida, S., Tatematsu, Y., Yanagisawa, K., Yatabe, Y., Takamizawa, J., Miyoshi, S., Mitsudomi, T.*, et al.* (2005). Reduced expression of Dicer associated with poor prognosis in lung cancer patients. Cancer science *96*, 111-115.

Kawahara, Y., Megraw, M., Kreider, E., Iizasa, H., Valente, L., Hatzigeorgiou, A.G., and Nishikura, K. (2008). Frequency and fate of microRNA editing in human brain. Nucleic acids research *36*, 5270-5280.

Ke, Y., Zhao, W., Xiong, J., and Cao, R. (2013). miR-149 Inhibits Non-Small-Cell Lung Cancer Cells EMT by Targeting FOXM1. Biochemistry research international *2013*, 506731.

Kea, B., Gamarallage, R., Vairamuthu, H., Fortman, J., Lunney, K., Hendey, G.W., and Rodriguez, R.M. (2013). What is the clinical significance of chest CT when the chest x-ray result is normal in patients with blunt trauma? The American journal of emergency medicine *31*, 1268-1273.

Ketting, R.F., Fischer, S.E., Bernstein, E., Sijen, T., Hannon, G.J., and Plasterk, R.H. (2001). Dicer functions in RNA interference and in synthesis of small RNA involved in developmental timing in C. elegans. Genes & development *15*, 2654-2659.

Kim, M.P., Zhang, Y., and Lozano, G. (2015). Mutant p53: Multiple Mechanisms Define Biologic Activity in Cancer. Frontiers in oncology *5*, 249.

Kitamura, T., Qian, B.Z., and Pollard, J.W. (2015). Immune cell promotion of metastasis. Nature reviews Immunology *15*, 73-86.

Kleeff, J., Ishiwata, T., Kumbasar, A., Friess, H., Buchler, M.W., Lander, A.D., and Korc, M. (1998). The cell-surface heparan sulfate proteoglycan glypican-1 regulates growth factor action in pancreatic carcinoma cells and is overexpressed in human pancreatic cancer. The Journal of clinical investigation *102*, 1662-1673.

Kleeff, J., Wildi, S., Kumbasar, A., Friess, H., Lander, A.D., and Korc, M. (1999). Stable transfection of a glypican-1 antisense construct decreases tumorigenicity in PANC-1 pancreatic carcinoma cells. Pancreas *19*, 281-288.

Kondo, T., Nakazawa, H., Ito, F., Hashimoto, Y., Osaka, Y., Futatsuyama, K., Toma, H., and Tanabe, K. (2006). Favorable prognosis of renal cell carcinoma with increased expression of chemokines associated with a Th1-type immune response. Cancer science *97*, 780-786.

Kong, Z., Raghavan, P., Xie, D., Boike, T., Burma, S., Chen, D., Chakraborty, A., Hsieh, J.T., and Saha, D. (2010). Epothilone B confers radiation dose enhancement in DAB2IP gene knock-down radioresistant prostate cancer cells. International journal of radiation oncology, biology, physics *78*, 1210-1218.

Krol, J., Loedige, I., and Filipowicz, W. (2010). The widespread regulation of microRNA biogenesis, function and decay. Nature reviews Genetics *11*, 597-610.

Krol, J., Sobczak, K., Wilczynska, U., Drath, M., Jasinska, A., Kaczynska, D., and Krzyzosiak, W.J. (2004). Structural features of microRNA (miRNA) precursors and their relevance to miRNA biogenesis and small interfering RNA/short hairpin RNA design. The Journal of biological chemistry *279*, 42230-42239.

Kunz, M., Toksoy, A., Goebeler, M., Engelhardt, E., Brocker, E., and Gillitzer, R. (1999). Strong expression of the lymphoattractant C-X-C chemokine Mig is associated with heavy infiltration of T cells in human malignant melanoma. The Journal of pathology *189*, 552-558.

Lang, G.A., Iwakuma, T., Suh, Y.A., Liu, G., Rao, V.A., Parant, J.M., Valentin-Vega, Y.A., Terzian, T., Caldwell, L.C., Strong, L.C.*, et al.* (2004). Gain of function of a p53 hot spot mutation in a mouse model of Li-Fraumeni syndrome. Cell *119*, 861-872.

Laptenko, O., and Prives, C. (2006). Transcriptional regulation by p53: one protein, many possibilities. Cell death and differentiation *13*, 951-961.

Lee, G.H., Kim, S.H., Homayouni, R., and D'Arcangelo, G. (2012). Dab2ip regulates neuronal migration and neurite outgrowth in the developing neocortex. PloS one *7*, e46592.

Lee, Y., Jeon, K., Lee, J.T., Kim, S., and Kim, V.N. (2002). MicroRNA maturation: stepwise processing and subcellular localization. The EMBO journal *21*, 4663-4670.

Leung, W.K., He, M., Chan, A.W., Law, P.T., and Wong, N. (2015). Wnt/beta-Catenin activates MiR-183/96/182 expression in hepatocellular carcinoma that promotes cell invasion. Cancer letters *362*, 97-105.

Li, M., Guan, X., Sun, Y., Mi, J., Shu, X., Liu, F., and Li, C. (2014a). miR-92a family and their target genes in tumorigenesis and metastasis. Experimental cell research *323*, 1-6.

Li, P., Shan, J.X., Chen, X.H., Zhang, D., Su, L.P., Huang, X.Y., Yu, B.Q., Zhi, Q.M., Li, C.L., Wang, Y.Q.*, et al.* (2015). Epigenetic silencing of microRNA-149 in cancer-associated fibroblasts mediates prostaglandin E2/interleukin-6 signaling in the tumor microenvironment. Cell research *25*, 588-603.

Li, P., Sheng, C., Huang, L., Zhang, H., Huang, L., Cheng, Z., and Zhu, Q. (2014b). MiR-183/-96/-182 cluster is up-regulated in most breast cancers and increases cell proliferation and migration. Breast cancer research : BCR *16*, 473.

Li, R., Sutphin, P.D., Schwartz, D., Matas, D., Almog, N., Wolkowicz, R., Goldfinger, N., Pei, H., Prokocimer, M., and Rotter, V. (1998). Mutant p53 protein expression interferes with p53-independent apoptotic pathways. Oncogene *16*, 3269-3277.

Li, X., Zhang, R., Luo, D., Park, S.J., Wang, Q., Kim, Y., and Min, W. (2005). Tumor necrosis factor alpha-induced desumoylation and cytoplasmic translocation of homeodomain-interacting protein kinase 1 are critical for apoptosis signal-regulating kinase 1-JNK/p38 activation. The Journal of biological chemistry *280*, 15061-15070.

Li, Y., and Prives, C. (2007). Are interactions with p63 and p73 involved in mutant p53 gain of oncogenic function? Oncogene *26*, 2220-2225.

Liao, H., Xiao, Y., Hu, Y., Xiao, Y., Yin, Z., and Liu, L. (2015). microRNA-32 induces radioresistance by targeting DAB2IP and regulating autophagy in prostate cancer cells. Oncology letters *10*, 2055-2062.

Lin, F., Ding, R., Zheng, S., Xing, D., Hong, W., Zhou, Z., and Shen, J. (2014). Decrease expression of microRNA-744 promotes cell proliferation by targeting c-Myc in human hepatocellular carcinoma. Cancer cell international *14*, 58.

Lin, R.J., Lin, Y.C., and Yu, A.L. (2010). miR-149* induces apoptosis by inhibiting Akt1 and E2F1 in human cancer cells. Molecular carcinogenesis *49*, 719-727.

Lin, S., and Gregory, R.I. (2015). MicroRNA biogenesis pathways in cancer. Nature reviews Cancer *15*, 321-333.

Lin, Y., Choksi, S., Shen, H.M., Yang, Q.F., Hur, G.M., Kim, Y.S., Tran, J.H., Nedospasov, S.A., and Liu, Z.G. (2004). Tumor necrosis factor-induced nonapoptotic cell death requires receptor-interacting protein-mediated cellular reactive oxygen species accumulation. The Journal of biological chemistry *279*, 10822-10828.

Liu, D.P., Song, H., and Xu, Y. (2010). A common gain of function of p53 cancer mutants in inducing genetic instability. Oncogene *29*, 949-956.

Liu, K., Ling, S., and Lin, W.C. (2011). TopBP1 mediates mutant p53 gain of function through NF-Y and p63/p73. Molecular and cellular biology *31*, 4464-4481.

Liu, N., Tang, L.L., Sun, Y., Cui, R.X., Wang, H.Y., Huang, B.J., He, Q.M., Jiang, W., and Ma, J. (2013). MiR-29c suppresses invasion and metastasis by targeting TIAM1 in nasopharyngeal carcinoma. Cancer letters *329*, 181-188.

Liu, S., Zhu, N., and Chen, H. (2012). Expression patterns of human DAB2IP protein in fetal tissues. Biotechnic & histochemistry : official publication of the Biological Stain Commission *87*, 350-359.

Llave, C., Xie, Z., Kasschau, K.D., and Carrington, J.C. (2002). Cleavage of Scarecrow-like mRNA targets directed by a class of Arabidopsis miRNA. Science *297*, 2053-2056.

Lu, J., Getz, G., Miska, E.A., Alvarez-Saavedra, E., Lamb, J., Peck, D., Sweet-Cordero, A., Ebert, B.L., Mak, R.H., Ferrando, A.A.*, et al.* (2005). MicroRNA expression profiles classify human cancers. Nature *435*, 834-838.

Ludes-Meyers, J.H., Subler, M.A., Shivakumar, C.V., Munoz, R.M., Jiang, P., Bigger, J.E., Brown, D.R., Deb, S.P., and Deb, S. (1996). Transcriptional activation of the human epidermal growth factor receptor promoter by human p53. Molecular and cellular biology *16*, 6009-6019.

Lunardi, A., Di Minin, G., Provero, P., Dal Ferro, M., Carotti, M., Del Sal, G., and Collavin, L. (2010). A genome-scale protein interaction profile of Drosophila p53 uncovers additional nodes of the human p53 network. Proceedings of the National Academy of Sciences of the United States of America *107*, 6322-6327.

Luo, D., He, Y., Zhang, H., Yu, L., Chen, H., Xu, Z., Tang, S., Urano, F., and Min, W. (2008). AIP1 is critical in transducing IRE1-mediated endoplasmic reticulum stress response. The Journal of biological chemistry *283*, 11905-11912.

Luo, G., Chao, Y.L., Tang, B., Li, B.S., Xiao, Y.F., Xie, R., Wang, S.M., Wu, Y.Y., Dong, H., Liu, X.D.*, et al.* (2015). miR-149 represses metastasis of hepatocellular carcinoma by targeting actin-regulatory proteins PPM1F. Oncotarget *6*, 37808-37823.

Ma, L., Teruya-Feldstein, J., and Weinberg, R.A. (2007). Tumour invasion and metastasis initiated by microRNA-10b in breast cancer. Nature *449*, 682-688.

MacRae, I.J., Ma, E., Zhou, M., Robinson, C.V., and Doudna, J.A. (2008). In vitro reconstitution of the human RISC-loading complex. Proceedings of the National Academy of Sciences of the United States of America *105*, 512-517.

Mantovani, A., Allavena, P., Sica, A., and Balkwill, F. (2008). Cancer-related inflammation. Nature *454*, 436-444.

Marian, C.O., Yang, L., Zou, Y.S., Gore, C., Pong, R.C., Shay, J.W., Kabbani, W., Hsieh, J.T., and Raj, G.V. (2011). Evidence of epithelial to mesenchymal transition associated with increased tumorigenic potential in an immortalized normal prostate epithelial cell line. The Prostate *71*, 626-636.

Markert, E.K., Mizuno, H., Vazquez, A., and Levine, A.J. (2011). Molecular classification of prostate cancer using curated expression signatures. Proceedings of the National Academy of Sciences of the United States of America *108*, 21276-21281.

Martynova, E., Pozzi, S., Basile, V., Dolfini, D., Zambelli, F., Imbriano, C., Pavesi, G., and Mantovani, R. (2012). Gain-of-function p53 mutants have widespread genomic locations partially overlapping with p63. Oncotarget *3*, 132-143.

Matas, D., Milyavsky, M., Shats, I., Nissim, L., Goldfinger, N., and Rotter, V. (2004). p53 is a regulator of macrophage differentiation. Cell death and differentiation *11*, 458-467.

Matsuda, K., Maruyama, H., Guo, F., Kleeff, J., Itakura, J., Matsumoto, Y., Lander, A.D., and Korc, M. (2001). Glypican-1 is overexpressed in human breast cancer and modulates the mitogenic effects of multiple heparin-binding growth factors in breast cancer cells. Cancer research *61*, 5562-5569.

Medema, J.P. (2013). Cancer stem cells: the challenges ahead. Nature cell biology *15*, 338-344.

Meek, D.W. (2009). Tumour suppression by p53: a role for the DNA damage response? Nature reviews Cancer *9*, 714-723.

Melo, S.A., Moutinho, C., Ropero, S., Calin, G.A., Rossi, S., Spizzo, R., Fernandez, A.F., Davalos, V., Villanueva, A., Montoya, G.*, et al.* (2010). A genetic defect in exportin-5 traps precursor microRNAs in the nucleus of cancer cells. Cancer cell *18*, 303-315.

Mendell, J.T. (2008). miRiad roles for the miR-17-92 cluster in development and disease. Cell *133*, 217-222.

Merritt, W.M., Lin, Y.G., Han, L.Y., Kamat, A.A., Spannuth, W.A., Schmandt, R., Urbauer, D., Pennacchio, L.A., Cheng, J.F., Nick, A.M.*, et al.* (2008). Dicer, Drosha, and outcomes in patients with ovarian cancer. The New England journal of medicine *359*, 2641-2650.

Min, J., Liu, L., Li, X., Jiang, J., Wang, J., Zhang, B., Cao, D., Yu, D., Tao, D., Hu, J.*, et al.* (2015). Absence of DAB2IP promotes cancer stem cell like signatures and indicates poor survival outcome in colorectal cancer. Scientific reports *5*, 16578.

Min, J., Zaslavsky, A., Fedele, G., McLaughlin, S.K., Reczek, E.E., De Raedt, T., Guney, I., Strochlic, D.E., Macconaill, L.E., Beroukhim, R.*, et al.* (2010). An oncogene-tumor suppressor cascade drives metastatic prostate cancer by coordinately activating Ras and nuclear factor-kappaB. Nature medicine *16*, 286-294.

Min, W., Lin, Y., Tang, S., Yu, L., Zhang, H., Wan, T., Luhn, T., Fu, H., and Chen, H. (2008). AIP1 recruits phosphatase PP2A to ASK1 in tumor necrosis factor-induced ASK1-JNK activation. Circulation research *102*, 840-848.

Min, W., and Pober, J.S. (2011). AIP1 in graft arteriosclerosis. Trends in cardiovascular medicine *21*, 229-233.

Mizuno, H., Spike, B.T., Wahl, G.M., and Levine, A.J. (2010). Inactivation of p53 in breast cancers correlates with stem cell transcriptional signatures. Proceedings of the National Academy of Sciences of the United States of America *107*, 22745-22750.

Mlecnik, B., Tosolini, M., Charoentong, P., Kirilovsky, A., Bindea, G., Berger, A., Camus, M., Gillard, M., Bruneval, P., Fridman, W.H.*, et al.* (2010). Biomolecular network reconstruction identifies T-cell homing factors associated with survival in colorectal cancer. Gastroenterology *138*, 1429-1440.

Moore, R.J., Owens, D.M., Stamp, G., Arnott, C., Burke, F., East, N., Holdsworth, H., Turner, L., Rollins, B., Pasparakis, M.*, et al.* (1999). Mice deficient in tumor necrosis factor-alpha are resistant to skin carcinogenesis. Nature medicine *5*, 828-831.

Morlando, M., Ballarino, M., Gromak, N., Pagano, F., Bozzoni, I., and Proudfoot, N.J. (2008). Primary microRNA transcripts are processed co-transcriptionally. Nature structural & molecular biology *15*, 902-909.

Morton, J.P., Timpson, P., Karim, S.A., Ridgway, R.A., Athineos, D., Doyle, B., Jamieson, N.B., Oien, K.A., Lowy, A.M., Brunton, V.G.*, et al.* (2010). Mutant p53 drives metastasis and overcomes growth arrest/senescence in pancreatic cancer. Proceedings of the National Academy of Sciences of the United States of America *107*, 246-251.

Muller, P.A., Caswell, P.T., Doyle, B., Iwanicki, M.P., Tan, E.H., Karim, S., Lukashchuk, N., Gillespie, D.A., Ludwig, R.L., Gosselin, P.*, et al.* (2009). Mutant p53 drives invasion by promoting integrin recycling. Cell *139*, 1327-1341.

Muller, P.A., and Vousden, K.H. (2013). p53 mutations in cancer. Nature cell biology *15*, 2-8.

Muller, P.A., and Vousden, K.H. (2014). Mutant p53 in cancer: new functions and therapeutic opportunities. Cancer cell *25*, 304-317.

Muller, P.A., Vousden, K.H., and Norman, J.C. (2011). p53 and its mutants in tumor cell migration and invasion. The Journal of cell biology *192*, 209-218.

Musacchio, A., Gibson, T., Rice, P., Thompson, J., and Saraste, M. (1993). The PH domain: a common piece in the structural patchwork of signalling proteins. Trends in biochemical sciences *18*, 343-348.

Nalefski, E.A., and Falke, J.J. (1996). The C2 domain calcium-binding motif: structural and functional diversity. Protein science : a publication of the Protein Society *5*, 2375-2390.

O'Donnell, K.A., Wentzel, E.A., Zeller, K.I., Dang, C.V., and Mendell, J.T. (2005). c-Myc-regulated microRNAs modulate E2F1 expression. Nature *435*, 839-843.

Offer, H., Wolkowicz, R., Matas, D., Blumenstein, S., Livneh, Z., and Rotter, V. (1999). Direct involvement of p53 in the base excision repair pathway of the DNA repair machinery. FEBS letters *450*, 197-204.

Oguma, K., Oshima, H., Aoki, M., Uchio, R., Naka, K., Nakamura, S., Hirao, A., Saya, H., Taketo, M.M., and Oshima, M. (2008). Activated macrophages promote Wnt signalling through tumour necrosis factor-alpha in gastric tumour cells. The EMBO journal *27*, 1671-1681.

Okamura, K., Liu, N., and Lai, E.C. (2009). Distinct mechanisms for microRNA strand selection by Drosophila Argonautes. Molecular cell *36*, 431-444.

Olive, K.P., Tuveson, D.A., Ruhe, Z.C., Yin, B., Willis, N.A., Bronson, R.T., Crowley, D., and Jacks, T. (2004). Mutant p53 gain of function in two mouse models of Li-Fraumeni syndrome. Cell *119*, 847-860.

Orom, U.A., Nielsen, F.C., and Lund, A.H. (2008). MicroRNA-10a binds the 5'UTR of ribosomal protein mRNAs and enhances their translation. Molecular cell *30*, 460-471.

Palmieri, D., Capponi, S., Geroldi, A., Mura, M., Mandich, P., and Palombo, D. (2014). TNFalpha induces the expression of genes associated with endothelial dysfunction through p38MAPK-mediated down-regulation of miR-149. Biochemical and biophysical research communications *443*, 246-251.

Park, B.K., Zhang, H., Zeng, Q., Dai, J., Keller, E.T., Giordano, T., Gu, K., Shah, V., Pei, L., Zarbo, R.J*., et al.* (2007). NF-kappaB in breast cancer cells promotes osteolytic bone metastasis by inducing osteoclastogenesis via GM-CSF. Nature medicine *13*, 62-69.

Pasquinelli, A.E. (2012). MicroRNAs and their targets: recognition, regulation and an emerging reciprocal relationship. Nature reviews Genetics *13*, 271-282.

Perkins, N.D. (2007). Integrating cell-signalling pathways with NF-kappaB and IKK function. Nature reviews Molecular cell biology *8*, 49-62.

Peters, L., and Meister, G. (2007). Argonaute proteins: mediators of RNA silencing. Molecular cell *26*, 611-623.

Petrocca, F., Vecchione, A., and Croce, C.M. (2008a). Emerging role of miR-106b-25/miR-17-92 clusters in the control of transforming growth factor beta signaling. Cancer research *68*, 8191-8194.

Petrocca, F., Visone, R., Onelli, M.R., Shah, M.H., Nicoloso, M.S., de Martino, I., Iliopoulos, D., Pilozzi, E., Liu, C.G., Negrini, M*., et al.* (2008b). E2F1-regulated microRNAs impair TGFbeta-dependent cell-cycle arrest and apoptosis in gastric cancer. Cancer cell *13*, 272-286.

Pillai, R.S., Artus, C.G., and Filipowicz, W. (2004). Tethering of human Ago proteins to mRNA mimics the miRNA-mediated repression of protein synthesis. RNA *10*, 1518-1525.

Pribluda, A., Elyada, E., Wiener, Z., Hamza, H., Goldstein, R.E., Biton, M., Burstain, I., Morgenstern, Y., Brachya, G., Billauer, H*., et al.* (2013). A senescence-inflammatory switch from cancer-inhibitory to cancer-promoting mechanism. Cancer cell *24*, 242-256.

Qian, B.Z., Li, J., Zhang, H., Kitamura, T., Zhang, J., Campion, L.R., Kaiser, E.A., Snyder, L.A., and Pollard, J.W. (2011). CCL2 recruits inflammatory monocytes to facilitate breast-tumour metastasis. Nature *475*, 222-225.

Qiao, S., Kim, S.H., Heck, D., Goldowitz, D., LeDoux, M.S., and Homayouni, R. (2013). Dab2IP GTPase activating protein regulates dendrite development and synapse number in cerebellum. PloS one *8*, e53635.

Qiu, G.H., Xie, H., Wheelhouse, N., Harrison, D., Chen, G.G., Salto-Tellez, M., Lai, P., Ross, J.A., and Hooi, S.C. (2007). Differential expression of hDAB2IPA and hDAB2IPB in normal tissues and promoter methylation of hDAB2IPA in hepatocellular carcinoma. Journal of hepatology *46*, 655-663.

Rao, E., Jiang, C., Ji, M., Huang, X., Iqbal, J., Lenz, G., Wright, G., Staudt, L.M., Zhao, Y., McKeithan, T.W.*, et al.* (2012). The miRNA-17 approximately 92 cluster mediates chemoresistance and enhances tumor growth in mantle cell lymphoma via PI3K/AKT pathway activation. Leukemia *26*, 1064-1072.

Restle, A., Farber, M., Baumann, C., Bohringer, M., Scheidtmann, K.H., Muller-Tidow, C., and Wiesmuller, L. (2008). Dissecting the role of p53 phosphorylation in homologous recombination provides new clues for gain-of-function mutants. Nucleic acids research *36*, 5362-5375.

Roberti, M.P., Arriaga, J.M., Bianchini, M., Quinta, H.R., Bravo, A.I., Levy, E.M., Mordoh, J., and Barrio, M.M. (2012). Protein expression changes during human triple negative breast cancer cell line progression to lymph node metastasis in a xenografted model in nude mice. Cancer biology & therapy *13*, 1123-1140.

Robinson, D., Van Allen, E.M., Wu, Y.M., Schultz, N., Lonigro, R.J., Mosquera, J.M., Montgomery, B., Taplin, M.E., Pritchard, C.C., Attard, G.*, et al.* (2015). Integrative clinical genomics of advanced prostate cancer. Cell *161*, 1215-1228.

Rody, A., Karn, T., Liedtke, C., Pusztai, L., Ruckhaeberle, E., Hanker, L., Gaetje, R., Solbach, C., Ahr, A., Metzler, D.*, et al.* (2011). A clinically relevant gene signature in triple negative and basal-like breast cancer. Breast cancer research : BCR *13*, R97.

Rudisch, A., Dewhurst, M.R., Horga, L.G., Kramer, N., Harrer, N., Dong, M., van der Kuip, H., Wernitznig, A., Bernthaler, A., Dolznig, H.*, et al.* (2015). High EMT Signature Score of Invasive Non-Small Cell Lung Cancer (NSCLC) Cells Correlates with NFkappaB Driven Colony-Stimulating Factor 2 (CSF2/GM-CSF) Secretion by Neighboring Stromal Fibroblasts. PloS one *10*, e0124283.

Sabapathy, K. (2015). The Contrived Mutant p53 Oncogene - Beyond Loss of Functions. Frontiers in oncology *5*, 276.

Sangodkar, J., Farrington, C., McClinch, K., Galsky, M.D., Kastrinsky, D.B., and Narla, G. (2015). All roads lead to PP2A: Exploiting the therapeutic potential of this phosphatase. The FEBS journal.

Sarig, R., Rivlin, N., Brosh, R., Bornstein, C., Kamer, I., Ezra, O., Molchadsky, A., Goldfinger, N., Brenner, O., and Rotter, V. (2010). Mutant p53 facilitates somatic cell reprogramming and augments the malignant potential of reprogrammed cells. The Journal of experimental medicine *207*, 2127-2140.

Sauer, L., Gitenay, D., Vo, C., and Baron, V.T. (2010). Mutant p53 initiates a feedback loop that involves Egr-1/EGF receptor/ERK in prostate cancer cells. Oncogene *29*, 2628-2637.

Schwitalla, S., Ziegler, P.K., Horst, D., Becker, V., Kerle, I., Begus-Nahrmann, Y., Lechel, A., Rudolph, K.L., Langer, R., Slotta-Huspenina, J.*, et al.* (2013). Loss of p53 in enterocytes generates an inflammatory microenvironment enabling invasion and lymph node metastasis of carcinogen-induced colorectal tumors. Cancer cell *23*, 93-106.

Scian, M.J., Stagliano, K.E., Anderson, M.A., Hassan, S., Bowman, M., Miles, M.F., Deb, S.P., and Deb, S. (2005). Tumor-derived p53 mutants induce NF-kappaB2 gene expression. Molecular and cellular biology *25*, 10097-10110.

Sfanos, K.S., and De Marzo, A.M. (2012). Prostate cancer and inflammation: the evidence. Histopathology *60*, 199-215.

Sharma, J., Gray, K.P., Harshman, L.C., Evan, C., Nakabayashi, M., Fichorova, R., Rider, J., Mucci, L., Kantoff, P.W., and Sweeney, C.J. (2014). Elevated IL-8, TNF-alpha, and MCP-1 in men with metastatic prostate cancer starting androgen-deprivation therapy (ADT) are associated with shorter time to castration-resistance and overall survival. The Prostate *74*, 820-828.

Shen, Y.J., Kong, Z.L., Wan, F.N., Wang, H.K., Bian, X.J., Gan, H.L., Wang, C.F., and Ye, D.W. (2014). Downregulation of DAB2IP results in cell proliferation and invasion and contributes to unfavorable outcomes in bladder cancer. Cancer science *105*, 704-712.

Siu, M.K., Tsai, Y.C., Chang, Y.S., Yin, J.J., Suau, F., Chen, W.Y., and Liu, Y.N. (2015). Transforming growth factor-beta promotes prostate bone metastasis through induction of microRNA-96 and activation of the mTOR pathway. Oncogene *34*, 4767-4776.

Smith, A.L., Iwanaga, R., Drasin, D.J., Micalizzi, D.S., Vartuli, R.L., Tan, A.C., and Ford, H.L. (2012). The miR-106b-25 cluster targets Smad7, activates TGF-beta signaling, and induces EMT and tumor initiating cell characteristics downstream of Six1 in human breast cancer. Oncogene *31*, 5162-5171.

Smits, M., van Rijn, S., Hulleman, E., Biesmans, D., van Vuurden, D.G., Kool, M., Haberler, C., Aronica, E., Vandertop, W.P., Noske, D.P.*, et al.* (2012). EZH2-regulated DAB2IP is a medulloblastoma tumor suppressor and a positive marker for survival. Clinical cancer research : an official journal of the American Association for Cancer Research *18*, 4048-4058.

Smyth, G.K. (2004). Linear models and empirical bayes methods for assessing differential expression in microarray experiments. Stat Appl Genet Mol Biol *3*, Article3.

Solomon, H., Buganim, Y., Kogan-Sakin, I., Pomeraniec, L., Assia, Y., Madar, S., Goldstein, I., Brosh, R., Kalo, E., Beatus, T.*, et al.* (2012). Various p53 mutant proteins differently regulate the Ras circuit to induce a cancer-related gene signature. Journal of cell science *125*, 3144-3152.

Solomon, H., Madar, S., and Rotter, V. (2011). Mutant p53 gain of function is interwoven into the hallmarks of cancer. The Journal of pathology *225*, 475-478.

Song, G., and Wang, L. (2008). MiR-433 and miR-127 arise from independent overlapping primary transcripts encoded by the miR-433-127 locus. PloS one *3*, e3574.

Song, H., Hollstein, M., and Xu, Y. (2007). p53 gain-of-function cancer mutants induce genetic instability by inactivating ATM. Nature cell biology *9*, 573-580.

Song, M.Y., Pan, K.F., Su, H.J., Zhang, L., Ma, J.L., Li, J.Y., Yuasa, Y., Kang, D., Kim, Y.S., and You, W.C. (2012). Identification of serum microRNAs as novel non-invasive biomarkers for early detection of gastric cancer. PloS one *7*, e33608.

Stambolsky, P., Tabach, Y., Fontemaggi, G., Weisz, L., Maor-Aloni, R., Siegfried, Z., Shiff, I., Kogan, I., Shay, M., Kalo, E.*, et al.* (2010). Modulation of the vitamin D3 response by cancer-associated mutant p53. Cancer cell *17*, 273-285.

Stuelten, C.H., DaCosta Byfield, S., Arany, P.R., Karpova, T.S., Stetler-Stevenson, W.G., and Roberts, A.B. (2005). Breast cancer cells induce stromal fibroblasts to express MMP-9 via secretion of TNF-alpha and TGF-beta. Journal of cell science *118*, 2143-2153.

Su, G., Meyer, K., Nandini, C.D., Qiao, D., Salamat, S., and Friedl, A. (2006). Glypican-1 is frequently overexpressed in human gliomas and enhances FGF-2 signaling in glioma cells. The American journal of pathology *168*, 2014-2026.

Sullivan, N.J., Sasser, A.K., Axel, A.E., Vesuna, F., Raman, V., Ramirez, N., Oberyszyn, T.M., and Hall, B.M. (2009). Interleukin-6 induces an epithelial-mesenchymal transition phenotype in human breast cancer cells. Oncogene *28*, 2940-2947.

Tan, Y.L., Bai, Z.G., Zou, W.L., Ma, X.M., Wang, T.T., Guo, W., Liu, J., Li, J.S., Jie, Y., Zang, Y.J.*, et al.* (2015). miR-744 is a potential prognostic marker in patients with hepatocellular carcinoma. Clinics and research in hepatology and gastroenterology *39*, 359-365.

Taylor, B.S., Schultz, N., Hieronymus, H., Gopalan, A., Xiao, Y., Carver, B.S., Arora, V.K., Kaushik, P., Cerami, E., Reva, B.*, et al.* (2010). Integrative genomic profiling of human prostate cancer. Cancer cell *18*, 11-22.

Tessitore, A., Cicciarelli, G., Del Vecchio, F., Gaggiano, A., Verzella, D., Fischietti, M., Vecchiotti, D., Capece, D., Zazzeroni, F., and Alesse, E. (2014). MicroRNAs in the DNA Damage/Repair Network and Cancer. International journal of genomics *2014*, 820248.

Thukral, S.K., Lu, Y., Blain, G.C., Harvey, T.S., and Jacobsen, V.L. (1995). Discrimination of DNA binding sites by mutant p53 proteins. Molecular and cellular biology *15*, 5196-5202.

Treilleux, I., Blay, J.Y., Bendriss-Vermare, N., Ray-Coquard, I., Bachelot, T., Guastalla, J.P., Bremond, A., Goddard, S., Pin, J.J., Barthelemy-Dubois, C.*, et al.* (2004). Dendritic cell infiltration and prognosis of early stage breast cancer. Clinical cancer research : an official journal of the American Association for Cancer Research *10*, 7466-7474.

Tsai, Y.S., Lai, C.L., Lai, C.H., Chang, K.H., Wu, K., Tseng, S.F., Fazli, L., Gleave, M., Xiao, G., Gandee, L.*, et al.* (2014). The role of homeostatic regulation between tumor suppressor DAB2IP and oncogenic Skp2 in prostate cancer growth. Oncotarget *5*, 6425-6436.

Valenti, F., Fausti, F., Biagioni, F., Shay, T., Fontemaggi, G., Domany, E., Yaffe, M.B., Strano, S., Blandino, G., and Di Agostino, S. (2011). Mutant p53 oncogenic functions are sustained by Plk2 kinase through an autoregulatory feedback loop. Cell Cycle *10*, 4330-4340.

Vasudevan, S., Tong, Y., and Steitz, J.A. (2007). Switching from repression to activation: microRNAs can up-regulate translation. Science *318*, 1931-1934.

Ventura, A., Young, A.G., Winslow, M.M., Lintault, L., Meissner, A., Erkeland, S.J., Newman, J., Bronson, R.T., Crowley, D., Stone, J.R.*, et al.* (2008). Targeted deletion reveals essential and overlapping functions of the miR-17 through 92 family of miRNA clusters. Cell *132*, 875-886.

Vidal, A.C., Howard, L.E., Moreira, D.M., Castro-Santamaria, R., Andriole, G.L., and Freedland, S.J. (2015). Aspirin, NSAIDs, and risk of prostate cancer: results from the REDUCE study. Clinical cancer research : an official journal of the American Association for Cancer Research *21*, 756-762.

Volinia, S., Calin, G.A., Liu, C.G., Ambs, S., Cimmino, A., Petrocca, F., Visone, R., Iorio, M., Roldo, C., Ferracin, M.*, et al.* (2006). A microRNA expression signature of human solid tumors defines cancer gene targets. Proceedings of the National Academy of Sciences of the United States of America *103*, 2257-2261.

von Bergh, A.R., Wijers, P.M., Groot, A.J., van Zelderen-Bhola, S., Falkenburg, J.H., Kluin, P.M., and Schuuring, E. (2004). Identification of a novel RAS GTPase-activating protein (RASGAP) gene at 9q34 as an MLL fusion partner in a patient with de novo acute myeloid leukemia. Genes, chromosomes & cancer *39*, 324-334.

Voronov, E., Shouval, D.S., Krelin, Y., Cagnano, E., Benharroch, D., Iwakura, Y., Dinarello, C.A., and Apte, R.N. (2003). IL-1 is required for tumor invasiveness and angiogenesis. Proceedings of the National Academy of Sciences of the United States of America *100*, 2645-2650.

Wajant, H. (2009). The role of TNF in cancer. Results and problems in cell differentiation *49*, 1-15.

Wajant, H., Pfizenmaier, K., and Scheurich, P. (2003). Tumor necrosis factor signaling. Cell death and differentiation *10*, 45-65.

Walch-Ruckheim, B., Mavrova, R., Henning, M., Vicinus, B., Kim, Y.J., Bohle, R.M., Juhasz-Boss, I., Solomayer, E.F., and Smola, S. (2015). Stromal Fibroblasts Induce CCL20 through IL6/C/EBPbeta to Support the Recruitment of Th17 Cells during Cervical Cancer Progression. Cancer research *75*, 5248-5259.

Wan, T., Liu, T., Zhang, H., Tang, S., and Min, W. (2010). AIP1 functions as Arf6-GAP to negatively regulate TLR4 signaling. The Journal of biological chemistry *285*, 3750-3757.

Wang, C.M., Wang, Y., Fan, C.G., Xu, F.F., Sun, W.S., Liu, Y.G., and Jia, J.H. (2011). miR-29c targets TNFAIP3, inhibits cell proliferation and induces apoptosis in hepatitis B virus-related hepatocellular carcinoma. Biochemical and biophysical research communications *411*, 586-592.

Wang, H., Fang, R., Wang, X.F., Zhang, F., Chen, D.Y., Zhou, B., Wang, H.S., Cai, S.H., and Du, J. (2013). Stabilization of Snail through AKT/GSK-3beta signaling pathway is required for TNF-alpha-induced epithelial-mesenchymal transition in prostate cancer PC3 cells. European journal of pharmacology *714*, 48-55.

Wang, J., Zhu, X., Hu, J., He, G., Li, X., Wu, P., Ren, X., Wang, F., Liao, W., Liang, L.*, et al.* (2015). The positive feedback between Snail and DAB2IP regulates EMT, invasion and metastasis in colorectal cancer. Oncotarget *6*, 27427-27439.

Wang, Y., Klijn, J.G., Zhang, Y., Sieuwerts, A.M., Look, M.P., Yang, F., Talantov, D., Timmermans, M., Meijer-van Gelder, M.E., Yu, J.*, et al.* (2005). Gene-expression profiles to predict distant metastasis of lymph-node-negative primary breast cancer. Lancet *365*, 671-679.

Wang, Y., Zheng, X., Zhang, Z., Zhou, J., Zhao, G., Yang, J., Xia, L., Wang, R., Cai, X., Hu, H.*, et al.* (2012). MicroRNA-149 inhibits proliferation and cell cycle progression through the targeting of ZBTB2 in human gastric cancer. PloS one *7*, e41693.

Wang, Z., Tseng, C.P., Pong, R.C., Chen, H., McConnell, J.D., Navone, N., and Hsieh, J.T. (2002). The mechanism of growth-inhibitory effect of DOC-2/DAB2 in prostate cancer. Characterization of a novel GTPase-activating protein associated with N-terminal domain of DOC-2/DAB2. The Journal of biological chemistry *277*, 12622-12631.

Weissmueller, S., Manchado, E., Saborowski, M., Morris, J.P.t., Wagenblast, E., Davis, C.A., Moon, S.H., Pfister, N.T., Tschaharganeh, D.F., Kitzing, T.*, et al.* (2014). Mutant p53 drives pancreatic cancer metastasis through cell-autonomous PDGF receptor beta signaling. Cell *157*, 382-394.

Weisz, L., Damalas, A., Liontos, M., Karakaidos, P., Fontemaggi, G., Maor-Aloni, R., Kalis, M., Levrero, M., Strano, S., Gorgoulis, V.G.*, et al.* (2007). Mutant p53 enhances nuclear factor kappaB activation by tumor necrosis factor alpha in cancer cells. Cancer research *67*, 2396-2401.

Werner, H., Karnieli, E., Rauscher, F.J., and LeRoith, D. (1996). Wild-type and mutant p53 differentially regulate transcription of the insulin-like growth factor I receptor gene. Proceedings of the National Academy of Sciences of the United States of America *93*, 8318-8323.

Winter, J., Jung, S., Keller, S., Gregory, R.I., and Diederichs, S. (2009). Many roads to maturity: microRNA biogenesis pathways and their regulation. Nature cell biology *11*, 228-234.

Wolf, M.J., Hoos, A., Bauer, J., Boettcher, S., Knust, M., Weber, A., Simonavicius, N., Schneider, C., Lang, M., Sturzl, M.*, et al.* (2012). Endothelial CCR2 signaling induced by colon carcinoma cells enables extravasation via the JAK2-Stat5 and p38MAPK pathway. Cancer cell *22*, 91-105.

Wolin, K.Y., Carson, K., and Colditz, G.A. (2010). Obesity and cancer. The oncologist *15*, 556-565.

Wu, K., Liu, J., Tseng, S.F., Gore, C., Ning, Z., Sharifi, N., Fazli, L., Gleave, M., Kapur, P., Xiao, G.*, et al.* (2014). The role of DAB2IP in androgen receptor activation during prostate cancer progression. Oncogene *33*, 1954-1963.

Wu, K., Wang, B., Chen, Y., Zhou, J., Huang, J., Hui, K., Zeng, J., Zhu, J., Zhang, K., Li, L.*, et al.* (2015a). DAB2IP regulates the chemoresistance to pirarubicin and tumor recurrence of non-muscle invasive bladder cancer through STAT3/Twist1/P-glycoprotein signaling. Cellular signalling *27*, 2515-2523.

Wu, K., Xie, D., Zou, Y., Zhang, T., Pong, R.C., Xiao, G., Fazli, L., Gleave, M., He, D., Boothman, D.A.*, et al.* (2013). The mechanism of DAB2IP in chemoresistance of prostate cancer cells. Clinical cancer research : an official journal of the American Association for Cancer Research *19*, 4740-4749.

Wu, L., Fan, J., and Belasco, J.G. (2006). MicroRNAs direct rapid deadenylation of mRNA. Proceedings of the National Academy of Sciences of the United States of America *103*, 4034-4039.

Wu, Y., Deng, J., Rychahou, P.G., Qiu, S., Evers, B.M., and Zhou, B.P. (2009). Stabilization of snail by NF-kappaB is required for inflammation-induced cell migration and invasion. Cancer cell *15*, 416-428.

Wu, Z., Liu, K., Wang, Y., Xu, Z., Meng, J., and Gu, S. (2015b). Upregulation of microRNA-96 and its oncogenic functions by targeting CDKN1A in bladder cancer. Cancer cell international *15*, 107.

Wullaert, A., Heyninck, K., and Beyaert, R. (2006). Mechanisms of crosstalk between TNF-induced NF-kappaB and JNK activation in hepatocytes. Biochemical pharmacology *72*, 1090-1101.

Xia, H., Chen, S., Chen, K., Huang, H., and Ma, H. (2014). MiR-96 promotes proliferation and chemo- or radioresistance by down-regulating RECK in esophageal cancer. Biomedicine & pharmacotherapy = Biomedecine & pharmacotherapie *68*, 951-958.

Xie, D., Gore, C., Liu, J., Pong, R.C., Mason, R., Hao, G., Long, M., Kabbani, W., Yu, L., Zhang, H.*, et al.* (2010). Role of DAB2IP in modulating epithelial-to-mesenchymal transition and prostate cancer metastasis. Proceedings of the National Academy of Sciences of the United States of America *107*, 2485-2490.

Xie, D., Gore, C., Zhou, J., Pong, R.C., Zhang, H., Yu, L., Vessella, R.L., Min, W., and Hsieh, J.T. (2009). DAB2IP coordinates both PI3K-Akt and ASK1 pathways for cell survival and apoptosis. Proceedings of the National Academy of Sciences of the United States of America *106*, 19878-19883.

Xin, C., Zhang, H., and Liu, Z. (2014). miR-154 suppresses colorectal cancer cell growth and motility by targeting TLR2. Molecular and cellular biochemistry *387*, 271-277.

Xu, K., Liu, X., Mao, X., Xue, L., Wang, R., Chen, L., and Chu, X. (2015a). MicroRNA-149 suppresses colorectal cancer cell migration and invasion by directly targeting forkhead box transcription factor FOXM1. Cellular physiology and biochemistry : international journal of experimental cellular physiology, biochemistry, and pharmacology *35*, 499-515.

Xu, Y., He, J., Wang, Y., Zhu, X., Pan, Q., Xie, Q., and Sun, F. (2015b). miR-889 promotes proliferation of esophageal squamous cell carcinomas through DAB2IP. FEBS letters *589*, 1127-1135.

Xue, L., Wang, Y., Yue, S., and Zhang, J. (2015). Low MiR-149 expression is associated with unfavorable prognosis and enhanced Akt/mTOR signaling in glioma. International journal of clinical and experimental pathology *8*, 11178-11184.

Yan, W., and Chen, X. (2009). Identification of GRO1 as a critical determinant for mutant p53 gain of function. The Journal of biological chemistry *284*, 12178-12187.

Yano, M., Toyooka, S., Tsukuda, K., Dote, H., Ouchida, M., Hanabata, T., Aoe, M., Date, H., Gazdar, A.F., and Shimizu, N. (2005). Aberrant promoter methylation of human DAB2 interactive protein (hDAB2IP) gene in lung cancers. International journal of cancer Journal international du cancer *113*, 59-66.

Yeudall, W.A., Vaughan, C.A., Miyazaki, H., Ramamoorthy, M., Choi, M.Y., Chapman, C.G., Wang, H., Black, E., Bulysheva, A.A., Deb, S.P.*, et al.* (2012). Gain-of-function mutant p53 upregulates CXC chemokines and enhances cell migration. Carcinogenesis *33*, 442-451.

Yi, R., Qin, Y., Macara, I.G., and Cullen, B.R. (2003). Exportin-5 mediates the nuclear export of pre-microRNAs and short hairpin RNAs. Genes & development *17*, 3011-3016.

You, J.S., and Jones, P.A. (2012). Cancer genetics and epigenetics: two sides of the same coin? Cancer cell *22*, 9-20.

Yu, J.J., Wu, Y.X., Zhao, F.J., and Xia, S.J. (2014). miR-96 promotes cell proliferation and clonogenicity by down-regulating of FOXO1 in prostate cancer cells. Med Oncol *31*, 910.

Yu, L., Qin, L., Zhang, H., He, Y., Chen, H., Pober, J.S., Tellides, G., and Min, W. (2011). AIP1 prevents graft arteriosclerosis by inhibiting interferon-gamma-dependent smooth muscle cell proliferation and intimal expansion. Circulation research *109*, 418-427.

Yun, E.J., Baek, S.T., Xie, D., Tseng, S.F., Dobin, T., Hernandez, E., Zhou, J., Zhang, L., Yang, J., Sun, H.*, et al.* (2015). DAB2IP regulates cancer stem cell phenotypes through modulating stem cell factor receptor and ZEB1. Oncogene *34*, 2741-2752.

Zeng, W., Chang, H., Ma, M., and Li, Y. (2014). CCL20/CCR6 promotes the invasion and migration of thyroid cancer cells via NF-kappa B signaling-induced MMP-3 production. Experimental and molecular pathology *97*, 184-190.

Zeng, Y., and Cullen, B.R. (2005). Efficient processing of primary microRNA hairpins by Drosha requires flanking nonstructured RNA sequences. The Journal of biological chemistry *280*, 27595-27603.

Zhang, H., He, Y., Dai, S., Xu, Z., Luo, Y., Wan, T., Luo, D., Jones, D., Tang, S., Chen, H.*, et al.* (2008). AIP1 functions as an endogenous inhibitor of VEGFR2-mediated signaling and inflammatory angiogenesis in mice. The Journal of clinical investigation *118*, 3904-3916.

Zhang, H., Zhang, H., Lin, Y., Li, J., Pober, J.S., and Min, W. (2007). RIP1-mediated AIP1 phosphorylation at a 14-3-3-binding site is critical for tumor necrosis factor-induced ASK1-JNK/p38 activation. The Journal of biological chemistry *282*, 14788-14796.

Zhang, H., Zhang, R., Luo, Y., D'Alessio, A., Pober, J.S., and Min, W. (2004). AIP1/DAB2IP, a novel member of the Ras-GAP family, transduces TRAF2-induced ASK1-JNK activation. The Journal of biological chemistry *279*, 44955-44965.

Zhang, R., He, X., Liu, W., Lu, M., Hsieh, J.T., and Min, W. (2003). AIP1 mediates TNF-alpha-induced ASK1 activation by facilitating dissociation of ASK1 from its inhibitor 14-3-3. The Journal of clinical investigation *111*, 1933-1943.

Zhou, G., Wang, J., Zhao, M., Xie, T.X., Tanaka, N., Sano, D., Patel, A.A., Ward, A.M., Sandulache, V.C., Jasser, S.A.*, et al.* (2014a). Gain-of-function mutant p53 promotes cell growth and cancer cell metabolism via inhibition of AMPK activation. Molecular cell *54*, 960-974.

Zhou, H.J., Chen, X., Huang, Q., Liu, R., Zhang, H., Wang, Y., Jin, Y., Liang, X., Lu, L., Xu, Z.*, et al.* (2014b). AIP1 mediates vascular endothelial cell growth factor receptor-3-dependent angiogenic and lymphangiogenic responses. Arteriosclerosis, thrombosis, and vascular biology *34*, 603-615.

Zhou, J., Ning, Z., Wang, B., Yun, E.J., Zhang, T., Pong, R.C., Fazli, L., Gleave, M., Zeng, J., Fan, J.*, et al.* (2015). DAB2IP loss confers the resistance of prostate cancer to androgen deprivation therapy through activating STAT3 and inhibiting apoptosis. Cell death & disease *6*, e1955.

Zhu, C., Li, J., Cheng, G., Zhou, H., Tao, L., Cai, H., Li, P., Cao, Q., Ju, X., Meng, X.*, et al.* (2013a). miR-154 inhibits EMT by targeting HMGA2 in prostate cancer cells. Molecular and cellular biochemistry *379*, 69-75.

Zhu, C., Shao, P., Bao, M., Li, P., Zhou, H., Cai, H., Cao, Q., Tao, L., Meng, X., Ju, X.*, et al.* (2014). miR-154 inhibits prostate cancer cell proliferation by targeting CCND2. Urologic oncology *32*, 31 e39-16.

Zhu, H., Mao, Q., Lin, Y., Yang, K., and Xie, L. (2011). RNA interference targeting mutant p53 inhibits growth and induces apoptosis in DU145 human prostate cancer cells. Med Oncol *28 Suppl 1*, S381-387.

Zhu, H.B., Yang, K., Xie, Y.Q., Lin, Y.W., Mao, Q.Q., and Xie, L.P. (2013b). Silencing of mutant p53 by siRNA induces cell cycle arrest and apoptosis in human bladder cancer cells. World journal of surgical oncology *11*, 22.

ACKNOWLEDGMENTS

First of all, I would like to express my sincere gratitude to my supervisor Professor Licio Collavin, who gave me the opportunity to work in his laboratory, and whose contribution with suggestions and encouragements, helped me to coordinate my project. I am grateful for his support, patience and motivation, especially in writing this Thesis.

A special gratitude I give to Giulio di Minin who has supported me during my first steps in laboratory, passed me curiosity and passion and helping me to conceive this project.

I would like also to thank Marco dal Ferro, Elena Valentino and Daria Sicari, for their insightful comments and encouragements, as well as the numerous questions that have incented me to widen my research from various perspectives.

I thank my colleagues at the LNCIB, especially old and new fellows of 117 room, for the stimulating discussion, and for all the fun we have had in the last four years.

I would like to thank our collaborators who provided insights and expertise that greatly assisted the research.

I am also grateful with my friends who encourage me in the hardest moments.

Finally, I would like to thank my parents, my sister, my brother and Simone for providing me with unfailing support and continuous encouragements throughout my years of study, and for their endless love. This accomplishment would not have been possible without them. Thank you.